

Characterising the function of CDK5RAP2 in the vertebrate centrosome

**This dissertation is submitted for the degree of Doctor of
Philosophy**

**Alexis Ruth Barr, MSci MA (Cantab.)
Trinity Hall**

Final word count: 52,557



**UNIVERSITY OF
CAMBRIDGE**

Cancer Research UK
- Cambridge Research Institute
Department of Oncology
University of Cambridge



Statement

This dissertation is the result of my own work and includes nothing which is the outcome of work done in collaboration except where specifically indicated in the text.

This dissertation is not substantially the same as any that I have submitted for a degree or diploma or other qualification at any other University.

Furthermore, I state that no part of this dissertation has been, or is being concurrently, submitted for any degree, diploma, or other qualification.

Alexis Ruth Barr

August 2010

Acknowledgements

I want to thank all the members of the Gergely lab, past and present, for making the lab a fantastic and fun place to work - Deborah, Joo-Hee, Hani, Carles, Monika, Jo, Chris (particularly for his proof-reading skills!), Tolou, Daniela, Thomas – and most of all Fanni. Especially huge thanks go to Fanni for her endless enthusiasm for the subject, her support and ideas. Some may have seen it as a risk doing a PhD with a new group leader but I never saw it as a risk and I always knew that working with Fanni would be productive and exciting. I believe that what I have learnt from her has helped me develop as an independent researcher and hopefully will stand me in very good stead throughout my career.

I would like to thank our collaborator – Geoff Woods and all his lab, especially for the entertaining group meetings. John Kilmartin deserves an extra special mention for teaching me serial sectioning and electron microscopy – probably the hardest technique I have had to master during my PhD! I would also like to thank the following people for reagents, without which my PhD would have been considerably more difficult: KJ Patel, Sean Munro, Viji Draviam, Peter Coopman, Lynne Cassimeris, Bill Earnshaw and Jon Pines. I also thank our neighbours – the Murrell lab for making the lab an entertaining place to be.

I thank Cancer Research UK for funding and the core facilities at CRI – particularly Microscopy - have been invaluable throughout my PhD and special thanks goes to Heather Zecchini for her training and expertise. Ann Kaminski also deserves a big thank you for her ‘unflappability’.

I thank all my friends (for too many to mention but you all know who you are) for all their support and encouragement through the more difficult times. I am also indebted to the love and support of all of my family – but particularly my Mum, Nannan and Richard. Without their backing I would not be where I am today and for that I am extremely grateful.

Finally, I thank Ben – for pretty much anything I can think of! For his endless love and support, his unshakeable belief in my abilities, the constant supply of meals and his patience during the long evenings and weekends. Thank you!

This PhD is dedicated to my wonderful cousin and godmother, Samantha Jane Barr.

Table of Contents

Statement

Acknowledgements

Summary	i
----------------	----------

Abbreviations	ii
----------------------	-----------

Chapter 1: Introduction	1
--------------------------------	----------

1.1 The cell cycle	2
---------------------------	----------

1.1.1 Phases of the cell cycle	2
--------------------------------	---

1.1.2 Control of the cell cycle by Cyclin-dependent kinases	3
---	---

1.1.3 Quality control of the cell cycle	5
---	---

1.2 The microtubule cytoskeleton	9
---	----------

1.2.1 Microtubule structure	9
-----------------------------	---

1.2.2 Microtubule dynamics	9
----------------------------	---

1.2.3 Microtubule organising centres (MTOCs)	12
--	----

1.2.4 Microtubule-associated proteins (MAPs)	14
--	----

1.2.5 Microtubules and bipolar spindle assembly	16
---	----

1.3 The centrosome	19
---------------------------	-----------

1.3.1 Centrosome structure	19
----------------------------	----

1.3.2 Microtubule organisation by centrosomes throughout the cell cycle	22
---	----

1.3.3 The Centrosome Cycle	23
----------------------------	----

1.3.4 Are centrosomes essential?	31
----------------------------------	----

1.3.5 The centrosome and the DNA damage response	34
--	----

1.4 Primary Microcephaly – a centrosomal disease?	40
--	-----------

1.4.1 Mammalian neurogenesis – a summary	40
--	----

1.4.2 Microcephaly and centrosomes	42
------------------------------------	----

1.5 CDK5RAP2: an uncharacterised centrosomal protein essential for proper brain development	49
--	-----------

1.5.1 CDK5RAP2 is an evolutionarily conserved centrosomal protein	49
---	----

1.5.2 CDK5RAP2: the story so far....	53
--------------------------------------	----

Aims of my PhD	54
-----------------------	-----------

Chapter 2: Materials and Methods	55
---	-----------

2.1 Cell Culture	55
-------------------------	-----------

2.1.1 ECM-coating of flasks for primary glioblastoma cell lines	55
---	----

2.1.2 Primary cilium formation in HB2 cells	56
---	----

2.1.3 Synchronisation of HeLa cells	56
-------------------------------------	----

2.1.4 Brefeldin A treatment of HeLa cells	56
---	----

2.1.5 Cold-induced depolymerisation of microtubules in HeLa cells	56
---	----

2.2 Molecular Biology	57
------------------------------	-----------

2.2.1 FLAG-tagging of CDK5RAP2	58
--------------------------------	----

2.2.2 Site-directed mutagenesis of FLAG-CDK5RAP2 constructs	59
---	----

2.3 Generating anti-human CDK5RAP2 antibodies	59
--	-----------

2.4 Immunostaining	61
---------------------------	-----------

2.4.1 Making metasilicated coverslips	61
2.4.2 Making poly-l-lysine coated coverslips	62
2.5 Image acquisition and analysis	62
2.5.1 Image acquisition	62
2.5.2 Image analysis	63
2.6 Electron Microscopy	64
2.6.1 Fixing and embedding cells	64
2.6.2 Serial sectioning and post-staining grids	64
2.7 Western blotting	65
2.8 Transient transfection of DNA into human cell lines	66
2.9 siRNA transfection into human cell lines	66
2.10 Retroviral shRNA	67
2.11 Lambda Phosphatase Treatments	68
2.12 Microtubule-pelleting assay	68
2.12.1 Making Taxol-stabilised microtubules	69
2.13 Immunoprecipitation	69
2.13.1 Cross-linking antibodies to beads	69
2.13.2 Coimmunoprecipitation reaction	70
2.14 DT40 methods	70
2.14.1 Design and creation of targeting constructs	70
2.14.2 Targeted integration of DNA into DT40	72
2.14.3 Non-targeted integration of DNA into DT40	72
2.14.4 Cre-mediated recombination of loxP sites in DT40	72
2.14.5 Transient transfection of DNA into DT40	73
2.14.6 DT40 Centrosome purification	73
2.14.7 Microtubule regrowth in DT40 cells	73
2.14.8 Taxol treatment of DT40 cells	74
2.14.9 Cell cycle analysis	74
2.14.10 DT40 clonogenic assay	74
2.14.11 Ionising radiation assays	74

Chapter 3 **81**

3.1 CDK5RAP2 localises to the centrosome and Golgi body and associates with microtubules	82
3.1.1 Making an anti-human CDK5RAP2 antibody	82
3.1.2 CDK5RAP2 localises to the centrosome and Golgi body	82
3.2 CDK5RAP2 is required for centrosome cohesion	86
3.2.1 Depleting CDK5RAP2 levels by siRNA and shRNA	86
3.2.2 CDK5RAP2 is required for centrosome cohesion	88
3.2.3 Restoration of CDK5RAP2 protein rescues centrosome splitting	90
3.2.4 CDK5RAP2 does not affect the localisation of other centrosome cohesion proteins	90
3.2.5 Split centrosomes are dynamic	92
3.2.6 CDK5RAP2 may mediate centrosome cohesion by regulating centrosome-microtubule interactions	96
3.3 CDK5RAP2 is a microtubule-associated protein and has two distinct centrosome-localisation signals	98
3.3.1 The N- and C-termini of CDK5RAP2 have distinct localisation patterns	98
3.3.2 Overexpression of the C-terminus of CDK5RAP2 leads to a loss of centrosome cohesion	100
3.3.3 FLAG-NT interacts with endogenous CDK5RAP2	102

3.3.4 Endogenous CDK5RAP2 can bind to microtubules	102
3.3.5 CDK5RAP2 is phosphorylated in mitosis	104
3.4 Myomegalin is not required for centrosome cohesion	108
3.4.1 Making an anti-human Myomegalin antibody	108
3.4.2 Myomegalin is not required to maintain centrosome cohesion	108
3.4.3 Myomegalin localisation varies between cell lines	110
3.5 Discussion	114
3.5.1 CDK5RAP2 mediates centrosome cohesion	114
3.5.2 CDK5RAP2 localises to the Golgi body	118
3.5.3 CDK5RAP2 is phosphorylated in mitosis	118
3.5.4 CDK5RAP2 localises to basal bodies but not to ciliary axonemes	120
3.5.5 Myomegalin localisation varies between cell lines	120
3.5.6 Myomegalin expression in cancer	121
Chapter 4	122
4.1 CDK5RAP2 interacts with AKAP450 and recruits it to the mitotic centrosome	123
4.1.1 CDK5RAP2 colocalises and interacts with AKAP450 throughout the cell cycle	123
4.1.2 CDK5RAP2 is required for the accumulation of AKAP450 in the mitotic centrosome	123
4.1.3 CDK5RAP2 is required to recruit AKAP450 to the mitotic centrosomes	126
4.1.4 AKAP450 does not mediate the localisation of CDK5RAP2 to the centrosome	128
4.1.5 AKAP450 is required for centrosome cohesion	128
4.1.6 Myomegalin regulates AKAP450 levels in mitotic centrosomes	131
4.2 CDK5RAP2 is not required for efficient γ-tubulin localisation to mitotic centrosomes	133
4.2.1 CDK5RAP2 is not required for the efficient localisation of γ -tubulin to mitotic centrosomes	133
4.2.2 CDK5RAP2 is not required for centrosome maturation	133
4.3 Discussion	137
4.3.1 CDK5RAP2 interacts with AKAP450 and recruits it to the centrosome in mitosis	137
4.3.2 AKAP450 is required for centrosome cohesion	137
4.3.3 CDK5RAP2 is not required for the efficient localisation of γ -tubulin to mitotic centrosomes	138
4.3.4 Myomegalin and AKAP450	140
Chapter 5	141
5.1 Creation and characterisation of <i>cdk5rap2</i>-disrupted cell lines	141
5.1.1 <i>cdk5rap2</i> conservation between human and chicken	142
5.1.2 Gene-disruption of <i>cdk5rap2</i> in DT40 cells	143
5.1.3 Characterisation of CNN1- and CNN2-disrupted DT40 cells	147
5.2 CDK5RAP2 connects centrosomes to mitotic spindle poles	150
5.2.1 Centrosomes detach from spindle poles in <i>cnn1</i> ^{-/-} and <i>cnn2</i> ^{-/-} DT40 cells	150
5.2.2 Expression of FLAG-FL CDK5RAP2 in <i>cnn1</i> ^{lox} cells rescues centrosome detachment	152
5.2.3 Centrosome detachment is a dynamic and reversible event	154
5.2.4 Dynamic microtubules are not required for centrosome detachment	158
5.2.5 Mitotic spindle pole organisation is intact in <i>cnn1</i> ^{-/-} cells	158
5.2.6 Centrosome structure is normal in <i>cnn1</i> ^{-/-} cells	161
5.2.7 Visualising AKAP450 in DT40 cells	161
5.2.8 CDK5RAP2 is critical for the centrosomal localisation of AKAP450	161
5.2.9 CDK5RAP2 is critical for the centrosomal localisation of p150 ^{glued} /dynactin	165
5.2.10 <i>cnn1</i> ^{-/-} centrosomes contain reduced levels of γ -tubulin but are not deficient in microtubule nucleation	168

5.2.11 The CNN1 domain of CDK5RAP2 is dispensable for centrosome maturation	170
5.3 The CNN1, but not the CNN2, domain in CDK5RAP2 is required for centrosome cohesion	173
5.3.1 <i>cnn1^{-/-}</i> , but not <i>cnn2^{-/-}</i> , DT40 cells have defects in centrosome cohesion	173
5.4 Discussion	175
5.4.1 CDK5RAP2 is a critical regulator of centrosome to spindle pole attachment	175
5.4.2 The CNN1, but not the CNN2, domain is required for centrosome cohesion	176
5.4.3 GS-TAP tagging as a way to identify interacting partners of CDK5RAP2 and AKAP450	178
<hr/>	
Chapter 6	179
<hr/>	
6.1 The CNN1 domain is required for an efficient G2 arrest after DNA damage	180
6.1.1 The CNN1 domain is essential for normal proliferation and clonogenic potential	180
6.1.2 The CNN1 domain is required for effective DNA damage-induced G2 arrest	182
6.1.3 The CNN1 domain is required for the centrosomal accumulation of Chk1	184
6.1.4 The CNN1 domain is involved in centrosome amplification in response to aphidicolin but not to hydroxyurea	186
6.2 Discussion	189
6.2.1 The role of CDK5RAP2 in DNA-damage induced G2 arrest	189
6.2.2 The function of the CNN1 domain in centrosome amplification	190
6.2.3 The respective contributions of the CNN1 and CNN2 domains to CDK5RAP2 function	190
<hr/>	
Chapter 7: Discussion	193
<hr/>	
7.1 CDK5RAP2 is required for centrosome to spindle pole attachment	193
7.1.1 Attachment of centrosomes to spindle poles	193
7.1.2 CDK5RAP2 maintains centrosome to spindle pole attachment via AKAP450 and dynactin	194
7.1.3 The relative contributions of the CNN1 and CNN2 domains in centrosome to spindle pole attachment	196
7.1.4 The interplay between CDK5RAP2 and dynein in the mitotic centrosome	197
7.2 CDK5RAP2 and AKAP450 may mediate centrosome cohesion by regulating microtubule interactions with the centrosome	199
7.3 CDK5RAP2 plays a role in the DNA damage response	201
7.4 Similarities and differences between CDK5RAP2 and its lower eukaryotic homologues	203
7.4.1 Centrosome maturation	203
7.4.2 PCM structure	204
7.4.3 Centrosome to spindle pole attachment	205
7.4.4 Centrosome cohesion	205
7.4.5 Functions of the CNN2 domain	205
7.4.6 Does CDK5RAP2 function redundantly with Myomegalin?	206
7.5 Inconsistencies between results obtained from DT40 and HeLa cell lines	208
7.5.1 DT40 versus HeLa cells as a system to study centrosomal proteins	208
7.5.2 Centrosome detachment	208
7.5.3 AKAP450 localisation in interphase	209
7.5.4 CDK5RAP2 in centrosome cohesion	209
7.6 Linking the function of CDK5RAP2 to microcephaly	211
7.6.1 Defects in spindle alignment	211
7.6.2 Defects in arrest after DNA damage	212

Chapter 8: Bibliography	214
Appendix	244

Summary

The centrosome is the major microtubule organising centre in vertebrate cells. CDK5RAP2 is a human protein that localises to the centrosome. At the start of this thesis work, the function of CDK5RAP2 was uncharacterised. Significantly, *cdk5rap2* is one of several centrosomal genes that are mutated in the developmental disorder Primary Microcephaly, where affected individuals have smaller brains than expected for the age- and sex-adjusted mean. Orthologues of CDK5RAP2 in the fruit fly (Centrosomin/Cnn) and in fission yeast (Mod20p) have been well characterised and are known to have important roles in maintaining centrosome structure and in regulating microtubule nucleation. CDK5RAP2 shares two evolutionarily conserved domains with Cnn, known as CNN motif 1 and 2. Using the chicken B-cell line, DT40, I have used gene-targeting methods to disrupt both of these domains in CDK5RAP2. This revealed a function for CDK5RAP2 in attaching centrosomes to mitotic spindle poles. Centrosome attachment to spindle poles is mediated by a binding partner of CDK5RAP2, AKAP450. AKAP450 also localises to centrosomes and provides anchorage sites for spindle poles in the centrosome. Disruption of the CNN1 and CNN2 domains of CDK5RAP2 causes mislocalisation of AKAP450 from the centrosome and detachment of centrosomes from spindle poles. My studies in DT40 and in human cell lines revealed that CDK5RAP2 and AKAP450 also cooperate during interphase to maintain the two centrioles in the centrosome as a pair. In addition to a structural role in the centrosome, I also find that CNN motif 1 of CDK5RAP2 plays a role in the cellular response to DNA damage. In the absence of CNN motif 1, cells no longer efficiently arrest the cell cycle in response to damage. Centrosome-mediated mitotic spindle alignment and the DNA damage response have both been implicated in microcephaly. Therefore, defects in these functions of CDK5RAP2 may explain how mutations in *cdk5rap2* may lead to microcephaly.

Abbreviations

APC/C	Anaphase Promoting Complex/Cyclosome
BFA	Brefeldin A
bp	basepair
Cdk	Cyclin-dependent kinase
DIC	Differential Interference Contrast
DMSO	Dimethyl Sulphoxide
DTT	Dithiothreitol
ECM	Extracellular Matrix
eMTOC	Equatorial Microtubule Organising Centre
EDTA	Ethylenediamine Tetraacetic Acid
EGTA	Ethylene Glycol Tetraacetic Acid
EST	Expressed Sequence Tag
EtBr	Ethidium Bromide
FBS	Foetal Bovine Serum
FKBP	FK506 Binding Protein
FRAP	Fluorescence Recovery After Photobleaching
GFP	Green Fluorescent Protein
GSC	Germline Stem Cell
γ -TuRC	γ -Tubulin Ring Complex
γ -TuSC	γ -Tubulin Small Complex
HEPES	4-(2-Hydroxyethyl)-1-Piperazineethane Sulphonic acid
hp	Hairpin
HR	Homologous Recombination
HRP	Horse Radish Peroxidase
HU	Hydroxyurea
IFT	Intraflagellar Transport
iMTOC	Interphase Microtubule Organising Centre
INM	Interkinetic Nuclear Migration
IP	Immunoprecipitation
IR	Ionising Radiation
kb	kilobases

kDa	kilodaltons
MAP	Microtubule Associated Protein
MBP	Maltose-Binding Protein
MCC	Mitotic Checkpoint Complex
MCPH	Microcephaly
MOPD II	Majewski Osteodysplastic Primordial Dwarfism type II
MRI	Magnetic Resonance Imaging
MTOC	Microtubule Organising Centre
MW	Molecular Weight
NA	Numerical Aperture
NEBD	Nuclear Envelope Break Down
NHEJ	Non-Homologous End Joining
NS	Neural Stem cell
NZ	Nocodazole
PACT	Pericentrin and AKAP450 Centrosome Targeting domain
PBS	Phosphate Buffered Saline
PCC	Premature Chromosome Condensation
PCM	Pericentriolar Material
PCR	Polymerase Chain Reaction
Pel	Pellet
PHH3	Phosphorylated serine 10 on Histone H3
PIPES	Piperazine-N,N'-bis (2-Ethanesulphonic acid)
RNAi	RNA interference
ROI	Region Of Interest
RT	Room Temperature
SAC	Spindle Assembly Checkpoint
SDS	Sodium Dodecyl Sulphate
shRNA	Short hairpin RNA
siRNA	Silencing RNA
SN	Supernatant
SPB	Spindle Pole Body
STD	Standard Deviation
TAP	Tandem Affinity Purification

TBS	Tris Buffered Saline
TEM	Transmission Electron Microscopy
wb	Western blot
WCE	Whole Cell Extract
wt	Wild type

Chapter 1: Introduction

There exists an enormous variety in cell shape and size. The architecture of a cell is determined by the cytoskeleton. As the name infers, the cytoskeleton provides the framework in the cell to which other cellular components are anchored and/or transported. It consists of a fibrous network extending throughout the cytoplasm and is made up of microtubules, actin and intermediate filaments. The cytoskeleton must be rigid enough to provide mechanical support for a cell but also dynamic enough to be able to respond to its environment. Perhaps one of the most dramatic alterations in the cytoskeleton occurs during cell division. During this time, the cytoskeleton completely rearranges in order to build the microtubule-based mitotic spindle. A robust mitotic spindle is necessary to accurately separate duplicated chromosomes into two new daughter cells and maintain genomic fidelity.

This thesis focuses on the study of the vertebrate centrosome – the major organiser of the microtubule network in animal cells. The centrosome cycle is intricately linked to the cell cycle by a series of kinase and protease activities and, therefore, it is difficult to discuss the centrosome without placing its function in the context of the cell cycle. In this introduction I shall begin by summarising the cell cycle and defining the major events that occur. I shall then go on to introduce the microtubule cytoskeleton and how it is organised before discussing microtubule organising centres, and, in detail, the centrosome. The centrosome is implicated in the rare congenital abnormality Primary Microcephaly ('small brain') and I shall introduce what is known so far of some of the centrosomal proteins implicated in this disorder. One such centrosomal protein is CDK5RAP2. At the start of this thesis work, CDK5RAP2 was uncharacterised in vertebrate cells. The study of this protein is the objective of this thesis and thus, finally, I shall introduce what is known of the potential functions of this protein from lower organisms, including the fission yeast, *Schizosaccharomyces pombe* and the fruit fly, *Drosophila melanogaster*.

1.1 The cell cycle

The cell cycle is the series of events that occur in a cell, culminating in the generation of two new daughter cells from one single mother cell. It consists of a series of discrete phases that must occur in a defined order. The transitions between these phases are tightly regulated in order to generate two genetically identical daughter cells. During the cell cycle, a cell must grow in size and replicate its DNA, such that the daughter cells can each inherit one copy of DNA. The consequences of defects in the cell cycle are genetic mutations or aneuploidy – the gain or loss of chromosomes. Aneuploidy can have serious consequences for human health – potentially leading to cancer or congenital abnormalities, such as Down's syndrome.

1.1.1 Phases of the cell cycle

The cell cycle in animal cells consists of four consecutive phases: G1, S, G2 and Mitosis (M). G1, S and G2 constitute interphase. Mitosis constitutes nuclear division and cytokinesis. G1 and G2 are 'gap' phases – periods of growth in the cell cycle. In S-phase, cells replicate their DNA to generate two copies of each chromosome, the so-called sister chromatids, which remain closely associated until late mitosis. Mitosis is the period of the cell cycle when the cell condenses, aligns and separates sister chromatids in such a way that each new daughter cell will inherit one complement of DNA. Alignment of sister chromatids and subsequent separation into the two daughter cells depends on the microtubule cytoskeleton. Microtubules are required to build a symmetrical, bipolar spindle and to align the DNA in the centre of this spindle, such that it can be partitioned equally into the two daughter cells. Faithful transmission of genetic information relies upon a robust and accurate mitosis. Mitosis itself is divided into discrete phases. This classification is based on the changes that can be observed when watching cells divide under the light microscope. First is prophase when chromosomes start to condense and resolve, that is chromosomes separate from one another (but sister chromatids remain paired). During late prophase, the nuclear envelope breaks down (NEBD) and microtubules begin to capture the condensed chromosomes. Microtubules need to be extremely dynamic at this point in order to "search and capture" the chromosomes and

incorporate them into the bipolar spindle (Hayden et al., 1990; Rieder and Alexander, 1990). The period of chromosome capture by microtubules constitutes prometaphase. Microtubules capture the chromosomes at the kinetochore, a proteinaceous complex that assembles on centromeric DNA (reviewed in (Maiato et al., 2004a)). Centromeres consist of highly repetitive DNA sequences that assemble into specialised higher order structures and persist in chromosomes throughout the cell cycle. Once a microtubule has captured a kinetochore it becomes less dynamic as the plus end of the microtubule is stabilised by interaction with proteins at the kinetochore ((Hayden et al., 1990; Mitchison et al., 1986) and reviewed in (Maiato et al., 2004a)). Captured chromosomes are brought to the equatorial plate where they are aligned between the two poles of the mitotic spindle. Importantly, microtubules attached to kinetochores are still able to grow and shrink over small distances at their plus ends to enable the alignment of chromosomes (Mitchison et al., 1986). During metaphase, all chromosomes are aligned at the plate. The transition from metaphase into anaphase occurs only when all chromosomes are aligned and attached to microtubules. In anaphase, the sister chromatids are separated and pulled apart by spindle microtubules. The spindle continues to elongate throughout anaphase and, during telophase, chromosomes are released from the microtubules and the nuclear envelope reforms around the decondensing, separated DNA. Microtubules are released from the mitotic spindle and, during cytokinesis, released microtubules direct the formation of an actomyosin contractile ring between the two daughter cells, which contracts to form a cleavage furrow. As the cleavage furrow continues to ingress, a structure known as the midbody is formed which is physically cleaved during the process of abscission (reviewed in (Barr and Gruneberg, 2007)). In this way, two genetically identical daughter cells are created.

1.1.2 Control of the cell cycle by Cyclin-dependent kinases

Transitions from one stage to the next throughout the cell cycle must be tightly controlled such that one phase of the cell cycle is completed before the next begins. For example, DNA replication must be completed before a cell enters mitosis and tries to segregate sister chromatids in anaphase. Transitions through the cell cycle are regulated by Cyclin-dependent kinases (Cdks). As their name suggests, these kinases must be associated with a cyclin to be active. The exception to this is Cdk5, which is

activated independently of cyclin association (Ching et al., 2000). Cyclins were first discovered in sea urchin eggs and named as such due to the cyclical nature of their synthesis and destruction (Evans et al., 1983). We now know that there are multiple cyclins present in cells, each regulating different cellular transitions.

1.1.2.1 G1 to S

Transition from G1 into S-phase is marked by the start of DNA replication (reviewed in (Sherr, 1993)). A peak of cyclin E/Cdk2 activity at the G1/S transition triggers initiation of DNA replication. Cyclin E is degraded shortly after this transition and Cdk2 is released to associate with cyclin A. Cyclin A/Cdk2 activity remains high throughout S-phase, up until the G2/M transition (Pines and Hunter, 1991).

1.1.2.2 G2 to M

Cdk2 plays a role in coordinating entry into mitosis, by regulating the activity of the master regulator of mitotic entry, Cdk1 (Mitra and Enders, 2004). Cdk1 phosphorylates a plethora of substrates to coordinate entry into mitosis by regulating such processes as chromosome condensation, NEBD and mitotic spindle assembly. Maximal activation of Cdk1 kinase activity requires both association with cyclin B and removal of inhibitory phosphorylations (reviewed in (Ohi and Gould, 1999)). Cdk1 is maintained in an inactive state in G2 by two inhibitory phosphorylations on threonine 14 and tyrosine 15. Cdc25 phosphatases (in particular cdc25B and C) are responsible for the removal of inhibitory phosphorylations on Cdk1. Cdk1 itself can phosphorylate and thus activate cdc25, leading to the generation of a positive feedback loop. Using a cyclin B/Cdk1 biosensor, Gavet and Pines were able to definitively show that activation of cyclin B/Cdk1 first occurs in the cytoplasm and is rapidly followed by its nuclear import (Gavet and Pines, 2010a; Gavet and Pines, 2010b). The authors were also able to show that activation of cyclin B/Cdk1 occurs gradually and that different levels of kinase activity correlated with different events occurring in the cell – for example, chromosome condensation occurring before NEBD (Gavet and Pines, 2010b).

1.1.3 Quality control of the cell cycle

To ensure faithful transmission of genetic material from mother to daughter, the cell must monitor each phase of the cycle for any errors. Moreover, the cell must respond to errors by arresting the cell cycle until such errors can be corrected, or, if correction is not possible, by committing the cell to programmed cell death. This quality control of the cell cycle is monitored by checkpoints that the cell must satisfy in order to progress through the cycle.

The aim of mitosis is to biorient sister chromatids in such a way that the kinetochore of each sister chromatid in a pair is attached to microtubules emanating from opposite poles of the bipolar spindle. This ensures that during anaphase, sister chromatids are pulled towards opposite poles and each daughter cell will inherit an identical copy of DNA. In mitosis, the major checkpoint is the Spinde Assembly Checkpoint (SAC). The SAC is active throughout prometaphase and metaphase and monitors the progress of chromosome alignment. The SAC generates a “wait anaphase” signal to ensure that all chromosomes are aligned in this way before anaphase starts (Figure 1.1). Unattached kinetochores maintain the SAC in an active state. Laser ablation of the last unattached kinetochore in rat kangaroo cells demonstrated that a single unattached kinetochore is sufficient to maintain an active SAC (Rieder et al., 1995).

1.1.3.1 Protein components of the SAC

Genetic screens in yeast uncovered many of the proteins that constitute the SAC and these proteins were named, appropriately, mad (mitotic arrest deficient) and bub (budding uninhibited by benzamidazoles) (reviewed in (Malmanche et al., 2006)). These proteins are conserved in higher eukaryotes, with the exception of the kinase, BubR1, which contains domains similar to both yeast bub1 and mad3. Mad and bub proteins accumulate on unattached kinetochores but there is still some debate as to the precise molecular mechanism(s) of how these proteins maintain an active SAC. What is agreed is that four proteins (mad2, BubR1, bub3 and cdc20) assemble a mitotic checkpoint complex (MCC) at kinetochores that is then active both at kinetochores and in the cytoplasm (Figure 1.1 and reviewed in (Maresca and Salmon; Nezi and Musacchio, 2009)). Cdc20 is required for substrate recognition by the Anaphase Promoting Complex/Cyclosome (APC/C). Sequestration of cdc20 by the MCC

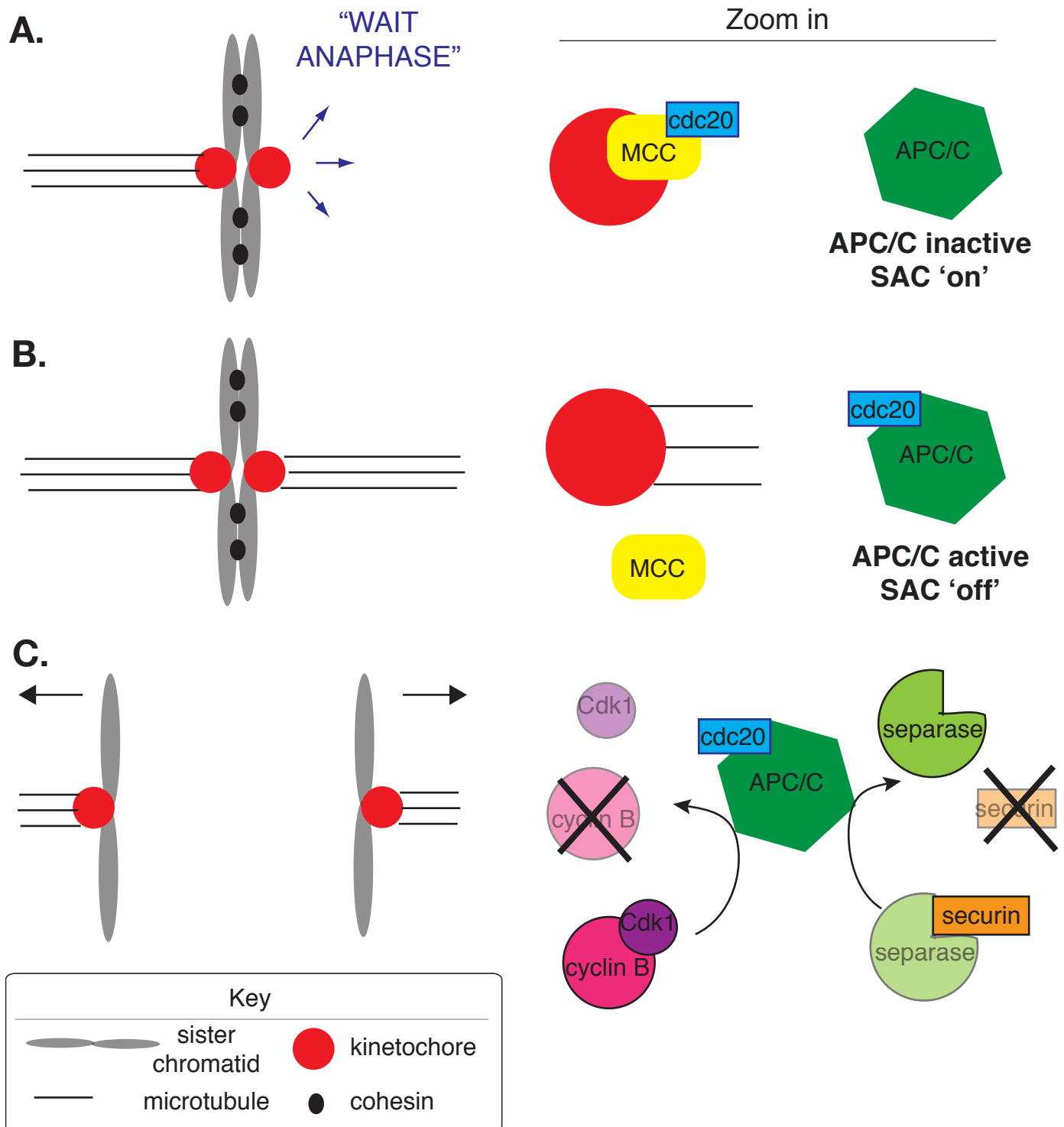


Figure 1.1 The Spindle Assembly Checkpoint. **A.** During prometaphase and metaphase, unattached kinetochores generate a “wait anaphase” signal (SAC on). In part, this is mediated by the accumulation of MCC proteins at unattached kinetochores. The MCC inhibits association of cdc20 with APC/C. Therefore APC/C is inactive. **B.** As the last kinetochore is captured, the SAC is switched off. Cdc20 can now associate with the APC/C and the APC/C becomes active. **C.** Activated APC/C targets cyclin B for degradation, therefore Cdk1 is no longer active and metaphase ends. APC/C also targets securin. Securin degradation activates separase which cleaves the cohesin “glue” between sister chromatids and allows sister chromatids to be pulled apart by microtubules in anaphase.

prevents activation of APC/C and entry into anaphase. Only once the SAC is satisfied will cdc20 be released to associate with the APC/C.

1.1.3.2 The tension versus attachment debate

The biggest question in the SAC field is what does the SAC actually monitor? One possibility is that the SAC only monitors microtubule attachment to kinetochores. The second is that the SAC only monitors the tension generated between sister chromatids by the biorientation of kinetochores between the poles of the bipolar spindle. The latter argument is further complicated by the fact that tension itself stabilises microtubule attachment and that tension can only be generated by microtubule attachment to both kinetochores on paired sister chromatids (reviewed in both (Nezi and Musacchio, 2009) and (Maresca and Salmon)). While evidence exists to support and contradict both sides, a new model has recently been proposed that may satisfy both those against and in favour of the tension hypothesis. Two recent papers have analysed a phenomenon called “intra-kinetochore stretch”, where the kinetochores themselves stretch upon attachment of microtubules (Maresca and Salmon, 2009; Uchida et al., 2009). Both papers found, in different cells lines (*Drosophila* S2 cells and human HeLa cells), that stretching of the kinetochore correlated with inactivation of the SAC. Future work in this area should hopefully provide a unifying model for how the SAC is monitored and inactivated.

1.1.3.3 Inactivation of the SAC and mitotic exit

The metaphase to anaphase transition and thus exit from mitosis is regulated by the coordinated proteolysis of specific proteins. Inactivation of the SAC permits the activation of the APC/C. The APC/C is an E3 ubiquitin protein ligase that targets proteins for degradation by the 26S proteasome (reviewed in (Acquaviva and Pines, 2006)). The APC/C targets several key regulators of cell cycle progression for proteolysis. One such target is cyclin B (Glotzer et al., 1991). Degradation of cyclin B marks the end of Cdk1 activity and the transition from metaphase into anaphase. A second APC/C target is securin, an inhibitor of the protease separase (Hornig et al., 2002). Separase cleaves the Scc1 subunit of the complex, cohesin, which is deposited onto sister chromatids during DNA replication and maintains them as a pair (Uhlmann and Nasmyth, 1998). Cleavage of Scc1 by separase allows cohesin to be removed

from sister chromatids, thus chromatids can separate and the cell can progress from metaphase into anaphase (Figure 1.1 and (Hauf et al., 2001; Uhlmann et al., 1999)).

As I have alluded to throughout this section, many stages of mitosis depend on the microtubule cytoskeleton. Dynamic microtubules are required to capture kinetochores on sister chromatids and align them on the equatorial plate. Microtubules are implicated in the SAC and required to physically separate the sister chromatids once a cell transitions from metaphase into anaphase. Therefore, the microtubule cytoskeleton must be highly regulated throughout mitosis in order to coordinate spindle assembly. The next section will introduce these crucial polymers and discuss how their dynamics and stability are regulated.

1.2 The Microtubule Cytoskeleton

1.2.1 Microtubule structure

Microtubules are hollow filaments assembled by the dynamic polymerisation of α - and β -tubulin heterodimers (Figure 1.2). In mammalian cells, the microtubule filament is made up of 13 protofilaments that associate laterally to form a closed cylinder that is 24 nm in diameter (reviewed in (Conde and Caceres, 2009)). Microtubules have an intrinsic polarity, with distinct plus and minus ends. This is inherent in the way that the tubulin heterodimers assemble: the β -tubulin subunit is exposed at the plus end and the α -tubulin subunit is exposed at the minus end (Figure 1.2A).

1.2.2 Microtubule dynamics

Microtubules are dynamic polymers. Both α - and β -tubulin are GTP-binding proteins and polymerisation of tubulin requires that both subunits are GTP-bound. *In vitro*, microtubules exhibit dynamic instability, where an individual microtubule can switch rapidly between growing and shrinking phases ((Mitchison and Kirschner, 1984a); Figure 1.2). *In vivo*, dynamic instability of microtubules is thought to be the basis of a “search and capture” mechanism in mitosis by which microtubules capture chromosomes ((Hayden et al., 1990; Rieder and Alexander, 1990); and reviewed in (O'Connell and Khodjakov, 2007)). “Search and capture” allows microtubules to probe the cytoplasm for condensed chromosomes and bring them to the equatorial plate. Dynamic instability is dependent on the GTP-binding capacity of the tubulin heterodimers. When a new tubulin dimer is added at the plus end, the α -tubulin subunit makes contact with the previously added β -tubulin subunit in the adjacent heterodimer. This contact stimulates GTP hydrolysis by the β -tubulin subunit. GTP bound to α -tubulin is stable and does not readily hydrolyse (reviewed in (Conde and Caceres, 2009; Howard and Hyman, 2009)). GTP hydrolysis in this manner ensures that there is usually a single GTP-tubulin layer at the plus end of the microtubule, known as a “GTP-cap”. GTP-tubulin has a linear conformation. In contrast, GDP-bound tubulin has a ‘kinked’ conformation. Therefore, if the GTP-cap is lost, GDP-bound tubulin at the plus end forces polymerised tubulin to adopt a ‘curved’

conformation (see Figure 1.2B, right hand side; reviewed in (Howard and Hyman, 2009)). This curvature generates tension at the plus end of microtubules and promotes microtubule depolymerisation, known as catastrophe. This can be prevented by the addition of a GTP-bound heterodimer, known as rescue. Addition of a GTP-cap in this way maintains the microtubule plus end in a linear conformation and therefore reduced the likelihood of depolymerisation. Due to the polarity of microtubules, polymerisation/depolymerisation events are faster at the plus end than the minus end.

In addition to dynamic instability, microtubules also exhibit treadmilling behaviour. In treadmilling, microtubules move uni-directionally by polymerisation at their plus end and depolymerisation at their minus end ((Margolis and Wilson, 1978) and reviewed in (Galjart, 2005; Waterman-Storer and Salmon, 1997); see Figure 1.2C). Treadmilling may be required to generate the lateral organisation of microtubules that is observed in columnar epithelial cells, such as those in the cochlea or kidney (see Section 1.2.3.3). In addition, treadmilling may be the underlying mechanism in generating 'poleward flux' of microtubules in mitotic spindles (see Section 1.3.2 and (Mitchison, 1989)).

The study of microtubules in cells has been aided by the use of pharmacological inhibitors. Two such inhibitors are Taxol and nocodazole. Taxol binds to the inside of microtubules and stabilises the polymer, thus preventing microtubule depolymerisation (Amos and Lowe, 1999; Nogales et al., 1995). Nocodazole is a derivative of benzimidazole and has the opposite mode of action to Taxol in that it promotes microtubule polymer disassembly. How nocodazole promotes depolymerisation is still not fully understood. While high doses of nocodazole and Taxol promote the effects described, lower doses inhibit the dynamic instability of microtubules (Jordan et al., 1993; Vasquez et al., 1997). Therefore, by varying the concentrations of inhibitors used, it is possible to probe different aspects of microtubule behaviour.

Although purified tubulin undergoes dynamic instability *in vitro*, microtubule dynamics in cells are controlled by a large number of proteins. These may be present in Microtubule Organising Centres (MTOCs) or on the microtubules themselves (hence they are known as Microtubule-Associated Proteins, or MAPs).

1.2.3 Microtubule organising centres (MTOCs)

The definition of an MTOC is a morphologically distinguishable domain of the cytoplasm whose significance depends on its quantitative capacity to nucleate microtubules (reviewed in (Archer and Solomon, 1994)). Microtubule nucleation can occur by self-assembly but such structures are inherently unstable (Murphy et al., 1977). The major MTOC in most animal cells is the centrosome. The primary MTOC in yeast is the Spinde-Pole Body (SPB). The high concentration of γ -tubulin at the centrosome and SPB defines these organelles as MTOCs.

1.2.3.1 The centrosome

The centrosome is a non-membranous organelle consisting of a pair of orthogonally arranged centrioles, surrounded by a proteinaceous matrix, known as the Pericentriolar Material, or PCM (Figure 1.3). Centrioles are microtubule-based structures consisting of nine triplet microtubules organised to form a cylinder (see inset in Figure 1.3). Centriolar microtubules are highly glutamylated and this reflects the stable nature of the centriolar microtubules, as compared to the highly dynamic microtubule cytoskeleton (Bobinnec et al., 1998b). Since the study of the centrosome constitutes the bulk of this thesis, an in-depth introduction is given in Section 1.3.

1.2.3.2 The SPB

The SPB in yeast is a proteinaceous complex embedded in the nuclear membrane. It does not contain centrioles. Although structurally quite different to the animal centrosome, the SPB shares conserved mechanisms of duplication and microtubule nucleation, making yeast a useful organism for understanding the molecular mechanisms involved in centrosome function in higher eukaryotes.

1.2.3.3 Other MTOCs

In addition to the centrosome and SPB, other MTOCs have been identified (reviewed in (Luders and Stearns, 2007)). Such MTOCs can be present in cells that lack centrosomes. One example is in differentiated muscle cells (known as myotubes) where microtubules are nucleated and organised by the nuclear membrane. Secondary MTOCs can also be present in cells where a centrosome or SPB is present. Three examples of secondary MTOCs are given below.

In animal cells, the Golgi body has been shown to act as an MTOC during interphase (Chabin-Brion et al., 2001; Rios et al., 2004). The Golgi is closely associated with the centrosome and its position and structure are maintained by the microtubule cytoskeleton (Sandoval et al., 1984). Depolymerisation of microtubules leads to the fragmentation of the Golgi body. Golgi-mediated nucleation of microtubules is controversial (Barr and Egerer, 2005) but, if true, represents an exciting new area of research.

In polarised epithelial cells (such as those in the cochlea or kidney) microtubules are organised in parallel arrays, with their minus ends anchored at the apical domain and their plus ends extending to the basal membrane. The majority of these microtubules are not associated with the centrosome. Instead, the minus ends of the microtubules are anchored near the apical membrane by γ -tubulin and a microtubule anchoring protein, ninein (Mogensen et al., 2000). Microtubules may first be nucleated by centrosomes and then move, by treadmilling behaviour, to apical sites (Luders and Stearns, 2007). However, it has not yet been shown whether this is truly the case or if microtubules are nucleated at apical sites directly.

In fission yeast, although the SPB is the major MTOC, there are two additional MTOCs. The first of these is the equatorial MTOC (eMTOC) that is required at the end of mitosis at the cell division site. The eMTOC is thought to provide the initial microtubule array in the two new daughter cells. The interphase MTOC (iMTOC) nucleates microtubules throughout the cytoplasm during interphase (Sawin et al., 2004).

1.2.3.4 Microtubule nucleation by γ -tubulin

Robust microtubule nucleation requires a microtubule nucleating protein and this role is fulfilled by γ -tubulin (Joshi et al., 1992; Oakley and Oakley, 1989). γ -tubulin was first identified in the fungus *Aspergillus nidulans* as a novel member of the tubulin protein family (Oakley and Oakley, 1989). Injection of anti- γ -tubulin antibodies into cells revealed that not only did γ -tubulin localise to centrosomes but that it was also essential for microtubule nucleation (Joshi et al., 1992). There are two main γ -tubulin containing complexes in cells. The smaller of the two is the γ -Tubulin Small Complex (γ -TuSC), which consists of two molecules of γ -tubulin and one molecule each of GCP-2 and -3 (for γ -tubulin Complex Proteins). Electron microscopy

revealed the second complex to be ring-shaped and hence this was designated the γ -Tubulin Ring Complex (γ -TuRC) (reviewed in (Raynaud-Messina and Merdes, 2007)). γ -TuRC contains multiple copies of γ -TuSC and additional proteins including GCP-4, -5 and -6 and NEDD1.

1.2.4 Microtubule-associated proteins (MAPs)

MAPs can be categorised into several classes determined by how they affect microtubule dynamics, structure and organisation. These include proteins that promote microtubule polymerisation and depolymerisation, plus end binding proteins, and microtubule motor proteins. Examples of each of these categories are given below.

1.2.4.1 Microtubule polymerases

Microtubule polymerising proteins promote the growth and elongation of microtubules. One example is XMAP215. XMAP215 was first purified from *Xenopus laevis* oocytes as a protein required for microtubule plus end elongation (Gard and Kirschner, 1987). More recent characterisation of this protein showed that XMAP215 tracks the plus ends of microtubules and acts as a microtubule polymerase, catalysing the addition of tubulin subunits (Brouhard et al., 2008). XMAP215 has homologues in human, known as ch-Tog (for colonic and hepatic Tumour overexpressed gene), and in *Drosophila*, known as Msps (Minispindles). Both homologues also have important roles in regulating microtubule dynamics ((Charrasse et al., 1998; Cullen and Ohkura, 2001) and see appendix for (Barr and Gergely, 2008)).

1.2.4.2 Microtubule depolymerases

In contrast to promoting microtubule polymerisation, proteins can also promote the depolymerisation of microtubules. A good example of such a MAP is MCAK (for Mitotic Centromere-Associated Kinesin). MCAK is capable of depolymerising microtubules both *in vivo* (when overexpressed) and *in vitro* (Maney et al., 2001). It induces depolymerisation by binding to and stabilising the curved conformation of the microtubule protofilaments (reviewed in (Howard and Hyman, 2007) and see Figure

1.2B). MCAK is a member of the kinesin family of microtubule motor proteins and therefore uses the energy generated by ATP hydrolysis to remove tubulin dimers from microtubules (see Section 1.2.4.4).

1.2.4.3 Plus end binding proteins

Plus end binding proteins, such as Eb1 (End-binding protein 1) and its binding partner APC (Adenomatous Polyposis Coli), track the plus ends of microtubules *in vivo* (Nakamura et al., 2001). *In vitro* experiments have suggested that Eb1 promotes sheet closure of microtubules (see ‘Growing microtubule’ in Figure 1.2B) at the plus end and thus can either stabilise the growing end of the microtubule or promote catastrophe by eliminating stressed microtubule lattices (i.e. lattices that do not contain 13 protofilaments) (Vitre et al., 2008).

1.2.4.4 Microtubule motor proteins

There are two large families of microtubule motors – dynein and kinesins. Both have ATPase domains and use the energy generated from ATP hydrolysis to propel themselves along microtubules (reviewed in (Hirokawa et al., 1998) and (Kardon and Vale, 2009)). Dynein moves towards the minus ends of microtubules, while kinesins (with the exception of kinesin 14 family members) move towards the plus ends. Dynein and kinesins not only mediate the transport of cargo along microtubules but also participate in microtubule organisation. For example, the kinesin 13 family member, MCAK, does not walk along microtubules, like other kinesin family members, but depolymerises microtubules from their plus ends (see Section 1.2.4.2). Dynein is also essential for microtubule and spindle organisation. All of the cytoplasmic-mediated minus end microtubule transport and microtubule-organising functions in vertebrate cells are carried out by a single dynein, cytoplasmic dynein (reviewed in (Kardon and Vale, 2009)). Cytoplasmic dynein is a large multisubunit complex. It consists of a homodimer of Dynein Heavy Chains (DHC), which contain the ATPase motor activity and the microtubule binding domains plus a long, slender tail domain that mediates homodimerisation and generates the ‘power stroke’ required for dynein movement along microtubules (Shima et al., 2006). Non-catalytic subunits are anchored onto the DHC dimer in the tail domain and these include: dynein intermediate chain (IC), dynein Light Intermediate Chain (LIC), dynein Light Chain 8 (LC8), LC7 and TCTEX-1. Diversity in cytoplasmic dynein function and cargo is

bestowed by interaction with adaptor proteins. One essential adaptor for dynein is Dynactin (for ‘dynein activator’). Dynactin itself is a large multiprotein complex, the largest subunit being p150^{glued}. Dynactin targets dynein to specific cellular locations, increases the processivity of dynein along microtubules and links dynein to its cargo (reviewed in (Kardon and Vale, 2009)).

1.2.5 Microtubules and bipolar spindle assembly

The centrosome nucleates dynamic microtubules during mitosis to allow microtubules to “search and capture” kinetochores and bi-orient chromosomes on the metaphase plate (Kirschner and Mitchison, 1986). Centrosomes are present at both poles of the bipolar spindle and centrosome microtubule nucleation represents a major pathway for mitotic spindle assembly. However, studies on the meiotic cells of females from several animal species have failed to detect centrioles, including *Drosophila* (Endow and Komma, 1997; Theurkauf and Hawley, 1992), *Xenopus* (Heald et al., 1996), mouse (Szollosi et al., 1972) and human (Hertig and Adams, 1967). Moreover, higher plant cells do not contain centrosomes and parthenogenetic development in the fly *Sciara* occurs in the absence of centrosomes (de Saint Phalle and Sullivan, 1998). Therefore, non-centrosomal pathways of spindle assembly must exist in these systems. In fact, there are at least two additional centrosome-independent spindle assembly pathways, discussed below.

1.2.5.1 Chromatin-mediated spindle assembly

DNA-coated beads in *Xenopus* cell-free extracts are capable of nucleating and organising microtubules into a bipolar spindle in the absence of centrosomes (Heald et al., 1996). Microtubules nucleate around chromatin in a Ran-GTP dependent manner (Carazo-Salas et al., 1999; Kalab et al., 1999). Ran is a GTP-binding protein that, in interphase, is required for transport between the nucleus and cytoplasm, through the nuclear pore complex. RCC1 is a chromatin-bound, Ran GDP to GTP exchange factor. Localisation of RCC1 to chromatin generates a gradient of Ran-GTP, such that the concentration of Ran-GTP is high around chromatin and is lower further away. A high Ran-GTP concentration promotes the release of microtubule assembly factors from importins (Nachury et al., 2001). Importins are protein complexes

required for the import of cargo into the nucleus during interphase. However, during mitosis, the nuclear envelope breaks down and thus the importins are not required for this role. Microtubule assembly factors required for chromatin-mediated microtubule assembly include microtubule-crosslinking proteins (e.g. TPX-2; (Gruss et al., 2001)), microtubule-bundling proteins (e.g. HURP; (Koffa et al., 2006)) and microtubule-polymerising proteins (e.g. XMAP215; (Koffa et al., 2006)).

Chromatin assembles microtubules in linear antiparallel arrays that require focussing in order to generate a bipolar spindle. Microtubule focussing is driven by the minus end directed motor protein, dynein, together with its activator, dynactin (Heald et al., 1997) (Gaglio et al., 1997). Dynein/dynactin drives the coalescence of microtubule minus ends into a focussed spindle pole. NuMA (Nuclear Mitotic Apparatus) is also released from importin by high RanGTP (Nachury et al., 2001). NuMA associates with dynein/dynactin and is transported to the spindle pole by their motor activity (Gaglio et al., 1997; Merdes et al., 1996). Immunodepletion in *Xenopus* egg extracts, silencing RNA (siRNA)-mediated depletion in *Drosophila* and human tissue culture cells, antibody interference in cells and egg extracts and gene-targeting in mouse, have all shown a requirement for NuMA, dynein and dynactin in spindle pole focussing and in attaching centrosomes to spindle poles (Gaglio et al., 1997; Goshima et al., 2007; Haren et al., 2009a; Morales-Mulia and Scholey, 2005; Silk et al., 2009). At the spindle pole, NuMA forms a matrix in which coalesced microtubule minus ends are anchored (Haren and Merdes, 2002; Saredi et al., 1996). Both spindle poles and centrosomes have a high concentration of microtubule minus ends and thus the relationship between spindle poles and centrosomes is not fully understood.

Until recently, the relative contribution of the kinetochore versus the chromosome arms for chromatin-mediated spindle assembly in cells was not known. However, careful analysis of cells undergoing mitosis with unreplicated genomes revealed that the kinetochore represents the major site for chromatin-mediated spindle assembly (O'Connell et al., 2009). Thus the kinetochore is not only important for maintaining stable microtubule connections during prometaphase and metaphase (see Section 1.1.1) but also significantly contributes to microtubule growth and spindle assembly.

1.2.5.2 Spindle-mediated microtubule assembly

Another pathway of bipolar spindle assembly has been characterised more recently. This pathway depends on the Augmin complex of proteins (from *Drosophila*), or

HAUS (Homologous to Augmin Subunits) as it is known in mammalian cells (Goshima et al., 2008; Lawo et al., 2009; Uehara et al., 2009). siRNA screens to identify new players in mitotic spindle assembly played a large part in identifying both the human and *Drosophila* complexes (Goshima et al., 2008; Lawo et al., 2009). This complex of proteins regulates γ -tubulin anchoring onto spindle microtubules. This leads to spindle-dependent microtubule nucleation.

1.3 The centrosome

As briefly introduced above, the centrosome is the major MTOC in animal cells. The name “centrosome” was first coined in 1888 by Theodor Boveri, who elegantly termed it the ‘especial organ of cell division’. 100 years later, this ‘especial organ’ is still fascinating scientists in its complexity.

1.3.1 Centrosome structure

The centrosome structure is outlined in Figure 1.3. The two centrioles within the pair differ in age. This difference arises as a consequence of semi-conservative duplication of the centrosomes in S-phase, where each centrosome contains old and new centriolar material (see Section 1.3.3.3). Electron microscopy revealed that the older ‘mother’ centriole is adorned with distal and sub-distal appendages ((Paintrand et al., 1992) and Figure 1.3). The younger ‘daughter’ centriole lacks these appendages but will acquire them in the next cell cycle. Structural differences between the mother and daughter centriole generates an inherent asymmetry within the centrosome. The function of sub-distal and distal appendages is not fully understood. Electron microscopy studies appear to show microtubules anchored specifically to the sub-distal appendages (reviewed in (Bornens, 2002)). The mother centriole is also required for basal body formation and primary cilium outgrowth and this role requires the sub-distal and distal appendages ((Ishikawa et al., 2005) and see Section 1.3.4.1).

While centrioles are able to nucleate microtubules, the vast majority of microtubule nucleation occurs in the PCM (Gould and Borisy, 1977). In electron microscopy studies, the PCM appears as an electron-dense material surrounding the centriolar pair. Proteomic analysis of purified human centrosomes identified over 100 proteins (Andersen et al., 2003). The majority of these are likely to reside in the protein-rich PCM. Centrioles are essential for the assembly of PCM into centrosomes. Loading of cells with anti-glutamylated tubulin causes the loss of centrioles and dispersal of PCM components throughout the cytoplasm (Bobinnec et al., 1998a). One of the key questions in centrosome biology is how the PCM is organised around the centrioles. For example, whether the PCM has a defined structure is a matter for debate. There is some evidence for a ‘Centromatrix’ – an inner core of PCM proteins to which other

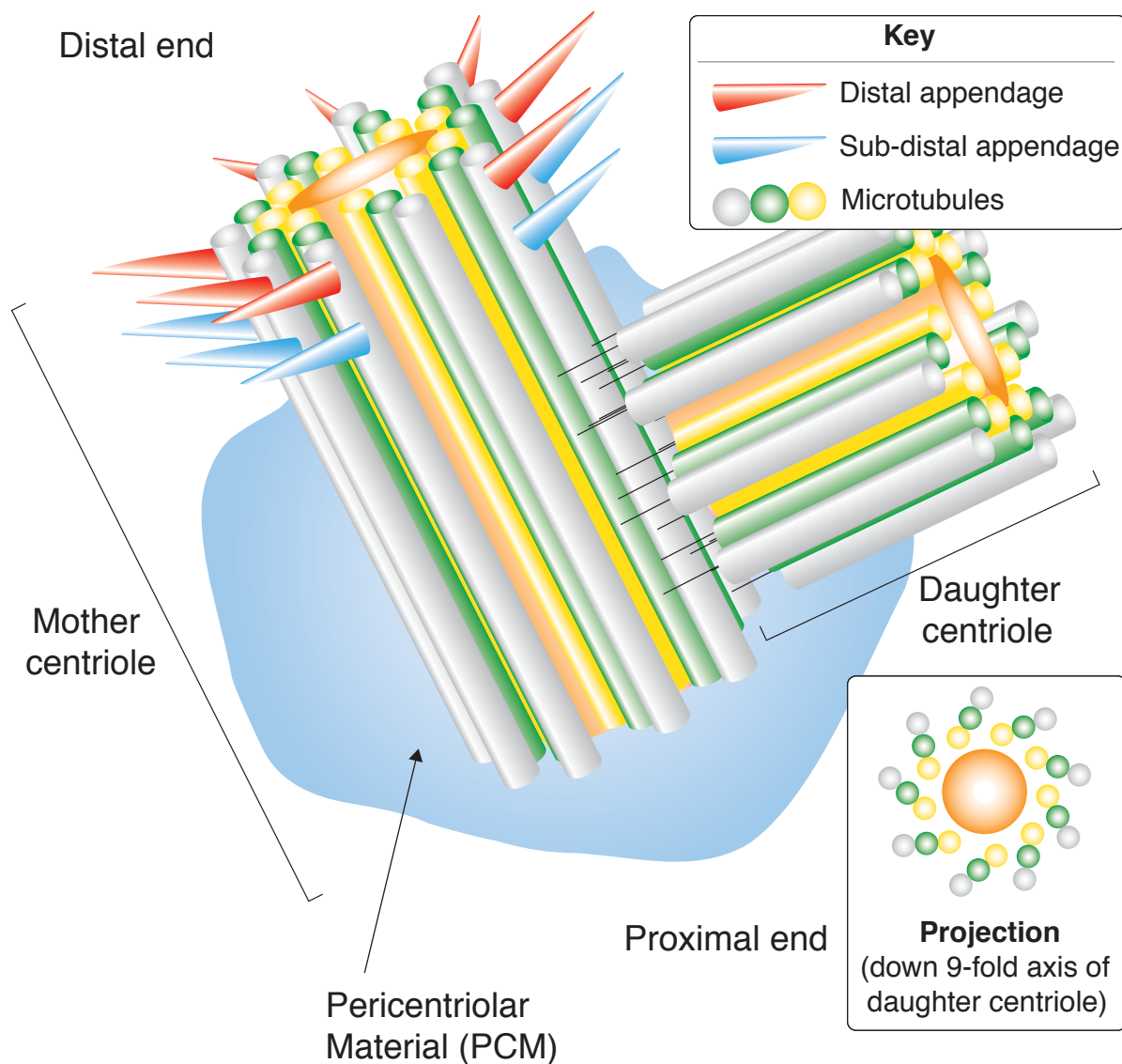


Figure 1.3 The vertebrate centrosome. The centrosome consists of two centrioles oriented perpendicularly to one another. Centrioles are microtubule-based structures with a nine-fold triplet radial symmetry (see inset). The two centrioles differ in age. The older, mother centriole can be distinguished by the presence of distal and sub-distal appendages. The two centrioles are surrounded by a protein-rich matrix, known as the Pericentriolar Material, or PCM. The PCM is the major site for microtubule nucleation. Note that this image represents the centrosome in S or G₂/Mitosis. In G₁, the two centrioles are further apart (see Figure 1.4). (Image is reproduced courtesy of Chris Stubbs).

proteins can anchor (reviewed in (Bornens, 2002)). This was first suggested over 25 years ago when it was found that treatment of purified centrosomes with a high concentration of salt destroyed the tubulin fraction (i.e. the centrioles) but the PCM remained intact (Mitchison and Kirschner, 1984b). Further evidence comes from Fluorescence Recovery After Photobleaching (FRAP) experiments. FRAP showed that GFP- γ -tubulin exists in two pools in the cell – one that is stably associated with centrioles and a second, dynamic pool that constantly exchanges with centrosomes (Khodjakov and Rieder, 1999). Similarly, FRAP studies of the centrosome-targeting domain in *Drosophila* embryos, GFP-PACT (for Pericentrin and AKAP450 Centrosome Targeting) revealed the presence of a stable centrosomal pool of this domain (Martinez-Campos et al., 2004). The PACT domain is conserved in two large, coiled-coil containing centrosomal proteins in humans – Pericentrin and AKAP450 (for A-Kinase Anchoring Protein, 450 kDa) (Gillingham and Munro, 2000). Complexes containing γ -tubulin and pericentrin have been isolated (Dictenberg et al., 1998). Moreover, *in vivo*, deconvolution microscopy revealed that γ -tubulin and pericentrin form a regular lattice structure at the centrosome (Dictenberg et al., 1998). AKAP450 has also been found in pericentrin and γ -tubulin-containing complexes (Takahashi et al., 2002) and AKAP450 has been implicated in the anchoring of multiple enzymes at the centrosome, including Protein Kinase N (PKN), Protein Kinase A (PKA) and Protein phosphatases 1 and 2A (Takahashi et al., 1999). With these data in mind, it seems feasible that at least γ -tubulin, pericentrin and AKAP450 could form part of a centromatrix and thus act as a scaffold in the centrosome. Moreover, many centrosomal proteins contain extensive coiled-coil regions, which can mediate protein-protein interactions, and this could further contribute to a PCM ‘structure’.

How do centrioles organise PCM proteins around them? An attractive model has been suggested in a review by Bornens (Bornens, 2002). He proposes that PCM proteins capable of binding the minus ends of microtubules could bind to the proximal ends of the centrioles. Proteins that can bind along microtubules or to the microtubule polymer (for example MAPs) could bind along the wall of the centrioles. Interactions between proteins bound at different centriolar positions could promote the formation of a matrix around the centrioles. Defining the interactions and molecular complexes that exist in the PCM, and how these complexes interact with centrioles, will help to

define if there is structure to the PCM. If there is a structure (and it seems likely that there is) then the next big question will be how the PCM can reorganise itself to adapt to the changing roles of the centrosome throughout the cell cycle (see Section 1.3.3).

1.3.2 Microtubule organisation by centrosomes throughout the cell cycle

Organisation of microtubules by centrosomes involves both microtubule nucleation and anchoring. The high concentration of γ -tubulin at centrosomes makes them very efficient nucleators of microtubules. Centrosomes nucleate microtubules in both interphase and mitosis yet microtubule dynamics are quite different in these two cell cycle phases. The centrosome must therefore be able to adapt to the different microtubule requirements of the cell. During interphase, the centrosome resides in the centre of the cell, close to the nucleus. Microtubules nucleated by the centrosome persistently grow out into the cytoplasm, leading with their dynamic plus ends. As microtubules near the cell cortex, microtubules undergo dynamic instability over short distances, effectively probing the cell boundary (Komarova et al., 2002). This probing activity by interphase microtubules has been proposed to allow cells to rapidly ‘sense’ changes in the cell boundary and respond quickly (Komarova et al., 2002).

In mitosis, the centrosome plays an important role in the nucleation of microtubules required to form the bipolar spindle. Analysis of microtubule growth on purified centrosomes (Kuriyama and Borisy, 1981) and time-lapse imaging of GFP-Eb1 expressing cells (Piehl et al., 2004), revealed an increase in the centrosomal nucleation of microtubules by up to five times in metaphase, compared with interphase. Moreover, microtubules become more dynamic in mitosis as their rate of catastrophe increases (Belmont et al., 1990). Increases in microtubule number and dynamicity allow mitotic microtubules to efficiently “search and capture” chromosomes and bring them to the metaphase plate (Mitchison and Kirschner, 1984a). Centrosome-nucleated microtubules can also interact with the cell cortex in mitosis. This subset of microtubules is known as the astral microtubules.

Microtubules nucleated by centrosomes are either anchored in the centrosome or can be released into the cytoplasm (Belmont et al., 1990). Proteins required for microtubule anchoring in the centrosome include ninein (Mogensen et al., 2000; Piel

et al., 2000), the TACC proteins (for Transforming Acidic Coiled-coil Containing) (Albee and Wiese, 2008; Lee et al., 2001) and Dynactin (Quintyne et al., 1999; Clark and Meyer, 1999; Waterman-Storer et al., 1995). Time-lapse imaging of microtubule dynamics in *Xenopus* egg extracts revealed that while microtubule release occurs in both interphase and mitosis, it is more frequent in mitosis (Belmont et al., 1990). This is consistent with the observation that microtubules within the mitotic spindle are not all anchored in centrosomes and the minus ends of microtubules can be more than 1 μm away from centrosomes in the spindle poles (Mastronarde et al., 1993). It is also consistent with the observation that the microtubule-severing protein, katanin, is localised in a hollow ring around the PCM in mitosis, suggestive of a microtubule release mechanism after nucleation from the PCM (McNally and Thomas, 1998). During mitosis, the minus ends of microtubules are principally anchored at the spindle pole by NuMA and the combined activities of the minus end directed microtubule motor, dynein and its activator complex, dynactin (Heald et al., 1996; Merdes et al., 1996). Thus dynactin can anchor microtubules both in the centrosome and in the spindle poles. The observation that microtubules in the mitotic spindle undergo 'poleward flux', i.e. movement towards the spindle pole, suggests that microtubule minus ends are not capped within the centrosome (Mitchison, 1989). Therefore, this switch in microtubule anchoring by the centrosome between interphase and mitosis may be required for the formation of a dynamic mitotic spindle.

1.3.3 The Centrosome Cycle

The centrosome cycles synchronously with the cell cycle. This ensures the centrosome is primed to perform its cell cycle functions when required. Figure 1.4 shows a summary of the centrosome cycle. Below I explain the different stages and what is known about their regulation. I have put particular emphasis on those parts that are relevant for the discussion of my data – including centriole disengagement and centrosome maturation.

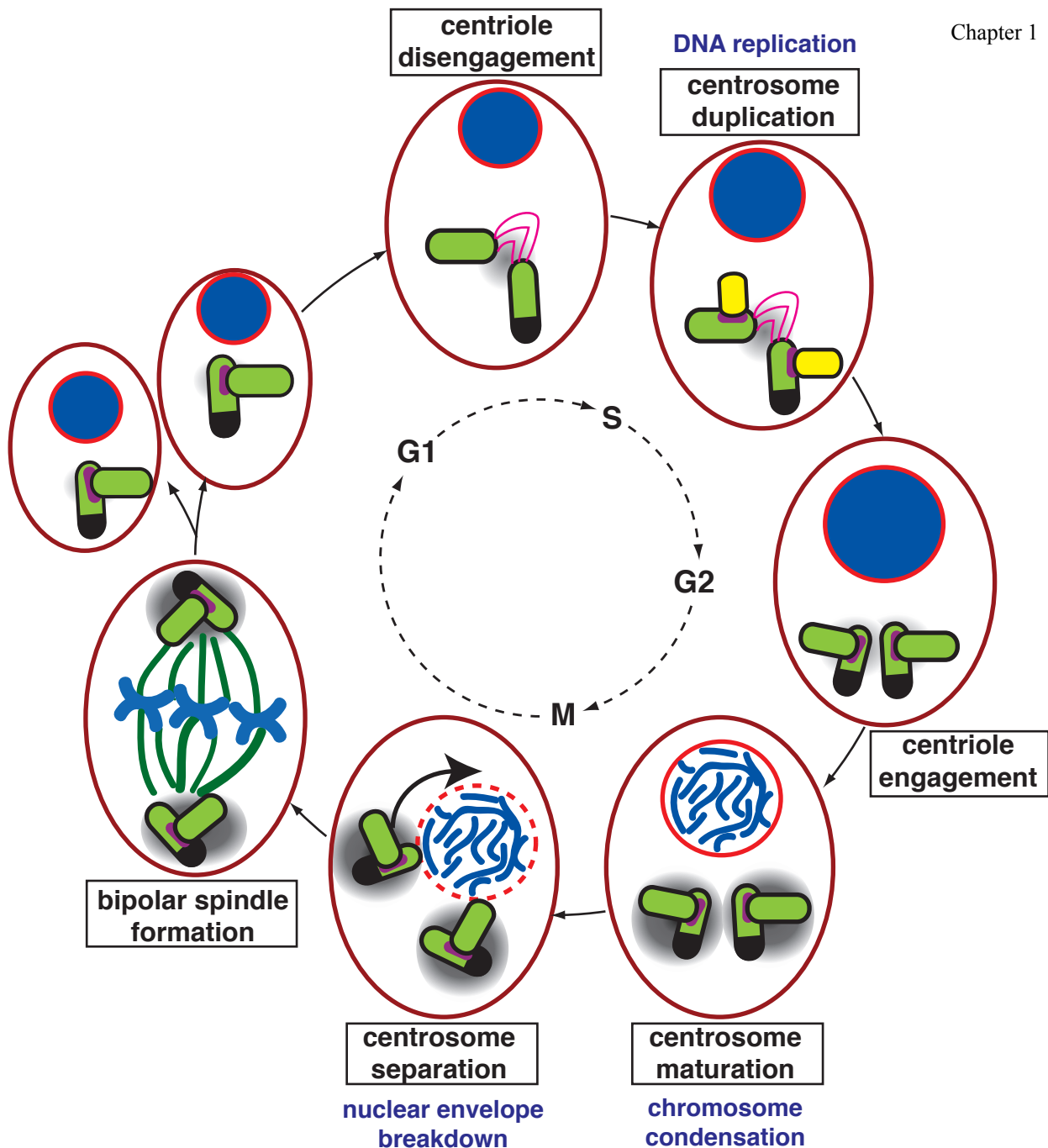


Figure 1.4 The centrosome cycle. The centrosome cycle is coordinated with the cell cycle (inner black circle). Disengagement of centrioles at the end of mitosis licenses centrosome duplication in S-phase. Each centriole nucleates the growth of one procentriole (yellow cylinders). As cells progress from S into G2, the daughter centriole from the previous cell cycle (green centriole) fully matures to become a mother centriole (distinguished by a black cap in the diagram). Duplicated centrosomes mature in the subsequent G2 by recruiting extra protein to the PCM (grey circle). Mature centrosomes separate from one another at the G2/M transition, such that they are ready to form the poles of the bipolar spindle in mitosis. The arrangement of centrosomes in a bipolar manner also ensures that after cytokinesis, each new daughter cell inherits one centrosome. The two centrosomes inherited differ in age: one centrosome contains a mother centriole that was made at least two cell cycles ago, while the other centrosome contains a mother that was made in the previous cell cycle. (Adapted from Barr and Gergely, *Journal of Cell Science*, 2007).

1.3.3.1 Centriole disengagement

In G1, cells possess a single centrosome consisting of two centrioles. The two centrioles are not strictly orthogonal to one another at this stage of the cell cycle and the centrosome is said to be 'disengaged'. Centriole disengagement occurs during anaphase (Piel et al., 2000) and requires the activity of a protease and a kinase. Separase, the protease required for cohesin cleavage and separation of sister chromatids (reviewed in (Nasmyth, 2002)), is also required for centriole disengagement (Tsou and Stearns, 2006a). Using *Xenopus* egg extracts and non-degradable securin, Tsou and colleagues demonstrated that separase activity is essential for centriole disengagement. In addition, the activity of Plk1, a centrosomally-localised kinase, is required and is thought to act upstream of separase activation (Tsou et al., 2009). The identities of separase and Plk1 substrates that mediate centriole disengagement are still not known and represent one of the outstanding questions in centrosome biology.

Centriole disengagement has been proposed to 'license' the centrosome for duplication in the subsequent S-phase (Tsou and Stearns, 2006b). Cell fusion experiments demonstrated that fusion of a G1 and a G2 cell permits duplication of the G1 centrosomes but not those in G2, suggestive of a centrosome-intrinsic block to centrosome reduplication in G2 (Wong and Stearns, 2003). Similarly, engaged centrioles cannot duplicate in interphase *Xenopus* egg extracts (Tsou and Stearns, 2006a). Centriole disengagement in anaphase would release the centrosome-intrinsic block to duplication. A mechanism of centriole engagement ensures that centrosomes cannot reduplicate until they have passed through the cell cycle and is an elegant safeguard implemented by the cell to prevent centrosome overduplication.

1.3.3.2 Centrosome cohesion

Although disengaged, centrioles are maintained as a pair throughout G1 and S phases by centrosome cohesion. Analysis of purified centrosomes by electron microscopy revealed the presence of a fibrous linker between the proximal ends of the two centrioles, the organisation of which is sensitive to Ca^{2+} ions (Figure 1.5A; (Paintrand et al., 1992)). Recent work suggests that this fibrous linker is likely to consist of the proteins c-Nap1 (for centrosomal Nek2-associated protein 1) and rootletin (Mayor et al., 2000; Bahe et al., 2005; Yang et al., 2006). Immunogold electron microscopy revealed rootletin-containing fibres extending from both centrioles and c-Nap1

anchored at the proximal ends of the centriolar pair (see Figure 1.5B). Rootletin localisation is dependent upon c-Nap1 and if the localisation of either protein is disrupted, for example by RNA interference (RNAi) technology or by antibody injection into cells, centrosome cohesion is lost (Figure 1.5C). Additional proteins have been implicated in maintaining centrosome cohesion – for example pericentrin (Jurczyk et al., 2004), the p150^{glued} subunit of dynactin (Quintyne and Schroer, 2002) and Dynamin 2 – a GTPase involved in vesicle trafficking and actin organisation (Thompson et al., 2004). Centrosome cohesion by p150^{glued} appears to be independent of c-Nap1 and indicates that centrosome cohesion may be regulated by several, non-overlapping pathways (Quintyne and Schroer, 2002). The interplay of dynamin-2 and pericentrin with c-Nap1/rootletin had yet to be investigated at the start of this thesis work. An intact microtubule network is also essential for centrosome cohesion (Jean et al., 1999; Meraldi and Nigg, 2001). Depolymerisation of microtubules using nocodazole leads to a loss in centrosome cohesion. Microtubules are thought to maintain a cohesive centrosome by balancing the kinase and phosphatase activities in the PCM (see Section 1.3.3.5 and (Meraldi and Nigg, 2001)). Pericentrin and p150^{glued} have both been implicated in regulating microtubule-centrosome interactions. p150^{glued} can anchor microtubules to centrosomes to generate a radial microtubule array (Quintyne et al., 1999). Pericentrin has been implicated in the organisation of microtubules around centrosomes in *Xenopus* extracts (Doxsey et al., 1994). Therefore, in addition to intercentriolar fibres, centrosome cohesion may also be mediated by maintaining the interaction of centrosomes with microtubules. Further characterisation of the structure of centrosomes will help in defining the mechanics of centrosome cohesion.

1.3.3.3 Centrosome duplication

Centrosome duplication is tightly linked to DNA duplication and occurs during the same (S) phase of the cell cycle (Figure 1.4). In a similar way to DNA duplication, centrosome duplication has been suggested to require the kinase activities of cyclin E/Cdk2 and/or cyclin A/Cdk2 (Lacey et al., 1999; Meraldi et al., 1999). Three substrates of Cdk2 that are implicated in centrosome duplication are nucleophosmin (Okuda et al., 2000), CP110 (Chen et al., 2002) and Mps1 (Kasbek et al., 2007). However, Cdk2 is not essential for centrosome duplication as this function can be

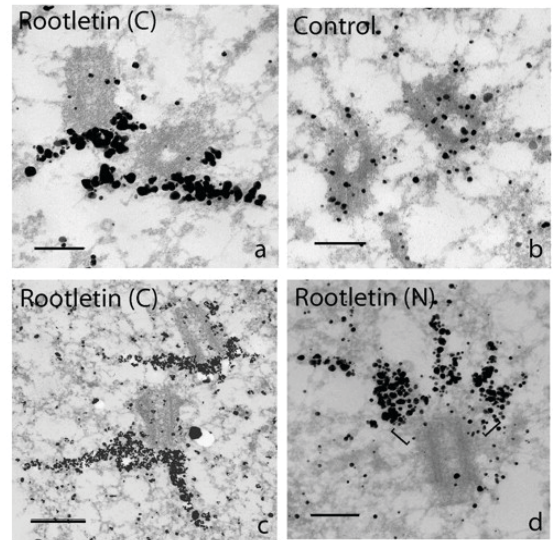
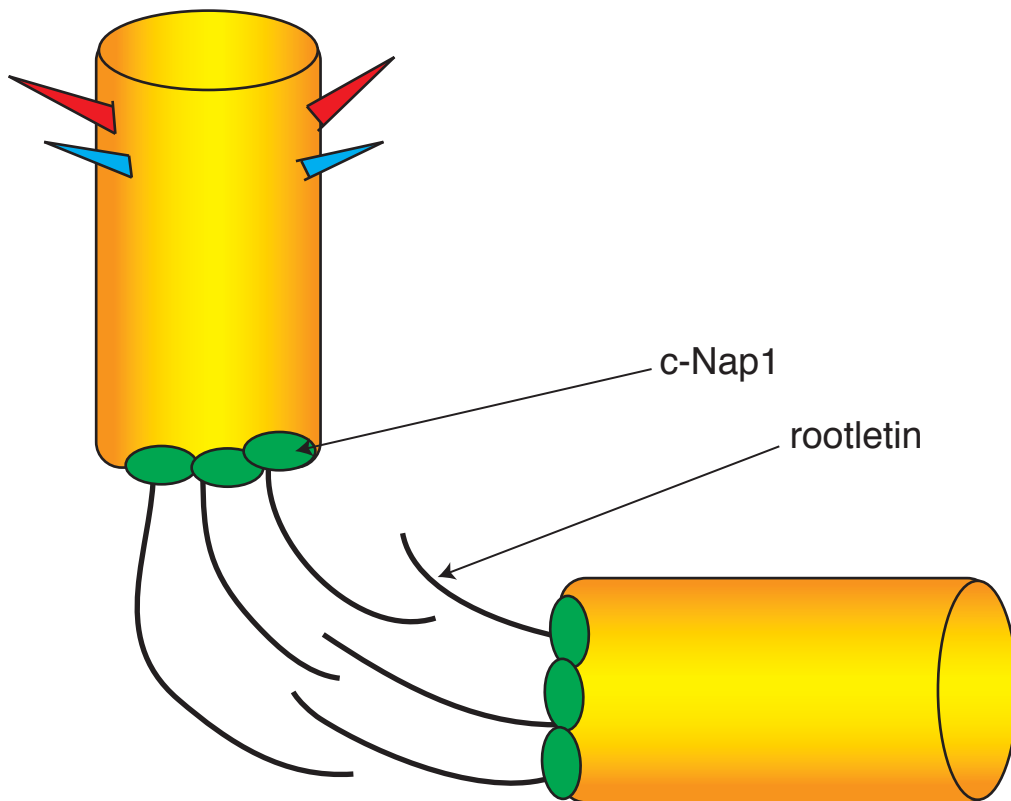
A.**B.****C.**

Figure 1.5 Centrosome cohesion. **A.** Electron microscopy of purified centrosomes revealed a fibrous linker between the two centrioles (small arrows; Paintrand *et al*, 1992). **B.** Using immunogold labelling of rootletin, Bahe *et al* confirmed that rootletin localised to fibres between the two centrioles (Bahe *et al*, 2005). **C.** The prevailing model is that the two centrioles are maintained as a pair in G1 and S phase, in part by the actions of c-Nap1 and rootletin. Rootletin forms fibres between the two centrioles that are proposed to intertwine and thus keep the centriole as a pair. c-Nap1 anchors rootletin to the proximal ends of the two centrioles.

compensated for by Cdk1 kinase activity (Aleem et al., 2005; Duensing et al., 2006; Hochegger et al., 2007). Chicken DT40 cells that lack Cdk2 require the kinase activity of Cdk1 to duplicate centrosomes. The presence of a single Cdk2 allele abrogates the need for Cdk1 in centrosome duplication, reflecting the redundancy of the two kinases in this pathway.

A second kinase, known as Plk4 in mammalian cells, SAK in *Drosophila* and zyg-1 in *Caenorhabditis elegans*, has also been implicated in centrosome duplication (Bettencourt-Dias et al., 2005; Kleylein-Sohn et al., 2007; O'Connell et al., 2001; Peel et al., 2007). Crucially, the substrates of Plk4/SAK activity are still unknown.

Centrosome duplication is semi-conservative. This was elegantly demonstrated over 20 years ago by monitoring tubulin incorporation into centrioles by injection of biotin-labelled tubulin into cells (Kochanski and Borisy, 1990). Only the new daughter centriole incorporated biotin-labelled tubulin. Each parental centriole nucleates the growth of a single procentriole at its proximal end. Procentrioles elongate throughout S-phase and into G2 until they form new daughter centrioles (Figure 1.4). The new daughter centriole is orthogonally aligned to its mother and the centrioles are 'engaged' at this point. Daughter centrioles will only become disengaged from their mothers on passage through anaphase.

1.3.3.4 Centrosome maturation

Centrosome maturation is the process of accumulating extra protein in the PCM during G2. Proteins are recruited to increase the microtubule nucleation capacity of the centrosome in mitosis. This increased nucleation capacity is generated by an increase in the amount of γ -tubulin in the PCM. Up to three times more γ -tubulin is recruited to the PCM during prophase and prometaphase, independently of microtubules (Khodjakov and Rieder, 1999; Piehl et al., 2004). Thus this reflects a centrosome-intrinsic mechanism for γ -tubulin accumulation.

The question then is what is this centrosome-intrinsic mechanism of protein recruitment during G2? The answer seems to lie with centrosome-associated kinases. It has been known for over 20 years that, on entry into mitosis the two centrosomes become highly phosphorylated (Vandre et al., 1984). More recent work has highlighted some of the kinases that are required for centrosome maturation, including CDK11 (Petretti et al., 2006), PAK1 (Zhao et al., 2005), Plk1 (Donaldson et al., 2001;

Lane and Nigg, 1996; Sunkel and Glover, 1988) and Aurora A ((Giet et al., 2002) and see appendix for review in (Barr and Gergely, 2007)). The substrates of some of these kinases are starting to be characterised which gives us some insight into how these kinases can regulate γ -tubulin recruitment. CDK11 and PAK1 are upstream of both Aurora A and Plk1 recruitment to centrosomes. PAK1 can interact with and phosphorylate Aurora A, including the phosphorylation of T288 in the activation loop of Aurora A. Phosphorylation of T288 in Aurora A is required for maximal kinase activity of Aurora A (Littlepage et al., 2002; Zhao et al., 2005; Bischoff et al., 1998; Walter et al., 2000). How Plk1 and Aurora A kinases recruit γ -tubulin to centrosomes is still not completely understood. In *Drosophila* cells, Aurora A binds to and recruits the centrosomal protein Centrosomin (Cnn) to centrosomes in G2. In turn, Cnn can bind to and recruit γ -tubulin to centrosomes (Megraw et al., 1999; Terada et al., 2003; Zhang and Megraw, 2007). Furthermore, Cnn was identified in a siRNA screen in *Drosophila* S2 cells as being essential for centrosome maturation (Dobbelaere et al., 2008). In the same paper, the authors find that Cnn is phosphorylated in a polo-kinase dependent manner. Polo is the fly homologue of human Plk1. It is essential for mitosis and also required for centrosome maturation in flies (Dobbelaere et al., 2008; Donaldson et al., 2001; Logarinho and Sunkel, 1998; Sunkel and Glover, 1988). Phosphorylation of Cnn may play a part in the function of Cnn in centrosome maturation, although this has yet to be characterised. Whatever the precise mechanism, it seems that at least in flies, Cnn plays an important role in centrosome maturation. Cnn has two orthologues in humans – CDK5RAP2 and Myomegalin. Whether these also have a role in centrosome maturation is not known.

In addition to γ -tubulin, Aurora A has also been implicated in the phosphorylation and recruitment of TACC proteins to the centrosome (Barros et al., 2005; Giet et al., 2002; Kinoshita et al., 2005; LeRoy et al., 2007; Peset et al., 2005). *Drosophila* and *Xenopus* have only one TACC protein: D-TACC and Maskin respectively (Gergely et al., 2000b; O'Brien et al., 2005; Peset et al., 2005). Mammals have three TACCs – known as TACC1, 2 and 3 (Gergely et al., 2000a). Of these three, TACC3 has been shown to be phosphorylated and recruited to the centrosome by interaction with Aurora A (Giet et al., 2002; LeRoy et al., 2007). Members of the TACC protein family are enriched in mitotic centrosomes, recruited during centrosome maturation. TACC proteins have been implicated in efficient microtubule growth and anchoring at

centrosomes (Albee and Wiese, 2008; Gergely et al., 2000a; Gergely et al., 2000b; Peset et al., 2005). The functions of the TACC proteins in microtubule growth are likely to be mediated by their interacting partner, the microtubule polymerase ch-TOG/Msps/XMAP215 (Gergely et al., 2003; Peset et al., 2005).

1.3.3.5 Centrosome separation

Centrosome separation is the movement of the two duplicated centrosomes to opposite sides of the nucleus during G2, in preparation to form the poles of the bipolar spindle in mitosis. For centrosome separation to occur, at least two things have to occur. First, centrosome cohesion between the parental centrioles has to be removed/broken. Secondly, the two centrosomes must be physically separated.

Nek2 kinase is involved in removing centrosome cohesion. Overexpression of Nek2 can induce centrosome splitting, and this phenotype is completely dependent on Nek2 kinase activity (Fry et al., 1998b). Nek2 is a cell-cycle regulated centrosomal kinase (Fry et al., 1998b; Fry et al., 1995). Kinase activity of Nek2 reaches a peak at the G2 transition. Protein Phosphatase 1 α (PP1 α) acts as a negative regulator of Nek2 kinase activity (Helps et al., 2000). PP1 α is inhibited at the onset of mitosis by high Cdk1 activity (Puntoni and Villa-Moruzzi, 1997). Thus Nek2 kinase activity can increase as Cdk1 kinase activity increases towards the end of G2. Nek2 phosphorylates both c-Nap1 and rootletin and promotes their displacement from centrosomes (Fry et al., 1998a; Bahe et al., 2005). Loss of the rootletin fibres connecting the parental centrioles allows the two duplicated centrosomes to separate. Intriguingly, the Wnt signalling pathway has been implicated in centrosome separation. The Wnt signalling pathway regulates cell proliferation and gene expression during development. Two downstream components of the Wnt pathway – β -catenin and conductin – localise to centrosomes and appear to be directly involved in the centrosome cohesion pathway (Bahmanyar et al., 2008; Hadjihannas et al., 2010). β -catenin binds to rootletin and is phosphorylated by Nek2 (Hadjihannas et al., 2010). Importantly, phosphorylation of β -catenin is required for Nek2-induced centrosome separation (Bahmanyar et al., 2008). The exact mechanism underlying this requirement for Wnt signalling in Nek2-mediated centrosome separation is still not fully understood. Cdk2 activity has also been implicated in centrosome

separation, in a pathway distinct to that requiring Nek2 (Meraldi and Nigg, 2001), but the mechanism of Cdk2-regulated centrosome separation is still not understood.

Duplicated centrosomes are separated by microtubules. In most animal cells, this occurs before NEBD but can also occur afterwards (Rattner and Berns, 1976; Aubin et al., 1980). One key motor required for centrosome separation is the plus end-directed kinesin, Eg5 (Blangy et al., 1995). Eg5 slides antiparallel interpolar microtubules past each other and in this way can drive apart the two centrosomes (Kapitein et al., 2005). The minus end-directed motor, dynein, is also required for centrosome separation (Vaisberg et al., 1993). These data imply that centrosome separation is driven by the counteracting forces of microtubule motors. In addition, Myosin II, present at the cell cortex, can also play a role in centrosome separation, but only after NEBD (Rosenblatt et al., 2004). Myosin II mediates the interaction of astral microtubules with the cell cortex and therefore mediates centrosome separation by physically attaching centrosomes to the cortex (Rosenblatt et al., 2004).

1.3.4 Are centrosomes essential?

As mentioned previously, the meiotic cells of females from several animal species lack centrosomes. Therefore, while centrosomes can and do organise bipolar spindles when present, they are not essential for this function. This is perhaps not too surprising since centrosome-independent pathways for spindle assembly do exist (see Section 1.2.5). However, the big question is, what happens in cells that normally use centrosomes for spindle assembly when centrosomes are no longer there? Laser ablation of centrosomes in mammalian cells revealed that cells are capable of assembling bipolar spindles and completing mitosis in the absence of centrosomes (Khodjakov et al., 2000). Acentriolar *Drosophila* cell lines exist that are capable of completing repeated rounds of mitosis (Debec et al., 1995). Moreover, adult flies have been generated that lack centrioles altogether (Basto et al., 2006). This shows that in cells with centrosomes, centrosome-independent spindle assembly pathways still exist.

It was suggested from work in *Xenopus* egg extracts that, when present, centrosomes are the dominant sites for spindle assembly, such that if only one centrosome is present, monopolar spindles are generated (Heald et al., 1997). Contrary to this hypothesis is that in *Drosophila* Ganglion Mother Cells (GMCs) in the brain,

centrosomes are present but the cell appears to build a mitotic spindle in a centrosome-independent manner (Bonaccorsi et al., 2000). These conflicting lines of evidence reveal that there is still some confusion as to the relative contributions of centrosome-dependent and -independent pathways in spindle assembly. The likelihood is that the importance of centrosome-mediated spindle assembly varies between organisms and cell type. For example, while *Drosophila* cell lines have been generated that lack centrioles (Debec et al., 1995), it has not been possible to generate acentriolar mammalian somatic cell lines that undergo repeated cell divisions. The reasons for this are uncertain but it may be due to the relative abundance of microtubule assembly factors present in different cell types.

If centrosomes are dispensable for spindle assembly, then what are they required for? In all systems lacking centrosomes, spindles lack astral microtubules (Bonaccorsi et al., 2000; de Saint Phalle and Sullivan, 1998; Khodjakov et al., 2000). Thus it seems that centrosomes are essential to generate astral microtubules. Astral microtubules are required to orient the spindle with respect to the cell cortex, for example in establishing asymmetric cell division. Therefore, centrosomes may be essential in systems requiring asymmetric divisions. In support of this is that in flies lacking centrioles, there is an increase in the number of neuroblasts that divide symmetrically rather than asymmetrically (percentage of symmetric neuroblast divisions: 0% in wild-type, 13.5% in flies lacking centrioles ((Basto et al., 2006)). Astral microtubules are also essential in the syncytial embryos of *Drosophila* and *Sciara* to separate adjacent spindles and prevent nuclei coalescing in the middle of the embryo (de Saint Phalle and Sullivan, 1998; Gergely et al., 2000b). In fact, even though flies can develop to adulthood in the absence of centrosomes, centrosomes are still essential for the rapid mitoses in the syncytial embryo. Additionally, micromanipulation of mammalian cells to physically remove centrosomes suggested a role for centrosomes in the G1/S transition (Hinchcliffe et al., 2001). Karyoplasts lacking centrosomes proceeded through and completed mitosis but arrested in the next cell cycle. Similar results were obtained after laser ablation of centrioles in mitosis (Khodjakov and Rieder, 2001). However, G1 arrest after centrosome removal in these experiments has since been attributed to the additional damage incurred by cells during time-lapse imaging with high intensity blue light (Uetake et al., 2007). Removal/ablation of centrosomes plus additional irradiation with blue light leads to a cumulative stress response in cells and activation of a p53-mediated G1 arrest. p53 is a transcription

factor that has been nicknamed “the guardian of the genome” for its ability to arrest cells in the cell cycle in a checkpoint-dependent manner. These data show that centrosomes are not essential for the G1 to S transition. However, centrosomes are indispensable for primary cilium formation (Basto et al., 2006)(see Section 1.3.4.1). Therefore, while centrosomes contribute to, and can be dominant in, spindle assembly in cells, this does not represent an essential function of this organelle.

1.3.4.1 The centrosome in primary cilium formation

The mother centriole is required to form the basal body for the generation of cilia and flagella. Cilia and flagella consist of a basal body and an axoneme - a membrane-bound, microtubule-based structure that extends out from the cell membrane into the extracellular milieu. They can be motile – flagella or motile cilia, or static – such as the primary cilium, which is found on most, non-cycling vertebrate cells (one exception are the nodal cilia found during development which structurally are primary cilia but can move). Motile cilia and flagella have a 9+2 arrangement of microtubules in the axoneme – nine doublets of microtubules organised around a central pair. In contrast, primary cilia have a 9+0 arrangement of microtubules, with no central pair. Amongst other roles, flagella are required for the motility of sperm and motile cilia are present on cells of the trachea and bronchial tubes where they mediate clearing of debris (reviewed in (Nigg and Raff, 2009)). The functions of the primary cilium are diverse and represented by the myriad of diseases associated with defective primary cilia. These include (but are not limited to) polycystic kidney disease, obesity, cranio-facial abnormalities, polydactyly and situs inversus (defects in left-right asymmetry) (reviewed in (Nigg and Raff, 2009)).

Ciliogenesis is the process of cilium assembly. In G1, the centrosome migrates to the cell membrane. The transition from centrosome to basal body is not completely understood. An early step is the encapsulation of the distal end of the mother centriole by a Golgi-derived vesicle (reviewed in (Satir and Christensen, 2007)). The mother centriole must anchor itself at the cell membrane and the distal and sub-distal appendages seem to be required for this process (Graser et al., 2007b; Ishikawa et al., 2005). Ciliogenesis and ongoing maintenance of the ciliary structure requires intraflagellar transport, or IFT. IFT was first described in the flagella of the green algae, *Chlamydomonas* (Kozminski et al., 1993). IFT is the microtubule-based transport of cargo from the cytoplasm to the tip of the cilium/flagella and back down

again (reviewed in (Scholey, 2008)). Axoneme growth occurs at the distal tip, therefore, IFT provides a way to deliver components required for axoneme growth to the tip and return turnover products back to the cytoplasm.

From an evolutionary point of view, it appears that the role for centrioles in ciliogenesis evolved before the role for centrioles in spindle assembly (Marshall, 2007). Marshall proposes that the position of centrioles at the poles of the bipolar spindle may have evolved to ensure the inheritance of a basal body into each daughter cell after cell division. During metazoan development, the centriole may then have become a more integral part of the spindle assembly pathway by organising the centrosome. It is interesting to note that an siRNA screen of proteins required for ciliogenesis in human cells revealed a number of centrosomal proteins that are required for genesis of the primary cilium and/or maintenance (Graser et al., 2007b). Some of the proteins required for ciliogenesis (for example ch-TOG) are PCM and not centriolar components. Therefore, how centrosomal proteins impact on the earlier evolved, centriolar-based mechanism of ciliogenesis is an interesting question and one that remains to be answered.

1.3.5 The centrosome and the DNA damage response

Outside of its well-characterised roles in mitosis and microtubule organisation, the centrosome is also known to function in the cellular response to DNA damage. Damage to DNA triggers a signalling cascade, the DNA damage response, in order to arrest the cell cycle, such that damaged DNA can be repaired, or (if the damage incurred is too great) that the cell can undergo programmed cell death. Arresting the cell cycle in response to DNA damage occurs by the activation of checkpoints – including the G1/S, Intra-S and G2 checkpoints. The G1/S checkpoint prevents cells with damage entering S-phase and starting replication of the damaged DNA. The intra-S checkpoint prevents the firing of new origins of DNA replication. The G2 checkpoint prevents cells with DNA damage from entering mitosis and thus prevents the transmission of damaged DNA to daughter cells. The DNA damage response and its related repair mechanisms are crucial to maintain genomic integrity and safeguard the cell against mutation and potential transformation (reviewed in (Shiloh, 2003)).

The DNA damage response is a typical signalling system mediated by a sensor-transducer-effector mechanism. The major sensors in the DNA damage response are two structurally related serine/threonine kinases – ATM (Ataxia Telangiectasia, Mutated) and ATR (ATM and Rad3 related) (reviewed in (Shiloh, 2003)). ATM predominantly responds to double strand breaks (DSBs) in DNA. ATR is activated predominantly in response to DNA replication stress (although ATR can also be activated in response to Ionising Radiation (IR), which generates DSBs). Activation of ATM and ATR leads to an increase in their kinase activity, such that they can phosphorylate downstream transducers. Two major DNA damage transducers activated by ATM/ATR are the Chk1 and Chk2 kinases (reviewed in (Bartek and Lukas, 2003)). Chk2 is phosphorylated by ATM in response to DSBs. Chk1 is phosphorylated by ATR in response to replicative stress. However, ATM can also phosphorylate Chk1 after exposure to IR.

The major response to DNA damage is activation of cell-cycle checkpoints. One of the major checkpoints is mediated by p53 in G1. ATM, Chk1 and Chk2 can all phosphorylate p53 (reviewed in (Bartek and Lukas, 2003; Rhind and Russell, 2000; Shiloh, 2003)). Phosphorylation of p53 leads to an enhancement in its transcriptional activity. One target of this activity is p21 – an inhibitor of the cyclin E/Cdk2 complex. Therefore, in response to DNA damage, p53 can activate the G1/S checkpoint and inhibit entry into G1.

Another important checkpoint is the G2 checkpoint. Chk1 and 2 both phosphorylate cdc25 phosphatases and in doing so either inhibit their phosphatase activity (as for cdc25C) or promote their degradation by the proteasome (as for cdc25A) (reviewed in (Bartek and Lukas, 2003)). Cdc25 phosphatase activity is crucial for the activation of cyclin B/Cdk1 in prophase and thus entry into mitosis (see Section 1.1.2.2). Maintenance of the inhibitory phosphorylations on T14 and Y15 on Cdk1 are partly required for G2 arrest after DNA damage (Blasina et al., 1997; Jin et al., 1996). However, interestingly, cells expressing the non-phosphorylatable Cdk1, Cdk1AF, still exhibit a G2 arrest, albeit a shorter one than in cells expressing wild-type Cdk1 (Jin et al., 1996). This implies that other, as yet unknown, mechanisms are also involved in maintaining a G2 arrest after DNA damage. It is also important to note that Chk1 also appears to regulate the G2 to M transition in unperturbed cell cycles (Kramer et al., 2004), via its effects on cdc25 phosphatases.

The relative contributions of Chk1 and Chk2 to the DNA damage response in G2 came from gene-targeting studies of these two kinases in chicken DT40 cells. Analysis of DT40 cells null for Chk1 revealed that this kinase is essential for the maintenance of a G2 arrest after DNA damage induced by IR (Zachos et al., 2003). Analysis of DT40 cells null for Chk2 kinase revealed that Chk2 is not essential for G2 arrest in response to IR in asynchronous cells but is required for a robust G2 arrest in response to damage incurred in G2 (Rainey et al., 2008). This implies that Chk1 is likely to be the major kinase mediating G2 arrest in response to IR while Chk2 may play a supporting role for Chk1. This may be required to maintain a robust arrest when DNA damage is incurred late in the cell cycle with less time for repair.

Chk1, Chk2, p53, cdc25 and cyclin B/Cdk1 have all been found to localise to centrosomes (Dutertre et al., 2004; Jackman et al., 2003; Kramer et al., 2004; Morris et al., 2000; Takada et al., 2003; Tsvetkov et al., 2003). These data indicate that the centrosome may be an important effector in the DNA damage response. The protein-rich PCM of the centrosome can concentrate signalling molecules and thus enhance the efficiency of signalling. In addition, phospho-specific antibodies recognising activated cyclin B/Cdk1, revealed that cyclin B/Cdk1 is first active on the centrosomes in prophase (Jackman et al., 2003). Therefore, by concentrating DNA damage effector proteins at the centrosome – cyclin B/Cdk1-mediated entry into mitosis can be prevented quickly and efficiently in the presence of DNA damage.

The centrosome can also exhibit a number of effector responses in the face of DNA damage. These responses are summarised below.

1.3.5.1 Centrosome amplification

One well-documented response of centrosomes to DNA damage is the amplification of centrosomes in response to IR (Sato et al., 2000). This amplification of centrosomes requires an extended G2 arrest (Dodson et al., 2004), which in turn requires the kinase activities of ATM, ATR and Chk1 (Bourke et al., 2007; Dodson et al., 2004). The mechanisms governing centrosome amplification in G2 after DNA damage are just beginning to be elucidated. Cdk2 activity is involved in the normal duplication of centrosomes (see Section 1.3.3.3). Bourke and colleagues found that Cdk2 kinase activity increases after IR and that Cdk2 is also required for centrosome amplification after IR (Bourke et al., 2010). Significantly, the increase in Cdk2 activity was dependent on Chk1 kinase. In addition, loss of centrosome cohesion

(implying loss of centriole engagement) correlates with centrosome amplification after IR (Saladino et al., 2009). These data imply that some of the same mechanisms that govern normal centrosome duplication may be involved in centrosome amplification in G2. Similar to the redundancy observed in centrosome duplication, Cdk1 can mediate centrosome amplification in the absence of Cdk2 (Bourke et al., 2010).

Centrosome amplification can also occur after extended inhibition of DNA synthesis in S-phase. Phenotypically, centrosome amplification in both G2 and S phase have the same endpoint – the generation of extra centrioles. Loffler and colleagues showed that ultra-violet (UV)-damage to human cells induced the activation of Chk1 kinase in S-phase and centrosome amplification (Loffler et al., 2006). Moreover, they were able to show, by fusing Chk1 to the PACT domain and thus forcing its centrosomal accumulation, that the centrosomal localisation of Chk1 alone is sufficient to mediate centrosome amplification (Loffler et al., 2006). These data suggested that Chk1 was responsible for centrosome amplification during extended S-phase arrest. However, more recent work suggests that Chk1 may not be required for S-phase centrosome amplification since DT40 cells null for Chk1 can still amplify their centrosomes after hydroxyurea (HU)-mediated inhibition of DNA synthesis (Bourke et al., 2010). Therefore, while Chk1 is activated during S-phase arrest it may not be essential for centrosome amplification during this stage. Significantly, Loffler and colleagues did not confirm the cell cycle stage of Chk1-PACT expressing cells and thus it is feasible that centrosome amplification in the absence of damage was occurring in G2. Alternatively, the differences observed may be due to the way in which S-phase arrest was induced (UV versus HU) or the cell lines used (human cell lines versus DT40). Clearly, further work is needed to deconstruct the pathways of centrosome amplification in S and G2. Importantly, S-phase mediated centrosome amplification does depend on ATM and ATR signalling since inhibition of their kinase activity by caffeine treatment prevented centrosome amplification (Loffler et al., 2006).

The centrioles generated during G2 or S-phase arrest appear to differ in their maturity. Centrioles generated after IR-mediated G2 arrest contain the mother centriole specific protein, Cep170, indicating that they are mature. Amplified centrosomes appear to contain complete centrosomes with mother centrioles nucleating the growth of single daughter centrioles. Centrioles generated during extended S-phase arrest do not contain Cep170, indicating that they are immature (Saladino et al., 2009). In S-phase

arrested cells, a single mother centriole can apparently generate multiple daughter centrioles. This may reflect the factors available in different cell cycle phases to induce centriole maturation or may represent different pathways present in S and G2 to amplify centrosomes.

Intriguingly, a recent paper has revealed a requirement for nuclear export for the amplification of centrosomes in S-phase arrested cells (Prosser et al., 2009). Treating S-phase arrested cells with an inhibitor of nuclear export caused the accumulation of the centriolar protein, centrin, in the nucleus and prevented the generation of extra centrosomes in the cytoplasm. This represents an exciting novel pathway involved in centrosome amplification and further work will hopefully characterise how general a mechanism this is in the amplification of centrosomes.

1.3.5.2 Centrosome splitting

In cells forced to go into mitosis in the presence of DNA damage (by the addition of caffeine – an inhibitor of ATM and ATR kinase activities), centrosomes appear structurally normal before NEBD but mother and daughter centrioles split after NEBD, generating multipolar spindles (Hut et al., 2003). The mechanism underlying this splitting event has not been investigated and represents an interesting future line of research.

1.3.5.3 Targeting centrosomal proteins

In addition to indirect effects on centrosome function mediated by downstream transducers, the DNA damage sensors ATM and ATR can also directly phosphorylate at least one centrosomal protein (Smith et al., 2009). Cep63 was identified in *Xenopus* egg extracts as an ATM and ATR target that is essential for spindle assembly. After induction of DNA damage, Cep63 is phosphorylated by ATM and ATR and mislocalised from the centrosome. Mislocalisation of Cep63 caused defects in spindle assembly. Some of this work has been validated in DT40 cells yet crucially, the residue phosphorylated by ATM/ATR in Cep63 is not conserved in higher eukaryotes. Therefore, while further work is needed to validate the role of Cep63 in somatic cells, these data provide a direct link between DNA damage sensing and a centrosomal response. It will be interesting to see if other centrosomal proteins are direct targets of ATM and ATR.

1.3.5.4 Centrosome inactivation

In *Drosophila* embryos, DNA damage triggers a process known as “centrosome inactivation” (Takada et al., 2003). During centrosome inactivation, components of the γ -TuRC are lost from the centrosome and thus the centrosome loses the capacity to nucleate microtubules, leading to defects in chromosome segregation. Significantly, centrosome inactivation requires Chk2 function in *Drosophila* and Chk2 accumulates on centrosomes after DNA damage (Takada et al., 2003). While centrosome inactivation *per se* has not been observed in mammalian cells (Mikhailov et al., 2002), many of the pathways downstream of Chk2 may be conserved in a centrosomal response to DNA damage.

Centrosome amplification and centrosome splitting both lead to generation of multipolar spindles in mitosis (Dodson et al., 2007; Hut et al., 2003). Mislocalisation of Cep63 is predicted to lead to defects in spindle assembly (Smith et al., 2009). These mechanisms ensure that cells with DNA damage that enter mitosis (by escaping the G2 arrest) will undergo mitotic catastrophe in response to spindle defects and arrest in mitosis. Mitotic catastrophe is a poorly characterised form of cell death that occurs during mitosis that is distinct to programmed cell death (apoptosis). Time-lapse imaging of cells with centrosome amplification generated by IR has shown a correlation between an increasing dose of IR and mitotic catastrophe (Dodson et al., 2007). In this way, cells with unrepaired DNA damage can be deleted from the population. Similarly, centrosome inactivation and subsequent defects in chromosome segregation would ensure that nuclei that have incurred DNA damage would be eliminated from the *Drosophila* embryo (Takada et al., 2003).

These data also suggest that while the centrosome may not be essential for spindle assembly, defective centrosomes can still exert a powerful influence on mitosis. Of course, it is also possible that centrosome amplification is merely a by-product of sustained Chk1 activity after DNA damage and that it has no particular physiological relevance. However, whether centrosome amplification is a true effector mechanism or merely a by-product of DNA damage, it still has consequences for cell division that could eliminate cells with damaged DNA from the population.

1.4 Primary Microcephaly – a centrosomal disease?

Autosomal Recessive Primary Microcephaly (Online Mendelian Inheritance in Man, OMIM, 251200) is a congenital neurodevelopmental disorder characterised by a brain size that is at least three standard deviations below the sex and age-adjusted mean. Magnetic Resonance Imaging (MRI) of brains of microcephaly-affected individuals revealed that, while the cerebral cortex is substantially reduced in size, the overall brain architecture is grossly normal (Bond et al., 2002; Trimborn et al., 2004). This is consistent with the fact that primary microcephaly is associated with mental retardation but not with other clinical problems, such as defects in motor or sensory function. Primary microcephaly has been suggested to be a disorder of neurogenic division, therefore I will briefly summarise mammalian neurogenesis below.

1.4.1 Mammalian neurogenesis – a summary

Neurogenesis is the generation of new neurons in the brain. All neurons of the mammalian cortex are derived from the neuroepithelium and the primary stem cells in the brain are the neuroepithelial cells (reviewed in (Farkas and Huttner, 2008)). Initially, it is thought that neuroepithelial cells undergo rapid symmetric, proliferative divisions, to expand the stem-cell pool. Later in neurogenesis, neuroepithelial cells undergo a neurogenic ‘switch’ and begin to carry out asymmetric, neurogenic divisions, in order to generate one neuroepithelial cell and one neural progenitor cell. These progenitor cells can then either undergo symmetric or asymmetric divisions before progressing on to differentiate into neurons (Figure 1.6). What causes the switch from proliferative to neurogenic divisions is unknown and remains a key question if we are to understand the basis of microcephaly. One argument suggests that cell-cycle timing could regulate the switch. It has been shown that by artificially increasing the length of the cell cycle in neuroepithelial cells it is possible to trigger a premature neurogenic switch in mouse whole embryo culture (Calegari and Huttner, 2003). Multiple lines of data also show that the length of the cell cycle increases concomitantly with the switch from proliferative to neurogenic cell division (Calegari et al., 2005; Takahashi et al., 1995). This has clear consequences for microcephaly. If the switch to neurogenic division occurs too early, then the progenitor pool will be depleted and hence the capacity to generate neurons will be reduced.

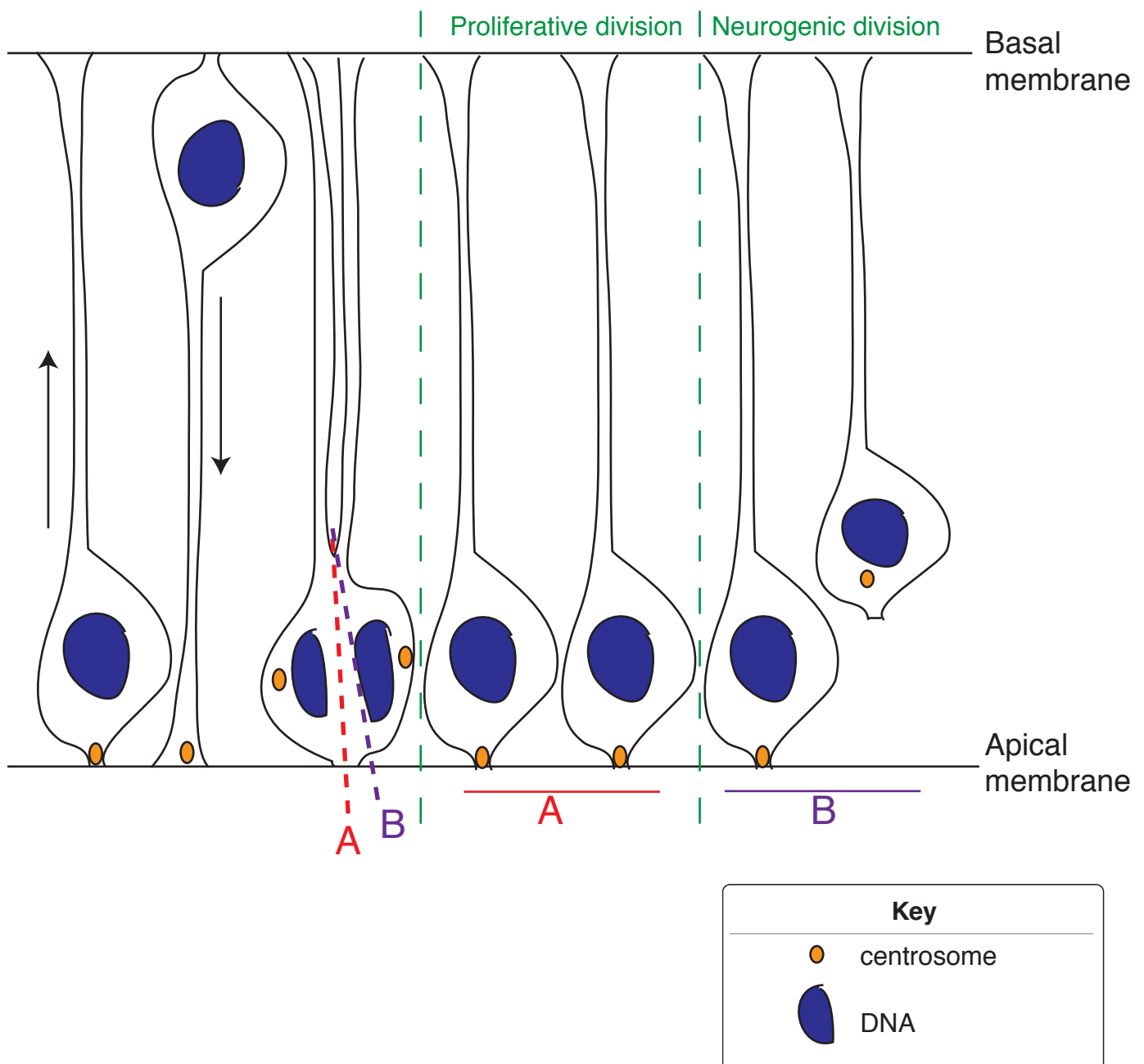


Figure 1.6 Mammalian Neurogenesis. Schematic represents a section through the mouse neuroepithelium. Neuroepithelial cells are anchored at both the apical and basal membranes. On the far left of the diagram is a neuroepithelial cell in G1. During Interkinetic Nuclear Migration (INM), the nucleus migrates to the basal membrane. At the basal membrane, the cell undergoes S-phase. The nucleus then migrates back to the apical membrane where it will go through mitosis. During cytokinesis at the apical membrane, the cleavage furrow ingresses from the basal membrane towards the apical membrane. The orientation of the cleavage plane determines the fate of the cell. If the cleavage plane is as in 'A' then the apical membrane is partitioned between the two cells and both cells are retained at the apical membrane as neuroepithelial cells. This is a proliferative division and expands the stem cell pool. If the cleavage plane is as in 'B', only one cell will inherit the apical membrane. This is a neurogenic division. One cell will leave the apical membrane and become a neural progenitor. This cell may divide again or differentiate into a neuron.

Neuroepithelial cells are anchored between the apical and basal membranes in the neuroepithelium. Before cell division, these cells undergo Interkinetic Nuclear Migration (INM) such that the nucleus migrates towards the basal membrane in G1, undergoes S-phase at the basal membrane and then moves to the apical membrane in G2. Cells then go through mitosis at the apical membrane (Figure 1.6; reviewed in (Farkas and Huttner, 2008)). It has been observed in mouse brain that, during proliferative divisions, dividing neuroepithelial cells equally inherit a portion of the apical membrane – thus generating two cells still attached to the membrane (see ‘A’ in Figure 1.6). During neurogenic divisions, only one daughter cell inherits apical membrane and thus the second is released and becomes a neural progenitor cell (Kosodo et al., 2004) (see ‘B’ in Figure 1.6). Mutations in genes that regulate mitotic spindle alignment could lead to a premature switch to neurogenic divisions and thus depletion of the stem cell pool.

1.4.2 Microcephaly and centrosomes

Seven loci have been linked to primary microcephaly and the mutated genes have been identified in five of these cases. The loci are numbered MCPH1-7 and intriguingly, all of the genes identified thus far encode centrosomal proteins: *MCPH1* – microcephalin; (Jackson et al., 2002), *MCPH3* – CDK5RAP2 (Bond et al., 2005), *MCPH5* - ASPM; (Bond et al., 2003), *MCPH6* – CenpJ (Bond et al., 2005) and *MCPH7* – STIL/SIL (Kumar et al., 2009). These findings indicate that the centrosome must play a significant role in the development of the brain, and in particular the cerebral cortex. Recently, the centrosome has been shown to have a very important role during neurogenesis in mouse. Wang *et al.* have shown that during the neurogenic divisions of neuroepithelial cells, the older centrosome is predominantly inherited by the neuroepithelial cell and the younger centrosome by the cell that will go on to differentiate (Wang et al., 2009). More significantly, if they depleted ninein, a mother centriole specific protein, by short hairpin RNA (shRNA), the asymmetric inheritance of centrosomes was perturbed and neuroepithelial cells were no longer retained at the apical membrane. While this is an exciting result, this conclusion is difficult to interpret, since if ninein depletion leads to randomisation of centrosome inheritance, then at least 50% of cells should inherit the older centrosome by chance and thus be retained. Therefore, a complete loss of neuroepithelial cells

after ninein depletion is surprising, unless ninein itself is required for retention of neuroepithelial cells independently of its role at the mother centrosome. Further work using this system should clarify this matter.

What is particularly interesting is that all of the *MCPH* genes are ubiquitously expressed (National Institutes of Health – Unigene) and therefore why their mutation should only affect brain development is an extremely interesting question in developmental biology. In addition to their localisation at centrosomes, all of the identified *MCPH* genes have been demonstrated to have a centrosomal function. It is still not known if mutations in microcephaly genes lead to a truncated protein product, or if affected individuals are null for the associated proteins. In the case of *ASPM*, at least one of the microcephaly-causing mutations causes a truncation of the protein (Kouprina et al., 2005). For microcephalin, one mutation has been shown to lead to a large reduction in the amount of protein while a different mutation led to no detectable protein product (Alderton et al., 2006). Therefore, how mutations in these centrosomal genes could cause microcephaly might be complicated by the effects of truncated or alternatively spliced proteins. Below, I will outline what is known of the functions of the genes mutated in primary microcephaly.

1.4.2.1 ASPM (MCPH5)

ASPM (Abnormal Spinde-like, Microcephaly associated) is the most frequently mutated gene in primary microcephaly, accounting for almost 50% of cases (Roberts et al., 2002). *ASPM* has closely related homologues in both *Drosophila* (*Asp* – Abnormal spindle) and *C. elegans* (*ASPM-1*). The *Drosophila* *Asp* protein was the first of these to be characterised in detail. *Drosophila* embryos mutant in *Asp* have defects in meiosis and mitosis, leading to arrest in metaphase (Ripoll et al., 1985). Subsequent cloning and immunolocalisation studies of the mutated gene identified *Asp* as a MAP that localises to spindle poles in a ‘hemisphere’ around the centrosome on the side of the chromosomes (Saunders et al., 1997). *Asp* is a *bona fide* centrosomal protein since it is present in partially-purified centrosomes (do Carmo Avides and Glover, 1999). Microtubule nucleation from the same partially purified centrosomes requires *Asp* to be phosphorylated and this is most likely mediated by polo kinase (do Carmo Avides and Glover, 1999; do Carmo Avides et al., 2001). *Asp* mutant larval neuroblasts display unfocussed spindle poles and γ -tubulin is mislocalised from the spindle pole region (do Carmo Avides and Glover, 1999).

Similarly in *C. elegans*, ASPM-1 interacts with the spindle pole localised NuMA-like protein, LIN-5 and is required to localise dynein to spindle poles (van der Voet et al., 2009). Therefore, by maintaining NuMA and dynein at spindle poles, ASPM may mediate spindle pole focussing.

The human homologue of Asp, ASPM, also localises to spindle poles in human cells (Kouprina et al., 2005; Zhong et al., 2005). Further analysis of ASPM identified that it is required for the continued proliferation of glioblastoma cell lines and for expansion of mouse neural stem (NS) cells (Horvath et al., 2006). ASPM expression decreased as mouse NS cells were forced to differentiate. This is similar to what was observed in mouse brain, that as neural progenitor cells begin to differentiate, they express less ASPM (Fish et al., 2006). This indicates that ASPM has an important role in mitosis, similar to its homologue in *Drosophila*.

An indication of how mutation of *ASPM* might cause microcephaly came from *in vivo* experiments of ASPM function in mouse brain. ASPM-targeting siRNAs were electroporated into embryonic mouse brain (Fish et al., 2006). Neuroepithelial cells transfected with *ASPM* siRNA had an increased propensity to undergo asymmetric, neurogenic divisions, rather than symmetric, proliferative divisions. This was due to a misalignment of the mitotic spindle such that only one of the two daughter cells inherited the apical membrane (Figure 1.6 'B'). Clues as to how ASPM may regulate spindle positioning in neuroepithelial cells come from studies in the *C. elegans* embryo. Knockdown of ASPM-1 in *C. elegans* causes defects in spindle rotation (van der Voet et al., 2009). ASPM-1-mediated spindle rotation is regulated by dynein. Therefore, ASPM may regulate spindle orientation in mouse neuroepithelial cells by ensuring the proper localisation of dynein at spindle poles. In telophase neuroepithelial cells depleted of ASPM, there is a striking detachment of centrosomes from the spindle poles. Detachment of centrosomes in this way would diminish the ability of centrosome-nucleated astral microtubules to orientate the mitotic spindle relative to the cortex and thus could lead to defects in spindle positioning. Further work is required to characterise the role of ASPM in spindle orientation in mammalian cells.

1.4.2.2 Microcephalin (*MCPH1*)

Mutations in Microcephalin (also known as MCPH1 or BRIT1) were the first to be identified in primary microcephaly (Jackson et al., 2002). Microcephalin is both a

nuclear and centrosomal protein (Brunk et al., 2007; Jeffers et al., 2008; Tibelius et al., 2009; Xu et al., 2004; Zhong et al., 2006). Many functions have been ascribed to microcephalin, including roles in chromosome condensation, the DNA damage response, DNA repair and regulating mitotic entry.

In patient cells with mutant microcephalin, or in cells depleted of microcephalin by siRNA, there are a high proportion of G2 cells that exhibit premature chromosome condensation (PCC) (Trimborn et al., 2004). The same cells also exhibit a delay in decondensing chromosomes after mitosis. The function of microcephalin in chromosome condensation is mediated via its physical interaction with condensin II subunits (Trimborn et al., 2006; Wood et al., 2008). Condensin II is one of two ATPase-containing complexes that mediate chromosome condensation in vertebrate cells, the other being condensin I (reviewed in (Hudson et al., 2009)). However, the molecular mechanism of how mutation or depletion of microcephalin should lead to PCC is not understood.

Microcephalin has been implicated extensively in the DNA damage response and in repair of DNA damaged lesions by Homologous Recombination (HR) and Non-Homologous End Joining (NHEJ). HR is the process of using the homologous chromosome as a template strand to repair the damaged lesion. NHEJ involves the resection and ligation of double-stranded DNA on either side of the lesion and can lead to loss of DNA base pairs. Microcephalin has three BRCT (BRCA1 C-terminal) domains (Jackson et al., 2002). These domains are predominantly found in cell cycle checkpoint functions responsive to DNA damage (SMART (Simple Modular Architecture Research Tool)). In response to DNA damage, histone H2AX is phosphorylated by ATM and ATR kinases to generate γ H2AX, which localises to sites of DNA damage (Stucki and Jackson, 2006). Microcephalin localises to these DNA damage foci, via its interaction with phosphorylated γ H2AX (Jeffers et al., 2008; Lin et al., 2005; Rai et al., 2006; Wood et al., 2007; Xu et al., 2004). This interaction mediates the recruitment of downstream DNA damage response proteins. Microcephalin also regulates cell cycle arrest in response to DNA damage and is required for both the intra S-phase and G2 checkpoints (Xu et al., 2004). The requirement for microcephalin in the G2 checkpoint has been well characterised. In the absence of microcephalin, Chk1 is mislocalised from the centrosome (Tibelius et al., 2009). Moreover, the inhibitory tyrosine phosphorylation, Y15, on Cdk1 is

reduced (Alderton et al., 2006). Thus, in the presence of reduced or mutated microcephalin, Chk1 is no longer at the centrosome and cannot inhibit the activation of Cdk1 kinase activity. Therefore, Cdk1 becomes active and cells enter mitosis in the presence of DNA damage. Work on *mcpH* mutant *Drosophila* embryos suggested that in the absence of microcephalin, nuclear and centrosome cycles become uncoupled, centrosomes detach from the mitotic spindles and cells arrest in mitosis (Brunk et al., 2007; Rickmyre et al., 2007). It has been reported that microcephalin can regulate the levels of Chk1 at a transcriptional level, however, the literature on this is conflicting (Xu et al., 2004; Yang et al., 2008).

As well as arresting the cell cycle to allow DNA damage to be repaired, microcephalin is also directly involved in the DNA repair process (Liang et al., 2010; Wu et al., 2009). Microcephalin interacts with and recruits chromatin-remodelling proteins to the sites of DNA damage (Peng et al., 2009). Targeting of remodelling proteins to sites of damage allows localised ‘opening up’ of the DNA structure to allow DNA repair factors to bind. Therefore, it seems that microcephalin is required to maintain the integrity of the genome by acting at multiple stages in the DNA damage response.

1.4.2.3 CDK5RAP2 (*MCPH3*)

Characterisation of the function of CDK5RAP2 forms the bulk of this thesis. At the start of this work, no functions had been ascribed to vertebrate CDK5RAP2. Description of the functions of orthologues of CDK5RAP2 in lower organisms is outlined in detail towards the end of this chapter.

1.4.2.4 CenpJ (*MCPH6*)

CenpJ is a highly-conserved centriolar protein that is involved in centrosome duplication. A siRNA screen in *C. elegans* embryos identified *sas-4* (as CenpJ is known in *C. elegans*) as being essential for centriole duplication (Kirkham et al., 2003; Leidel and Gonczy, 2003). Sas-4 is a stable, core component of the centrioles in *C. elegans* and is required for the assembly of centriolar microtubules onto the daughter centriole (Pelletier et al., 2006). Sas-4 is also essential for centrosome duplication in *Drosophila* (*Dsas-4*; (Basto et al., 2006)) and in human cells (CenpJ/CPAP; (Kleylein-Sohn et al., 2007; Kohlmaier et al., 2009)). Mutation (*Dsas-4*) or siRNA-depletion (*CenpJ/CPAP*) of *sas-4* homologues leads to an inability to

generate new centrioles. Intriguingly, in human cells, CenpJ can bind to the tubulin heterodimer (Hung et al., 2004) and is required for the elongation of centrioles by the addition of tubulin subunits to the growing centrioles (Kohlmaier et al., 2009; Schmidt et al., 2009; Tang et al., 2009). Conversely, CenpJ has also been shown to destabilise the microtubule polymer and promote depolymerisation of microtubules (Hsu et al., 2008; Hung et al., 2004). This microtubule-destabilising role of CenpJ is hard to reconcile with its proposed role in centriole elongation and requires further characterisation.

In addition to its role in centrosome duplication, CenpJ has also been implicated in mediating centrosome cohesion (Zhao et al., 2010). By forming a homodimer, CenpJ can maintain a link between the two centrioles. It would be interesting to see if this function of CenpJ is also linked to the ability of CenpJ to bind to tubulin heterodimers, since an intact microtubule cytoskeleton is required for centrosome cohesion (Jean et al., 1999; Meraldi and Nigg, 2001).

1.4.2.5 STIL/SIL (*MCPH7*)

Microcephaly-causing mutations in the *STIL* gene are the most recent mutations to be characterised (Kumar et al., 2009). *STIL* is a cell cycle regulated protein and localises to the centrosomal region only in mitosis (Pfaff et al., 2007). *STIL* has been reported to be the orthologue of the *Drosophila* protein, Ana2 (Stevens et al., 2010). Ana2, in turn, is functionally related to the *C. elegans* protein, Sas-5. In the *C. elegans* embryo, Sas-5 is essential for centrosome duplication (Delattre et al., 2004), and is upstream of sas-4 (CenpJ) in the centrosome duplication pathway (Delattre et al., 2006; Pelletier et al., 2006). Ana2 is required in *Drosophila* S2 cells for centriole duplication (Dobbelaere et al., 2008) and for *de novo* centriole formation in unfertilised *Drosophila* eggs (Stevens et al., 2010). These data imply that *STIL* may also be involved in centrosome duplication in human cells, but, as yet, no requirement for *STIL* in centrosome duplication has been demonstrated. *STIL* only localises to centrosomes in mitosis (Pfaff et al., 2007) and thus how it might regulate centrosome duplication in S-phase is uncertain. However, zebrafish mutants that are null for the *STIL* protein, and human cells where *STIL* protein has been depleted by siRNA, do have an increased number of monopolar spindles (Pfaff et al., 2007), which could arise due to a failure in centrosome duplication. A closer analysis of centriole number after *STIL* depletion would be required to determine if this is true. Zebrafish null for

the STIL protein also display mitotic spindles where the centrosomes have detached (Pfaff et al., 2007).

Mouse embryos null for *Stil* have defects in left-right asymmetry (Izraeli et al., 1999). Defects in left-right patterning have been attributed to defective ciliogenesis and therefore it would be interesting to investigate if STIL has a role in primary cilium formation and/or maintenance.

As can be seen from the data available, MCPH proteins have diverse functions at the centrosome – including functions in centrosome duplication, centrosome cohesion, centrosome attachment to spindle poles, spindle orientation and centrosome-mediated G2 arrest in response to DNA damage. Therefore, there does not seem to be a unifying theory for how mutations in any one of these genes could lead to microcephaly. Defining which of these functions are important in neurogenesis is a fascinating area of future research.

1.5 CDK5RAP2: an uncharacterised centrosomal protein essential for proper brain development

Cyclin-Dependent Kinase 5 Regulatory subunit Associated Protein 2, or CDK5RAP2 (also known as Cep215), is a human protein that localises to the centrosome (Andersen et al., 2003; Bond et al., 2005). Mutations in the *CDK5RAP2* gene can cause primary microcephaly (Bond et al., 2005). Therefore, clearly CDK5RAP2 is an important centrosomal protein that warrants further study. At the start of this thesis, the functions of CDK5RAP2 were completely uncharacterised. However, potential orthologues of CDK5RAP2 in fission yeast and fly have been extensively characterised and may give some clue as to the functions of CDK5RAP2.

1.5.1 CDK5RAP2 is an evolutionarily conserved centrosomal protein

Based on sequence homology, CDK5RAP2 is a potential orthologue of Centrosomin (Cnn) in *Drosophila* and mod20p in fission yeast (Bond et al., 2005; Sawin et al., 2004). No equivalent protein has been identified in *C. elegans*. All three proteins are large (100-300 kDa), coiled-coil domain containing proteins that share a region of homology at their amino-termini – known as ‘CNN motif 1’ (Zhang and Megraw, 2007) (Figure 1.7). In addition, a second region of significant homology has been recently identified at the C-terminus of Cnn and CDK5RAP2 which is termed ‘CNN motif 2’ (Zhang and Megraw, 2007). This region does not appear to be conserved in mod20p.

1.5.1.1 Mod20p in *Schizosaccharomyces pombe*

As mentioned above (see Section 1.2.3), fission yeast have at least three MTOCs: the SPB, iMTOCs and eMTOCs. Mod20p (also known as mto1 and mbo1) is essential for microtubule nucleation from both iMTOCs and eMTOCS, but not SPBs (Sawin et al., 2004). In the absence of mod20p, intranuclear microtubule assembly during mitosis is unaffected (since this is mediated exclusively by the SPB). However, the growth of astral microtubules from the SPB and the growth of microtubules from eMTOCs and iMTOCs is severely impaired (Sawin et al., 2004). Mod20p binds to γ -tubulin and recruits it to the iMTOCs and eMTOCs. Binding of mod20p to γ -tubulin

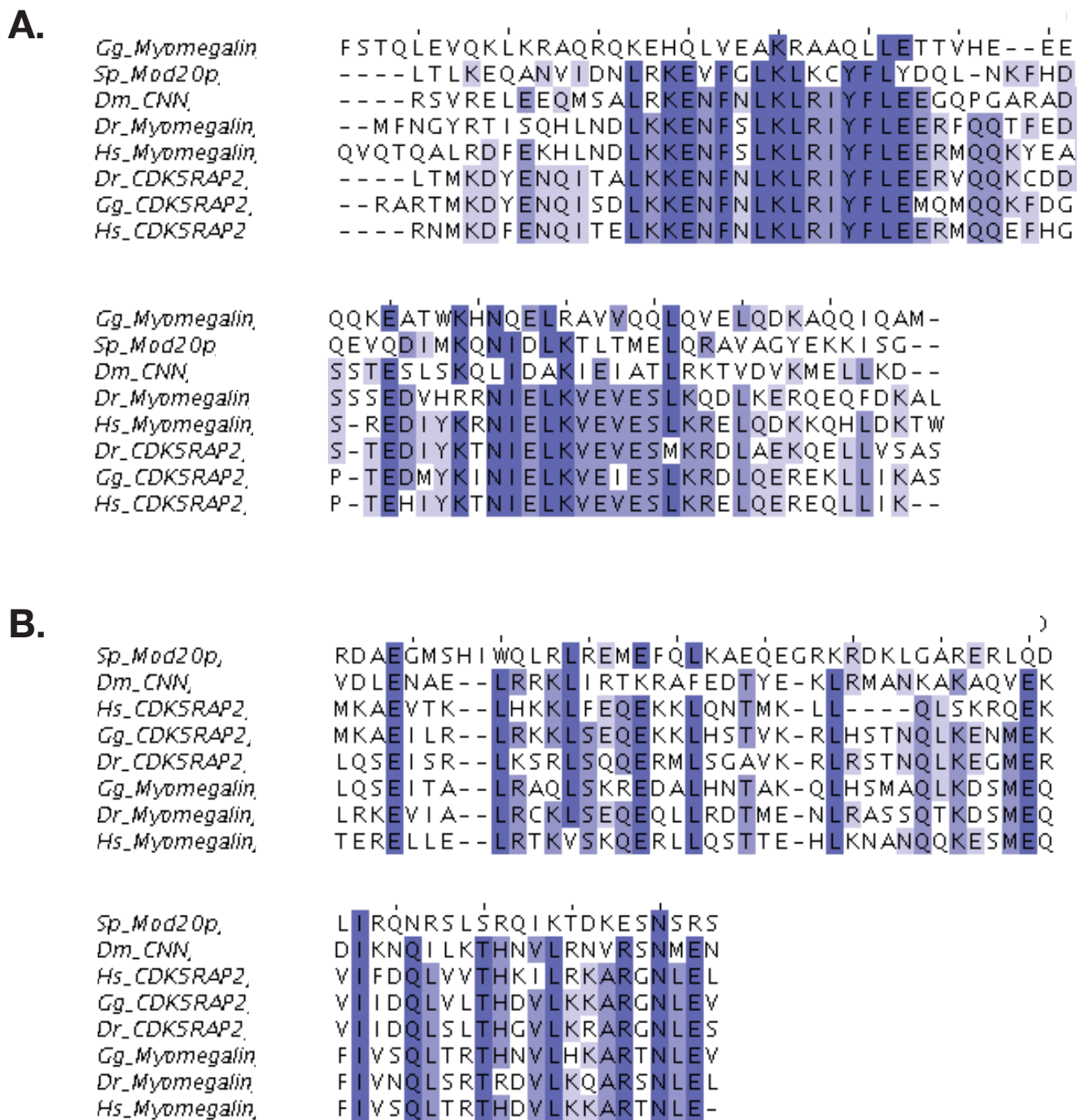


Figure 1.7 Multiple sequence alignment of CNN motifs 1 and 2 across species. A. Multiple sequence alignment of CNN motif 1. Note that *Gg_Myomegalin* has a divergent N-terminus to other CNN-motif containing proteins. **B.** Multiple sequence alignment of CNN motif 2. Note that *Sp_Mod20p* has a divergent C-terminus. Abbreviations: *Gg* - *Gallus gallus*, *Sp* - *Schizosaccharomyces pombe*, *Dm* - *Drosophila melanogaster*, *Dr* - *Danio rerio*, *Hs* - *Homo sapiens*.

is modulated by a second microtubule-regulating protein, mto2p (Samejima et al., 2005; Samejima et al., 2008). In the absence of mto2p, mod20p cannot bind to γ -tubulin. Significantly, CNN motif 1 in mod20p is essential for its interaction with γ -tubulin (Samejima et al., 2008).

1.5.1.2 Centrosomin (Cnn) in *Drosophila melanogaster*

Cnn is a core centrosomal component in flies. Cnn is required to assemble PCM components around the centrioles (Lucas and Raff, 2007; Megraw et al., 2001). In fly embryos lacking Cnn protein, the PCM is disorganised and separated from the centrioles. Centrioles thus become detached from the spindle pole and spindles are no longer properly spaced in the syncytium (due to the lack of astral microtubules at the spindle poles). Cnn is also required for proper centrosome maturation by recruiting several PCM components to centrosomes, including D-TACC, γ -tubulin, Msp, CP60, CP190, Aurora and Polo (Dobbelaere et al., 2008; Megraw et al., 2001; Megraw et al., 1999; Terada et al., 2003; Zhang and Megraw, 2007). In fact, in an siRNA screen to identify regulators of centrosome maturation in *Drosophila* S2 cells, Cnn was found to be one of two master regulators of centrosome maturation, the second being Polo kinase (Dobbelaere et al., 2008). In a similar manner to mod20p in *S. pombe*, recruitment of γ -tubulin and D-TACC to centrosomes by Cnn is dependent on CNN motif 1 (Zhang and Megraw, 2007). Moreover, Cnn interacts with γ -tubulin via the N-terminus of Cnn (which includes CNN motif 1) (Terada et al., 2003). This again highlights the importance of CNN motif 1 in centrosome function.

Unlike mod20p, Cnn also has an evolutionarily conserved CNN motif 2 at its C-terminus. Recently, the requirement for this domain in Cnn function has been characterised (Kao and Megraw, 2009; Sullivan, 2009). A missense mutation in CNN Motif 2 of *cnn* (known as *cnn*^{B4}) produces a protein product that is still able to localise to centrosomes in fly embryos (Kao and Megraw, 2009). Wild-type fly embryos undergo nine rounds of rapid and synchronous divisions in the interior of the embryo, after which syncytial nuclei organise in a monolayer around the surface of the embryo. Cleavage furrows then form around each nucleus to cellularise the embryo. Centrosomes expressing Cnn^{B4} protein can nucleate microtubules and recruit PCM

components. However, Cnn^{B4} expression disrupts cleavage furrow assembly and so prevents cellularisation of the embryo.

Adult flies null for Cnn protein are viable (Megraw et al., 1999). This is in spite of the fact that centrosomes lacking Cnn are non-functional (Megraw et al., 2001). This is not too surprising since bipolar spindles can still assemble via the chromatin-mediated pathway (Megraw et al., 2001). However, centrosomes lacking Cnn do not have astral microtubules. As a consequence, 4% of dividing neuroblasts in the brain divide symmetrically in Cnn null flies, compared with 0% in wild-type flies (Lucas and Raff, 2007). In addition, centrosomes appear to detach from spindle poles in dividing neuroblasts lacking Cnn protein (Lucas and Raff, 2007).

In divisions of the male germline stem cells (GSCs) in *Drosophila*, the mother centrosome is preferentially inherited by the stem cell, while the daughter cell inherits the daughter centrosome (Yamashita and Fuller, 2008). Mutation of *cnn* leads to random segregation of mother and daughter centrosomes into daughter cells and even misorientated mitotic spindles. The lack of astral microtubules in *cnn* mutant flies means that the mother centrosome is no longer anchored to the hub and the segregation of centrosomes is randomised. Work on ageing flies suggests that centrosome misorientation in the GSCs may cause a delay in the cell cycle (Cheng et al., 2008).

1.4.1.3 Myomegalin in humans

In addition to CDK5RAP2, there is a second human protein that contains both CNN motifs 1 and 2. This protein is known as Myomegalin (or Phosphodiesterase 4D Interacting Protein – PDE4DIP) (see Figure 1.7). Myomegalin localises both to the centrosome and Golgi body in COS-7 cells (kidney cells derived from the African Green Monkey) (Verde et al., 2001). Expression of Myomegalin is highest in heart and skeletal muscle, with relatively little expression in brain, lung and liver. The function of Myomegalin (either at the centrosome or otherwise) is, as yet, unknown. Two interacting partners have been identified. One binding partner is myopodin – an actin-bundling protein that shuttles between the nucleus and Z-disc in myocytes (precursor muscle cells). The second is the centrosomal protein Cep120, which is required for INM during neurogenesis (see Figure 1.6) (Faul et al., 2007; Xie et al., 2007). However, the significance of these interactions has yet to be characterised.

1.5.2 CDK5RAP2: the story so far....

CDK5RAP2 was first identified as an interacting partner of p35^{nk5a} – the activator protein for Neuronal cdc2-like kinase (Nclk) (Ching et al., 2000). Nclk is a kinase involved in the regulation of neuro-cytoskeletal dynamics (Lew et al., 1992; Paudel et al., 1993; Sun et al., 1996) and neuronal differentiation and neurite outgrowth (Chae et al., 1997; Nikolic et al., 1996; Ohshima et al., 1996). Nclk consists of a catalytic subunit – Cdk5, and a 25kDa activator protein (p25), derived from the larger precursor, p35^{nk5a}. A C-terminal fragment of CDK5RAP2 ('C48') was shown to bind to p35^{nk5a} and to be phosphorylated by Nclk (Ching et al., 2000). The significance of this interaction is unclear as the interaction between C48 and p35^{nk5a} did not affect p35^{nk5a}-activated Cdk5 activity (Wang et al., 2000). Importantly, while the Cdk5 activator, p35^{nk5a}, is detected almost exclusively in neurons (Lew et al., 1994; Tsai et al., 1994), Cdk5 kinase activity has been demonstrated outside of the brain (Turner et al., 2008) and Northern blot analysis showed that 'C48' was ubiquitously expressed in all tissues tested, including heart, brain, lung, liver, skeletal muscle, kidney and pancreas (Ching et al., 2000). These observations imply that 1. Cdk5 may have other, as yet uncharacterised activators in non-neuronal tissues, and, 2. CDK5RAP2 is likely to have functions outside of the nervous system. The expression pattern of CDK5RAP2 is quite different to that seen for Myomegalin (Verde et al., 2001) and may reflect different requirements for CNN-domain containing proteins in different tissues.

Two mutations in *CDK5RAP2* have been linked to primary microcephaly (Bond et al., 2005). The first of these is a mutation at 243T→A that causes the nonsense amino acid substitution S81X, thus causing a premature stop. The second is in intron 26 and causes a change in the splice-acceptor site, leading to the addition of four amino acids and then a stop (E385fsX4). Whether these mutations are hypomorphic or null for CDK5RAP2 protein is not known. Significantly, the S81X mutation is in CNN motif 1 of *CDK5RAP2*. CNN motif 1 has been shown to be important for the centrosomal functions of both mod20p and Cnn (Samejima et al., 2008; Zhang and Megraw, 2007). Furthermore, truncation of CDK5RAP2 protein after amino acid E385 may lead to loss of the conserved CNN motif 2 from CDK5RAP2 protein. How the functions of CNN motif 2 in cleavage furrow assembly in flies may translate into a function in humans is difficult to imagine but will be interesting to investigate.

Aims of my PhD

The aims of this thesis are to characterise the function(s) of CDK5RAP2 in vertebrate somatic cells. Data from CNN domain-containing proteins of yeast and fly, together with the identification of mutations in the *cdk5rap2* gene in patients with primary microcephaly, suggest that CDK5RAP2 will have an important centrosomal function in vertebrates. Although this thesis will not focus on the characterisation of the second human CNN-domain protein, Myomegalin, I will explore some aspects of Myomegalin function with respect to CDK5RAP2, in order to investigate if the two proteins can function redundantly.

Chapter 2: Materials and Methods

2.1 Cell Culture

HeLa (kind gift of Jon Pines, Gurdon Institute, Cambridge, UK), U251MG, HEK293T (from ATCC – American Type Culture Collection) and Phoenix cells (kind gift of Masashi Narita, CRUK Cambridge Research Institute, Cambridge, UK) were maintained in a standard medium of Dulbecco's modified eagle medium, supplemented with 10% Foetal Bovine Serum (FBS) and 1% penicillin-streptomycin. For maintenance of GFP-centrin1 HeLa cells (kind gift of Jon Pines), the standard medium was supplemented with 500 µg/ml G418. For HB2 cells (from ATCC), the standard medium was supplemented with 5 µg/ml hydrocortisone and 10 µg/ml insulin (both from Sigma). All human cell lines were maintained at 37°C. DT40 cells (kind gift of KJ Patel, MRC-Laboratory of Molecular Biology, Cambridge, UK) and derivatives were propagated at 40°C in RPMI, supplemented with 10% FBS, 5% chicken serum (Sigma), 50 µM β-mercaptoethanol and penicillin-streptomycin. Primary glioblastoma cell lines (kind gift of Colin Watts, Cambridge Centre for Brain Repair, Cambridge, UK) were maintained in Neurobasal A (NBA) medium (no phenol red) supplemented with 20 mM L-glutamine, 1% penicillin-streptomycin, 20 ng/ml Epidermal Growth Factor, 20 ng/ml Fibroblast Growth Factor, 5 µg/ml heparin, 2% B27 and 1% N2 (all from Invitrogen). These cell lines were grown on Extracellular Matrix (ECM)-coated flasks (see 2.1.1). All cells were grown at 5% CO₂, except HeLa cells which were grown at 6% CO₂. All tissue culture reagents were from Invitrogen, unless otherwise stated.

2.1.1 ECM-coating of flasks for primary glioblastoma cell lines

Neat ECM Gel solution (from Engelbreth-Holm-Swarm murine sarcoma; Sigma) was diluted 1/10 in NBA medium. 5 ml of this was added to a T-75 tissue culture flask and left to polymerise at room temperature (RT) for 10 minutes. Excess liquid was removed before flasks were used.

2.1.2 Primary cilium formation in HB2 cells

HB2 cells were seeded onto metasilicated coverslips (see 2.4.1) at 20% cell density. Cells were allowed to expand to confluency and then left for a further two days for primary cilia to form. Primary cilia were identified by immunostaining with anti-acetylated tubulin antibody (see Table 2.5 at the end of this chapter).

2.1.3 Synchronisation of HeLa cells

2.1.3.1 Synchronising cells in mitosis

Nocodazole (Sigma; 40 µg/ml stock in dimethyl sulphoxide (DMSO)) was added to HeLa cells at a final concentration of 40 ng/ml for 16 hours. Cells were then either processed for immunostaining (see 2.4) or mitotic cells were removed from the plate by a mitotic shake-off and cells were processed for Lambda Phosphatase treatment (see 2.11) or for immunoprecipitation (see 2.13).

2.1.3.2 Synchronising cells in G1/S

Cells were treated with 2 mM thymidine (Sigma, dissolved in MilliQ water) for 18 hours.

2.1.4 Brefeldin A treatment of HeLa cells

Brefeldin A (Sigma; 10 mg/ml stock in Methanol) was added to HeLa cells at 10 µM for 1 hour. Methanol alone was added as a vehicle control. After 1 hour, cells were fixed and processed for immunostaining (see 2.4).

2.1.5 Cold-induced depolymerisation of microtubules in HeLa cells

Microtubules were depolymerised by incubating coverslips on ice for 30 minutes. Coverslips were then washed in ice-cold Phosphate Buffered Saline (PBS – 2.68 mM KCl, 1.47 mM KH₂PO₄, 136.89 mM NaCl, 8.1 mM Na₂HPO₄), fixed in methanol (-20 °C) and processed for immunostaining (see 2.4).

2.2 Molecular Biology

DNA transformations were performed by 1 minute heat-shock at 42°C into chemically competent DH5 α *Escherichia coli*. All *E. coli* strains used in this study are listed at in Table 2.1

Table 2.1 List of *E. coli* strains used in this study

Name and source	Genotype	Purpose
DH5 α (NEB)	$\phi 80(lacZ)M15;recA;endA;hsdR17;fhuA2$	Standard cloning
Dam-/dcm- (NEB)	$dam13::Tn9(Cam^R),dcm-6;endA;hsdR2;mcrA, mcrB1;fhuA31$	Standard cloning if using methylation-sensitive restriction endonucleases
T7 Express (NEB)	$lacZ::T7gene1;[lon]ompT;sulA11;endA;(\Delta(mcrC^-mrr)114::1510 and R(mcr-73::miniTn10--Tet^s)2);fhuA2$	Protein expression

Plasmid extraction was carried out using a Qiagen Mini-Prep or HiSpeed Midi-prep kit, according to the manufacturer's instructions. Briefly, overnight bacterial cultures were lysed and cell debris and precipitated protein was removed by centrifugation. Clarified lysates were added to Qiagen DNA-binding columns. Plasmid DNA bound to the column was washed with 70% ethanol. DNA was eluted in MilliQ water (Millipore) and stored at -20°C. Gel extraction of PCR products and digested plasmid DNA was carried out using a Qiagen Gel Extraction kit, according to the manufacturer's instructions. Briefly, this involved dissolving agarose gel slices in a buffer containing a pH indicator to ensure DNA-binding to the column occurred at an optimal pH (pH \leq 7.5). DNA bound to the column was washed in 70% ethanol and then eluted in MilliQ water and stored at -20°C.

Restriction enzyme digests were performed using New England Biolabs (NEB) restriction enzymes.

Products of Polymerase Chain Reactions (PCRs) and Restriction enzyme digests were run on 1% agarose gels containing 0.5 µg/ml ethidium bromide (EtBr; Fisher Scientific) in 1xTBE (8.9 mM Tris pH 8.2, Boric acid 8.9 mM, 50 mM EDTA) buffer. If the expected product was less than 1 kb, 2% agarose gels were used. DNA base pair (bp) ladders (1 kb or 100 bp ladder (NEB)) were always run in parallel to confirm the size of products.

For ligations, the 5' ends of plasmid DNA were dephosphorylated to prevent vector self-ligation. Digested vector DNA was treated with Calf Intestinal Phosphatase (Roche) at concentrations recommended by the manufacturer. Ligations were performed using NEB T4 ligase. PCR products with A base-overhangs were ligated into the pGEM-T vector kit (Promega). Blunt-ended PCR products were ligated into pJet2.1 vector (Fermentas).

RNA extraction from vertebrate cells was carried out using the Qiagen RNeasy Mini Kit, according to the manufacturer's instructions. Briefly, cells were lysed and homogenised by vortexing. Ethanol was added to the lysates to improve binding to the RNA-binding column. Lysates were centrifuged through the column to allow RNA to bind. DNase digestion was performed on the column to remove contaminating genomic DNA. Column-bound RNA was then washed and eluted with RNase free water. RNA was stored at -20°C.

cDNA was prepared from total RNA using the Superscript II Reverse Transcriptase and random primers (Invitrogen), using 500 ng total RNA per reaction. Reactions were performed exactly as stated by the manufacturer, including the addition of RNaseOUT (Invitrogen) to the mixture. In addition, a negative control reaction with no Reverse Transcriptase (RT-) was carried out in parallel to check for genomic DNA contamination.

2.2.1 FLAG-tagging of CDK5RAP2

Fragments of *CDK5RAP2* were PCR amplified from human *CDK5RAP2* cDNA (kind gift of Geoff Woods, Cambridge Institute for Medical Research, Cambridge, UK), using primers shown in Table 2.4. PCR was carried out using Phusion high-fidelity

polymerase (NEB). Reactions were set up exactly according to manufacturer's instructions and the PCR conditions used were: 98°C 2 minutes, then 30 cycles of 98°C 10 seconds, 60°C 30 seconds and 72°C 6 minutes, followed by an extra elongation step at 72°C for 10 minutes and a final hold step at 10°C. PCR amplified fragments were run on an agarose gel to confirm the size and then gel extracted (see above). Gel-extracted PCR products were sub-cloned into pJet2.1 (Fermentas) and sequenced. PCR products were removed from pJet2.1 by restriction digest, run on agarose gels, gel extracted and finally sub-cloned into the pCMV-Tag2 vector (Stratagene). Final constructs were sequenced to confirm the FLAG-tag was in frame with the cDNA and that the cloning procedure had not introduced any DNA base changes.

2.2.2 Site-directed mutagenesis of FLAG-CDK5RAP2 constructs

Site-directed mutagenesis was performed using Phusion high fidelity polymerase (NEB) using complementary primers containing the mutation site flanked by arms of at least 12 bp each (see Table 2.4). PCR was performed on 0.5 µg of plasmid DNA and reactions were set up according to the manufacturer's instructions. PCR conditions used were: 98°C 2 minutes, then 30 cycles of 98°C 10 seconds, 60°C 30 seconds and 72°C 10 minutes, followed by an extra elongation step at 72°C for 20 minutes and a final hold step at 10°C. After the PCR was completed, 10% of the PCR mix was digested with DpnI restriction enzyme in a 20 µl reaction, containing 40 U of enzyme, for 1 hour at 37°C. This was to remove methylated (template) DNA. 10 µl of this digest was then transformed into chemically competent DH5α *E. coli* (as above; Table 2.1). The next day, colonies were picked and plasmid DNA prepared by Qiagen Mini Prep. Plasmid DNA was sequenced to determine which clones had the desired mutation. The mutated cDNA was then sub-cloned into a clean vector background (i.e. one that had not been through multiple PCR cycles).

2.3 Generating anti-human CDK5RAP2 antibodies

An N-terminal Maltose Binding Protein (MBP)-fusion protein of amino acids 40-375 of CDK5RAP2 was generated using the cloning procedures outlined in 2.2.1. The

CDK5RAP2 fragment was cloned in frame into the pMal vector (NEB). For protein expression, pMal-CDK5RAP2 was transformed into T7 Express Competent *E. coli* (NEB: Table 2.1) by heat-shock transformation (see 2.2). A 1 litre culture of bacteria was used for protein purification. 0.1 mM IPTG was added to the culture to induce protein expression. 4 hours after IPTG addition, bacterial cells were pelleted. All subsequent purification steps were performed at 4°C. Cell pellets were washed twice in ice-cold 1xPBS, resuspended in Bacterial Lysis buffer (50 mM Tris pH 8.0, 1 mM EDTA 100 mM KCl) and 100 µg/ml of lysozyme (Amersham) added. Cells were sonicated twice (40% output, 1 minute pulse) and cell debris and DNA removed by centrifugation at 16000g for 20 minutes at 4°C. Amylose resin (Amersham) was equilibrated with Bacterial Lysis buffer and the clarified lysates added to the resin and rotated for 1 hour. After binding of MBP-CDK5RAP2 to the amylose resin, the amylose column was washed in bacterial lysis buffer containing 0.05% Tween20, three times for 10 minutes each. A final wash was done in the absence of Tween20. MBP-CDK5RAP2 was eluted by batch elution with 10 mM Maltose (Amersham; in Bacterial Lysis buffer). The concentrations of the peak and side-fractions were determined by Bradford assay (Bradford, 1976) and then pooled.

To prepare the protein for antibody injections, half of the purified protein was run on a 1-well Bis-Tris NuPage protein gel (Invitrogen; see 2.7). The gel was stained with Coomassie Blue (2% Coomassie Blue, 10% acetic acid and 50% methanol in MilliQ water) for 30 minutes before destaining with Destain solution (7.5% acetic acid, 5% methanol in MilliQ water) overnight at RT. The destained gel was rinsed extensively with MilliQ water and the band of protein cut out. The protein that was not subjected to gel electrophoresis was mixed with the gel piece and the mixture homogenised using a drill. This mixture was injected into rabbits (Eurogentech).

Antibodies were purified from sera against the MBP-CDK5RAP2 fusion protein, as described in (Huang and Raff, 1999). Briefly, the fusion protein was coupled to covalently coupled to either Affigel 15 resin (Bio-Rad). Immune serum was first depleted of anti-MBP antibodies by passing the serum over an Amino-link-MBP column until no anti-MBP antibodies remained. Anti-CDK5RAP2 antibodies were then purified by passing the serum over the column of MBP-CDK5RAP2 fusion protein. The column was washed extensively with PBS/0.5 M KCl, and antibodies were eluted in 0.1 M glycine, pH 2.2. The antibodies were neutralized with 1 M Tris pH 8.5. Glycerol was added to 50%, and antibodies were stored at -20°C.

2.4 Immunostaining

Adherent cells were grown on metasilicated coverslips (see 2.4.1) and suspension cells were spotted onto poly-L-lysine-coated coverslips (see 2.4.2) and left to settle for 15 minutes at 37°C/40°C (human cells/DT40). Coverslips were washed briefly in 1xPBS before fixation.

For visualisation of centrosomal proteins, cells were fixed in methanol (MeOH) at -20°C for 5 minutes, washed in PBST (PBS/0.1% Tween20) for 3 minutes at RT and then blocked in Blocking solution (5% BSA in PBS) for 5 minutes at RT. For visualisation of kinetochore proteins, cells were fixed in either 4% formaldehyde (Form) in PHEM buffer (60 mM PIPES pH 6.8, 25 mM HEPES, 10 mM EGTA and 2 mM MgCl₂) at 37°C for 5 minutes, or 3% paraformaldehyde (PFA) in PHEM for 20 minutes at RT. Cells fixed in formaldehyde or paraformaldehyde were then permeabilised in PBS/0.2% TritonX-100 for 5 minutes at RT, before blocking as above. Specific fixation conditions for the antibodies used are listed in Table 2.5.

Primary antibodies (listed in Table 2.5) were diluted to 0.25-1 µg/ml in blocking solution and incubated on coverslips for 2 hours at 37°C or at 4°C overnight. After incubation in primary antibody, coverslips were washed 3 times for 5 minutes each in PBST. Alexa 488-, 555- or 637-coupled secondary antibodies (Invitrogen) were used at a final concentration of 1 µg/ml for 1 hour at 37°C. Coverslips were then washed 3 times for 5 minutes each in PBST and once for 5 minutes in MilliQ water before mounting in Prolong Gold antifade mounting medium (Invitrogen) containing 1 µg/ml of Hoechst 33258 (Sigma).

2.4.1 Making metasilicated coverslips

13 mm round coverslips were boiled in Silicating solution (78 g of Sodium Metasilicate and 8 g Sodium Hexametaphosphate dissolved in 1 l of MilliQ water) for 20 minutes. Coverslips were rinsed in MilliQ water and then boiled in MilliQ water for 20 minutes. Coverslips were then washed in absolute ethanol, dried on Whatman filter paper, collected in a glass Petri dish and oven-baked for 90 minutes.

2.4.2 Making poly-l-lysine coated coverslips

Poly-l-lysine (Sigma) was dissolved in MilliQ water to a final concentration of 2 mg/ml and filter-sterilised through 0.22 μm filters (Millipore). Poly-l-lysine solution was spotted onto glass coverslips and incubated at 37°C for 30 minutes. Poly-l-lysine solution was then removed and coverslips were washed 6 times in MilliQ water. Coverslips were left to dry at 37°C.

2.5 Image acquisition and analysis

2.5.1 Image acquisition

For fixed cell analysis, images were acquired as Z-stacks (0.4 μm steps) using a Nikon Eclipse 90i microscope fitted with a Nikon Eclipse C1Si camera. Images were acquired using Nikon EZ-C1 software. Human cell lines and DT40 cells were imaged using a Nikon 60x oil/1.40 Numerical Aperture (N.A.) and Nikon 100x oil/1.40 N.A. objective, respectively. Images were imported into Volocity 4.0 (Improvision) and exported as 2D volume-rendered images into Photoshop CS3 (Adobe). Images were adjusted to use the full range of pixel intensities in Photoshop CS3. All images from a single experiment were treated in exactly the same way.

For live imaging of GFP-centrin1 in HeLa cells, control hp1-1 and CDK5RAP2 hp1d clonal cells were plated into 1 well each of an 8-well glass bottomed chamber slide (LabTek) and transfected with GFP-centrin1 (Piel et al., 2000). 24 hours later, the medium was changed to Liebowitz medium (no Phenol Red, +10% FBS; Invitrogen) and cells were placed at 37 °C in a Tokai hit incubation chamber (without CO₂) on a spinning disc confocal system (Improvision), mounted on an inverted microscope (Nikon Eclipse TE2000-S) equipped with a C9100-13 EM-CCD digital camera (Hamamatsu). Imaging was performed with a Nikon 60x oil/1.40 N.A. objective. Cells were imaged every 5 minutes, taking Z-stacks at each point – 1 μm apart, for 4 hours. Images were processed and analysed using Volocity (Improvision).

For time-lapse imaging of GFP-tubulin (kind gift of Peter Coopman, Centre National de la Recherche Scientifique UMR5539, Université Montpellier II, Montpellier, France) or mCherry-tubulin/GFP-PACT (kind gifts of Viji Draviam (Dept of Genetics, University of Cambridge, UK) and Sean Munro (MRC-Laboratory of Molecular Biology, Cambridge,

UK); (Gillingham and Munro, 2000)) expressing DT40 cells, transiently transfected DT40 cells (see 2.14.5) were settled onto Ibidi 60 μm dishes. Cells were imaged in Liebowitz medium containing 10% FBS. Imaging was performed with a Nikon 100x oil/1.40 N.A. objective on a spinning disk confocal (see above). Cells were kept at 40°C, without CO₂. Images were acquired either at 1 or 3 minute intervals as Z-stacks (1.5 μm steps) using Volocity 4.0. 2D volume-rendered image sequences were exported as QuickTime files. For movie stills, snapshot images were taken in Volocity and were processed as for fixed-cell analysis.

For differential interference contrast (DIC) microscopy of DT40 cells, images were acquired on a Nikon Eclipse TE2000-E microscope fitted with a Nikon Digital Sight Camera (DS-2MBW) using a 60x oil/1.40 N.A. objective (Nikon) with the NIS-Elements AR software from Nikon. Images were acquired every 15 minutes, at 40°C and 5% CO₂.

2.5.2 Image analysis

For all quantification of fixed cells, images were taken at sub-saturation levels on the Nikon Eclipse 90i confocal microscope and imported into Volocity (Improvision) for measurements.

1. *Quantifying AKAP450 levels in control hp1-1 and CDK5RAP2 hp1d centrosomes (HeLa cells)*

A 40-100% intensity cut off was set in the centrin-3 channel in Volocity. This selected centrioles only. The mean AKAP450 intensity in that area was taken as a measure of AKAP450 levels in the centrosome.

2. *Quantifying levels of AKAP450 in myomegalin siRNA targeted mitotic cells (U251MG cells)*

A defined region of interest (ROI) was positioned over mitotic centrosomes in Volocity. The mean intensity of AKAP450 fluorescence in these ROIs was taken as a measure of AKAP450 levels in the centrosome. This method also ensured that the volumes measured in each image were the same.

3. *Quantifying volume of α -tubulin (DT40) and γ -tubulin (HeLa and DT40 cells)*

To quantify α - and γ -tubulin signals volumes that contained α -tubulin-staining intensity over the cut-off value of '1500' or γ -tubulin-staining intensity over the cut-off value of '900', thus defining α - and γ -tubulin-positive volumes, were selected. Volumes were converted to μm^3 . In the case of α -tubulin, the cut-off value was

determined to allow separation of centrosomal asters from chromatin-associated microtubule asters. In the case of γ -tubulin the cut-off value allowed me to exclude contribution from spindle-bound protein.

4. *Quantifying CDK5RAP2 and Protein G levels (DT40 cells)*

To quantify CDK5RAP2 and Protein G levels in the centrosomes of wild-type, tag-cnn1^{lox} and cnn2^{-/-} cells, γ -tubulin-positive 3D volumes (cut-off value of 1300) were selected and the mean signal intensities of CDK5RAP2 or of Protein G were determined across the volume.

2.6 Electron Microscopy

2.6.1 Fixing and embedding cells

2 x 10⁶ DT40 cells were pelleted and washed once in pre-warmed (37°C) PHEM buffer. Cell pellets were fixed in pre-warmed (37°C) 1% glutaraldehyde (EM grade, Sigma) in PHEM for 1 hour at RT. Cell pellets were washed once in 0.1 M Sodium Cacodylate buffer, pH 7.2, 5 minutes at RT. Pellets were post-fixed in 1% Osmium Tetroxide (Agar Scientific) in 0.1 M Sodium Cacodylate buffer pH 6.8, for 1 hour at RT. Pellets were then washed 2 times for 30 minutes each at RT in 0.1 M Sodium Cacodylate buffer pH 6.8. Pellets were then transferred to scintillation vials using a wooden spatula. Pellets were dehydrated through an ethanol series: 10 minutes each of 50%, 70%, 90% and 3 x 100% ethanol.

Epon embedding medium (Epoxy – Embedding kit, Fluka) was made up according to the manufacturer's exact instructions. Cell pellets were equilibrated in 1:1 100% ethanol:final epoxy mixture and then in 1:2 100% ethanol:epoxy embedding medium, each for 90 minutes at RT. Small cell pellets were then moved to embedding moulds and immersed in epoxy embedding medium. Sample containing moulds were polymerised at 45°C for 12 hours and then 60°C for 24 hours. Blocks were left at RT for 2 days to air-cure, to improve the quality of the sections.

2.6.2 Serial sectioning and post-staining grids

All sectioning was performed on a Reichert-Jung Microtome Ultra-cut 701701 (Leica) using a diamond knife. Serial sections were collected onto Formvar-coated copper grids. Grids were post-stained in 1% Uranyl Acetate (see 2.6.2(i)) in 50% Methanol

for 15 minutes at RT. Grids were then washed in a stream of deionised water and blotted dry with Whatman filter paper. Grids were then stained in Reynolds' Lead Citrate (Reynolds, 1963) for 2 minutes at RT and washed in a stream of deionised water again before being washed in 20 mM NaOH for 5 seconds, washed in deionised water and dried with Whatman filter paper.

2.6.2(i) Making up Uranyl Acetate solution:

A 2% stock solution of Uranyl Acetate was made up in deionised water. The solution was incubated in a boiling water bath to allow it to dissolve. The final mixture is stored in the dark at RT. For 1% Uranyl Acetate solution, the 2% stock solution was mixed 1:1 with 100% methanol.

2.7 Western blotting

Samples for Western blotting were boiled in sodium dodecyl sulphate (SDS)-loading buffer (200 mM Tris-HCl pH 6.8, 400 mM dithiothreitol (DTT), 8% SDS, 0.4% Bromophenol blue and 50% glycerol). Proteins were separated on 3-8% Tris-Acetate or 4-12% Bis-Tris NuPage Novex precast gels (Invitrogen) and transferred to nitrocellulose (BioRad) in 1XTransfer Buffer (Invitrogen) plus 20% methanol at a constant voltage of 40 V for 90 minutes at RT. Membranes were blocked in 10% milk in Tris Buffered Saline (TBS, 50 mM Tris-HCl pH 7.4, 150 mM NaCl) at RT for a minimum of 2 hours. After blocking, membranes were incubated in primary antibody (listed in Table 2.5) at 0.25-1 µg/ml final concentration in 5% milk in TBS, overnight at 4°C. Unbound primary antibody was removed with 3 times 20 minutes washes in TBST (TBS/0.05% TritonX-100). Horse Radish Peroxidase (HRP)-coupled secondary antibodies (Dako cytometry) were used 1/2000 in 5% milk/TBS for 1 hour at RT. Membranes were washed 3 times for 20 minutes each in TBST and antibody binding was detected by LumiLight chemiluminescence kit (Roche). The exception to this procedure is when immunoblotting was performed with anti-protein-G-HRP antibody (AbCam). Since this antibody is directly conjugated to HRP, the incubation in secondary antibody is not required.

2.8 Transient transfection of DNA into human cell lines

Cells were seeded onto metasilicated coverslips (for immunostaining, see 2.4) or into 6-well plates (for immunoprecipitations, see 2.13) the day before transfection such that they would be 80% confluent on the day of transfection. Cells were seeded in standard medium (see 2.1) but without the addition of penicillin-streptomycin. Plasmid DNA was transfected into cells using Lipofectamine 2000 (Invitrogen). Plasmid DNA and Lipofectamine 2000 were diluted in fresh OPTIMEM (Invitrogen), using volumes and concentrations recommended by the manufacturer. Generally, for transfection in a 24-well, 0.8 μg DNA and 2 μl of Lipofectamine 2000 were dissolved in 100 μl of OPTIMEM. Transfected cells were incubated at 37°C. Cells were further processed 24 or 48 hours after transfection.

2.9 siRNA transfection into human cell lines

Cells were seeded onto metasilicated coverslips or into 6-well plates the day before transfection such that they would be 40% confluent on the day of transfection. Cells were washed 3 times in PBS and put into fresh OPTIMEM (Invitrogen). Per 24-well, 15 pmol of silencing RNA (siRNA) was transfected using Oligofectamine (Invitrogen), using volumes and concentrations recommended by the manufacturer. 4 hours after transfection, the medium was changed. Cells were further processed 48 or 72 hours after transfection. siRNA target sequences used in this study are listed in Table 2.2.

Table 2.2 siRNA targets used in this study

Target	Target Sequence 5'-3'	siRNA ID	Source
hsAKAP450	AAATCCCTTGCCAGCACATGA		Ambion (custom) (Larocca et al., 2004)
hsCDK5RAP2	CCTAAAGCTCCGCATCTAT	132391	Ambion
hsMyomegalin	1. CTAACGAGCTGGAGAAATA 2. GAAGGGAATAGTAACTTA 3. AGAGCGAGATCATGACTTA 4. GCAAGAAAATGGTCCCTTA	M-021870-00-0005	Dharmacon SMARTpool
Negative control 1	N/A	4611	Ambion

2.10 Retroviral shRNA

110 bp oligonucleotides containing short hairpin RNAs (shRNAs) targeting CDK5RAP2, and their corresponding mismatch controls, were designed as follows. Target sequences were selected using the Biopredsi design tool at www.biopredsi.org/start and shRNAs were designed using the Hannon lab website at <http://katahdin.cshl.org:9331/homepage/siRNA/RNAi.cgi?type=shRNA>. Targeted sequences for the human hairpins are shown in Table 2.3. XhoI and EcoRI overhangs were added for direct cloning into the modified MSCV-miR30puro vector (kind gift of Masashi Narita, CRUK Cambridge Research Institute, Cambridge, UK). The final 110 bp oligonucleotides were produced by Sigma. Oligonucleotides were annealed by incubating 0.25 µg/ml of each primer in 1xAnnealing Buffer (5 x stock: 500 mM potassium acetate, 150 mM HEPES-KOH pH 7.4, 10 mM magnesium acetate) and incubating on a PCR machine at 95°C for 5 minutes, 70°C for 10 minutes followed by a ramp from 70°C to 4°C (-0.5°C every 2.5 minutes). Annealed oligonucleotides were sub-cloned into EcoRI/XhoI digested MSCV-miR30puro vector. Retroviruses were packaged using amphoteric Phoenix cells and target cells were infected as shown previously (Serrano et al., 1997). Cells with stable integration were selected with 3 µg/ml puromycin (Sigma) for 3 days.

For generating single cell clones, HeLa cells were trypsinised and transferred to 150 mm plates after viral transfection and selected in puromycin for 10 days. Single colonies were transferred to 24-well plates using cloning cylinders (Sigma). Stable, single cell clones obtained in this way (for example control hp1-1 and CDK5RAP2 hp1-d cell lines (see Chapter 3)) were maintained in 3 µg/ml puromycin. Knockdown of CDK5RAP2 was confirmed both by immunostaining (see 2.4) and Western blotting (see 2.7) of protein lysates.

Table 2.3 Target sequences of human CDK5RAP2 for shRNA

Target name	shRNA target sequence 5'-3'
hCDK5RAP2 hp1	GAAGGAGAATGACAAATTA
hCDK5RAP2 control hp1	GAAGGATAAGGACACATTA
hCDK5RAP2 hp2	CCGTGATCTTAGAAATGAA
hCDK5RAP2 control hp2	CCGTGCTCTGAGAACTGAA

2.11 Lambda Phosphatase Treatments

Asynchronous HeLa cells or HeLa cells arrested in mitosis (see 2.1.3) were washed in ice-cold PBS and cell pellets divided into three. The three samples were treated as such: one sample had nothing added, one sample had PhosSTOP added and the third had Lambda Phosphatase added. Cell pellets were lysed in 150 mM NaCl, 50 mM Tris-HCl pH 7.4, 1 mM EDTA, 0.5% NP-40 and protease inhibitor cocktail (Sigma). PhosSTOP (Roche) was included in the lysis buffer of one of the three samples (+PhosSTOP on Western blot in Figure 3.3.5). Cells were lysed by passing 15 times through a 23G needle. Lysates were clarified by spinning at 14000g for 15 minutes at 4°C. After lysis, Lambda Phosphatase buffer and MnCl₂ were added to all three lysates. 1 µl of Lambda Phosphatase (per 100 µl of lysate) was added to one sample (+PPase, Figure 3.3.5). All tubes were incubated at 30 °C for 1 hour. After 1 hour, 4xSDS-loading buffer was added to each sample and samples prepared for Western blotting (see 2.7).

2.12 Microtubule-pelleting assay

Whole cell extracts were prepared by washing HB2 cells twice in ice-cold PBS and adding 0.5 ml lysis buffer (50 mM Tris-HCl pH 7.4, 5 mM MgCl₂, 0.1 mM EGTA, 0.5% Triton X-100, 1:1000 protease inhibitor cocktail (Sigma)) per 100 mm plate. Cells were rocked at 4°C for 10 minutes and scraped into 1.5 ml tubes. Samples were rotated at 4°C for 15 minutes and passed through a 23G needle to homogenise cells. Samples were centrifuged at 16000g at 4°C for 15 minutes to pellet unbroken nuclei and the supernatant transferred to a clean tube. The extract was pre-cleared by ultracentrifugation in a TLA100 (Beckman Coulter) at 189000g for 20 minutes at 4°C. The supernatant was transferred immediately to a clean tube on ice. Extracts were split into two: a 'control extract' and a 'Taxol extract'. To the Taxol extract, 0.5 mM MgGTP was added. 2 mM MgATP was added to both extracts and extracts were warmed to RT. 5 µM Taxol (Sigma) was added to the Taxol extract, which was incubated for 2-3 minutes before an additional 15 µM Taxol was added. In addition, 0.2 mg/ml of Taxol-stabilised microtubules (see 2.12.1) was added to the Taxol extract and 0.2 mg/ml non-Taxol-treated tubulin was added to the control extract (see

2.12.1). Both extracts were incubated for 30 minutes at 30°C. The polymerised mixture was layered onto a 1 M sucrose cushion in BRB80 buffer (80 mM PIPES pH 6.8, 1 mM MgCl₂ and 1 mM EGTA) containing 0.5 mM ATP, protease inhibitor cocktail and with or without 10 µM Taxol. Microtubules were pelleted at 69500g in a TLA100 for 20 minutes at 22°C. The supernatants were removed and saved for Western blot analysis. The microtubule pellet was washed twice in BRB80 and resuspended in 1xSDS-loading buffer to 1/5th volume of the supernatant. All samples were analysed by Western blotting (see 2.7).

2.12.1 Making Taxol-stabilised microtubules

To make Taxol-stabilised microtubules, purified tubulin (Cytoskeleton) was diluted to 2 mg/ml in BRB80 (80 mM PIPES pH 6.8, 1 mM MgCl₂ and 1 mM EGTA) with 1 mM GTP and 1 mM DTT and incubated on ice for 5 minutes. The mixture was warmed to 37°C and 1:100 of 0.02 mM Taxol in DMSO was added. This was incubated for 5 minutes at 37°C before a further 1:100 volume of 0.2 mM Taxol was added and incubated for a further 5 minutes at 37°C. Finally, 1:100 volume of 2 mM Taxol was added and incubated for 15 minutes at 37°C. For the non-Taxol treated sample, no Taxol was added but the extract was incubated at 37°C.

2.13 Immunoprecipitation

2.13.1 Cross-linking antibodies to beads

Immunoprecipitations were carried out using magnetic Protein G Dynabeads (Invitrogen). Beads were washed twice in 0.5 ml Citrate Phosphate buffer, pH 5.0 (4.7 g Citric acid and 9.2 g Dibasic Sodium Phosphate dehydrate dissolved in 1 l of MilliQ water). 10 µg of primary antibody in 100 µl total volume of Citrate Phosphate buffer, pH 5.0 was added to 20 µl of beads and incubated at RT for 1 hour, with gentle agitation. Beads were washed 3 times in 0.5 ml of Citrate Phosphate buffer/0.01%Tween20, followed by two washes in 1 ml 0.2 M triethanolamine, pH 8.2. Antibodies were crosslinked to beads by resuspending in 1 ml of freshly-made 20 mM dimethyl pimelimidate x 2HCl (Sigma) in 0.2 M triethanolamine, pH 8.2 and

incubating at 20°C for 1 hour, with gentle agitation. The reaction was stopped by removal of the crosslinker and addition of 50 mM Tris-HCl pH 7.4 for 15 minutes at RT. Uncrosslinked antibodies were removed by a 10 minutes wash in 0.1 M glycine pH 2.2. The beads were brought back to neutral pH by the addition of 0.1 M Sodium Phosphate buffer, pH 8.0 (5.3 ml 0.2 M sodium phosphate monobasic, 94.7 ml 0.2 M sodium phosphate dibasic in 100 ml MilliQ water). Beads were washed 2 times in PBS/0.01%Tween20 and stored in PBS/0.01%Tween20 containing 0.04% sodium azide at 4°C until needed.

2.13.2 Coimmunoprecipitation reaction

Cells were washed 2 times in ice-cold PBS and lysed in Immunoprecipitation Lysis Buffer (25 mM Tris-HCl, pH 7.4, 0.5% NP-40, 100 mM NaCl, 5 mM MgCl₂, 5 mM NaF and 1 mM DTT) plus protease inhibitor cocktail (Sigma) at 4°C by passing through a 23G needle. Lysates were centrifuged at 16000g at 4°C for 15 minutes to remove unbroken nuclei. 1/5th of the sample was removed as 'Input'. Dynabeads covalently coupled to antibody were washed 3 times for 5 minutes each in Immunoprecipitation Lysis Buffer before use. Lysates were incubated with antibody-coupled Dynabeads for 2 hours at 4°C. After this time, supernatants were removed and kept for Western blot analysis. Dynabeads were washed 3 times for 5 minutes each in Immunoprecipitation Lysis Buffer. Antibody-bound proteins were eluted at low pH by the addition of 0.1 M glycine, pH 2.2 for 15 minutes at 4°C. Eluates were removed and brought back to neutral pH by the addition of 1/10th volume of Tris-HCl buffer, pH 8.0. 4xSDS-loading buffer was added to all samples that were then processed for Western blot analysis (see 2.7).

2.14 DT40 methods

2.14.1 Design and creation of targeting constructs

Primers to amplify the left and right arms of the targeting constructs are listed in Table 2.4. These primers contained restriction sites at their 5' ends in order to sub-clone the PCR fragments into plasmids. Genomic DNA was extracted from wild-type (wt) DT40 cells using the Puregene cell kit (Qiagen), according to the manufacturer's

instructions. Briefly, cells were lysed and RNA removed by digestion with RNase A at 37°C for 5 minutes. Protein precipitates and cell debris were removed by centrifugation. Genomic DNA was precipitated by the addition of 100% isopropanol and precipitated DNA pelleted by centrifugation. Pelleted DNA was washed in 70% ethanol and air-dried. Air-dried DNA pellets were resuspended in MilliQ water by incubation at 65°C for 1 hour. Resuspended genomic DNA was stored at 4°C (short-term, <one week) or -20°C (long-term).

Homologous left and right arms were PCR amplified from genomic DNA using LA Taq DNA polymerase (Takara). PCRs were set up exactly as stated by the manufacturer, using LA PCR Buffer II (Mg²⁺ free) and adding MgCl₂ to the reaction. PCR conditions used were: 94°C 1 minute, then 30 cycles of 98°C 5 seconds and 68°C 5 minutes followed by an extra elongation step at 72°C for 10 minutes and a final hold step at 10°C. 68°C was used as a combined annealing and extension step, as recommended for LA Taq polymerase. If no product was obtained, the annealing/extension temperature was decreased 1°C per PCR to as low as 65°C. PCR products were run on an agarose gel, gel-extracted (see 2.2) and the gel-extracted DNA was sub-cloned into pGEM-T (Promega) and sequenced. PCR products were then digested out of the pGEM-T vector using the appropriate restriction enzymes (see Table 2.4). Restriction digests were run on an agarose gel to confirm the digestion and the homologous arms were gel-extracted. Gel-extracted, homologous arms were sub-cloned into pSKBsr, pSKNeo or pSKPuro (Arakawa et al., 2001). For GS-TAP tagging, the GS-TAP tag (kind gift of KJ Patel) (Burckstummer et al., 2006) was also sub-cloned into this vector, immediately after the left arm and in-frame with the end of the gene.

Prior to transfection into DT40 cells, plasmid DNA carrying the targeting construct was linearised with restriction enzyme digestion for 2 hours. A sample of the restriction digest was taken and run on an agarose gel to confirm linearisation. Linearised DNA was precipitated with 70% ethanol at -20°C for 1 hour, centrifuged to pellet precipitated DNA, washed in 70% ethanol, air-dried and then resuspended in 300 µl of sterile PBS.

2.14.2 Targeted integration of DNA into DT40

For transfection of targeting constructs into DT40 cells, 2×10^7 cells were washed in ice-cold PBS, transferred to a pre-chilled 4 mm electrocuvette (Biorad) containing 60 μg of linearised plasmid DNA in 300 μl sterile PBS and incubated on ice for 10 minutes. Cells were electroporated at 550 V and 25 μF and immediately transferred into 65 ml of pre-warmed medium. 100 μl of the cell-containing medium was aliquotted into each well of 6 times 96-well plates. After 24 hours recovery, antibiotic was added for selection of stable integrants. Final antibiotic concentrations used were 0.5 $\mu\text{g}/\text{ml}$ puromycin (Sigma), 1.5 mg/ml G418 and 50 $\mu\text{g}/\text{ml}$ Blastcidin-S HCl (both from Invitrogen). Resistant colonies were picked after 7 days selection and screened for targeted integration by PCR on genomic DNA using the primers listed in Table 2.4 and LA Taq enzyme (Takara) and the protocol as detailed in 2.14.1.

2.14.3 Non-targeted integration of DNA into DT40

For non-targeted integration of DNA into DT40 cells, 1×10^7 cells were washed in ice-cold PBS, transferred to a pre-chilled 4 mm electrocuvette (Biorad) containing 10 μg of plasmid DNA and adjusted to a final volume of 600 μl with sterile PBS. The mixture was incubated on ice for 10 minutes. Cells were electroporated at 250 V and 950 μF and immediately transferred into 32 ml of pre-warmed medium. 100 μl of this medium was aliquotted into each well of 3 times 96-well plates. After 24 hours recovery, antibiotic was added for selection of stable integrants (see 2.14.2).

2.14.4 Cre-mediated recombination of loxP sites in DT40

3×10^6 DT40 cells were washed once in 1xPBS and resuspended in 100 μl Amaxa Nucleofection solution T (Lonza) containing 2 μg of the cre recombinase expressing plasmid, pCaggsCre (kind gift of KJ Patel). Cells were nucleofected on program B-009 and immediately transferred to 4 ml of pre-warmed DT40 medium in a 6-well plate. Cells were left to recover for 24 hours. The next day, viable cells were counted using a haemocytometer and trypan blue exclusion. Cells were serially diluted and plated into three 96-well plates at a density of 1 cell/well. Plates were left at 40°C for 7 days. After this time, 24 single-cell colonies were picked and transferred to fresh medium in a 24-well plate. Cells were expanded and replica plated to two 24-well

plates. The appropriate drug was added singly to each of the replica plates and plates were incubated at 40°C for 7 days. After this time, colonies that were no longer drug-resistant were expanded and confirmed for loss of the resistance cassettes by PCR on genomic DNA template.

2.14.5 Transient transfection of DNA into DT40

Cells were transfected the same way as in 2.14.4. After 24 hours recovery, cells were processed for either live imaging (see 2.5) or immunostaining (see 2.4).

2.14.6 DT40 Centrosome purification

Centrosome purification was performed as in (Bornens and Moudjou, 1999) with the following modifications. Briefly, 8×10^7 tagAKAP-wt and tagAKAP-cnn1^{lox} DT40 cells were arrested in mitosis by incubation with 500 ng/ml nocodazole for 12 hours. The microtubule and actin cytoskeletons were then depolymerised by treatment with 1 µg/ml nocodazole (final) and 1 µg/ml Cytochalasin D for 1 hour at 40°C. Cell lysates were spun onto 2 ml of 60% sucrose cushion in a SW40 rotor (Beckman Coulter) at 10000g for 30 minutes. The discontinuous sucrose gradient consisted of 1 ml 70% sucrose, 600 µl 50% sucrose and 600 µl 40% sucrose. Sucrose buffers were made up w/v in 10 mM PIPES, pH 7.2, 0.1% Triton X-100 and 0.1% β-mercaptoethanol. After addition of the centrosome-containing supernatant onto this gradient, samples were centrifuged for 2 hours at 120000g in a SW55 Ti rotor (Beckman Coulter). 400 µl fractions were collected by punching a small hole in the bottom of the centrifuge tube and collecting droplets. After addition of 10 mM PIPES-KOH, pH 7.2, centrosomes in each fraction were pelleted at 115000g in the MLA 55 rotor in a Beckman ultracentrifuge. The supernatant was discarded and centrosome pellets were resuspended in 40 µl boiling 1xSDS-Loading buffer. Samples were analysed by Western blotting (see 2.7).

2.14.7 Microtubule regrowth in DT40 cells

Microtubules were depolymerised by addition of 2 µg/ml nocodazole for 2 hours at 40°C. Cells were washed three times in ice-cold 1xPBS (supplemented with 1:1000 volume DMSO) by centrifuging at 1100g for 2 minutes. Cells were then resuspended in 100 µl pre-warmed culture medium and spotted onto poly-L-lysine-coated

coverslips. Coverslips were incubated at 40°C for 5 minutes before methanol fixation. Fixed cells were immunostained for centrin-3 and phospho-histone H3 (see 2.4). After staining with secondary antibodies, coverslips were washed extensively for 4 hours with PBST. Cells were then post-stained with Dm1 α antibodies.

2.14.8 Taxol treatment of DT40 cells

DT40 cells were treated with 6 μ M of the Cdk1 inhibitor RO3306 (Calbiochem) for 3 hours to ensure that cells to be scored for spindle morphology entered mitosis in the presence of Taxol. Cells were washed three times in pre-warmed culture medium to remove RO3306 and resuspended in fresh medium containing either 5 nM Taxol or DMSO. Cells were incubated in Taxol or DMSO for 2 hours before being fixed and processed for immunostaining (see 2.4).

2.14.9 Cell cycle analysis

For analysis of cell cycle profiles, samples were centrifuged at 800g for 3 minutes and cell pellets were resuspended in 0.75 ml 70% ethanol and fixed at -20°C overnight. Tubes were topped up with 1xPBS and spun at 800g for 5 minutes. The supernatant was removed and cell pellets were resuspended in 0.5 ml of 1xPBS/0.1%TritonX-100 containing 20 μ g/ml propidium iodide (Sigma) and 0.2 mg/ml RNase A (Sigma). Cells were filtered into 5 ml BD-falcon tubes through the filter cap to remove cell clumps. Samples were analysed using BD FACS Calibur and FlowJo. Data was further analysed using the “Cell Cycle” platform on FlowJo.

2.14.10 DT40 clonogenic assay

DT40 cells were counted using a haemocytometer and trypan blue exclusion. Cells were then serially diluted and plated onto a 96-well plate at a density of 40 cells/plate. Plates were incubated at 40°C for 7 or 10 days and the number of colonies scored.

2.14.11 Ionising radiation assays

To assess the efficiency of G2 arrest following DNA damage, 1×10^6 cells were either irradiated with 20 Gy (gamma-irradiator, ^{137}Cs source) and then treated with 1 μ g/ml nocodazole for 10 hours, or treated with nocodazole only or DMSO only for 10 hours.

Cells were then fixed in methanol, processed for immunostaining (see 2.4) and stained with anti-phosphohistone H3 antibodies and Hoechst 33258. Tiled images of slides were acquired using the iCys Compucyte system coupled to an Olympus IX71 microscope, fitted with a Sony 3CCD camera. Images were acquired using a 40x air/0.75 N.A objective (Olympus). Analysis of phosphohistone H3-positive cells was carried out in an automated fashion using the iCys software.

Table 2.4 Primers used in this study

Primer name	Sequence 5' - 3'	Purpose
DT40		
Exon 43b reverse (D in Fig. 5.1.1A)	TGTTCTTCTTTAACCTCC	To check expressed CDK5RAP2 in DT40
Exon 43a forward (B in Fig. 5.1.1A)	TGGTTTTAACTCATGATG	To check expressed CDK5RAP2 in DT40
Exon 44 reverse (E in Fig. 5.1.1A)	TTTTCCAGGTCTGAGAGC	To check expressed CDK5RAP2 in DT40
Exon 42 forward (A in Fig 5.1.1A)	GATGAAGGAATGAAAGCA	To check expressed CDK5RAP2 in DT40
Exon 43a Reverse (C in Fig. 5.1.1A)	TTACTTCCAGGTTTCCTC	To check expressed CDK5RAP2 in DT40
cep215 TAG LAF EcoRI (Fig. 5.1.3C)	<u>GAATTC</u> GCAGTTTCTAGTCCAG	To amplify LA for CDK5RAP2 TAP tag
cep215 TAG LAR XbaI (Fig. 5.1.3C)	<u>TCTAGAG</u> GAGAATCCTTTTTTTGCT	To amplify LA for CDK5RAP2 TAP tag
cep215 TAG RAF SpeI (Fig. 5.1.3C)	<u>ACTAGT</u> TGAAGGAGAAAGGTCCAC	To amplify RA for CDK5RAP2 TAP tag
cep215 TAG RAR NotI (Fig. 5.1.3C)	<u>GCGGCCG</u> CCACTCTGCACATGGAATG	To amplify RA for CDK5RAP2 TAP tag
TAP tag check 1 (B in Fig. 5.1.3C,D)	GATCGTCTCTTCCAGAAG	To check targeted insertion of CDK5RAP2 TAP tag
DT40 CT LAFor ClaI (Fig. 5.1.2A)	<u>ATCGATT</u> GCCCTGCTGCCAGCAG	To amplify LA for CNN2-targeting construct
DT40 CT LARev EcoRI (Fig. 5.1.2A)	<u>GAATTC</u> TTGCAGCGATCACTGGTCTGGTAC	To amplify LA for CNN2-targeting construct
DT40 CT RAFor SpeI (Fig. 5.1.2A)	<u>ACTAGT</u> AAGGCTAGATGAAACCTGGAAG	To amplify RA for CNN2-targeting construct
DT40 CT RARev NotI (Fig. 5.1.2A)	<u>GCGGCCG</u> CGATAGAGCTGTGAGCAG	To amplify RA for CNN2-targeting construct
86467bp For (A in Fig. 5.1.2A)	ATGCAGTTGTGAGCTGCC	To check targeted insertions of CNN2-targeting construct
DT40 NT LAFor EcoRV (B in Fig. 5.1.2A)	<u>GATATC</u> ACCATGAAGGACTAAGAAAATGTAA GC	To amplify LA for CNN1-targeting construct
DT40 NT LARev BamHI (C in Fig. 5.1.2A)	<u>GGATC</u> CTGAGCCAACACTACGTCATGAGTTTC	To amplify LA for CNN1-targeting construct
DT40 NT RAFor SpeI (H in Fig. 5.1.2A)	<u>ACTAGT</u> GTGAGTGCCTAAAATGGAATGAAT	To amplify RA for CNN1-targeting construct
DT40 NT RARev NotI (I in Fig. 5.1.2A)	<u>GCGGCCG</u> CAGAGCTCCTTACTCCACACAGCC T	To amplify RA for CNN1-targeting construct
Neo Check (D in Fig. 5.1.3A)	CTGAATGAACTGCAGGACGAG	To check targeted insertions of targeting constructs
Puro Check (E in Fig. 5.1.3A)	ACGACCCCATGGCTCCGACCGAAG	To check targeted insertions of targeting constructs
Blasti 1 (F in Fig. 5.1.3A)	CTCATCAATGTATCTTATCAT	To check targeted insertions of targeting constructs
Chk2 new (G in Fig. 5.1.3A)	CATGTCTCAAAGCAATGGTAA	To check targeted insertions of CNN1-targeting construct
Chk1 new (A in Fig. 5.1.2A)	CTGCTGGTATTCCCTGGGATG	To check targeted insertions of CNN1-targeting construct
chAKAP TAG LAF EcoRI (Fig. 5.2.7A)	<u>GAATTC</u> CCAGCAGCAAACCTGTTGC	To amplify LA for AKAP450 TAP tag
chAKAP TAG LAR XbaI (Fig. 5.2.7A)	<u>TCTAGAT</u> CTTCTCATAGCAGAGTG	To amplify LA for AKAP450 TAP tag
chAKAP TAG RAF2 SpeI (Fig. 5.2.7A)	<u>ACTAGT</u> TCCATCACTGGCAGCGAT	To amplify RA for AKAP450 TAP tag

chAKAP TAG RAR NotI (Fig. 5.2.7A)	<u>GCGGCCGCTTATATTGGAGTTTATTC</u>	To amplify RA for AKAP450 TAP tag
chAKAP 82142bp Rev (B in Fig. 5.2.7A,B)	TCAAGCCTGACCGCTATC	To check targeted insertion of AKAP450 Neo TAP tag
AKAPTAP check F (D in Figure 5.2.7A,B)	AGTCAGAGTGTCCATTGC	To check targeted insertion of AKAP450 Bsr TAP tag
CNN1lox EIF	GTATGGATTCTCTGCCAG	To check splice-forms of CDK5RAP2 expressed
CNN1lox E6R	CATATCCAGATCCTTCGC	To check splice-forms of CDK5RAP2 expressed
Myomegalin RT-PCR (Human)		To check Myomegalin splice forms expressed in HeLa and U251MG
HsMyomeg E8F 1	AATGGCAAAGCTTCGAGAAA	
HsMyomeg E9R 1	ACACATTGTTTGGCATCAGC	
Hs Myomeg E39F 1	TCCGGGATGTTGGTATGAAT	
Hs Myomeg E40R 1	TTATTGGCAAAGGAGCCATC	
Myo Exon 10F	ATTCTTCAAGAGAAACTT	
Myo Exon 11R	GTGAAGTTGTCCAAGCTG	
Myo Exon 16F	AGTATGGAGAGTCTCCTG	
Myo Exon 17R	TTGGCTTTCCTGCTCCCT	
Myo Exon 18F	GCTGCTGCAGAGAAGTTG	
Myo Exon 19R	CTAATGTGGATCTGGGTA	
Myo Exon 20F	GAGACTTGGACACAGTTG	
Myo Exon 21R	CTTTATGAGATCTTCTTT	
Myo Exon 24F	CTCTGAGAGAGACCGGAAC	
Myo Exon 25R	TTGCTGGTACTATGGTG	
Myo Exon 12F	AGCTCAGAGGGTACTTCT	
Myo Exon 13R	CTGAAGCAACTGCTCCTT	
Myo Exon 22F	GACCTGCAAAATGCAACTG	
Myo Exon 23R	CTCTCTGGATGGGCATGG	
Myo Exon 33F	CAGGAGAAGGAGAAAGTG	
Myo Exon 33R	CTGAGTACTGGGAGAAG	
Myo Exon 1F	GCTCTGAGTCCAGCCTCC	
Myo Exon 2R	CTGCTGTGTACTCGTTC	
Myo Exon 3F	CTTAGTGACACTAAAGAT	
Myo Exon 4R	CCGCTTGTAGATGTCCTC	
Myo Exon 5F	AACATTGAGCTGAAGGTT	
Myo Exon 6R	CTCCTGCAGAAGCTGGAT	
Myo Exon 7F	GAATCCAGGCTAGCAAAG	
Myo Exon 7R	TTGTCCCTCTGGGCCAGG	
Myo Exon 14F	GAATTCGGGAGCTCCTA	
Myo Exon 15R	TTGCATAGTAGCTTCATT	
Myo Exon 26F	CTTGTCAAGGTGGCTTTG	
Myo Exon 27R	CTCGCCCTTCTCCTTGTC	
Myo Exon 29R	CAGGACTGGTGGTTTCCCT	
Myo Exon 28F	CAGGTGAATCCTTGGTGA	
Myo Exon 30F	AGTGTGAGGAGCACACA	
Myo Exon 31F	GAAATATGATTCCTGAT	
Myo Exon 31R	TGGTGCTGAGTTTGCTGG	

Myo Exon 32F	AGGATCATAAAAAGTGAGA	
Myo Exon 32R	CTGAGGGCCAGTGGCTCA	
Myo Exon 34F	ATTCCATCCATCATTCGA	
Myo Exon 35R	CTGTGGGTTGGAGTTAA	
Myo Exon 36F	GGGCTGACCTGCTGGAAG	
Myo Exon 36R	CCCTTCCACGAGCAGTAG	
Myo Exon 37F	GATCCACTTCTAACTTCT	
Myo Exon 38R	CTGGAGTCGTTTTCTGG	
Myo Exon 41F	ATTCAGCTGTGTCCCCTC	
Myo Exon 42R	CTCTGTGCCTTGGGCTTC	
Myo Exon 43F	GTGCTAGGCAGCCAAGGT	
Myo Exon 44R	GCTGGCTGACAATGAACT	
Myomegalin RT-PCR (DT40)		To check if Myomegalin is expressed in DT40
ggMyomeg Ex7F	CAGGCCCAAGAACAGAGAGT	
ggMyomeg Ex8R	TTTCTCCAGCATAGCATCCA	
ggMyomeg Ex11F	GCTTCTCAGTGACAGGAATCG	
ggMyomeg Ex12R	CGACAGGCTTCTTCTCAAC	
FLAG-tagged CDK5RAP2		To clone CDK5RAP2 into FLAG-tag vector
CDK5RAP2 TAG2B FOR	<u>GAATTC</u> ATGATGGACTTGGTGTG	
CDK5RAP2 TAG2B REV	<u>GTCGACT</u> CAGGAGCCTGGTCTGCT	
3600bp 3' end	<u>GTCGACC</u> AGCTGCTGTTGAGGTT	
3600bp 5' end tag2B	<u>GAATTC</u> GAAACAGGAATACAAGCTG	
CDK5RAP2 1	ATGAAGAAGATGCACGAG	To sequence hCDK5RAP2
CDK5RAP2 2	GAATTCAGGGGTCTGAA	To sequence hCDK5RAP2
CDK5RAP2 3	GATGGCCATGGCATCTGT	To sequence hCDK5RAP2
S1238 Phos SDM F	AGAATAAGTTCAGAGATCTCGCACCTCCCAG ATACGATTCA	To mutate S1238 to alanine
S1238 Phos SDM R	TGAATCGTATCTGGGAGGTGCGAGATCTCTG AACTTATTCT	To mutate S1238 to alanine
S1074 Phos SDM F	AAAATCCTGAAGATGTTCTGGCCCCAACTTC AGTAGCTACTT	To mutate S1074 to alanine
S1074 Phos SDM R	AAGTAGCTACTGAAGTTGGGGCCAGAACATC TTCAGGATTTT	To mutate S1074 to alanine
2 nd Ser815 Phosmut	CTATTCTTGACAGAGCAGGAAGTTGCTGGAG AACACCTTGATGGTAAAA	To mutate S815 to alanine
2 nd Ser815 Phos Rev	TTTTACCATCAAGGTGTTCTCCAGCAACTTCC TGCTCTGTCAAGAATAG	To mutate S815 to alanine
Thr890 mut	TGAGATTCAAGCATGAAGCAGCAAGAGAGG CTTGGGAAGAG	To mutate T890 to alanine
Thr890 mut rev	CTCTTCCCAAGCCTCTCTTGCTGCTTCATGCT TGAATCTCA	To mutate T890 to alanine
Hp1 gac to gat FOR	GATAAACAGAAGGAGAATGATAAATTACGA GAGCCCCTCTC	To mutate hCDK5RAP2 to generate FLAG-FL*
Hp1 gac to gat REV	GAGAGGGGCTCTCGTAATTTATCATTCCTT CTTGTTTATC	To mutate hCDK5RAP2 to generate FLAG-FL*
ARBhp1a	TCGAGAAGGTATATTGCTGTTGACAGTGAGC GCGAAGGAGAATGACAAATTACGTAGTGAA GCCACAGATGTACGTAATTTGTCATTCTCCTT CTTGCCTACTGCCTCGG	Primers to anneal to generate shRNA CDK5RAP2 hp1 to sub-clone into MSCV-miR30Puro.

ARBhp1b	AATCCGAGGCAGTAGGCAAGAAGGAGAAT GACAAATTACGTACATCTGTGGC TTCACACTACGTAATTTGTCATTCTCCTTCGCGC TCACTGTCAACAGCAATATACCTTC	Primers to anneal to generate shRNA CDK5RAP2 hp1 to sub-clone into MSCV-miR30Puro.
ARBhp2a	TCGAGAAGGTATATTGCTGTTGACAGTGAGC GCCCGTGATCTTAGAAATGAAGTTAGTGAAG CCACAGATGTAACCTTCATTTCTAAGATCACG GATGCCTACTGCCTCGG	Primers to anneal to generate shRNA CDK5RAP2 hp2 to sub-clone into MSCV-miR30Puro.
ARBhp2b	AATCCGAGGCAGTAGGCATCCGTGATCTTA GAAATGAAGTTACATCTGTGGCTTCACTAAC TTCATTTCTAAGATCACGGGCGCTCACTGTCA ACAGCAATATACCTTC	Primers to anneal to generate shRNA CDK5RAP2 hp2 to sub-clone into MSCV-miR30Puro.
ARBhpcont1a	TCGAGAAGGTATATTGCTGTTGACAGTGAGC GCGAAGGATAAGGACACATTACGTAGTGAAG CCACAGATGTACGTAATGTGTCTTATCCTTC TTGCCTACTGCCTCGG	Primers to anneal to generate shRNA CDK5RAP2 control hp1 to sub-clone into MSCV-miR30Puro.
ARBhpcont1b	AATCCGAGGCAGTAGGCAAGAAGGATAAG GACACATTACGTACATCTGTGGCTTCACTACG TAATGTGTCTTATCCTTCGCGCTCACTGTCA ACAGCAATATACCTTC	Primers to anneal to generate shRNA CDK5RAP2 control hp1 to sub-clone into MSCV-miR30Puro.
ARBhpcont2a	TCGAGAAGGTATATTGCTGTTGACAGTGAGC GCCCGTGCTCTGAGAACTGAAGTTAGTGAAG CCACAGATGTAACCTTCAGTTCTCAGAGCACG GATGCCTACTGCCTCGG	Primers to anneal to generate shRNA CDK5RAP2 control hp2 to sub-clone into MSCV-miR30Puro.
ARBhpcont2b	AATCCGAGGCAGTAGGCATCCGTGCTCTGA GAACTGAAGTTACATCTGTGGCTTCACTAACT TCAGTTCTCAGAGCACGGGCGCTCACTGTCA ACAGCAATATACCTTC	Primers to anneal to generate shRNA CDK5RAP2 control hp2 to sub-clone into MSCV-miR30Puro.

Underlined residues represent restriction sites.

All primers were from Sigma and were of Desalt quality.

Table 2.5 Antibodies used in this study

Antibody name	Species	Origin	Fixation for immunostaining	Reference
α -tubulin (DM1 α)	Ms	Sigma	MeOH, 3% PFA, 4% Form	
γ -tubulin (GTU88)	Ms	Sigma	MeOH	
γ -tubulin	Rb	Novus	MeOH	
acetylated tubulin	Ms	Sigma	MeOH	
AKAP450	Ms	BD	MeOH	
Aurora A	Ms	BD	MeOH	
β -actin (AC-15)	Ms	Sigma	-	
CDK5RAP2-SK56	Rb	Gergely lab	MeOH	
CDK5RAP2-A550	Rb	Bethyl	MeOH, 3% PFA	
centrin-1	Rb	Sigma	-	
centrin-3	Ms	Abnova	MeOH	
chBubR1	Ms	Earnshaw lab	4% Form	(Vagnarelli et al., 2004)
Chk1	Ms	Sigma	MeOH	
chTACC3	Rb	Gergely lab	MeOH, 4% Form, 3% PFA	
ch-Tog	Rb	Cassimeris lab	MeOH	(Charrasse et al., 1998)
c-Nap1	Ms	BD	MeOH	
cyclin A	Ms	Sigma	-	
FLAG-M2	Ms	Sigma	MeOH	
gm130	Ms	Sigma	MeOH	
Myomegalin	Rb	Gergely lab	MeOH	
Nek2	Ms	BD	MeOH	
ninein	Rb	AbCam	MeOH	
NuMA	Ms	BD	MeOH, 3% PFA	
p150 ^{glued}	Ms	BD	3% PFA	
pericentrin	Rb	Covance	MeOH	
Plk1	Ms	AbCam	MeOH (with high extraction)	
protein G	Rb	AbCam	MeOH	
protein G-HRP	Rb	AbCam	-	
pSer10HistoneH3	Rb	Millipore	MeOH	
pT288AurA	Rb	BD	MeOH	
Ran	Ms	BD	MeOH	(Keryer et al., 2003)
TGN46	Sh	Abnova	MeOH	

Key: Ms – Mouse; Rb – Rabbit; Sh – Sheep; PFA – Paraformaldehyde; Form – Formaldehyde; (-) –was not tested in immunostaining. “with high extraction” refers to a 5 minute, 1xPBS/1%TritonX-100/0.5%NP-40 wash after fixation.

Chapter 3

CDK5RAP2 is required for centrosome cohesion

Mutations in the centrosomal gene *CDK5RAP2* can lead to microcephaly, thus *CDK5RAP2* must play a role in brain development. However, *CDK5RAP2* is a ubiquitously expressed protein and has been shown to be expressed in the heart, brain, lung, liver, skeletal muscle, kidney and pancreas (Ching et al., 2000). *CDK5RAP2* has two evolutionarily conserved domains, known as the CNN1 and CNN2 domains (Kao and Megraw, 2009; Sawin et al., 2004; Zhang and Megraw, 2007). Both these domains are also present in a second human centrosomal protein, Myomegalin (Verde et al., 2001). The functions of both *CDK5RAP2* and Myomegalin were completely uncharacterised at the start of this thesis work. However, studies of orthologues of *CDK5RAP2* and Myomegalin in lower organisms suggest that CNN-domain containing proteins have important roles in MTOC function (Lucas and Raff, 2007; Megraw et al., 2001; Sawin et al., 2004). Therefore, for these reasons, I wanted to study the role of CNN domain proteins in somatic cells. The major focus of this work is on *CDK5RAP2* as I deemed this to be the most interesting protein because it has been linked to the human developmental disease, microcephaly. However, I also study Myomegalin function to a lesser extent and mostly to explore if Myomegalin and *CDK5RAP2* function redundantly.

In this chapter I describe the generation of specific antibodies and cell lines to study the function(s) of *CDK5RAP2* in human cells. I find that *CDK5RAP2* is a microtubule-associated protein that not only localises to the centrosome (as has been shown previously (Andersen et al., 2003; Bond et al., 2005)) but also localises to the Golgi body. Moreover, using RNA interference (RNAi) methods to deplete *CDK5RAP2*, I find that *CDK5RAP2* is required to mediate centrosome cohesion. Overexpression studies reveal that centrosome cohesion is likely to be mediated by the N-terminal domain of *CDK5RAP2*. In terms of maintaining centrosome cohesion, Myomegalin is not functionally redundant to *CDK5RAP2*. Finally, I show that the subcellular localisation of Myomegalin varies between cell lines.

3.1 CDK5RAP2 localises to the centrosome and Golgi body and associates with microtubules

3.1.1 Making an anti-human CDK5RAP2 antibody

At the start of the project, no commercial antibodies for CDK5RAP2 were available. Therefore, I made an N-terminal fusion protein between Maltose-Binding Protein (MBP) and amino acids 40-375 of human CDK5RAP2. This was used to immunise rabbits (Figure 3.1.1A; Section 2.3 in Materials and Methods). This epitope in CDK5RAP2 contains the highly evolutionarily conserved CNN1 domain and thus potentially this antibody will also be useful in other species (Sawin et al., 2004; Zhang and Megraw, 2007). I depleted sera of anti-MBP antibodies and then affinity purified anti-CDK5RAP2 antibodies against the MBP-CDK5RAP2 fusion protein used to inoculate rabbits. I named this antibody 'SK56' and further characterised it in a series of experiments to check its specificity.

Purified SK56 antibody recognised a single band in HeLa whole cell extract at just below the predicted molecular weight (MW) of 215 kDa (Figure 3.1.1B). In addition, silencing RNA (siRNA)-mediated depletion of CDK5RAP2, or overexpression of FLAG-tagged human CDK5RAP2 cDNA, in HeLa cells caused, respectively, a reduction and an increase in the Western blot signal of the SK56 antibody (Figure 3.1.1C and D). After starting this project, a commercial antibody recognising CDK5RAP2 became available (Bethyl-550A, see Table 2.5, Materials and Methods). This antibody recognised CDK5RAP2 specifically, although also recognised a non-specific band not depleted by CDK5RAP2-targeting siRNA (see asterisk in Figure 3.4.2B). Note that, unless otherwise stated, the CDK5RAP2 antibody used is SK56.

3.1.2 CDK5RAP2 localises to the centrosome and Golgi body

CDK5RAP2 has previously been shown to localise to the centrosome (Andersen et al., 2003; Bond et al., 2005). To see if SK56 recognised CDK5RAP2 at the centrosome, HeLa cells were fixed in methanol and co-stained with purified anti-CDK5RAP2 and γ -tubulin, a centrosomal marker. As expected, CDK5RAP2 was present at the centrosome throughout the cell cycle (Figure 3.1.2A). Moreover, in interphase, a punctate pericentrosomal staining was also visible (yellow arrow in

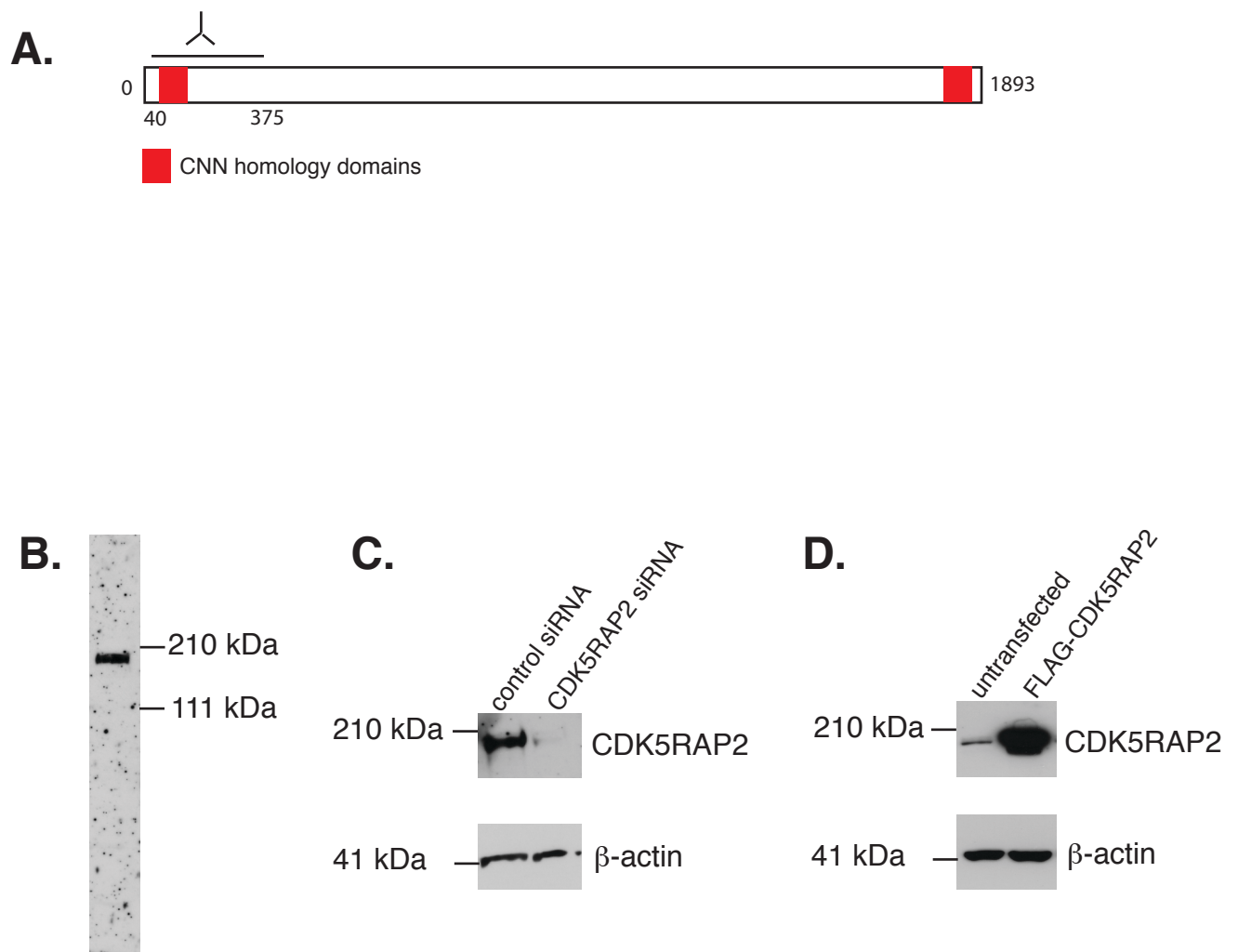


Figure 3.1.1 Making an anti-human CDK5RAP2 antibody. **A.** Schematic shows position of epitope within the human CDK5RAP2 protein used to raise antibodies. **B.** Western blot of HeLa cell whole cell extract with purified SK56 antibody. **C.** Western blot of HeLa whole cell extract 72 hr after transfection with CDK5RAP2 or negative control siRNA. β -actin serves as a loading control. **D.** Western blot of HeLa whole cell extract 24 hr after transfection with FLAG-tagged full-length (FLAG-FL) CDK5RAP2 (see also Figure 3.3.1A). β -actin serves as a loading control.

Figure 3.1.2A). This localisation of CDK5RAP2 was seen in all cell lines tested (HB2 (breast epithelial), Jurkat (T-lymphocyte), U251MG (glioblastoma) and U2OS (osteosarcoma)). To test if the pericentrosomal staining represented Golgi localisation of CDK5RAP2, cells were co-stained with anti-CDK5RAP2 and the cis-Golgi marker, gm130. The two antibody signals overlapped in the Golgi region, suggesting that CDK5RAP2 also localises to the Golgi body (lower panels in Figure 3.1.2B). To confirm this localisation, cells were treated with Brefeldin A (BFA), an antiviral antibiotic that blocks protein transport from the Endoplasmic Reticulum to the Golgi and leads to dispersal of the Golgi body (Klausner et al., 1992). Treatment of HeLa cells with BFA caused dispersal of the Golgi, as shown by dispersal of the gm130 signal (Figure 3.1.2B). After BFA treatment, CDK5RAP2 no longer localises to the Golgi, indicating that CDK5RAP2 is not an integral Golgi protein (Bascom et al., 1999) but can localise to the intact Golgi body, in particular the cis Golgi (Figure 3.1.2B). Treatment with BFA did not affect the localisation of CDK5RAP2 to the centrosome, indicating that Golgi localisation of CDK5RAP2 is not required for its localisation to the centrosome in interphase (Figure 3.1.2B).

CDK5RAP2 was identified as one of 23 centrosomal genes required for the formation or maintenance of primary cilia in a siRNA screen (Graser et al., 2007b). Therefore, in addition to its centrosomal and Golgi localisation I wondered if CDK5RAP2 localised to primary cilia. HB2 breast epithelial cells form a primary cilium when allowed to reach confluency (see Section 2.1.2, Materials and Methods). Immunostaining of confluent HB2 cells revealed that while CDK5RAP2 does localise to basal bodies, it does not localise along the axoneme (Figure 3.1.2C).

It has been reported that CDK5RAP2 localises to the midbody in HeLa cells (Paramasivam et al., 2007). However, I was unable to detect CDK5RAP2 at the midbody in HeLa cells with the available CDK5RAP2 antibodies using multiple different fixation conditions (methanol, paraformaldehyde and formaldehyde).

In summary, CDK5RAP2 localises to the centrosome throughout the cell cycle, to basal bodies and to the Golgi body in human cells.

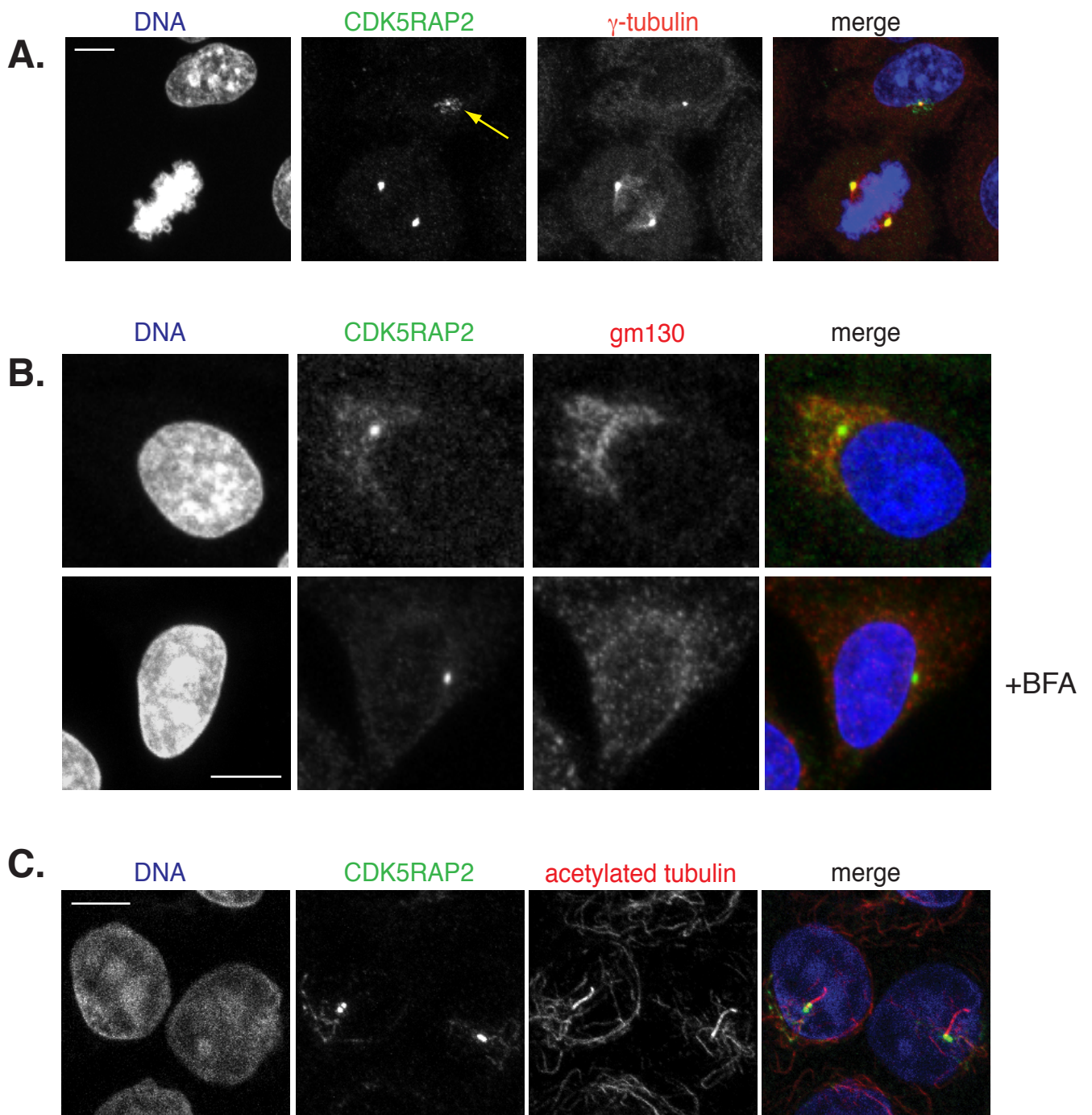


Figure 3.1.2 CDK5RAP2 localises to the centrosome and to the Golgi body. **A.** Subcellular localisation of CDK5RAP2 in HeLa cells, stained with SK56 antibody. Yellow arrow indicates punctate pericentrosomal staining. DNA is blue, CDK5RAP2 is green and γ -tubulin is red in merged image. **B.** CDK5RAP2 localises to the Golgi body as shown by colocalisation with the cis Golgi marker, gm130. Brefeldin A (BFA) leads to dispersal of the Golgi body and loss of CDK5RAP2 from the Golgi. DNA is blue, CDK5RAP2 is green and gm130 is red in merged images. **C.** Subcellular localisation of CDK5RAP2 in ciliated HB2 cells. DNA is blue, CDK5RAP2 is green and acetylated tubulin is red in merged images. Scale bars are 5 μ m.

3.2 CDK5RAP2 is required for centrosome cohesion

3.2.1 Depleting CDK5RAP2 levels by siRNA and shRNA

siRNA is a powerful method to study cellular function in the absence of a particular protein. Therefore, to analyse CDK5RAP2 function, I used siRNA to deplete CDK5RAP2 from human cells (Figure 3.2.1A and Figure 3.1.1C). Western blotting and immunostaining of cells 72 hours after transfection with CDK5RAP2-targeting siRNA showed that CDK5RAP2 protein was successfully depleted from cells and that the CDK5RAP2 signal at both the centrosome and the Golgi was diminished (further proving the specific localisation of CDK5RAP2 to the Golgi). However, even 72 hours after transfection, a small amount of CDK5RAP2 protein was still detectable in centrosomes (pink arrow in Figure 3.2.1A). Moreover the remaining CDK5RAP2 protein appeared to localise asymmetrically to the two centrioles. The remaining protein might be a stable fraction of CDK5RAP2 that is infrequently turned over and thus cannot fully be depleted. An alternative explanation is that full depletion of CDK5RAP2 may lead to cell death. However, I never saw an increase in cell death in cells treated with CDK5RAP2-targeting siRNAs.

To try another method to deplete CDK5RAP2 levels, I used short hairpin RNA (shRNA) vectors to generate cell lines depleted of CDK5RAP2 (Section 2.10, Materials and Methods). These vectors carry an shRNA targeting sequence under the control of a U6 promoter and a puromycin resistance gene such that cells carrying shRNA can be selected for. I reasoned that by generating stable cell lines carrying an shRNA vector, the target protein would be continuously depleted from cells over a long period of time and would thus potentially yield cell lines with little or no CDK5RAP2 protein. I generated retrovirus carrying shRNAs targeting CDK5RAP2 or scrambled shRNAs and tested their ability to deplete CDK5RAP2 protein on a population of HeLa cells. Figure 3.2.1B shows that the shRNAs tested could deplete CDK5RAP2 protein from cells. I used these same shRNAs to generate stable, clonal HeLa cells lines carrying either scrambled or CDK5RAP2-targeting shRNAs. I first checked depletion of CDK5RAP2 by immunostaining and then screened those clones deemed to have the lowest levels of CDK5RAP2 protein by Western blotting (Figure 3.2.1C). In this way, I made stable clonal HeLa cell lines where every cell in the population has reduced CDK5RAP2 protein. However, even these cell lines

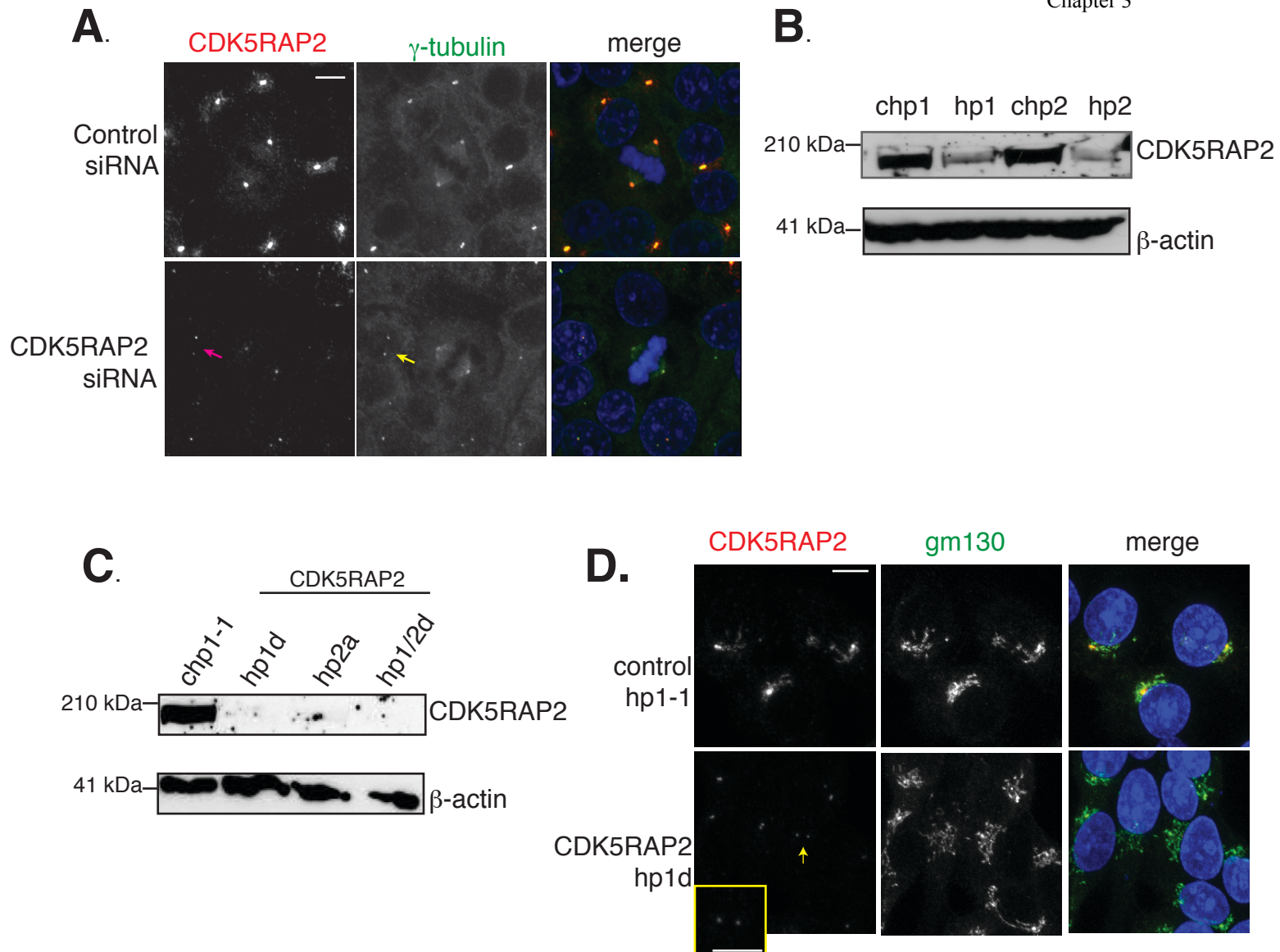


Figure 3.2.1 CDK5RAP2 protein levels were depleted by siRNA and shRNA. **A.** Immunofluorescence images showing depletion of CDK5RAP2 by siRNA in HeLa cells, 72 hr after transfection. Pink arrow shows an example of CDK5RAP2 remaining at the centrosome after siRNA depletion. Yellow arrow shows loss of centrosome cohesion when CDK5RAP2 is depleted. DNA is blue, CDK5RAP2 is red and γ -tubulin is green in merged images. Scale bar is 5 μ m. **B.** Western blot of HeLa whole cell extracts 72 hr after transfection with shRNA-carrying retrovirus. chp = control (scrambled) shRNA. hp = CDK5RAP2-targeting shRNA. '1' and '2' refer to two different shRNA targeting sequences (see Table 2.4). β -actin serves as a loading control. **C.** Western blot of whole cell extracts from clonal shRNA-carrying HeLa cells. Each clone (chp1-1, hp1d, hp2a, hp1/2d) was generated from a single cell and thus is a homogenous population. β -actin serves as a loading control. **D.** Immunofluorescence images of shRNA clonal HeLa cell lines. The cis Golgi remains structurally intact after CDK5RAP2 depletion. Yellow arrow indicates split centrosomes in CDK5RAP2-depleted cells. Inset is zoomed in image of cell marked with an arrow. DNA is blue, CDK5RAP2 is red and gm130 is green in merged images. Scale bars are 5 μ m.

contained a small amount of CDK5RAP2 protein at the centrosome. This implies that there may be a very stable portion of CDK5RAP2 at the centrosome that turns over very infrequently and is thus difficult to deplete using RNAi approaches.

It is worth noting here that depletion of CDK5RAP2 from cells did not perturb Golgi architecture in cells, since gm130 localisation appeared normal (Figure 3.2.1D).

In summary, I can successfully deplete CDK5RAP2 from human cell lines using both siRNA and shRNA. Moreover, using shRNA, I have generated clonal cell lines in which every cell in the population has low CDK5RAP2 protein levels. These cell lines provide useful tools for analysis of CDK5RAP2 function.

3.2.2 CDK5RAP2 is required for centrosome cohesion

I noted that in a high proportion of cells depleted of CDK5RAP2 protein, two distinct, separated γ -tubulin spots were clearly visible (Figure 3.2.1A – yellow arrow). This phenotype is present in approximately 30% of siRNA-depleted cells and 40% of shRNA-depleted cells (Figure 3.2.2A; these values were independently verified by a colleague “blind-scoring” one experiment). There are several reasons why depletion of CDK5RAP2 could lead to this phenotype. Firstly, the PCM could have fragmented and γ -tubulin containing PCM may have disintegrated from the centrosome. Alternatively, cells may be arrested in G2 with separated, duplicated centrosomes (Figure 1.4). Finally, the centrosome may have split (that is the mother and daughter centrioles have separated from one another and are no longer a pair - termed ‘centrosome splitting’ or ‘loss of centrosome cohesion’ (Meraldi and Nigg, 2001)).

To test the first of these hypotheses, siRNA depletion of CDK5RAP2 was performed in a HeLa cell line that stably expressed GFP-centrin1, to fluorescently label centrioles (kind gift of J. Pines). Figure 3.2.2B confirms that the separated γ -tubulin spots do contain centrioles (green arrows) and the presence of distinct γ -tubulin spots is not due to fragmented PCM. Moreover, each γ -tubulin spot contains one centriole, implying that centrosomes have separated before duplication.

Duplicated centrosomes separate in G2 in preparation to form the poles of the bipolar spindle in mitosis (Figure 1.4). To test if the presence of cells with distinct γ -tubulin spots are arrested in G2 with separated centrosomes, control hp1-1 and CDK5RAP2 hp1d clonal cells (Figure 3.2.1C, D) were immunostained for γ -tubulin and an antibody recognising Phosphorylated serine 10 on Histone H3 (PHH3), a marker of

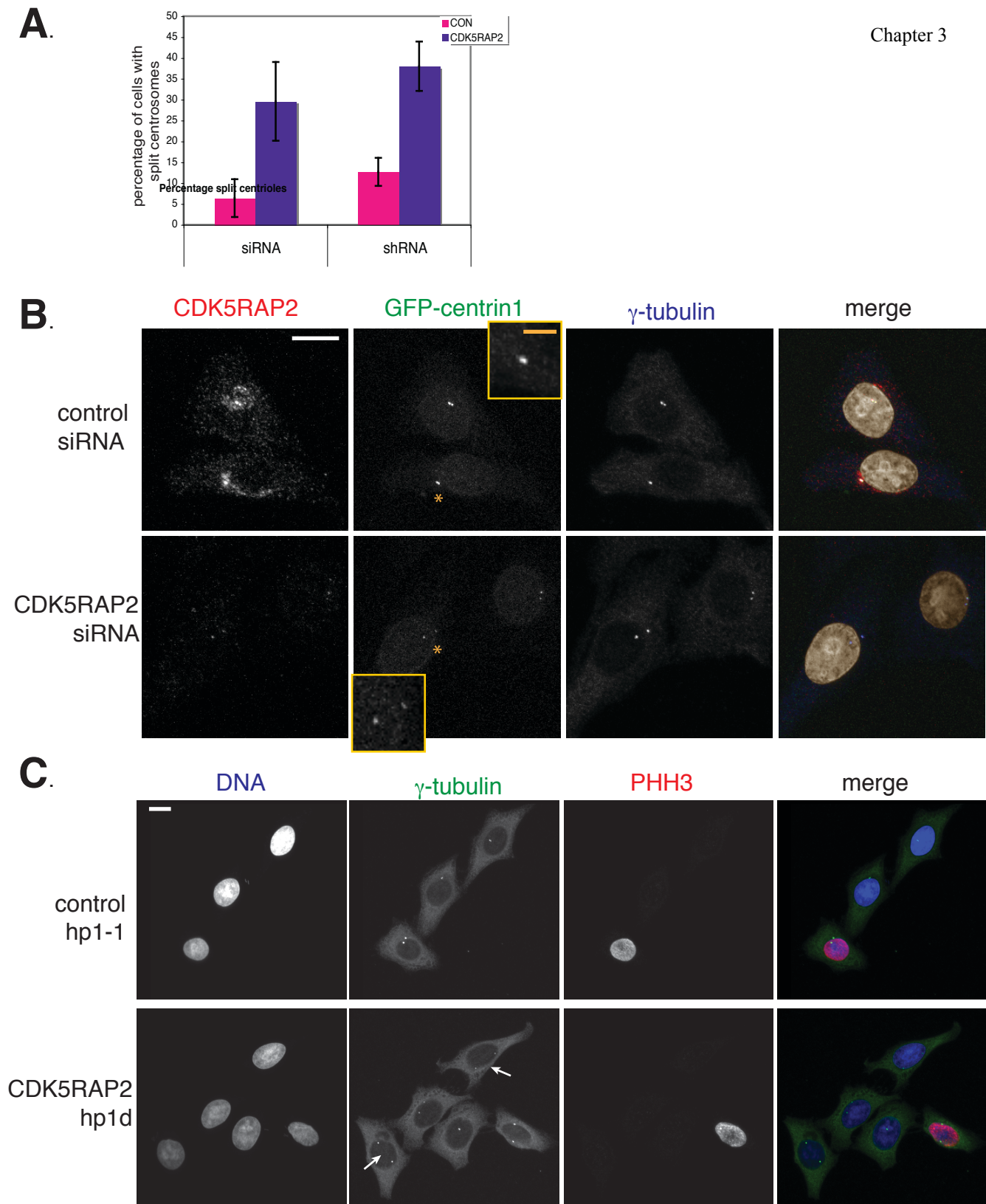


Figure 3.2.2 CDK5RAP2 is required for centrosome cohesion. A. Graph quantifying the number of cells with split centrosomes in siRNA and shRNA treated cells. siRNA experiments $n=3$, 250 cells counted per condition, per experiment. shRNA experiments represent three different stable clones for control hps and CDK5RAP2 hps, 250 cells counted for each clone. Error bars represent standard deviations (STD). **B.** Immunofluorescence images show that split centrosomes contain centrioles, shown by the presence of GFP-centrin1 in γ -tubulin containing spots. Yellow boxes are zoomed in images of centrioles marked by yellow asterisks. DNA is grey, CDK5RAP2 is red, GFP-centrin1 is green and γ -tubulin is blue in merged images. **C.** Immunofluorescence images of CDK5RAP2 shRNA clones. PHH3 marks those cells that are in G2 or Mitosis. White arrows indicate CDK5RAP2-depleted cells that have split centrosomes but are not in G2. Note that these images are from shRNA-depleted clones and thus every cell in CDK5RAP2 hp1d is depleted of CDK5RAP2 protein. DNA is blue, γ -tubulin is in green and PHH3 is in red in merged images. White scale bars are 5 μ m. Yellow scale bar is 2.5 μ m.

G2 and mitosis (Figure 3.2.2C). Separated centrosomes can be detected in the absence of PHH3 staining in CDK5RAP2-depleted cells. Again, this implies that the centrioles have split before G2.

These data imply that the third hypothesis is correct – that when CDK5RAP2 is depleted, the centrosome prematurely loses cohesion – leading to centrosome splitting. This suggests that normally CDK5RAP2 is required to maintain centrosome cohesion until the regulated separation of centrosomes in G2.

3.2.3 Restoration of CDK5RAP2 protein rescues centrosome splitting

siRNA and shRNA methods can have off-target effects that can lead to false-positive results. In this case, this seems unlikely since both siRNA and shRNA methods give the same phenotype, including two different shRNA targets in CDK5RAP2 (see Table 2.3 in Materials and Methods for targeted sequences). However, to be certain that the effects seen are due to loss of CDK5RAP2 function, I took advantage of the stable CDK5RAP2-depleted clonal cell lines to perform rescue experiments. Using a FLAG-tagged Full length (FL) human CDK5RAP2 construct (Figure 3.3.1A), I made a construct that would be insensitive to the shRNA integrated in the HeLa cell clones – referred to as FLAG-FL* (see Section 2.2.2, Materials and Methods). This construct was transiently transfected into control hp1-1 or CDK5RAP2 hp1d HeLa cell clones and cells analysed by immunostaining 24 hours later. The FLAG-FL* construct had the same localisation pattern as FLAG-FL (as one would expect since no amino acids were changed). Figure 3.2.3 shows that cells transfected with FLAG-FL* have a reduced number of split centrosomes, compared to untransfected cells (see yellow arrow in Figure 3.2.3A and graph in Figure 3.2.3B). This confirms that CDK5RAP2 is required for centrosome cohesion.

3.2.4 CDK5RAP2 does not affect the localisation of other centrosome cohesion proteins

Several proteins required to mediate centrosome cohesion have already been characterised (Figure 1.5). Two of these proteins are c-Nap1 and Nek2 (Fry et al., 1998b; Fry et al., 1998a). C-Nap1 is proposed to form part of a physical linker between the two centrioles, while Nek2 is a cell-cycle regulated kinase that binds to

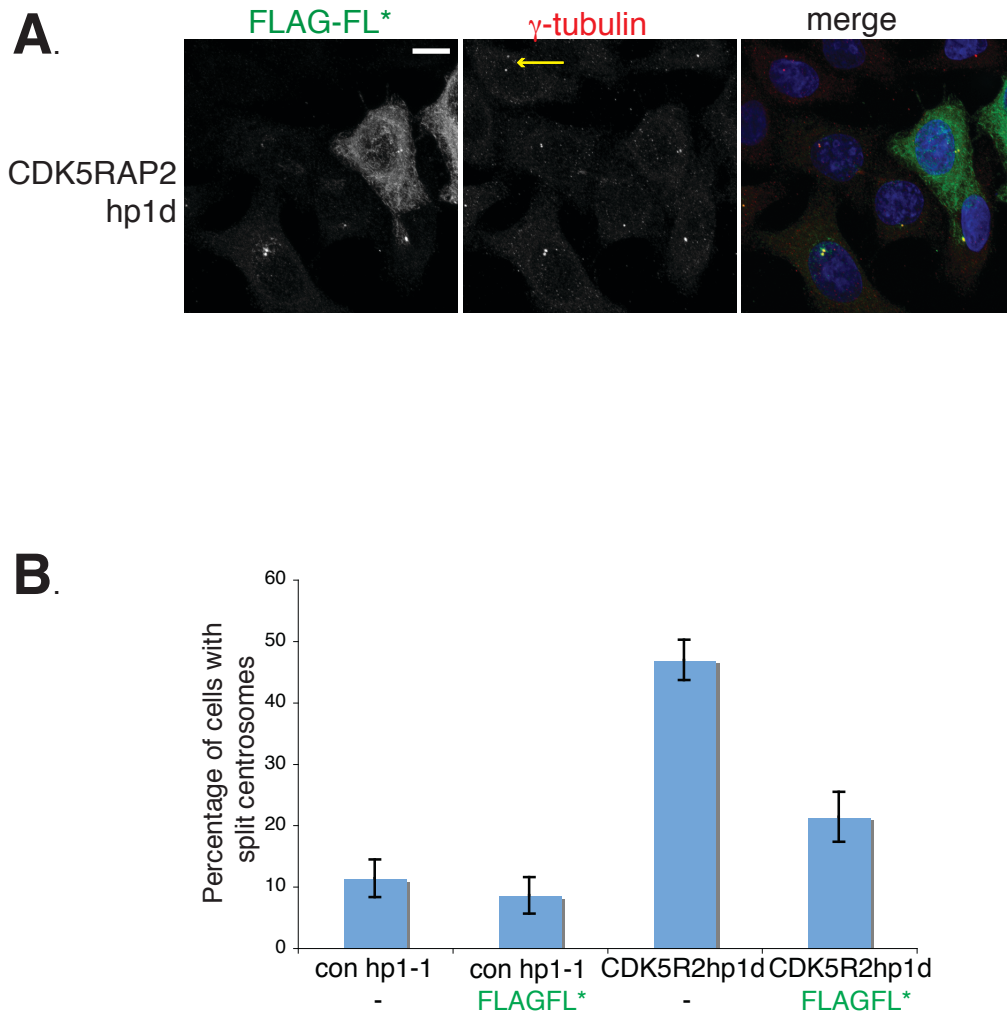


Figure 3.2.3 Restoration of CDK5RAP2 rescues centrosome splitting. **A.** Immunofluorescence images showing CDK5RAP2 hp1d cells transfected with FLAG-FL* and analysed 24 hrs later. Most cells in the image are transfected with FLAG-FL*, apart from the cell indicated by the yellow arrow. Note the rescue of centrosome cohesion in FLAG-FL* containing cells. DNA is blue, FLAG-FL* is green and γ -tubulin is red in merged image. Scale bar is 5 μ m. **B.** Graph quantifying the extent of rescue on transfection of FLAG-FL*. Error bars represent STD. n=3, at least 150 cells counted per condition, per experiment.

and phosphorylates c-Nap1 (Mayor et al., 2000; Fry et al., 1998). Phosphorylation of c-Nap1 by Nek2 has been suggested to promote the dissolution of c-Nap1 from centrioles and therefore permit centrosome separation in G2 (Figures 1.4 and 1.5).

To test if CDK5RAP2 was part of this same mechanism, I analysed the localisation of other proteins involved in centrosome cohesion. C-Nap1 and Nek2 still localise to split centrosomes even when CDK5RAP2 is depleted (Figure 3.2.4A, B). This implies that CDK5RAP2 is either downstream of c-Nap1 and Nek2 or is involved in a distinct centrosome cohesion mechanism.

3.2.5 Split centrosomes are dynamic

shRNA-mediated depletion of CDK5RAP2 leads to centrosome splitting in only approximately 40% of cells even though, due to the stable nature of this depletion, every cell in the population contains reduced CDK5RAP2 levels. Since after depletion of CDK5RAP2 centrosomes can split before G2 (i.e. in G1 and S) and 81% of cells are in G1/S, centrosomes could be split in as many as 81% of cells (taken from HeLa flow cytometry analysis: G1/S 81% and G2/M 14%). I hypothesised that one reason for only 40% of cells containing split centrosomes could be that centrosome splitting is dynamic.

To test this, I fluorescently-labelled centrioles by transiently transfecting control hp1-1 and CDK5RAP2-hp1d clonal cells with GFP-centrin1 (Piel et al., 2001). I then analysed GFP-centrin1-expressing cells by time-lapse microscopy. Images were acquired every 5 minutes for 4 hours to record centrosome movement. Any cell in which two pairs of centrioles were visible was excluded from the analysis as these cells were likely to be in G2 and thus their centrosomes would be expected to separate anyway (Figure 3.2.5B). Live analysis confirmed that overexpression of GFP-centrin1 did not rescue the centrosome splitting phenotype (CDK5RAP2 hp1d: 45 +/- 4.58% centrosomes split (179 total cells scored) versus 14 +/- 3.16% in control hp1-1 (229 total cells scored); n=3). Live imaging of centrosome dynamics revealed that in all cases where centrosomes split, the two centrioles exhibited a dynamic behaviour where they frequently moved apart and together over the 4 hours time period. The number of times this occurred varied widely from cell to cell (movie stills – Figure 3.2.5A; Movies 3.1, 3.2 and 3.3 on Supplementary CD). However, even taking into account this behaviour, the total number of cells that did split their

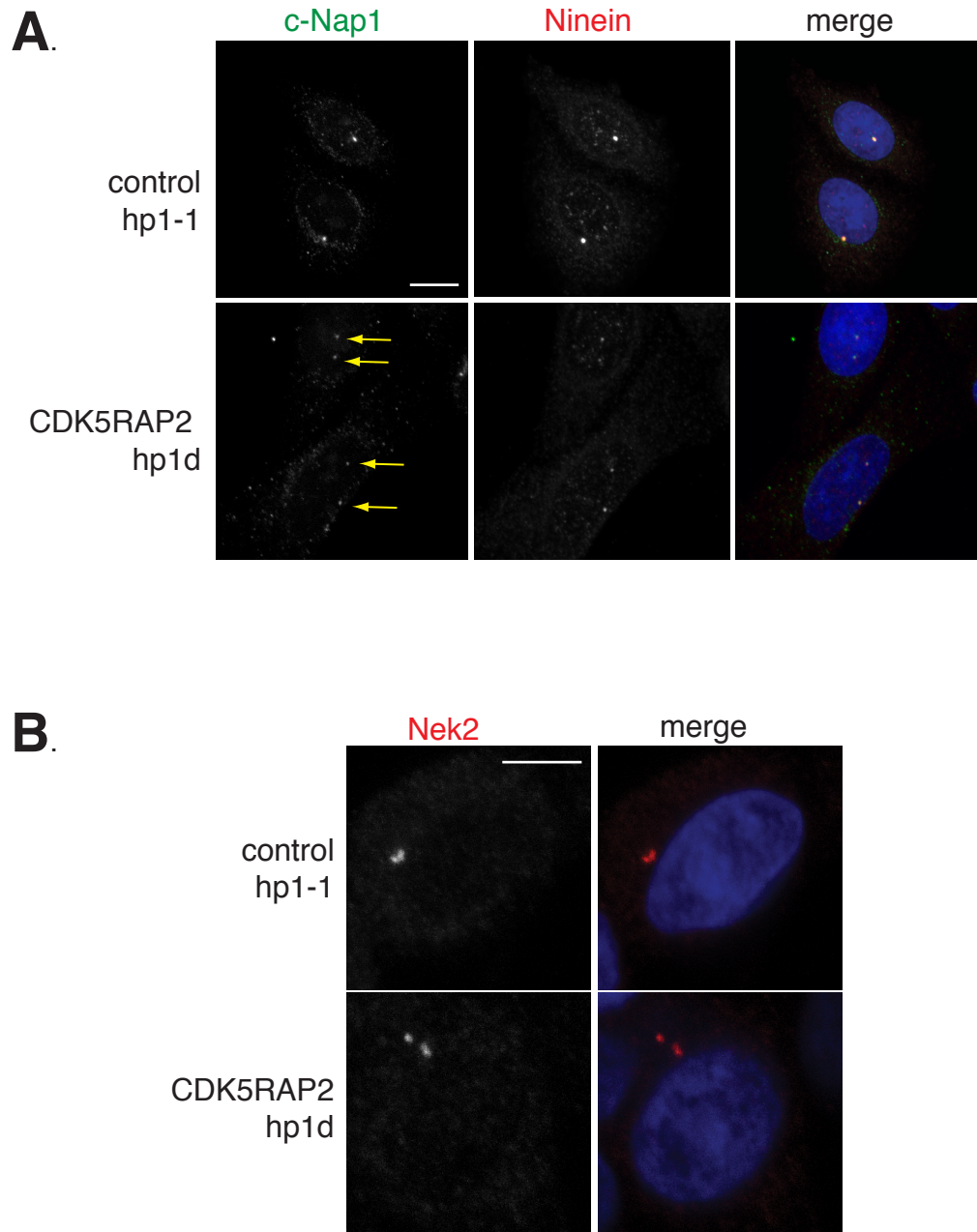


Figure 3.2.4 c-Nap1 and Nek2 still localise to split centrosomes when CDK5RAP2 is depleted. **A.** Subcellular localisation of c-Nap1 in CDK5RAP2-depleted cells. Ninein is used as a centriolar marker. c-Nap1 localisation at split centrosomes is highlighted by yellow arrows. DNA is blue, c-Nap1 is green and Ninein is red in merged images. **B.** Subcellular localisation of Nek2 in CDK5RAP2-depleted cells. DNA is blue and Nek2 is red in merged images. Scale bars are 5 μm .

centrosomes over the 4 hours period was similar to that seen in fixed cell analysis (compare figures in text above and Figure 3.2.2A). Therefore, the dynamicity of centrosome splitting does not account for the incomplete penetrance of the phenotype. It has been shown that in unperturbed cells, the mother and daughter centrioles can move apart (Piel et al., 2000). Using GFP-centrin1 stably transfected mammalian cell lines to differentiate between mother and daughter centrioles, combined with live imaging, Piel *et al.* showed that if centrioles do move apart from one another then the mother centriole remains relatively stationary at the cell centre and the daughter centriole migrates away. This was attributed to the difference in the capacity of the two centrioles to anchor microtubules (see Section 1.3.2). The mother centriole is able to anchor microtubules while the daughter centriole is not. Thus, by anchoring microtubules, the mother centriole can maintain a stable position at the centre of the cell. With this in mind, I wanted to know if there was a difference in the respective movements of the two centrioles in cells where centrosome cohesion has been perturbed. Therefore, using the time-lapse GFP-centrin1 imaging data, I first analysed control hp1-1 splitting events and noted if the centriole that moved was the mother or daughter centriole. Each individual splitting of the centrioles was scored as an independent splitting event. 15% of splitting events were not scored since I was unable to distinguish between the two centrioles as both contained equal amounts of GFP-centrin1. This is likely to represent centrioles in S-phase, when GFP-centrin1 is equally distributed between the two centrioles (Piel et al., 2000). Taking into account only those cells where I could differentiate between the mother and daughter centrioles, I did not observe a statistically significant difference between the movement of the mother versus daughter centriole (29 splitting events recorded: the mother migrated away in 15 of these cases and the daughter in 14). My data are therefore inconsistent with Piel *et al.* (Piel et al., 2000).

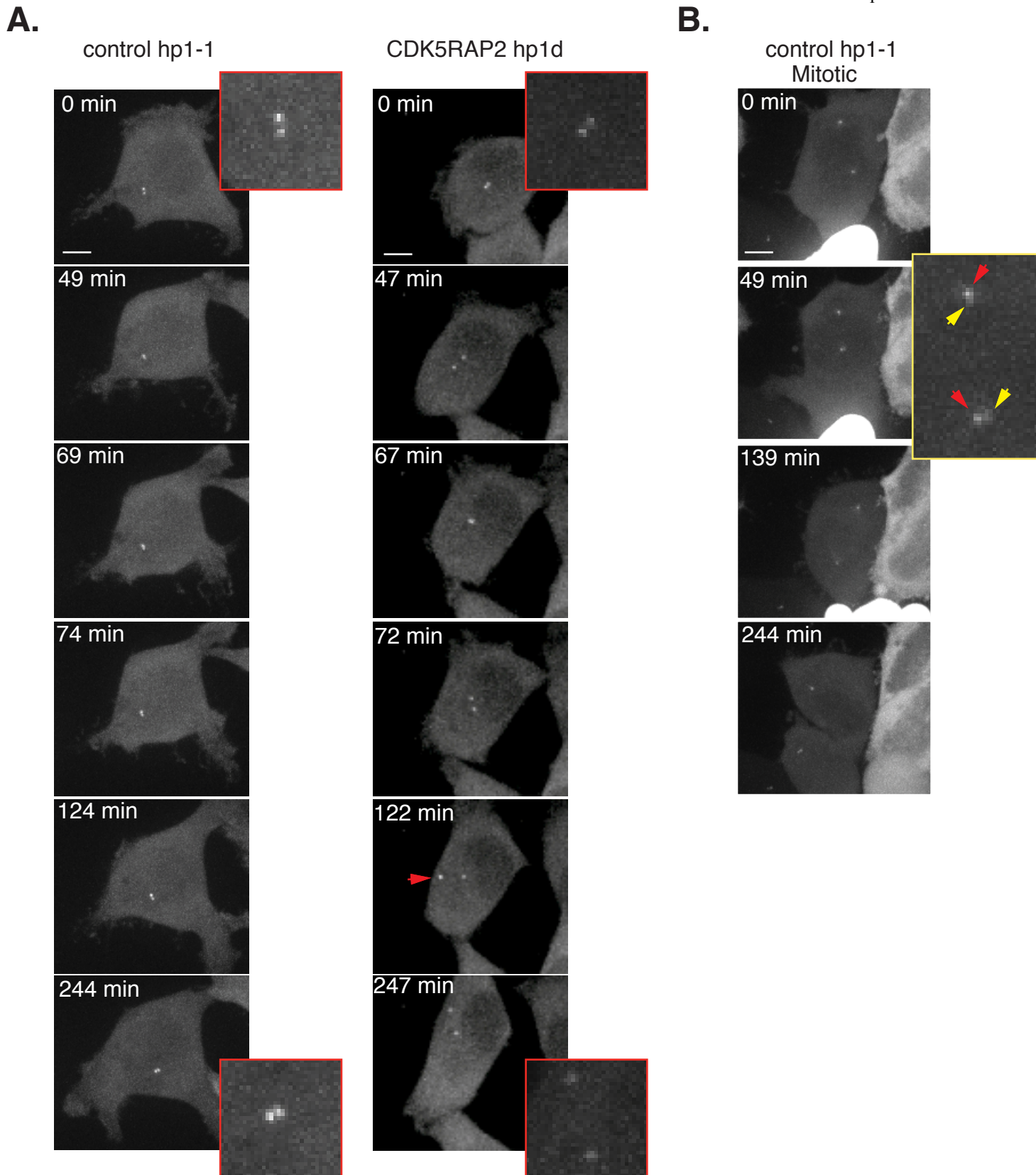
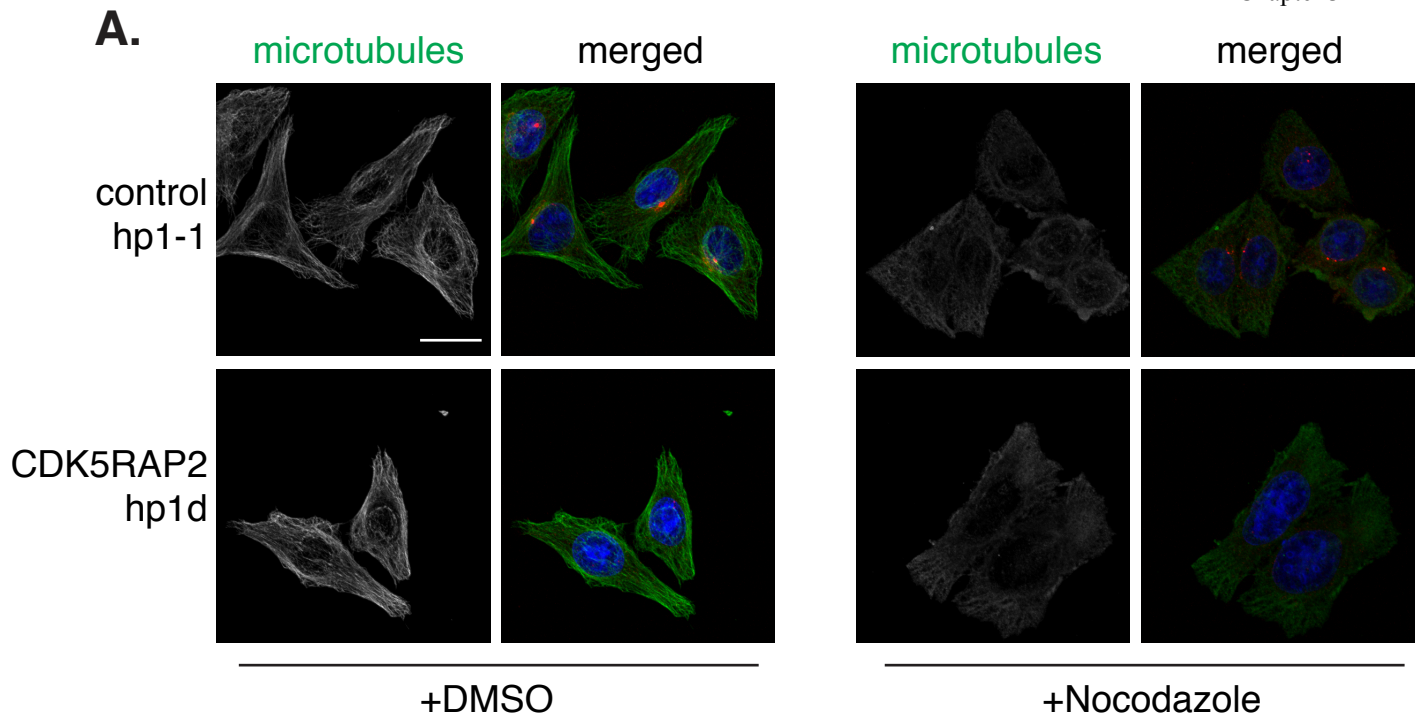


Figure 3.2.5 Split centrosomes are dynamic. Figures show movie stills taken from Movies 3.1, 3.2 and 3.3 (Supplementary CD). Control hp1-1 and CDK5RAP2 hp1d clonal cell lines were transiently transfected with GFP-centrin1 to visualise centriole dynamics. Cells were filmed every 5 min for 4 hr. **A.** Stills show centriole dynamics in control hp1-1 and CDK5RAP2 hp1d cells. In CDK5RAP2 hp1d, centrosomes move apart and come together frequently. Zoomed in images (red box) show centrosomes – only two centrosomes are present. **B.** Stills show centriole dynamics in G2 and Mitosis. Zoomed image (yellow box) shows that two pairs of centrosomes are visible. Mother centrosome is indicated by red arrows and daughter centrosome with yellow arrows. Scale bars are 5 μ m.

3.2.6 CDK5RAP2 may mediate centrosome cohesion by regulating centrosome-microtubule interactions

An intact microtubule network is essential for maintenance of centrosome cohesion (Jean *et al.*, 1999; Meraldi and Nigg, 2001). Meraldi and Nigg expanded on the earlier work by Jean *et al.* to suggest that the microtubule cytoskeleton is required to maintain a balance of kinase and phosphatase activities at the centrosome, such that if the microtubule cytoskeleton is perturbed by nocodazole (NZ) treatment then this balance is disturbed, kinases become overactive and centrosomes lose their cohesion. Therefore, I wanted to investigate if CDK5RAP2 mediated centrosome cohesion by an effect on the microtubule cytoskeleton. To investigate this, I depolymerised microtubules by nocodazole treatment in control hp1-1 and CDK5RAP2 hp1d cells. Microtubules were successfully depolymerised by a 1 hour treatment with 1 µg/ml Nocodazole in both control hp1-1 and CDK5RAP2 hp1d cells (Figure 3.2.6A). Note that CDK5RAP2 still localises to the centrosome in nocodazole treated cells and thus any loss of cohesion in nocodazole treated cells is not due to the loss of CDK5RAP2 from the centrosome. Consistent with previous reports, depolymerisation of microtubules in control hp1-1 cells led to centrosome splitting in 40% of interphase cells (Figure 3.2.6B; (Meraldi and Nigg, 2001)). In CDK5RAP2 hp1d cells treated with nocodazole, the extent of centrosome splitting was similar to that in CDK5RAP2 hp1d vehicle-treated cells (Figure 3.2.6B). Although these are only preliminary data, it suggests that loss of centrosome cohesion in CDK5RAP2-depleted cells could be due to perturbation of the microtubule cytoskeleton.



B.

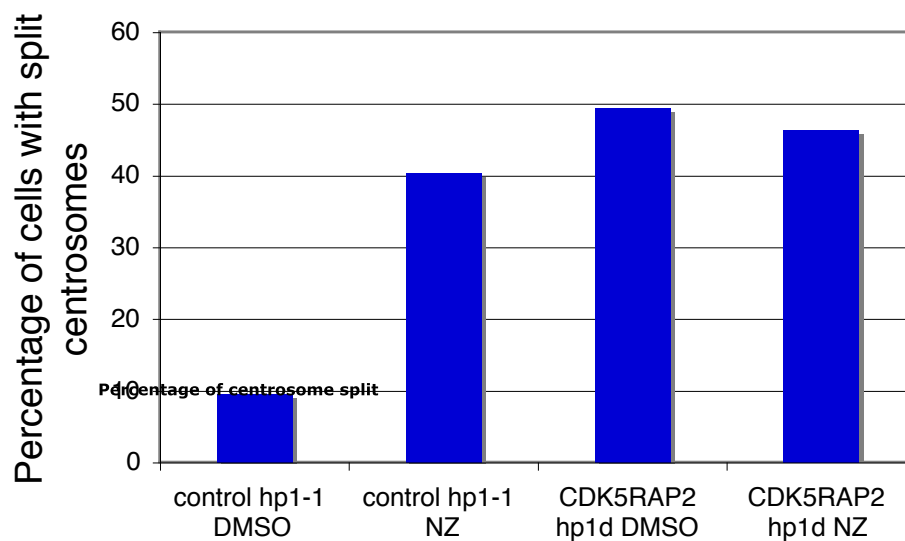


Figure 3.2.6. CDK5RAP2 may mediate centrosome cohesion by regulating microtubule-centrosome interactions. **A.** Immunostaining of control hp1-1 and CDK5RAP2 hp1d cells treated with either DMSO or nocodazole (NZ) for 1 hour. DNA is blue, microtubules are green and CDK5RAP2 is red in merged images. Scale bar is 5 μ m. **B.** Graph showing quantification of centrosome splitting in control hp1-1 or CDK5RAP2 hp1d cells treated with DMSO or nocodazole for 1 hour. n=1, 250 cells scored per condition.

3.3 CDK5RAP2 is a microtubule-associated protein and has two distinct centrosome-localisation signals

3.3.1 The N- and C-termini of CDK5RAP2 have distinct localisation patterns

CDK5RAP2 is a large (1893 amino acid) protein. The conserved CNN1 and CNN2 domains are, respectively, at the extreme N- and C-termini of the protein. To investigate which domains of CDK5RAP2 are required for its localisation, I made N-terminal FLAG-tag fusions of smaller fragments of CDK5RAP2. In designing the constructs, I was careful to conserve the secondary structure of the protein by avoiding areas with predicted coiled coils (Lupas et al., 1991). FLAG-NT consists of amino acids 1-1205 and contains the evolutionarily conserved CNN1 domain (Sawin et al., 2004; Zhang and Megraw, 2007). FLAG-CT consists of amino acids 1206-1893 and contains the conserved CNN2 domain (Figure 3.3.1A, (Kao and Megraw, 2009)). To analyse the localisation of these constructs, HeLa cells were transfected with either FLAG-FL, FLAG-NT or FLAG-CT and analysed 24 hours later. As predicted from the localisation of endogenous CDK5RAP2, FLAG-FL localised to interphase and mitotic centrosomes and to the Golgi body (Figure 3.3.1B, C). Note that TGN46 is a trans-Golgi marker and therefore the FLAG and TGN46 signals do not overlap precisely. This marker was used since both anti-FLAG and anti-gm130 antibodies were raised in mouse.

FLAG-CT had a similar localisation pattern to FLAG-FL. FLAG-CT localises to the interphase and mitotic centrosomes and to the Golgi body (Figure 3.1.3B, C). However, FLAG-NT had a quite different localisation pattern to FLAG-FL and FLAG-CT. FLAG-NT does localise to the centrosome in mitosis but is absent from the centrosome in interphase (Figure 3.3.1B). The timing of the localisation of FLAG-NT to the centrosome coincides with the appearance of activated Aurora A kinase on the centrosome in G₂, indicated by an antibody recognising Aurora A phosphorylated on T288 (pT288AurA, Figure 3.3.1B; (Barr and Gergely, 2007)). This implies that FLAG-NT is recruited to the centrosome during G₂ and remains there throughout mitosis. FLAG-NT does not localise to the Golgi body (Figure 3.3.1C).

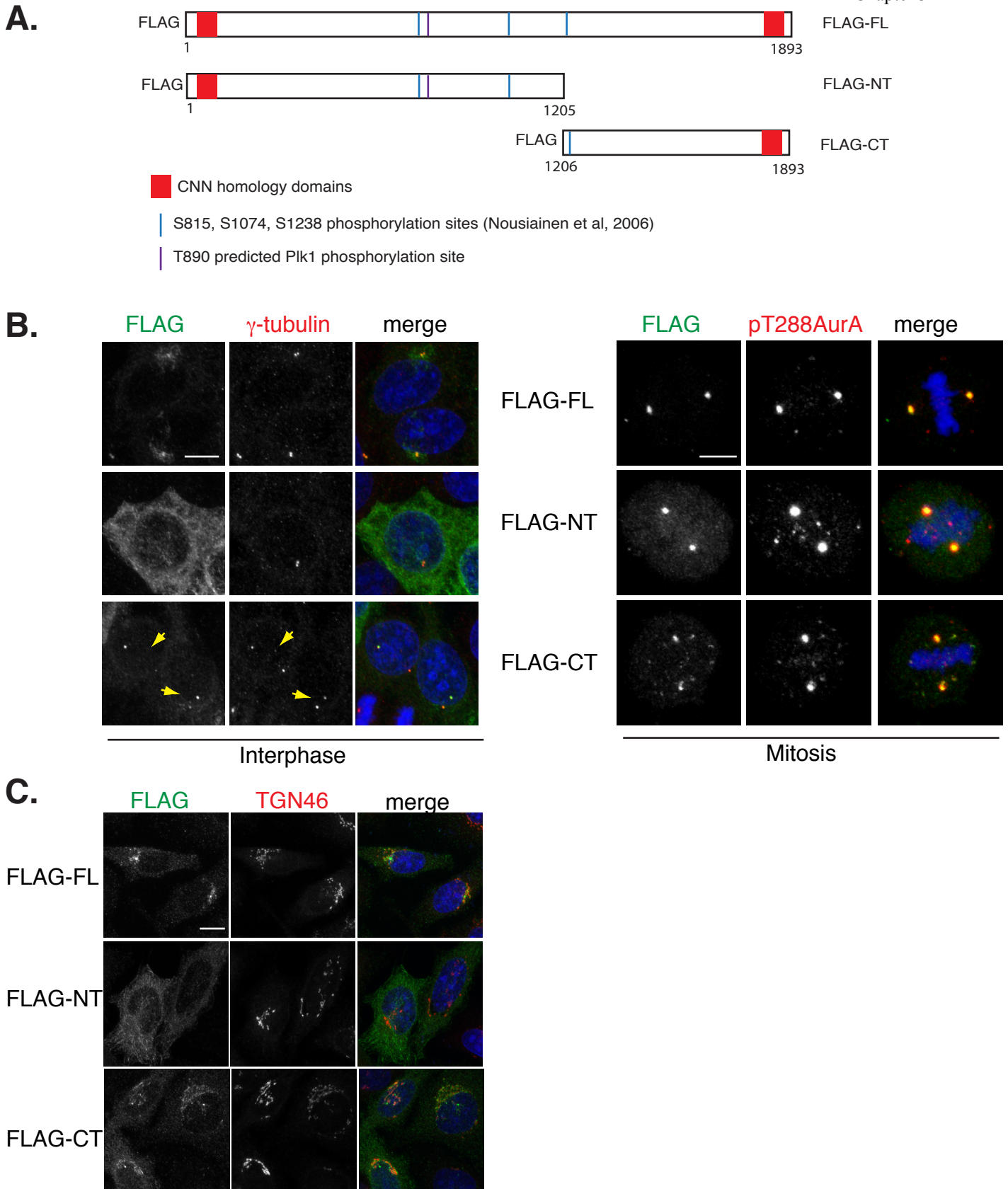


Figure 3.3.1 The N- and C-termini of CDK5RAP2 have distinct localisation patterns.

A. Schematic showing FLAG-tagged human CDK5RAP2 constructs used in this study. **B.** Subcellular localisation of FLAG-tagged CDK5RAP2 constructs in HeLa cells 24 hr after transfection. Yellow arrowheads mark split centrosomes in cells transfected with FLAG-CT. DNA is blue, FLAG-construct is green and γ -tubulin (left) or pT288Aurora-A (right) is red in merged images. **C.** FLAG-FL and FLAG-CT localise to the Golgi body as seen by proximity to the trans-Golgi marker, TGN46. DNA is blue, FLAG-constructs are green and TGN46 is red in merged images. Scale bars are 5 μ m.

In summary, while FLAG-FL and CT localise to the centrosome throughout the cell cycle, FLAG-NT only localises to the centrosome in late G2 and mitosis. This implies that there are at least two distinct centrosomal localisation signals in CDK5RAP2.

Interestingly, overexpression of CDK5RAP2 does not prevent centrosome separation as cells can still form bipolar spindles in the presence of overexpressed FLAG-FL CDK5RAP2 (Figure 3.3.1B).

3.3.2 Overexpression of the C-terminus of CDK5RAP2 leads to a loss of centrosome cohesion

During domain analysis of CDK5RAP2, I noticed that there was a high frequency of FLAG-CT expressing cells that had split centrosomes (Figure 3.3.1B and 3.3.2A). Scoring of cells transfected with FLAG-FL, FLAG-NT or FLAG-CT confirmed that almost 40% of cells expressing FLAG-CT had split centrosomes (Figure 3.3.2B). This was similar to the extent of centrosome splitting caused by depletion of CDK5RAP2 by siRNA/shRNA. Neither FLAG-FL nor FLAG-NT overexpression caused centrosome splitting.

To investigate why FLAG-CT overexpression would cause centrosome splitting, I analysed CDK5RAP2 localisation in cells transfected with FLAG-FL, FLAG-NT or FLAG-CT. Strikingly, cells overexpressing FLAG-CT (but not those overexpressing FLAG-FL or FLAG-NT) had little or no endogenous CDK5RAP2 at the centrosome or Golgi (Figure 3.3.2C). Therefore, it appears that FLAG-CT has a higher affinity for the centrosome than endogenous CDK5RAP2 and thus endogenous CDK5RAP2 protein is displaced.

Interestingly, FLAG-CT appeared to be asymmetrically distributed at the two split centrioles, while γ -tubulin was, predominantly, equally present at both (see yellow arrowheads, Figure 3.3.1B). To check if this represents a preferential localisation of CDK5RAP2 to the mother or daughter centriole, I triple-stained FLAG-CT transfected cells for FLAG-CT, ninein - a centrosomal protein that preferentially associates with the mother centriole (Piel et al., 2000), and centrin-3 - a centriolar marker. FLAG-CT mimics the localisation of ninein and also preferentially localises to the mother centriole (Figure 3.3.2D). Endogenous CDK5RAP2 that remained at the centrioles after RNAi also appeared to localise asymmetrically between the two

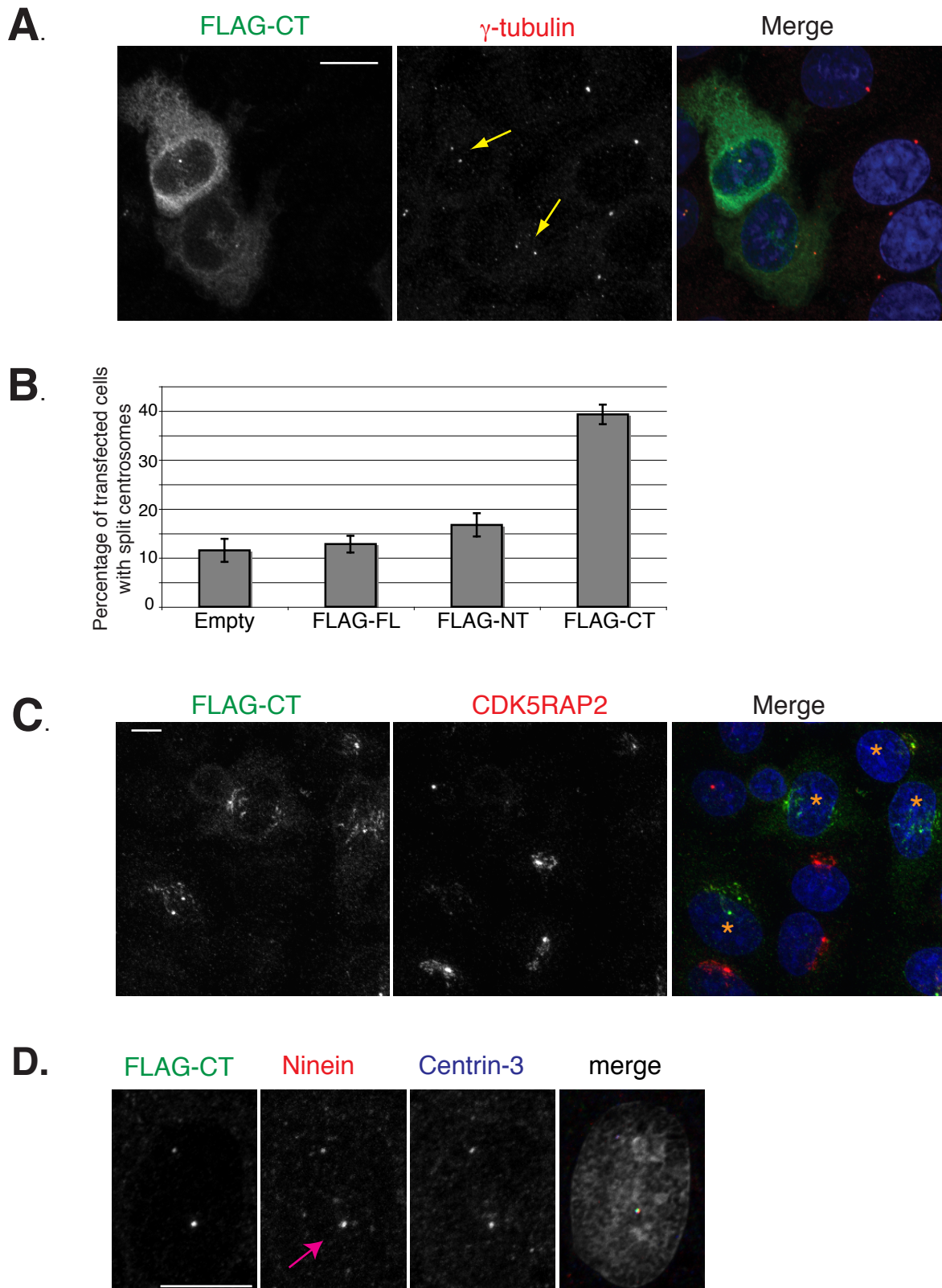


Figure 3.3.2 Expression of the C-terminus of CDK5RAP2 leads to loss of centrosome cohesion. **A.** Immunofluorescence images showing cells that express FLAG-CT often have split centrosomes. DNA is blue, FLAG-CT is in green and γ -tubulin is in red in merged images. **B.** Graph quantifying the number of cells with split centrosomes in cells transfected with FLAG-tagged CDK5RAP2 constructs. Cells were analysed 24 hr after transfection. $n=3$, at least 200 cells counted per condition, per experiment. Error bars represent STD. **C.** Subcellular localisation of CDK5RAP2 in FLAG-CT expressing HeLa cells. Cells expressing FLAG-CT are marked with an asterisk in merged image. DNA is blue, FLAG-CT is green and CDK5RAP2 is red in merged images. **D.** FLAG-CT of CDK5RAP2 preferentially localises to the mother centriole, as seen by colocalisation with ninein. Pink arrow indicates mother centriole. DNA is grey, FLAG-CT is green, ninein is red and centrin-3 is blue in merged image. Scale bars are 5 μ m.

centrioles (Figure 3.2.1D). These results suggest that CDK5RAP2 may preferentially localise to the mother centriole. However, to definitively prove this I would need to use immunolabelling and electron microscopy. The separation of the two centrioles in FLAG-CT transfected and CDK5RAP2-depleted cells provide a useful tool to study this asymmetric localisation.

In summary, overexpression of the C-terminus of CDK5RAP2 displaces endogenous CDK5RAP2 from the centrosome and causes a loss of centrosome cohesion. Furthermore, this implies that the C-terminus of CDK5RAP2 alone is not sufficient for centrosome cohesion.

3.3.3 FLAG-NT interacts with endogenous CDK5RAP2

A second centrosomal protein mutated in microcephaly, CenpJ, has been shown to be required for centrosome cohesion (Zhao et al., 2010). In a set of elegant experiments, the authors show that CenpJ mediates centrosome cohesion via homo-dimerisation. Therefore, I wanted to investigate if CDK5RAP2 might also homo-dimerise.

To do this, I immunoprecipitated FLAG-tagged CDK5RAP2 constructs (Figure 3.3.1A) from HeLa cells and looked for the coprecipitation of endogenous CDK5RAP2 (Figure 3.3.3). Since FLAG-FL and endogenous CDK5RAP2 are very similar in size, I was unable to determine if FLAG-FL coprecipitated endogenous CDK5RAP2. However, FLAG-NT and FLAG-CT migrate faster on SDS-PAGE than the endogenous protein. I was able to detect an interaction between FLAG-NT and endogenous CDK5RAP2 (Figure 3.3.3). I could not detect an interaction between FLAG-CT and endogenous CDK5RAP2. However, the relative amount of FLAG-NT immunoprecipitated was higher than the amount of FLAG-CT immunoprecipitated (Figure 3.3.3), therefore FLAG-CT may coprecipitate endogenous protein if more FLAG-CT was immunoprecipitated. What I can conclude is that CDK5RAP2 can either homodimerise or oligomerise and that this interaction is, at least in part, mediated by its N-terminus.

3.3.4 Endogenous CDK5RAP2 can bind to microtubules

At higher levels of expression, FLAG-FL and FLAG-NT appear to colocalise with the interphase microtubule network, as shown by colocalisation with β -tubulin (Figure 3.3.4A). Neither construct colocalises with the whole microtubule network,

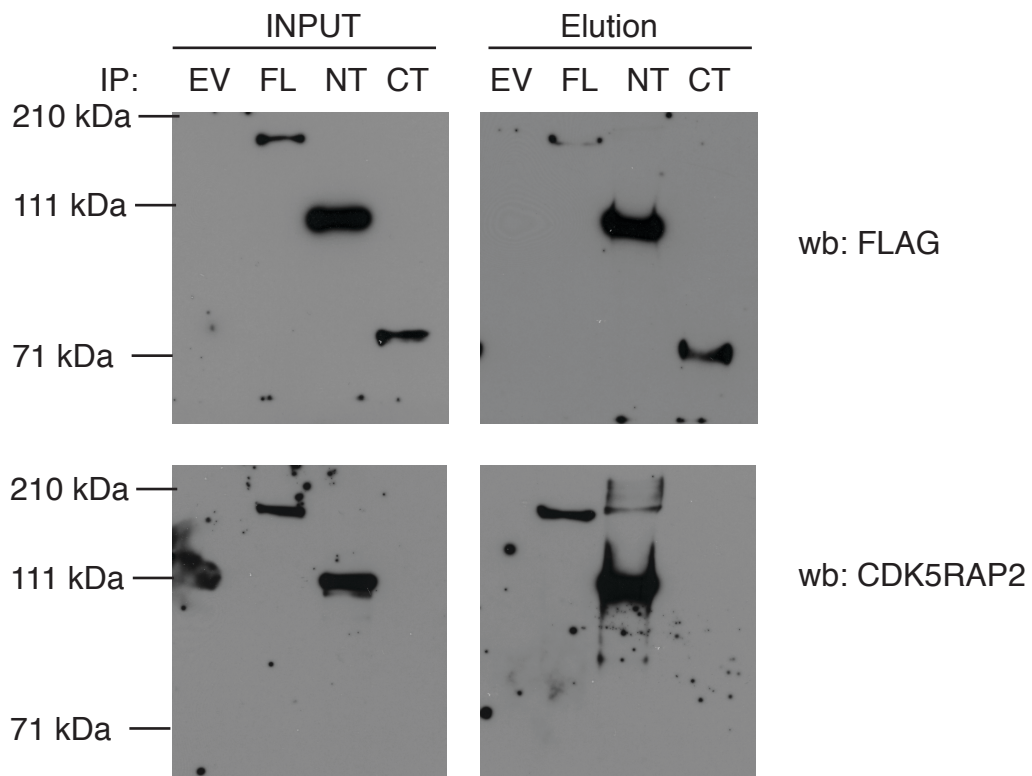


Figure 3.3.3 CDK5RAP2 may dimerise via its N-terminus. Western blot of immunoprecipitation of FLAG-tagged CDK5RAP2 constructs (see 3.3.1A) from asynchronous HeLa cell extracts, 24 hr after transfection. Immunoprecipitation of FLAG-NT coprecipitated endogenous CDK5RAP2. Input is one third of the elution amount. 'EV' refers to empty vector. 'FL', 'NT' and 'CT' refer to constructs in Figure 3.3.1A. 'IP' is Immunoprecipitation. 'wb' is Western blot.

suggesting that FLAG-FL and FLAG-NT only localise to a subset of microtubules – perhaps long-lived microtubules. FLAG-CT does not localise to microtubules. I have never detected endogenous CDK5RAP2 on microtubules by immunostaining, even in multiple different fixation conditions (methanol, 3% paraformaldehyde and 4% formaldehyde). Therefore, to see if localisation of overexpressed CDK5RAP2 to microtubules was physiologically relevant, I performed a microtubule-pelleting assay on endogenous protein from asynchronous cell extracts (Section 2.12, Materials and Methods). Figure 3.3.4B shows that a fraction of endogenous CDK5RAP2 can associate with microtubule polymer.

Thus it seems that CDK5RAP2 can localise to microtubules, when expressed at high levels, and that this requires the N-terminus of the protein. Moreover, endogenous CDK5RAP2 co-pelleted with Taxol-stabilised microtubules in an *in vitro* assay. Figure 3.3.4C summarises the localisation of the FLAG-constructs.

3.3.5 CDK5RAP2 is phosphorylated in mitosis

The specific localisation of FLAG-NT to the centrosome during G2 and mitosis led me to question whether this could be a phosphorylation-dependent event. Multiple kinases are known to regulate centrosome maturation during G2, for example Plk1 and Aurora A, and this regulation depends on their kinase activity. In *Drosophila* S2 cells, Cnn and Polo (the fly orthologue of Plk1) have been shown to be co-dependent for their localisation to the centrosome during centrosome maturation, and Cnn is phosphorylated in mitosis in a Polo dependent manner (Dobbelaere et al., 2008). Multiple centrosomal proteins are phosphorylated upon entry into mitosis and phosphorylation is required for their recruitment to the centrosome (for example, TACC3; (Kinoshita et al., 2005; LeRoy et al., 2007)). Therefore, I asked if CDK5RAP2 was phosphorylated during mitosis. To test this hypothesis, we made asynchronous and mitotic HeLa cell extracts and subjected them to one of three conditions: no treatment, addition of PhosSTOP (to inhibit phosphatases present in the cell extract) or addition of lambda phosphatase (to remove phosphate groups from proteins). Figure 3.3.5A shows that CDK5RAP2 is phosphorylated in mitosis. It seems that not the whole pool of CDK5RAP2 is phosphorylated, since in the untreated and PhosSTOP lanes, two closely positioned bands are present, the lower of which is of a similar size to that of the lambda phosphatase-treated protein.

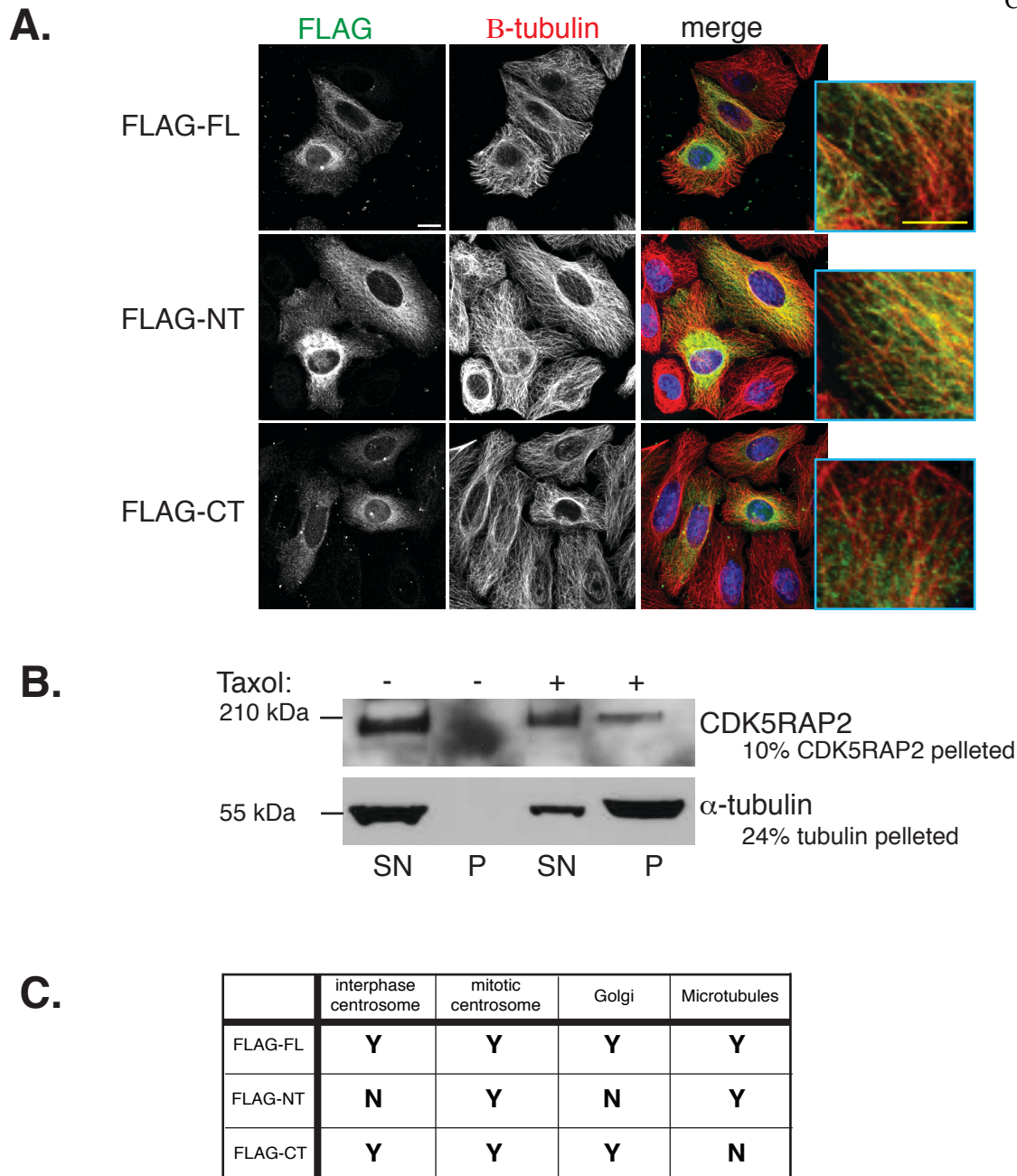


Figure 3.3.4 Endogenous CDK5RAP2 binds to microtubules and overexpressed CDK5RAP2 localises to microtubules. A. Subcellular localisation of FLAG-tagged CDK5RAP2 constructs in HeLa cells 24 hr after transfection. Insets (blue boxes) show zoomed in images to illustrate colocalisation of FLAG-FL and FLAG-NT with microtubules. DNA is blue, FLAG is green and β -tubulin is red in merged images. White scale bar is 5 μ m. Yellow scale bar is 2.5 μ m. **B.** Western blot shows that a fraction of endogenous CDK5RAP2 can bind to microtubules in a microtubule-pelleting assay. Percentages of protein pelleted were calculated using NIH ImageJ software based on the fact that the amount of pellet loaded is five times more concentrated than the supernatant. Fractions precipitated are measured relative to ‘–Taxol SN’ which is effectively equal to input. SN = supernatant (free tubulin and unbound material), P=microtubule pellet (plus any bound material). **C.** Table summarising localisation of FLAG-tagged constructs. Y=Yes, N=No.

To find out which domain is phosphorylated in CDK5RAP2, we used the FLAG-tagged constructs (Figure 3.3.1A) in the same lambda phosphatase assay. However, we were unable to detect a size shift upon lambda phosphatase treatment in any of the FLAG-CDK5RAP2 constructs. Therefore, we were unable to find which domain(s) of CDK5RAP2 are phosphorylated.

Several phosphorylation sites have been identified in CDK5RAP2 in an analysis of the phosphoproteome of the mitotic spindle (Nousiainen et al., 2006). In this paper, mitotic spindles were purified from HeLa cells and phosphorylated proteins present in the preparations were identified by mass spectrometry. The phosphorylation sites identified in CDK5RAP2 are highlighted in Figure 3.3.1A. I identified a Plk1 kinase consensus site (D/E-X-S/T-Φ-X-D/E; (Nakajima et al., 2003)) in the N-terminus of CDK5RAP2 at T890. To see if any of these phosphorylation sites were involved in localisation of CDK5RAP2 protein, I mutated each of these four sites individually, and in combination, to alanine to generate non-phosphorylatable constructs. None of the S815A, T890A S1074A or S1238A mutations alone, or in combination, affected the localisation of any of the FLAG-tagged CDK5RAP2 constructs (Figure 3.3.5B).

Therefore, while we know that endogenous CDK5RAP2 protein is phosphorylated in mitosis (Figure 3.3.5A and (Nousiainen et al., 2006)) we still do not know which domain(s) are phosphorylated and what consequence this has on CDK5RAP2 localisation or function.

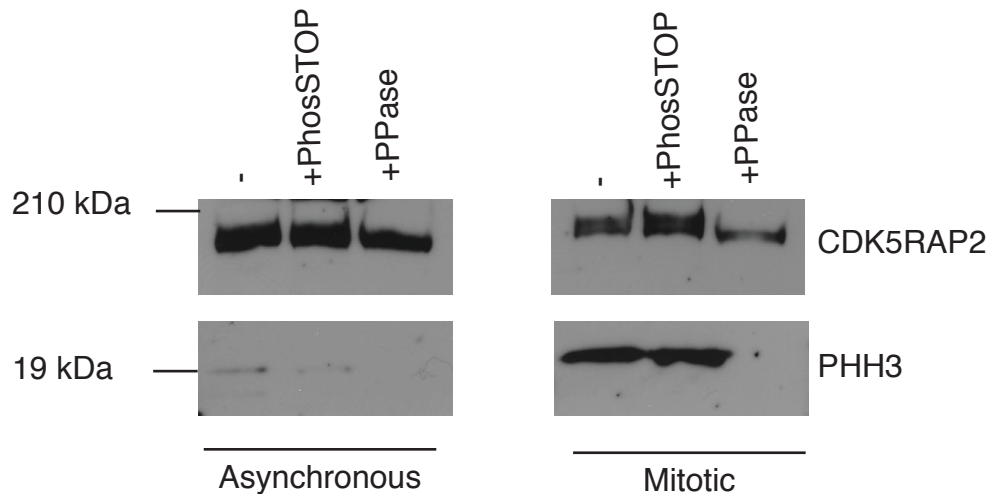
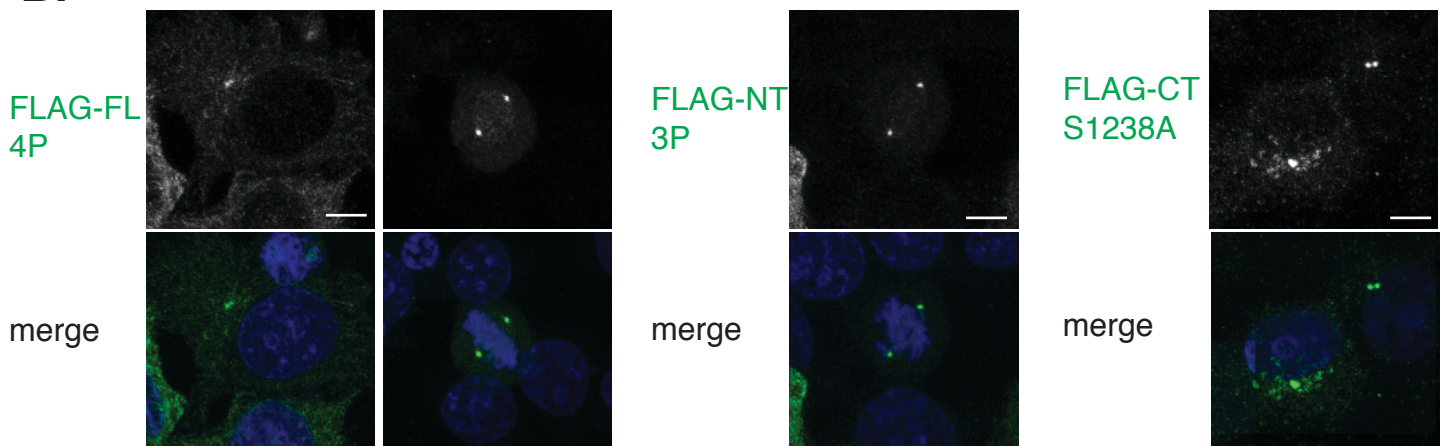
A.**B.**

Figure 3.3.5 CDK5RAP2 is phosphorylated in mitosis. **A.** Western blot showing asynchronous (left) and mitotic (right) HeLa cytoplasmic extracts either untreated (-), treated with PhosSTOP, or treated with lambda phosphatase (+PPase). In the mitotic extract treated with lambda phosphatase CDK5RAP2 migrates faster, indicating that CDK5RAP2 is normally phosphorylated in mitosis. Phosphorylated Serine 10 on Histone H3 (PHH3) is higher in mitotically arrested cells, indicating they are in mitosis. In addition, PHH3 staining acts as a positive control for phosphatase treatment. Treatment of the mitotic sample with lambda phosphatase removes the phosphate group from Ser10 and thus the PHH3 signal is absent in this lane. (Note – this experiment was designed by ARB but performed by a Masters student, Tolou Golkar, under the supervision of ARB). **B.** Subcellular localisation of FLAG-tagged CDK5RAP2 constructs that have had potential phosphorylation sites mutated to alanine (see Figure 3.3.1A for positions of these sites) . FLAG-FL 4P (S815A, T890A, S1074A, S1238A), FLAG-NT 3P (S815A, T890A, S1074A). DNA is blue and FLAG-constructs are green in merged images. Scale bars are 5 μm .

3.4 Myomegalin is not required for centrosome cohesion

3.4.1 Making an anti-human Myomegalin antibody

At the start of the project, no commercial antibodies for Myomegalin were available. Therefore, an N-terminal fusion protein between MBP and amino acids 19-223 of human Myomegalin was made and purified in the lab (D. Zyss) (Figure 3.4.1A). This epitope contains the highly evolutionarily conserved CNN1 domain and thus, like the CDK5RAP2 antibody, is potentially useful in other species (Sawin et al., 2004; Zhang and Megraw, 2007).

On Western blots of HeLa and U251MG (glioblastoma) whole cell extracts, the Myomegalin antibody recognised a band of greater than 210 kDa, which corresponds to the predicted MW of the full-length protein of 265kDa (Figure 3.4.1B). The antibody also recognised two smaller bands at approximately 41 kDa in both cell lines. Ensembl predicts eight splice variants of the human Myomegalin gene. Three of these are identical and correspond to the protein Myomegalin isoform 3 (accession number NP_071754.3), with a predicted MW of 36 kDa and therefore this could correspond to one of the bands at 41 kDa.

3.4.2 Myomegalin is not required to maintain centrosome cohesion

Since CDK5RAP2 is required for centrosome cohesion, I wanted to see if Myomegalin was also involved in this process. Therefore, I used siRNA to deplete Myomegalin from U251MG cells. Immunostaining of U251MG cells showed that Myomegalin localised to the centrosome throughout the cell cycle and Golgi body in interphase, as reported previously by (Verde et al., 2001) (Figure 3.4.2A). This signal was significantly reduced after siRNA depletion of Myomegalin (Figure 3.4.2A). Western blot analysis showed a reduction in the signal of Myomegalin antibody in the Myomegalin-depleted lysates (Figure 3.4.2B). Moreover, despite the extensive homology between the CNN1 domains of CDK5RAP2 and Myomegalin, the Myomegalin antibody did not cross react with CDK5RAP2 antibody, and vice-versa, since neither antibody showed a reduction in signal on depletion of the homologous protein (Figure 3.4.2B).

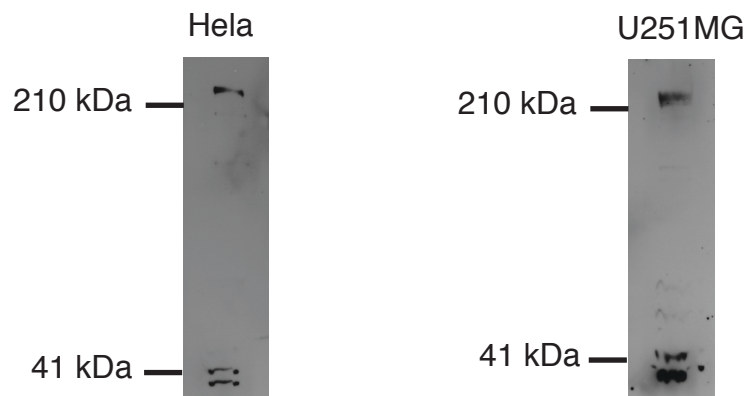
A.**B.**

Figure 3.4.1 Making a anti-human Myomegalin antibody **A.** Schematic showing the position of the epitope within Myomegalin, relative to the CNN1 and CNN2 domains. **B.** Western blotting of HeLa (epithelial) and U251MG (glioblastoma) whole cell extracts with our purified Myomegalin antibody.

To see if centrosome cohesion was affected in Myomegalin-depleted cells, I scored siRNA-treated cells for the presence of split centrosomes (based on γ -tubulin staining). Depletion of Myomegalin protein did not lead to a loss of centrosome cohesion in U251MG cells, while depletion of CDK5RAP2 protein did (Figure 3.4.2C). Moreover, co-depletion of both CDK5RAP2 and Myomegalin did not lead to a further increase in loss of centrosome cohesion (the difference between CDK5RAP2 siRNA alone and CDK5RAP2/Myomegalin siRNA is not statistically significant; Figure 3.4.2C). Therefore, Myomegalin is not required for centrosome cohesion.

3.4.3 Myomegalin localisation varies between cell lines

In the U251MG glioblastoma cell line, Myomegalin specifically localises to the centrosome and Golgi, as expected from previous observations in COS-7 cells (derived from the kidney of the African Green Monkey; (Verde et al., 2001)). Myomegalin also recognised the centrosome and Golgi in the T-lymphoblastic cell line, Jurkat (D. Zyss, personal communication). However, immunostaining of the epithelial cell lines HeLa (cervical carcinoma, epithelial) and HB2 (normal breast epithelial) did not show a centrosomal, basal body or Golgi staining of Myomegalin (Figure 3.4.3A). In fact, in these cell lines, Myomegalin did not stain any recognisable structure in the cell in a variety of different fixation conditions (Methanol (Figure 3.4.3A), 3% Paraformaldehyde, 4% Formaldehyde; data not shown). This seemed confusing as Myomegalin is clearly expressed in HeLa and recognises a band of the same size as that in U251MG cells, at over 210 kDa (Figure 3.4.1B) that most likely corresponds to the full-length Myomegalin protein of predicted MW 265 kDa.

In order to try and work out why Myomegalin had different localisation patterns in HeLa and U251MG cells, I used Reverse Transcription (RT)-PCR to systematically amplify all exons from Myomegalin cDNAs made from these cell lines to try and identify any differences in splice forms. I extracted RNA from both cell lines and generated cDNA in a RT reaction, using random primers. I used this cDNA to specifically PCR Myomegalin exon pairs (Figure 3.4.3B), which were then gel extracted and sequenced to confirm the PCR products. All of the exon pairs tested

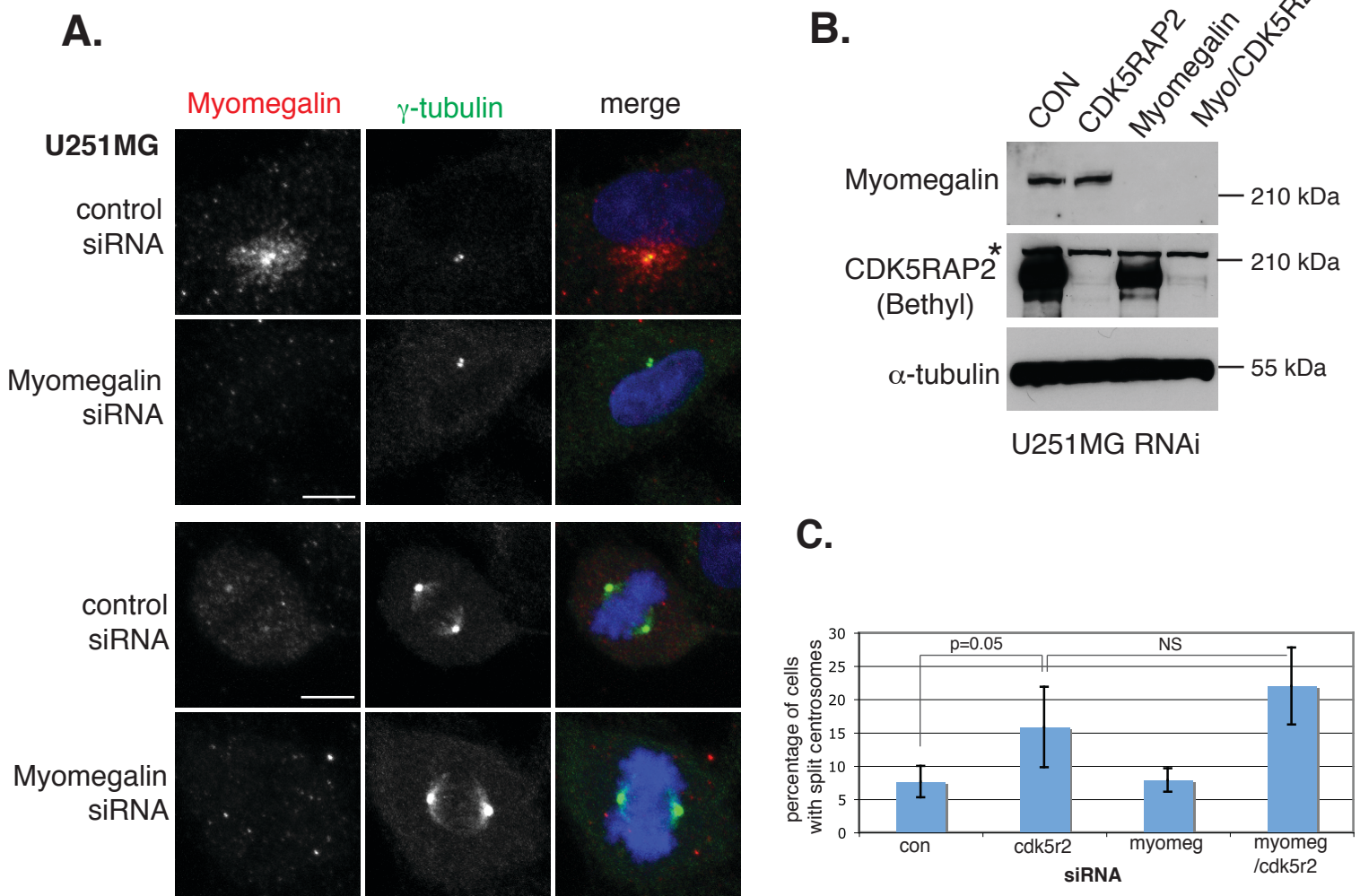


Figure 3.4.2 Myomegalin is not required for centrosome cohesion. **A.** Subcellular localisation of Myomegalin in U251MG cells shows that Myomegalin localises to the centrosome and Golgi. This staining is specific for Myomegalin protein as it is reduced after treatment with Myomegalin-targeting siRNAs (lower panels). DNA is blue, myomegalin is red and γ -tubulin is green in merged images. Scale bar is 5 μ m. **B.** Western blot of whole cell extracts 48 hr after transfection of U251MG cells with control, Myomegalin or CDK5RAP2 siRNA. Myomegalin antibody is specific and does not cross-react with CDK5RAP2 antibody. This blot also shows the specificity of the commercial Bethyl antibody for CDK5RAP2 protein (epitope is amino acids 300-554 in human CDK5RAP2). β -actin serves as a loading control. Asterisk marks a non-specific band. **C.** Graph indicating number of cells with split centrosomes in U251MG cells depleted of proteins shown on x-axis. $n=3$, at least 100 cells scored per condition, per experiment. Two-tailed Mann-Whitney test revealed the difference between CDK5RAP2 siRNA treated cells and double CDK5RAP2/Myomegalin siRNA treated cells, not to be statistically significant at ($p=0.37$).

(from exons 1-44) were expressed in both HeLa and U251MG cell lines (Figure 3.4.3B). I was unable to amplify more than approximately 700 bp from the cDNA generated using this method, therefore it is possible that those pairs tested are in different transcripts between the two cell lines. In summary, I was unable to identify the reason for the difference in Myomegalin localisation in different cell lines.

The localisation of Myomegalin to the centrosome and Golgi in the glioblastoma and T-lymphoblastic cell lines, yet not in epithelial cell lines, was intriguing. I had access to three glioblastoma primary cell lines (generous gift from Colin Watts). Therefore, I tested Myomegalin localisation in these three cell lines to see if the localisation was consistent between glioblastoma lines. Interestingly, while Myomegalin did localise to the centrosome and Golgi in all three of the cell lines, the level of Myomegalin expression varied from cell to cell, even within a population (Figure 3.4.3C, D). G19 had the highest expression and in immunostaining, Myomegalin was clearly expressed in every cell in the population. However, lines G23 and G25 had considerably lower expression and only a small proportion of cells had visible Myomegalin staining. These differences were independent of cell density and passage number. Moreover, I could observe no morphological differences between the cells within a cell line that might suggest that there were multiple cell types present that could explain the difference in Myomegalin localisation.

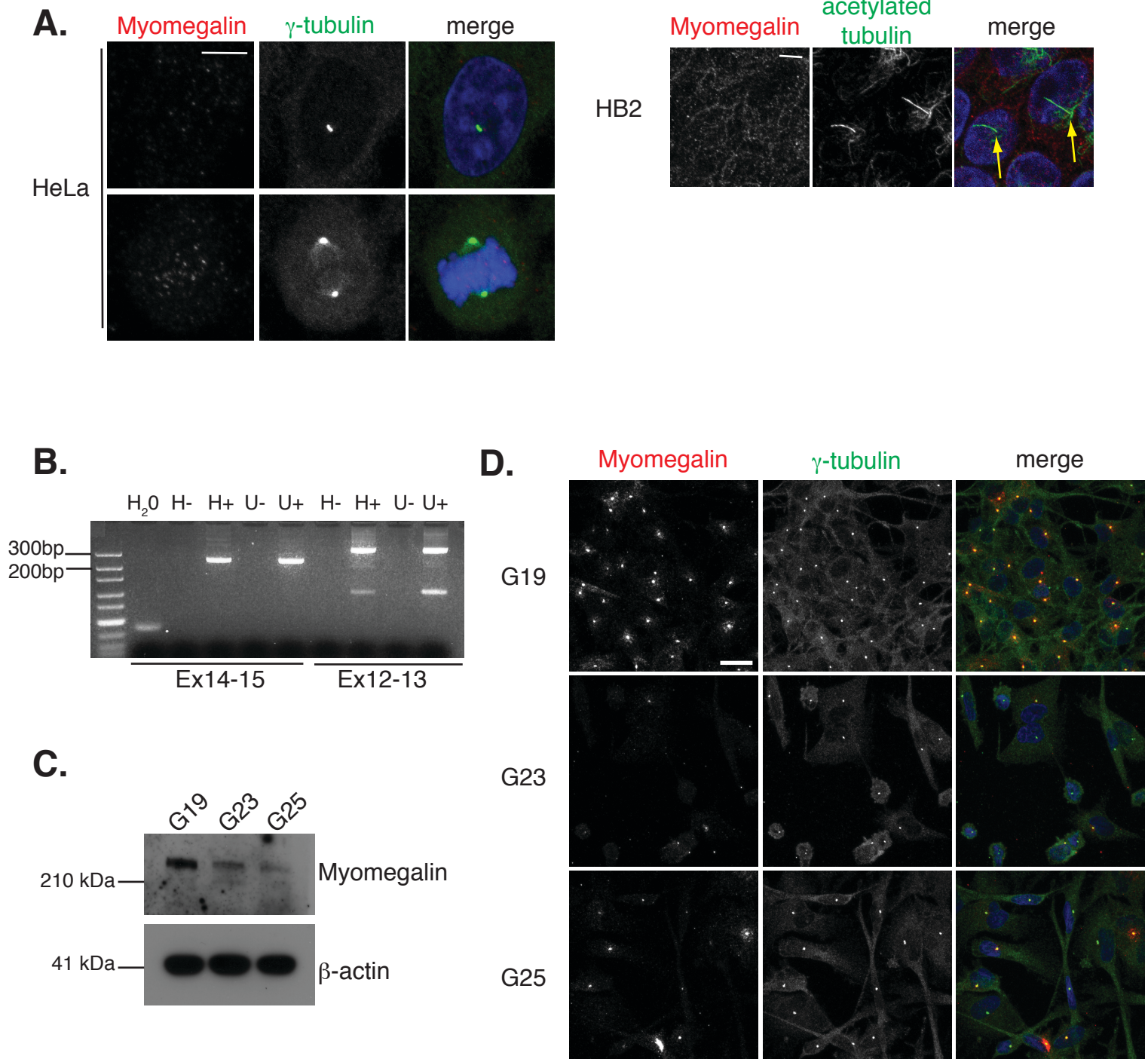


Figure 3.4.3 Myomegalin localisation varies between cell lines. **A.** Subcellular localisation of Myomegalin in HeLa (left) and HB2 (right) cells reveals that Myomegalin does not localise to the centrosome or Golgi in HeLa cells, nor to the basal body in HB2 cells (position of basal body indicated by yellow arrows in merged image). DNA is blue, myomegalin is red and γ -tubulin is green in merged images. Scale bars are 5 μ m. **B.** 2% ethidium bromide stained agarose gel showing example of PCR products obtained. HeLa (H) and U251MG (U) have identical products. ‘-/+’ refer to absence or presence of reverse transcriptase in the RT reaction. First lane is 100 bp DNA ladder. **C.** Western blot of whole cell lysates of glioblastoma cell lines. G19, G23 and G25 refer to the names of the cell lines. β -actin serves as a loading control. **D.** Subcellular localisation of Myomegalin in the three glioblastoma cell lines shown in ‘C’. Note that in lines G23 and G25, Myomegalin levels vary between cells in the same population. DNA is blue, myomegalin is red and γ -tubulin is green in merged images. Scale bar is 10 μ m.

3.5 Discussion

3.5.1 CDK5RAP2 mediates centrosome cohesion

3.5.1.1 CDK5RAP2 mediates centrosome cohesion independently of known centrosome cohesion proteins

Depletion of CDK5RAP2 revealed a role for this protein in maintaining centrosome cohesion during interphase (Figure 3.2.2A). During the course of my PhD, the same conclusion was reached by another group using a different cell line (U2OS) (Graser et al., 2007a). Graser and colleagues used an siRNA screen targeting centrosomal genes to determine if loss of centrosome cohesion was a general defect of disrupting centrosome structure, or if it was due to a specific defect caused by depletion of specific proteins. They concluded that centrosome cohesion is maintained by a subset of centrosomal proteins and furthermore identified two novel mediators of centrosome cohesion – CDK5RAP2 and cep68. Further investigation of cep68 revealed that it is part of the known centrosome cohesion pathway involving c-Nap1 and rootletin. However, consistent with my data, they found that CDK5RAP2 appeared to be part of an independent centrosome cohesion pathway. I found that depletion of CDK5RAP2 did not lead to mislocalisation of c-Nap1 or Nek2 (Figure 3.2.4A, B). My data do not exclude the possibility that CDK5RAP2 is downstream of c-Nap1 and Nek2. However, Graser *et al.* performed an extensive study to analyse the potential function of CDK5RAP2 in known centrosome cohesion pathways. They depleted known centrosome cohesion proteins and analysed CDK5RAP2 localisation. They found no change in CDK5RAP2 localisation upon depletion of c-Nap1, rootletin or cep68. Similarly, they depleted CDK5RAP2 and analysed the localisation of these three proteins and again found no defect. This indicates that CDK5RAP2 is not downstream of known cohesion proteins.

Further evidence for an independent role for CDK5RAP2 in mediating cohesion is that c-Nap1, rootletin and cep68 are all dissociated from the centrosome to allow centrosomes to separate in G2 (c-Nap1 is only partially dissociated but its mitotic centrosomal levels are lower than those in interphase) (Bahe et al., 2005; Fry et al., 1998a; Graser et al., 2007a). In contrast, CDK5RAP2 remains associated with the centrosome in mitosis and I did not observe a reduction in the amount of CDK5RAP2

at the centrosome in mitotic cells (Figure 3.1.2A; (Graser et al., 2007a)). This does not rule out the possibility that in G2 a small amount of CDK5RAP2 is removed from the centrosomes to allow centrosomes to separate. However, it does indicate that perhaps, unlike cep68 and rootletin, CDK5RAP2 may have roles in the cell cycle that are outside of its centrosome cohesion role. A further argument supporting an independent role for CDK5RAP2 in centrosome cohesion is that overexpression of rootletin causes the formation of fibres and it is these fibres that are proposed to act as a physical linker between the two centrioles. CDK5RAP2 did not localise to these fibres nor did it localise to intercentriolar fibres seen by immunogold electron microscopy (Graser et al., 2007a). Therefore, CDK5RAP2 is unlikely to mediate centrosome cohesion by forming a physical linker between the two centrioles, in the same way as that suggested for rootletin, c-Nap1 and cep68.

3.5.1.2 Potential mechanisms of centrosome cohesion mediated by CDK5RAP2

If CDK5RAP2 does not form a physical linker, how does it mediate centrosome cohesion? Below I outline two possibilities.

A role for CDK5RAP2 in regulating centrosome-microtubule interactions?

I have shown that endogenous CDK5RAP2 can bind to Taxol-stabilised microtubules (Figure 3.3.4B). Depletion of CDK5RAP2 and disruption of the microtubule network by nocodazole did not exacerbate loss of centrosome cohesion in interphase cells over either treatment alone (Figure 3.2.6). This suggests that the loss of centrosome cohesion observed in CDK5RAP2-depleted cells is due to perturbation of the microtubule network, such that further perturbation of the microtubule cytoskeleton has no additional effect.

Overexpression of the C-terminus of CDK5RAP2 (and consequent displacement of endogenous CDK5RAP2 from the centrosome (Figure 3.3.2C)) also leads to the loss of centrosome cohesion (Figure 3.3.2B), even though this C-terminal domain localises to the centrosome in interphase. These data imply that the N-terminus of CDK5RAP2 is involved in mediating centrosome cohesion. FLAG-NT of CDK5RAP2 can localise to microtubules when expressed at high levels (Figure 3.3.4A). Fong *et al.* have defined the microtubule-binding region of CDK5RAP2 to be in the N-terminal domain of CDK5RAP2 (Fong et al., 2008). Therefore, the N-terminus of CDK5RAP2 may regulate centrosomal-microtubule interactions to coordinate

centrosome cohesion. A more recent paper by the same group suggests that CDK5RAP2 binds to the plus end binding protein, Eb1 (Fong et al., 2009). *In vitro* experiments with Eb1 and the purified Eb1-binding domain of CDK5RAP2, suggest that CDK5RAP2 and Eb1 cooperate to promote microtubule elongation. Again, this is further evidence for a role of CDK5RAP2 in regulating microtubule dynamics.

Meraldi and Nigg suggested that the role of the microtubule cytoskeleton in maintaining centrosome cohesion was to maintain delivery of kinases and phosphatases to the PCM and thus balance in their opposing activities at the centrosome (Meraldi and Nigg, 2001). In particular, Nek2 kinase activity at the centrosome had to be balanced, since overexpression of a catalytically inactive Nek2 together with nocodazole treatment of cells prevented centrosome splitting. While further work is needed to confirm this, depletion of CDK5RAP2 may either disrupt centrosome-microtubule interactions, such that kinases and phosphatases become imbalanced in the PCM, or it may be directly required for the recruitment of a specific kinase or phosphatase to the centrosome. Since CDK5RAP2 depletion does not affect Nek2 localisation (Figure 3.2.4B), I favour the hypothesis that CDK5RAP2 is required for a more general role in mediating centrosome-microtubule interactions.

Homodimerisation of CDK5RAP2 may maintain centrosome cohesion

A second centrosomal protein that is mutated in microcephaly, CenpJ, has also been shown to mediate centrosome cohesion (Zhao et al., 2010). In an elegant set of experiments, the authors use FK506-binding protein (FKBP) fusions to CenpJ to force dimerisation on addition of the chemical inducer AP20187. In this way, they show that the dimerisation of CenpJ is essential for centrosome cohesion. I have shown that FLAG-NT can co-precipitate endogenous CDK5RAP2 (Figure 3.3.3). Therefore, the N-terminal domain of CDK5RAP2 could be required for the dimerisation of CDK5RAP2. Thus while the C-terminus of CDK5RAP2 anchors the protein to the centrioles, the N-terminus may be required to dimerise and maintain cohesion. However, one question that Figure 3.3.3 does raise is that if FLAG-NT can bind to endogenous CDK5RAP2, why is it not present on the centrosomes and Golgi in interphase cells? Therefore, it might be that the interaction between FLAG-NT and endogenous CDK5RAP2 only occurs in G2 and/or mitosis, which may reflect the dimerisation/oligomerisation of CDK5RAP2 only at this cell cycle stage. If this is the case, then CDK5RAP2 homodimerisation/oligomerisation would be present at the

wrong cell cycle stage to mediate centrosome cohesion. This raises the intriguing possibility is that homodimerisation of CDK5RAP2 may be required during the loss of centrosome cohesion as centrosomes separate during G2. Further experiments would be required to pinpoint the cell cycle stage of CDK5RAP2 homodimerisation/oligomerisation.

3.5.1.3 Myomegalin does not function redundantly with CDK5RAP2 in maintaining centrosome cohesion

Depletion of Myomegalin protein did not cause centrosome splitting and, as such, it appears that CDK5RAP2 and Myomegalin do not function redundantly in maintaining centrosome cohesion (Figure 3.4.2C). Depletion of Myomegalin leads to a complete absence of Myomegalin protein in the centrosomes of transfected cells (at least in immunostaining with our antibody) and thus it seems unlikely that a small amount of remaining Myomegalin is masking a centrosome splitting phenotype.

3.5.1.4 Split centrosomes are dynamic

Live imaging of GFP-centrin1 expressing CDK5RAP2 shRNA-depleted clones revealed that split centrosomes are dynamic (Figure 3.2.5A). All of the centrosomes imaged that split apart at some point over the 4 hour filming period, also showed periods of being together. Split centrosomes may re-group because the c-Nap1/rootletin/cep68 centrosome cohesion pathway is intact (since I have no evidence to suggest that this pathway should be perturbed by CDK5RAP2 depletion). Thus, while centrosome cohesion is diminished in CDK5RAP2-depleted cells, it is not completely absent. The linker between the two centrioles – maintained by rootletin/c-Nap1/cep68 function – may be very flexible and allow the mother and daughter centrioles to move apart yet still remain loosely connected. It has already been shown that in HeLa cells undergoing cytokinesis, mother and daughter centrioles can separate from one another by up to 12 μm (Piel et al., 2001). Co-depleting CDK5RAP2 with one of cep68/c-Nap1/rootletin and visualising GFP-centrin1 dynamics could address if there are two distinct centrosome cohesion pathways.

3.5.2 CDK5RAP2 localises to the Golgi body

In addition to its centrosomal localisation, I also found that CDK5RAP2 specifically localised to the Golgi body during interphase (Figure 3.1.2A). This is a similar pattern of localisation to that which has been reported for the second human CNN-domain containing protein, Myomegalin (Verde et al., 2001). From domain analysis, it appears that it is the last 687 amino acids of CDK5RAP2 that are required for this localisation (Figure 3.3.1B, C). The C-terminus of CDK5RAP2 contains the conserved CNN2 domain and thus it could be that it is this region in CDK5RAP2 and Myomegalin that mediates localisation to the Golgi. Further domain analysis would be required to find the precise Golgi-targeting region.

The significance of CDK5RAP2 localisation to the Golgi is still not known. Depletion of CDK5RAP2 does not appear to affect the Golgi structure (Figure 3.2.1D), although I cannot rule out that there are subtle changes in Golgi morphology. CDK5RAP2 may have a role in trafficking through the Golgi apparatus and this is something I have not investigated. It is perhaps interesting to note that the Golgi body has been shown to act as an MTOC itself. Since CDK5RAP2 can bind to microtubules (Figure 3.3.4B) it could be that CDK5RAP2 is involved in microtubule organisation at the Golgi body.

3.5.3 CDK5RAP2 is phosphorylated in mitosis

Localisation of Cnn to centrosomes in *Drosophila* has been reported to depend on two cell-cycle dependent kinases, Polo and Aurora (Dobbelaere et al., 2008; Terada et al., 2003). The mammalian homologues of these proteins, Plk1 and Aurora A kinase respectively, also have cell-cycle regulated activity - with maximal activity in G2 (coincident with centrosome maturation) and mitosis. In *Drosophila*, Cnn is phosphorylated in mitosis in a Cnn dependent manner (Dobbelaere et al., 2008). Thus it seems plausible that Cnn may be recruited to the centrosome by Polo in a phosphorylation-dependent reaction.

We have shown that CDK5RAP2 is phosphorylated in mitosis and that FLAG-NT CDK5RAP2 is recruited to the centrosome specifically in G2 and mitosis (Figure 3.3.1B). In addition, CDK5RAP2 has been shown to be phosphorylated in purified mitotic spindles (Nousiainen et al., 2006). Extrapolating from the regulation of Cnn to the regulation of CDK5RAP2, it might be that extra CDK5RAP2 protein is

recruited to the centrosome in G2 in a phosphorylation-dependent manner. Indeed, a recent paper showed that inhibition of Plk1 kinase activity in human cells with a small molecule inhibitor caused a substantial reduction in CDK5RAP2 in mitotic centrosomes (Haren et al., 2009b). This suggests, that like Cnn in *Drosophila*, CDK5RAP2 requires Plk1 kinase activity to localise to the centrosomes in mitosis. However, the authors do not show that the centrosomal levels of CDK5RAP2 are cell-cycle regulated or that Plk1 phosphorylates CDK5RAP2. Since Plk1 has been shown to be required for centrosome maturation in G2 (Lane and Nigg, 1996; Sunkel and Glover, 1988) it may be that the reduction in CDK5RAP2 is not specific to Plk1 but actually reflects an overall defect in centrosome maturation. Therefore, while this is a very interesting result, it remains a preliminary one. From my own data, there is little evidence to suggest that CDK5RAP2 is recruited to the centrosome in a phosphorylation-dependent manner in G2. First, endogenous CDK5RAP2 is present at the centrosome throughout the cell cycle and I have not observed a substantial increase in CDK5RAP2 protein at the centrosome during mitosis. Second, although FLAG-NT CDK5RAP2 is only present at centrosomes in G2 and mitosis, we have been unable to show that this domain is phosphorylated. Furthermore, mutation of the known phosphorylation sites in CDK5RAP2 to alanines did not affect the localisation of FLAG-NT, or any of the FLAG constructs, to the centrosome ((Nousiainen et al., 2006); Figure 3.3.5B). Therefore, in the absence of further evidence, it seems unlikely that CDK5RAP2 is recruited to the centrosome in G2 in a phosphorylation-dependent manner.

If this is the case, then why does FLAG-NT localise specifically to mitotic centrosomes? I suggest that this may be due to the presence of a binding partner of the N-terminus of CDK5RAP2 in the centrosome in G2 and mitosis. Many proteins are only recruited to the centrosome during centrosome maturation, for example TACC3. If any of the recruited proteins have a high affinity for the N-terminus of CDK5RAP2, they would recruit FLAG-NT to the centrosome specifically in G2 and mitosis.

The specific localisation of FLAG-NT to the centrosome in G2 and mitosis could be a useful tool. By fusing this domain to a protein of interest that protein could be targeted to the centrosome specifically in G2 and mitosis. This is in contrast to the PACT domain of AKAP450/pericentrin that targets proteins to the centrosome throughout the cell cycle (Gillingham and Munro, 2000). In this way, FLAG-NT of

CDK5RAP2 could be useful to separate a mitotic function of a centrosomal protein from functions in the rest of the cell cycle.

3.5.4 CDK5RAP2 localises to basal bodies but not to ciliary axonemes

Since CDK5RAP2 was shown to be required for primary cilium formation or maintenance (Graser et al., 2007b), I checked to see if CDK5RAP2 localised to primary cilia. I found that while CDK5RAP2 did localise to basal bodies, it did not localise to the ciliary axoneme (Figure 3.1.2C). Endogenous CDK5RAP2 and FLAG-CT localise asymmetrically between the two centrioles (Figure 3.2.1A and 3.3.1B). Immunogold labelling of CDK5RAP2 at the centrosome also appeared to show an asymmetry (Graser et al., 2007a). This probably reflects a preferential localisation to the mother centriole (Figure 3.3.2D). Sub-distal and distal appendages on the mother centriole are thought to be required for the formation of primary cilia (Ishikawa et al., 2005). Therefore, while it is still unknown how CDK5RAP2 is involved in primary cilium formation, this asymmetric localisation of CDK5RAP2 may be implicated.

3.5.5 Myomegalin localisation varies between cell lines

Although both anti-CDK5RAP2 antibody (SK56) and anti-Myomegalin antibody recognise epitopes in the conserved CNN1 domains of these proteins, the two antibodies do not cross-react and are specific for the protein they were raised against (Figure 3.1.1C, 3.2.2B and 3.4.3A). This specificity allows the separate study of the two proteins.

It has been reported that Myomegalin localises to the centrosome and Golgi in Cos-7 cells (Verde et al., 2001). I saw a similar localisation for Myomegalin in glioblastoma (Figure 3.4.1A) and T-lymphoblastic cell lines (D. Zyss, personal communication). However, Myomegalin was absent from the centrosome and Golgi in all epithelial cell lines tested (Figure 3.4.3A). RT-PCR of Myomegalin exon pairs from cDNA did not reveal any differences between HeLa and U251MG cell lines and thus the reason underlying this difference is still unknown. Ideally, a Northern blot with multiple Myomegalin probes should be done to identify the different splice forms. Alternatively, it may be that the same isoforms of Myomegalin are expressed in both cell types but that a binding partner required for the subcellular localisation of

Myomegalin is missing in HeLa cells. Future identification of binding partners of Myomegalin should help in answering this question.

3.5.6 Myomegalin expression in cancer

Analysis of Myomegalin expression in three patient-derived glioblastoma primary cell lines showed that levels of Myomegalin protein varied between all three lines (Figure 3.4.3C,D). Since I was unable to obtain patient data about these samples I do not know how expression levels correlate with prognosis. Potentially, it may be relevant to extend this study of Myomegalin expression both in glioblastomas and in other tumour types to see if Myomegalin has any link to cancer progression or prognosis.

Chapter 4

Identification of AKAP450 as a binding partner of CDK5RAP2

Clues to the function of a protein can often be derived from identification of the interacting partners of that protein. Here, I describe a novel interacting partner of CDK5RAP2 – the centrosomal protein, AKAP450. AKAP450 has been proposed to act as a scaffolding protein in the PCM, required to anchor proteins to the centrosome (Takahashi et al., 1999). I show that CDK5RAP2 is required for the recruitment of AKAP450 to the centrosome in mitosis. Intriguingly, I find that, like CDK5RAP2, AKAP450 is required for centrosome cohesion, most likely participating in the same pathway as CDK5RAP2.

Orthologues of CDK5RAP2 in *Drosophila* and fission yeast have been implicated in the binding and recruitment of γ -tubulin to sites of microtubule nucleation (Sawin et al., 2004; Zhang and Megraw, 2007). I present evidence that suggests that CDK5RAP2 in vertebrates is less critical for the efficient localisation of γ -tubulin to the centrosome. This suggests that γ -tubulin recruitment to the centrosome is not a major function of CDK5RAP2 in human cells, unlike its lower eukaryotic orthologues.

4.1 CDK5RAP2 interacts with AKAP450 and recruits it to the mitotic centrosome

4.1.1 CDK5RAP2 colocalises and interacts with AKAP450 throughout the cell cycle

The localisation of CDK5RAP2 to the centrosome and to the Golgi body was reminiscent of the centrosomal scaffolding protein, AKAP450 (Takahashi et al., 2002). Therefore, I co-stained cells with CDK5RAP2 and AKAP450 antibodies. This showed that the two proteins colocalise throughout the cell cycle (Figure 4.1.1A). Due to their striking overlap in localisation pattern, I checked if the two proteins could interact. Immunoprecipitation of endogenous CDK5RAP2 from asynchronous HeLa cell extracts coprecipitated endogenous AKAP450, indicating that these two proteins exist in the same molecular complex (Figure 4.1.1B). Synchronisation of HeLa cells in mitosis or at the G1/S boundary (see Section 2.1.3, Materials and Methods) revealed that this interaction is maintained throughout the cell cycle (Figure 4.1.1C). By expressing FLAG-tagged CDK5RAP2 constructs (Figure 3.3.1A), I found that the interaction with AKAP450 is mediated through the C-terminus of CDK5RAP2 (Figure 4.1.1D).

4.1.2 CDK5RAP2 is required for the accumulation of AKAP450 in the mitotic centrosome

To see if the interaction of CDK5RAP2 with AKAP450 had any functional relevance I immunostained CDK5RAP2-depleted cells with anti-AKAP450 antibody. In interphase, AKAP450 still localised to the centrosome and Golgi body when CDK5RAP2 protein was depleted (Figure 4.1.2A, orange arrows). However, in mitotic cells depleted of CDK5RAP2, AKAP450 was depleted from the centrosome (Figure 4.1.2A, B; yellow asterisks). This effect was seen in both siRNA and shRNA CDK5RAP2-depleted cells and in different cell lines – including HeLa (Figure 4.1.2B), U251MG (Figure 4.1.2A) and U2OS (data not shown). I quantified the extent of the reduction of AKAP450 in CDK5RAP2-depleted mitotic centrosomes. To do this I used the control hp1-1 and CDK5RAP2 hp1d cell lines (Figure 3.2.1) costained with centrin-3, a centriolar marker, and AKAP450 antibodies. I was then

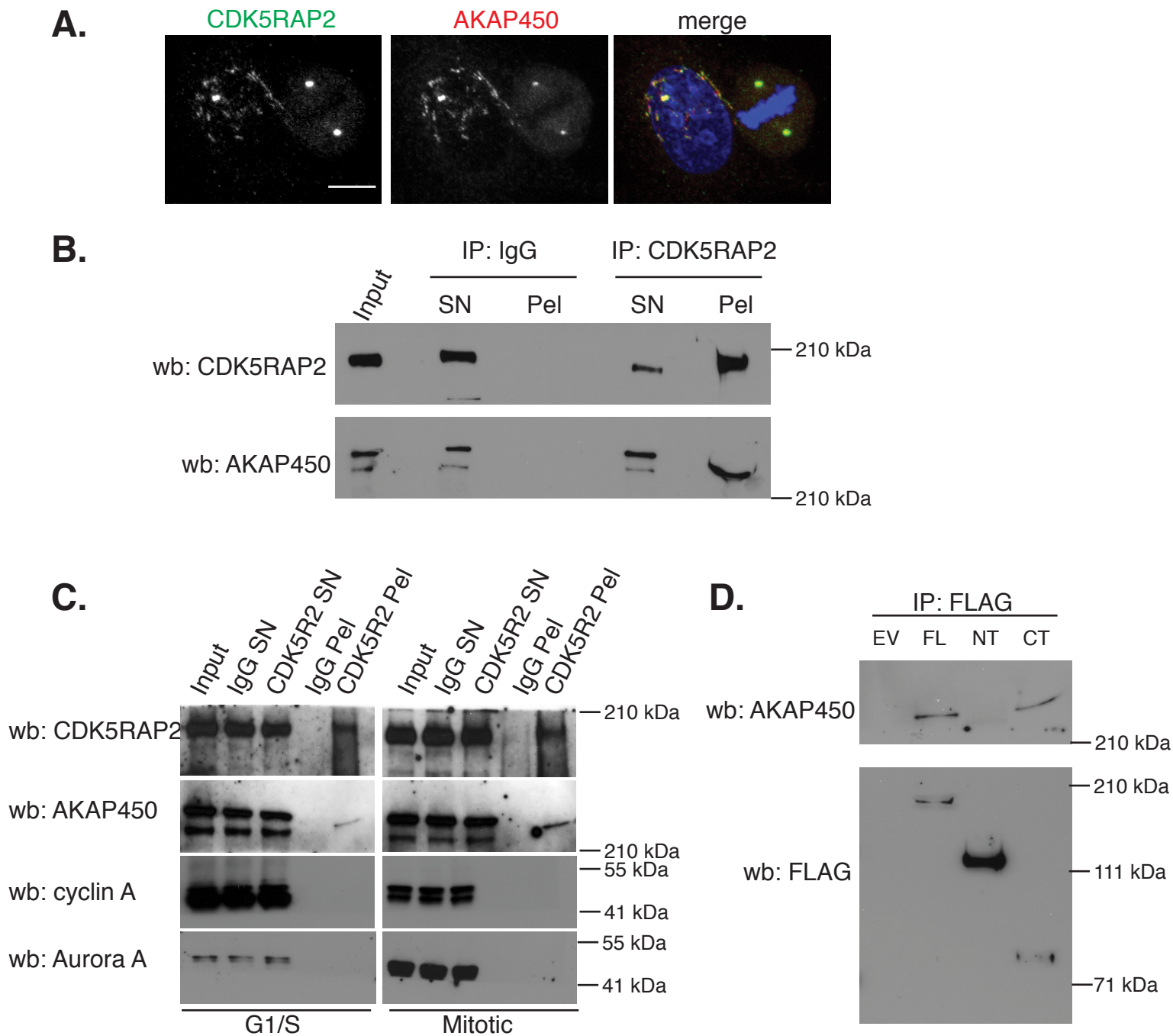


Figure 4.1.1 CDK5RAP2 localises and interacts with AKAP450 throughout the cell cycle. A. Subcellular localisation of CDK5RAP2 and AKAP450 in HeLa cells. DNA is blue, CDK5RAP2 is red and AKAP450 is green in merged image. Scale bar is 5 μ m. **B.** Western blot of immunoprecipitation of CDK5RAP2 from asynchronous HeLa cytoplasmic extracts. CDK5RAP2 antibody (Bethyl A300-550) immunoprecipitated 26% of total CDK5RAP2 and 40% of total AKAP450 protein. Proportions were calculated using NIH ImageJ. The amount of CDK5RAP2 immunoprecipitated may be underestimated, since the CDK5RAP2 signal is saturated. **C.** Western blot of immunoprecipitation of CDK5RAP2 from HeLa cytoplasmic extracts from cells enriched in G1/S or mitosis. CDK5RAP2 co-precipitates AKAP450 from both G1/S and mitotic enriched extracts. Aurora-A is a marker of G2 and mitosis (Kimura *et al.*, 1997) and cyclin A is degraded during mitosis and is thus higher in the G1/S arrested extract (Pines and Hunter, 1991). ‘SN’ – supernatant, ‘Pel’ – Pellet. A rabbit IgG mix serves as a negative control. **D.** Western blot of immunoprecipitation of FLAG-tagged CDK5RAP2 constructs (Figure 3.1.3A) 24 hr after transfection in HeLa cells. CDK5RAP2 interacts with AKAP450 via its C-terminus. (Note that this Immunoprecipitation experiment is the same as in Figure 3.3.3).

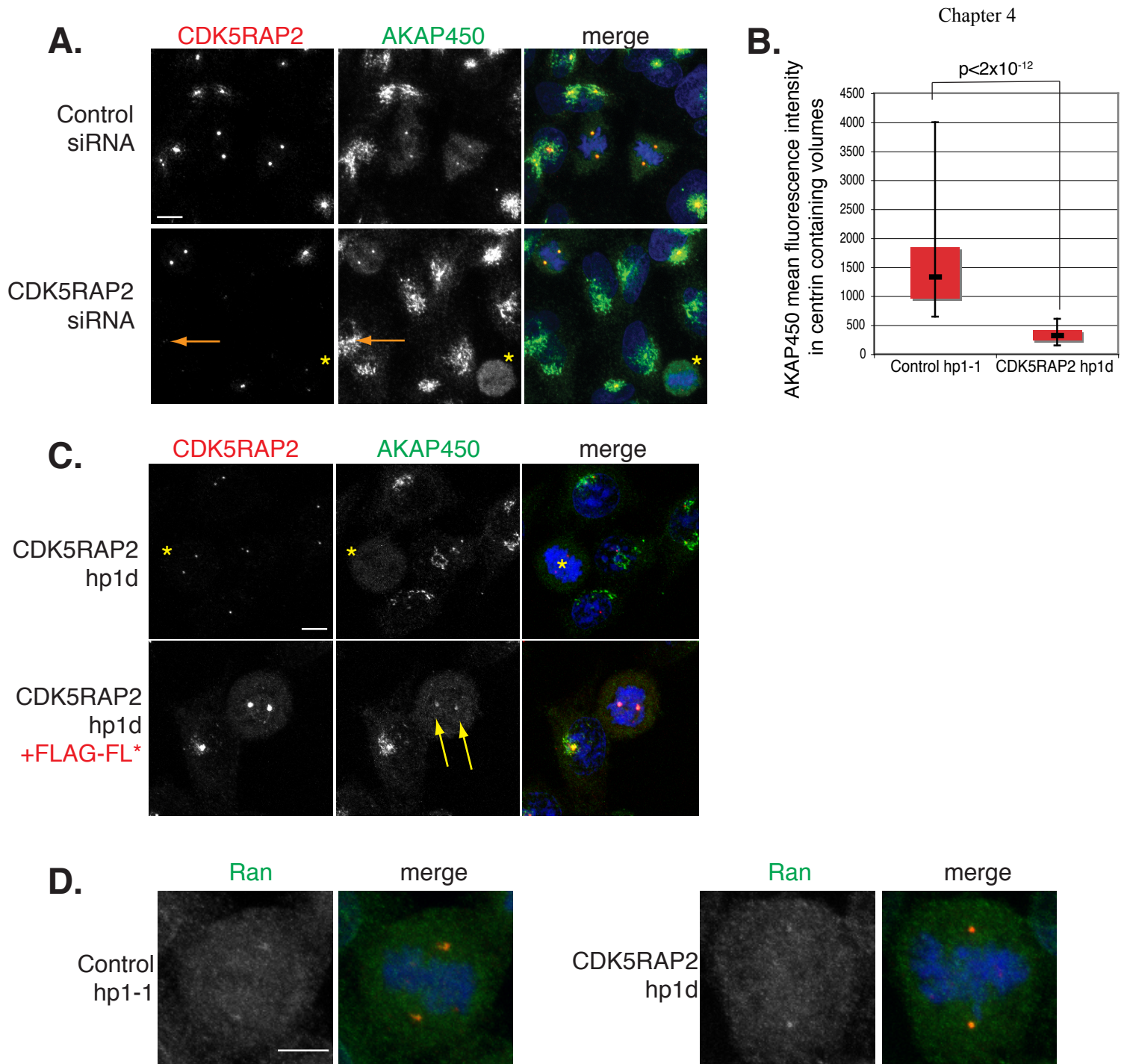


Figure 4.1.2 CDK5RAP2 is required for the accumulation of AKAP450 in the mitotic centrosome. **A.** Subcellular localisation of AKAP450 in U251MG cells 72 hr after transfection with AKAP450 or control siRNA. When CDK5RAP2 is depleted, AKAP450 is absent from mitotic centrosomes (yellow asterisks) but still present at the Golgi and centrosome in interphase (orange arrows). DNA is blue, CDK5RAP2 is red and AKAP450 is green in merged images. **B.** Graph showing the quantification of AKAP450 mean fluorescence levels in mitotic centrosomes. Centrin-3 containing volumes were selected and the mean AKAP450 intensity in that volume taken as a measure of AKAP450 levels in the centrosome. p -value was calculated from a two-tailed, unpaired student's t -test. 32 centrosomes were measured for each cell line. **C.** Immunofluorescence images show that expression of FLAG-FL* CDK5RAP2 can rescue AKAP450 localisation. Top panels shows untreated CDK5RAP2 hp1d HeLa cell clone. Note the absence of AKAP450 from mitotic centrosomes (yellow asterisks). Bottom panel shows the same cell line transfected with FLAG-FL* CDK5RAP2 and analysed 24 hr later. AKAP450 is now at the mitotic centrosome in the presence of CDK5RAP2 (yellow arrows). DNA is blue, CDK5RAP2 is red and AKAP450 is green in merged images. **D.** Immunostaining of Ran in control hp1-1 and CDK5RAP2 hp1d clonal HeLa cells. Ran is green, pT288AurA is in red and DNA is blue in merged images. Scale bars are 5 μ m.

able to measure the amount of AKAP450 in the centrin-3 containing volumes (see 2.5.2, Materials and Methods). Figure 4.1.2B shows that there is a significant reduction in AKAP450 in the mitotic centrosomes of CDK5RAP2-depleted cells.

To confirm that the depletion of AKAP450 from mitotic centrosomes was due to the absence of CDK5RAP2, I performed rescue experiments in the CDK5RAP2 hp1d clonal cell line. I transfected the hairpin resistant, FLAG-FL* into the CDK5RAP2 hp1d cell line and analysed AKAP450 localisation 24 hours later. Figure 4.1.2C shows that on restoration of CDK5RAP2 protein, AKAP450 now accumulates in the mitotic centrosome (yellow arrow, lower panels).

Intriguingly, it is known that a fraction of Ran is associated with AKAP450 at the centrosomes (Keryer et al., 2003). Ran is a small GTPase binding protein that is required for chromatin-mediated spindle assembly. At the centrosome Ran appears to be involved in microtubule anchoring (Keryer et al., 2003). Keryer *et al.* showed that overexpression of the C-terminal domain of AKAP450 mislocalises both endogenous AKAP450 and Ran from the centrosome in interphase. This implies that full-length AKAP450 is required to localise Ran to the centrosome, at least in interphase cells. In CDK5RAP2-depleted cells I observed a reduction in centrosomal AKAP450 only in mitosis. Therefore, I wondered if the absence of AKAP450 in mitotic centrosomes affected the localisation of Ran. To investigate this, I immunostained CDK5RAP2-depleted cells with anti-Ran antibody. I found that Ran localisation in mitotic cells was weak and variable between cells on the same coverslip. In spite of this variability, Ran localised to mitotic centrosomes in both control hp1-1 and CDK5RAP2 hp1d cells (Figure 4.1.2D). Therefore, it may be that the centrosomal accumulation of Ran in mitosis either requires only very little AKAP450 or is not dependent on AKAP450.

4.1.3 CDK5RAP2 is required to recruit AKAP450 to mitotic centrosomes

Absence of AKAP450 from mitotic centrosomes in CDK5RAP2-depleted cells could reflect a defect in the recruitment of AKAP450 to the centrosome or an inability to maintain AKAP450 in the PCM in the presence of microtubule-based forces. To distinguish between these possibilities, I depolymerised microtubules in HeLa control

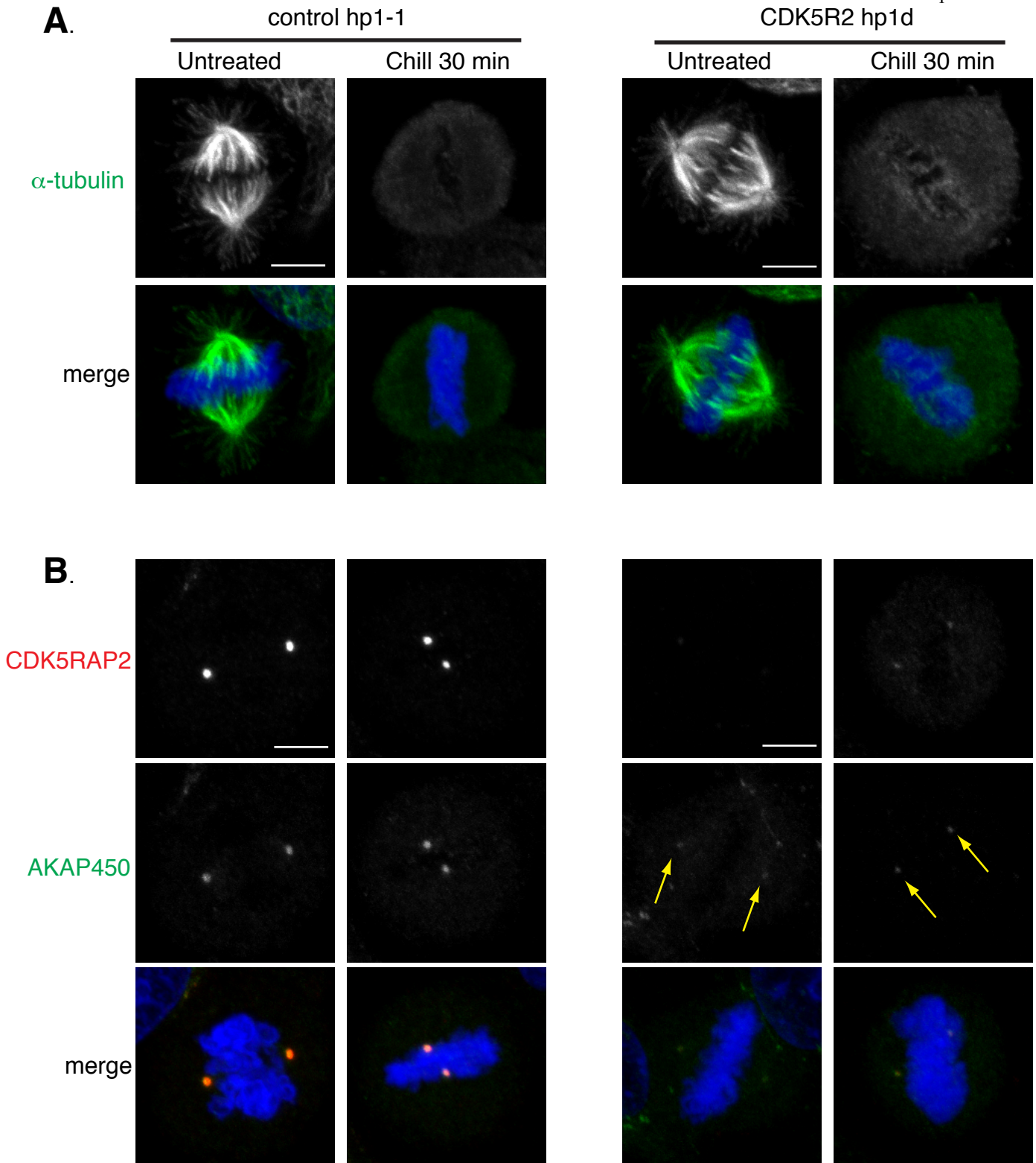


Figure 4.1.3 CDK5RAP2 is required to recruit AKAP450 to the mitotic centrosomes.

A. Chilling HeLa control hp1-1 or CDK5RAP2 hp1d stable clones on ice for 30 min depolymerises microtubules in the mitotic spindle in both control hp1-1 and CDK5RAP2 hp1d cell lines. DNA is blue and microtubules are green in merged image. **B.** Subcellular localisation of AKAP450 in untreated and chilled control hp1-1 and CDK5RAP2 hp1d clonal cell lines. Depolymerising microtubules does not restore AKAP450 levels in the mitotic centrosome (yellow arrows). DNA is blue, CDK5RAP2 is red and AKAP450 is green in merged images. Scale bars are 5 μ m.

hp1-1 or CDK5RAP2 hp1d clones by incubating them on ice for 30 minutes. Cells were immunostained to look at microtubules to ensure all microtubules had been depolymerised (Figure 4.1.3A). Immunostaining of untreated and cold-treated cells showed that AKAP450 is reduced in CDK5RAP2-depleted centrosomes, even when microtubules are depolymerised (Figure 4.1.3B). This implies that CDK5RAP2 is required for the recruitment of AKAP450 to the mitotic centrosome.

4.1.4 AKAP450 does not mediate the localisation of CDK5RAP2 to the centrosome

Since CDK5RAP2 affects the localisation of AKAP450, I wanted to see if the two proteins are mutually required for each other's localisation. To deplete AKAP450, I used a custom-made siRNA based on the target sequence reported in Larocca *et al.* ((Larocca et al., 2004); see Table 2.2). Figure 4.1.4A shows that this siRNA depleted AKAP450 from HeLa cells. This siRNA has been reported to cause dispersal of the Golgi body and immunostaining for gm130 (a cis Golgi marker) showed this to be the case (Figure 4.1.4B).

Depletion of AKAP450 did not affect CDK5RAP2 localisation to the centrosome in interphase or mitosis (Figure 4.1.4C). Since AKAP450 depletion leads to dispersal of the Golgi body, CDK5RAP2 no longer localises to the Golgi. However, dispersal of the Golgi is not due to the absence of CDK5RAP2 because depletion of CDK5RAP2 has no effect on Golgi structure (Figure 3.2.1D).

In summary, AKAP450 is not required for the localisation of CDK5RAP2 to the centrosome.

4.1.5 AKAP450 is required for centrosome cohesion

I noticed that a high proportion of cells depleted of AKAP450 contained split centrosomes. I scored the number of cells with split centrosomes and I found that, similar to CDK5RAP2 depletion, depletion of AKAP450 by siRNA gave rise to an increase in the number of cells with split centrosomes (Figure 4.1.5). Treatment of cells with nocodazole is known to give rise to an increased frequency of split centrosomes (Jean et al., 1999; Meraldi and Nigg, 2001). This has been attributed to the depolymerisation of microtubules but it is also known that depolymerisation of microtubules causes dispersal of the Golgi body (Rogalski and Singer, 1984).

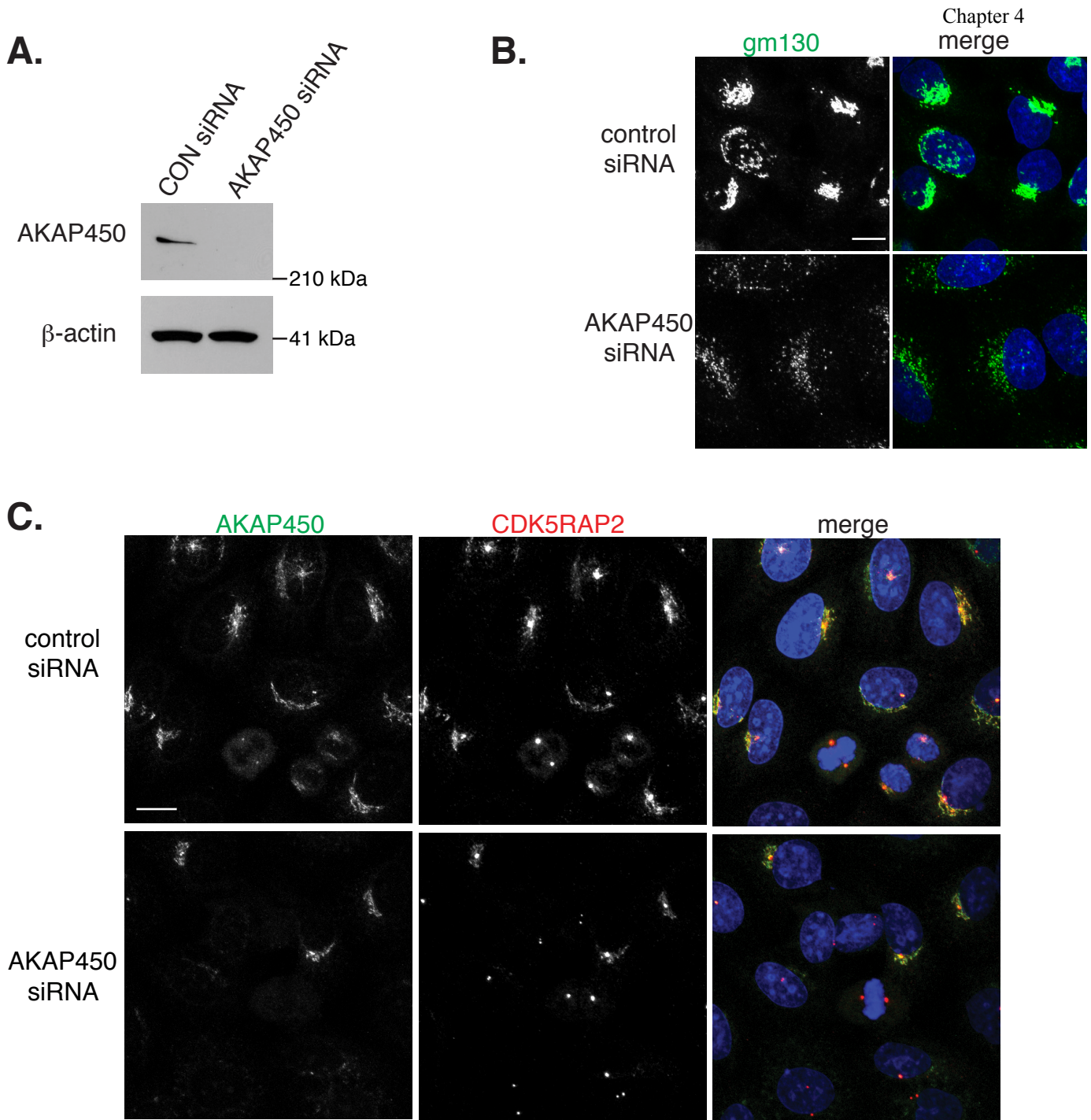


Figure 4.1.4 AKAP450 does not mediate the localisation of CDK5RAP2 to the centrosome. **A.** Western blot showing depletion of AKAP450 by siRNA 72 hr after transfection of HeLa cells. β -actin serves as a loading control. **B.** Subcellular localisation of the cis Golgi in AKAP450-depleted cells. DNA is blue and gm130 is green in merged images. **C.** Subcellular localisation of CDK5RAP2 in HeLa cells 72 hr after transfection with control or AKAP450 siRNA. DNA is blue, CDK5RAP2 is red and AKAP450 is green in merged images. Scale bars are 5 μ m.

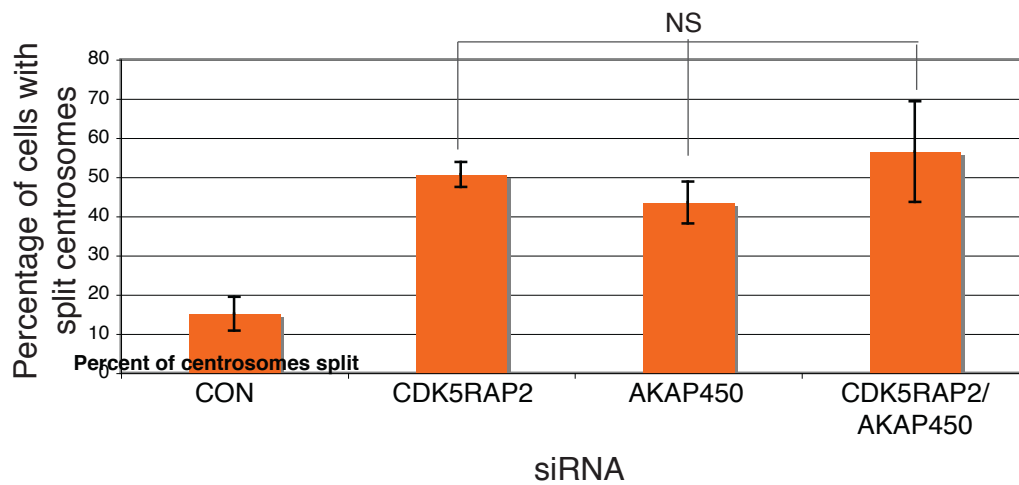


Figure 4.1.5 AKAP450 is required for centrosome cohesion. Graph showing that depletion of AKAP450 by siRNA in HeLa cells leads to a loss of centrosome cohesion. $n=4$, at least 100 cells scored per condition, per experiment. Difference between CDK5RAP2, AKAP450 and double depletion is not statistically significant at $p=0.05$ cut off in a Mann-Whitney 2-tailed test.

Therefore, I wanted to test if it was the dispersal of the Golgi body in AKAP450-depleted cells that caused the loss of centrosome cohesion. However, treatment of cells with the Golgi-disrupting agent BFA did not lead to an increase in centrosome splitting (vehicle-treated HeLa: no BFA = 11.9% centrosomes split; +BFA = 6.6% centrosomes split, n=1).

Co-depletion of CDK5RAP2 and AKAP450 did not further increase centrosome splitting when compared to the single siRNAs (Figure 4.1.5). Therefore, it seems that these two proteins are required in the same pathway to maintain centrosome cohesion.

4.1.6 Myomegalin regulates AKAP450 levels in mitotic centrosomes

Since CDK5RAP2 interacts with AKAP450 and recruits it to the centrosome in mitosis, I wondered if AKAP450 had a similar molecular interplay with Myomegalin. I was unable to efficiently immunoprecipitate either Myomegalin or AKAP450 to be able to test if the two proteins are in the same molecular complex. However, siRNA-mediated depletion of Myomegalin from U251MG cells (Figure 3.4.2B) appeared to lead to an increase in AKAP450 in the mitotic centrosome (Figure 4.1.6A). U251MG cells were chosen for these experiments since Myomegalin is centrosomal and colocalises with AKAP450 in these cells (Figure 4.1.6A, top panels). Quantification of AKAP450 levels in mitotic centrosomes from both control and Myomegalin-depleted cells suggested that there was an increase in AKAP450 levels when Myomegalin was depleted (Figure 4.1.6B (volumes of equal size were selected to quantify AKAP450 centrosomal levels in these cells, see Section 2.5.2, Materials and Methods)). While very preliminary, these data suggest a potential interplay between CDK5RAP2 and Myomegalin in regulating AKAP450 levels in the mitotic centrosome.

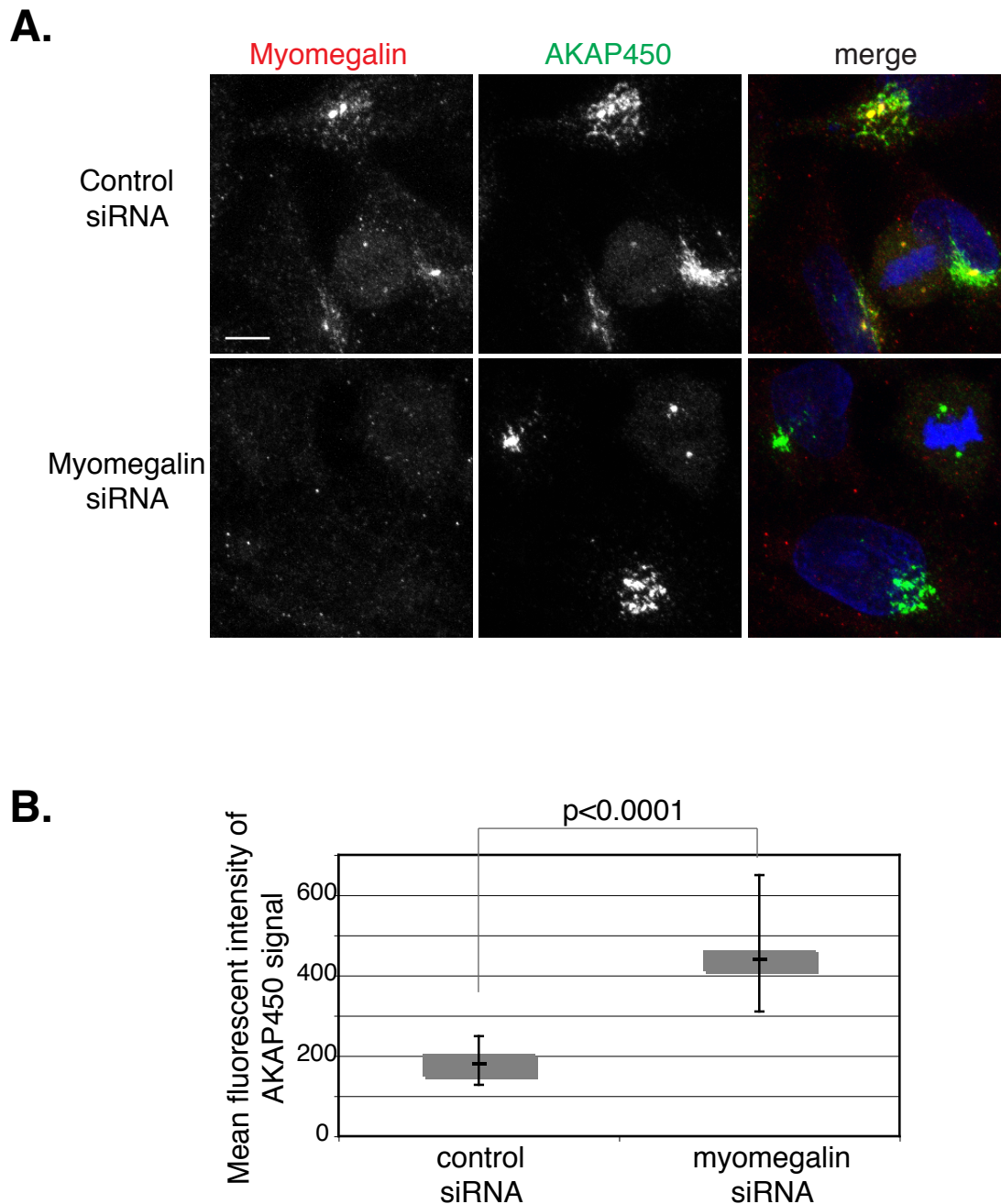


Figure 4.1.6 Myomegalin regulates AKAP450 levels in mitotic centrosomes. A. Subcellular localisation of AKAP450 72 hr after siRNA depletion of Myomegalin from U251MG cells. AKAP450 localises to the centrosome and Golgi, even in the absence of Myomegalin protein. Note that in Myomegalin-depleted cells, the levels of AKAP450 appear higher in mitotic centrosomes. DNA is blue, Myomegalin is red and AKAP450 is green in merged images. Scale bar is 5 μm . **B.** Box and whisker plot shows that AKAP450 levels are significantly higher in mitotic centrosomes after depletion of Myomegalin. AKAP450 mean intensity levels were measured in mitotic centrosomes using Volocity (see Materials and Methods). 10 centrosomes were scored for each condition. p-value was determined by a two-tailed unpaired student's t-test.

4.2 CDK5RAP2 is not required for efficient γ -tubulin localisation to mitotic centrosomes

4.2.1 CDK5RAP2 is not required for the efficient localisation of γ -tubulin to mitotic centrosomes

Orthologues of CDK5RAP2 in fission yeast (*mod20p*) and *Drosophila* (*Cnn*) have been implicated in binding and recruiting γ -tubulin complexes to microtubule-nucleation sites (Lucas and Raff, 2007; Megraw et al., 1999; Sawin et al., 2004; Terada et al., 2003; Vaizel-Ohayon and Schejter, 1999; Zhang and Megraw, 2007). Therefore, I wondered if depletion of CDK5RAP2 would affect γ -tubulin in human cells.

By immunostaining, depletion of CDK5RAP2 by siRNA appeared to lead to a reduction in γ -tubulin in mitotic centrosomes (Figure 4.2.1A, yellow arrows). However, the same effect was not seen in CDK5RAP2 hp1d or hp12d clonal cells (Figure 4.2.1B). Quantification of γ -tubulin levels in mitotic centrosomes in control hp1-1 and CDK5RAP2 hp1d cells revealed no statistically significant difference between fluorescence levels in the two cell lines. I did not quantify γ -tubulin levels in interphase centrosomes due to the high incidence of centrosome splitting. Since the level of CDK5RAP2 depletion was comparable between siRNA and shRNA treated cells, the reduction in γ -tubulin observed in HeLa cells treated with CDK5RAP2-targeting siRNA may be due to off target effects of the siRNA. Moreover, immunoprecipitation of endogenous CDK5RAP2 did not coprecipitate γ -tubulin, and *vice versa* (Figure 4.2.1C). Therefore, it appears that recruitment of γ -tubulin to the centrosome is not a major role of CDK5RAP2 in human cells.

4.2.2 CDK5RAP2 is not required for centrosome maturation

In an siRNA screen for centrosome maturation in *Drosophila* S2 cells, Dobbelaere *et al.* (Dobbelaere et al., 2008) found that *Cnn* was required for centrosome maturation. Similarly, *Cnn* is known to interact with Aurora A and be required for the efficient localisation of Aurora A to the centrosome in mitosis (Terada et al., 2003). While I

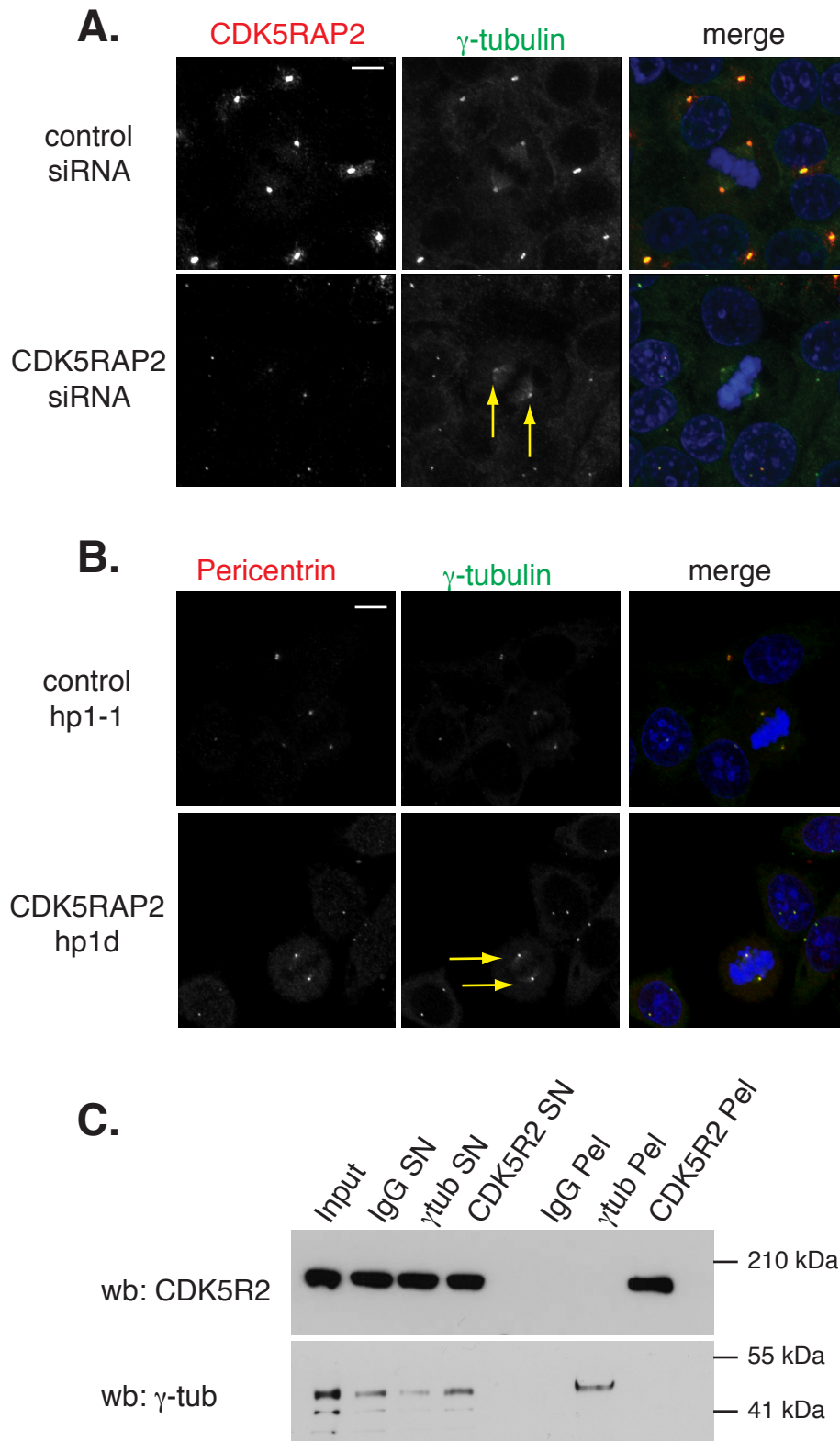


Figure 4.2.1 CDK5RAP2 is not required for the efficient recruitment of γ -tubulin to the centrosome. **A.** Subcellular localisation of γ -tubulin in HeLa cells, 72 hr after transfection with control or CDK5RAP2-targeting siRNA. γ -tubulin appears to be reduced in CDK5RAP2-depleted centrosomes (yellow arrows). DNA is blue, CDK5RAP2 is red and γ -tubulin is green in merged images. **B.** Subcellular localisation of γ -tubulin in control hp1-1 and CDK5RAP2 hp1d clonal HeLa cells. γ -tubulin is not reduced in CDK5RAP2-depleted centrosomes (yellow arrows). DNA is blue, pericentrin is red and γ -tubulin is green in merged images. Scale bars are 5 μ m. **C.** Western blot showing that immunoprecipitation of CDK5RAP2 from asynchronous HeLa cytoplasmic extracts does not coprecipitate γ -tubulin and vice-versa. 'SN' – supernatant, 'Pel' – Pellet. A rabbit IgG mix serves as a negative control.

have not found a role for CDK5RAP2 in γ -tubulin recruitment to the centrosome in mitosis, I wanted to investigate if depletion of CDK5RAP2 affected the recruitment of other centrosomal proteins implicated in centrosome maturation. Therefore, I analysed the localisation of Aurora A, and the activated form of Aurora A, pT288 Aurora A (Barr and Gergely, 2007), in CDK5RAP2-depleted cells. Both Aurora A and pT288 Aurora A were present in CDK5RAP2-depleted centrosomes indicating that centrosome maturation was intact (Figure 4.2.2A). I also checked the localisation of a protein that requires phosphorylation by Aurora A for its recruitment to the centrosome during centrosome maturation – TACC3 (Barros et al., 2005; Kinoshita et al., 2005). Again, TACC3 was recruited normally to CDK5RAP2-depleted centrosomes (Figure 4.2.2B). These results were consistent between siRNA and shRNA-targeted cells. Together, these data imply that CDK5RAP2 is not required for centrosome maturation.

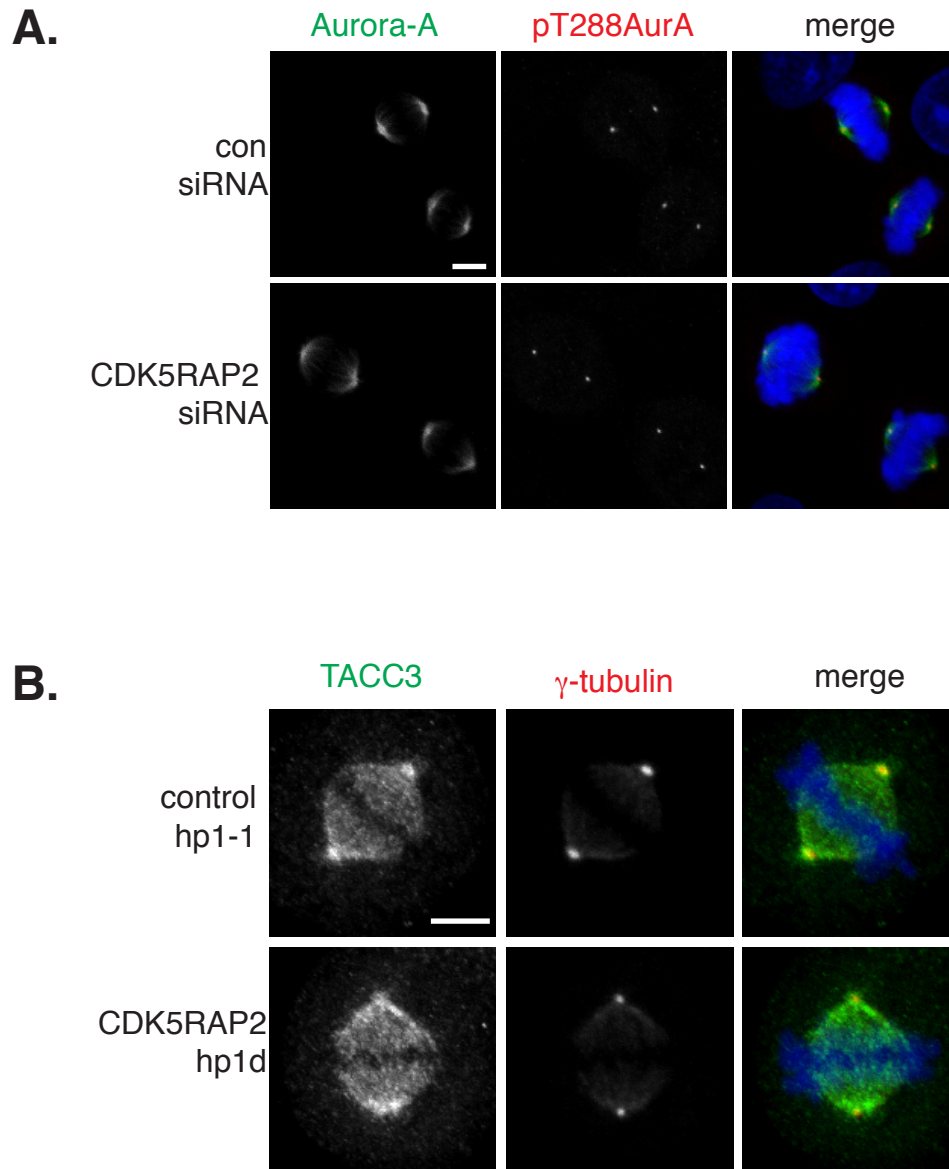


Figure 4.2.2 CDK5RAP2 is not required for centrosome maturation. **A.** Subcellular localisation of Aurora-A and activated Aurora-A (pT288AurA) in HeLa cells, 72 hr after transfection with control or CDK5RAP2-targeting siRNA. DNA is blue, Aurora-A is green and pT288AurA is red in merged images. **B.** Subcellular localisation of TACC3 in control hp1-1 and CDK5RAP2 hp1d clonal HeLa cells. DNA is blue, TACC3 is green and γ -tubulin is red in merged images. Scale bars are 5 μ m.

4.3 Discussion

4.3.1 CDK5RAP2 interacts with AKAP450 and recruits it to the centrosome in mitosis

I have shown that CDK5RAP2 and AKAP450 colocalise and interact throughout the cell cycle and that CDK5RAP2 is required for the recruitment of AKAP450 to the centrosome in mitosis (Figure 4.1.2A, B). The interaction between CDK5RAP2 and AKAP450 is mediated by the C-terminus of CDK5RAP2 (Figure 4.1.1D). This domain of CDK5RAP2 mimics the localisation of AKAP450 throughout the cell cycle. Therefore, the reason why CDK5RAP2 is only required for the mitotic localisation of AKAP450 and not its localisation in interphase is intriguing. This could be due to the incomplete depletion of CDK5RAP2. Alternatively, it may reflect a differing interplay between CDK5RAP2 and AKAP450 in interphase and mitosis. Perhaps, during interphase, the functions of CDK5RAP2 and AKAP450 are to regulate centrosome cohesion. Then, as cells prepare to go into mitosis, centrosomes separate and the Golgi body breaks down (Shorter and Warren, 2002). The breakdown of the Golgi potentially releases additional AKAP450 and CDK5RAP2. Therefore, in G₂, CDK5RAP2 may be required to recruit this extra AKAP450 to the centrosomes.

AKAP450 has recently been shown to be required for efficient microtubule nucleation from the Golgi (Rivero et al., 2009). Since CDK5RAP2 also localises to the Golgi and has been implicated in regulating microtubule nucleation (Fong et al., 2008), I tested to see if CDK5RAP2 was also involved in this process. However, I was unable to visualise microtubule regrowth at the Golgi body consistently in RPE1 cells (RPE1 cells were used as this was the cell line used in (Rivero et al., 2009)). I found that microtubule nucleation from the Golgi only occurred in a small proportion of cells and was only visible when centrosomes and the Golgi were spatially separated in the cell. Therefore, it still remains to be seen if CDK5RAP2 plays a role in this process.

4.3.2 AKAP450 is required for centrosome cohesion

One surprising result is that AKAP450 is required for centrosome cohesion (Figure 4.1.5). AKAP450 appears to operate in the same pathway as CDK5RAP2, since there

was no additional increase in centrosome splitting upon the simultaneous depletion of both proteins. The second PACT-domain containing protein in human cells, pericentrin, has also been shown to mediate centrosome cohesion ((Jurczyk et al., 2004)). In their siRNA screen for proteins that mediate centrosome cohesion, Graser *et al.* found that CDK5RAP2 and pericentrin were mutually dependent for their localisation to the centrosome in interphase (Graser et al., 2007a). Therefore, depletion of either pericentrin or CDK5RAP2 would lead to a reduction of the other protein at the centrosome and, as such, it is easy to see how these two proteins could collaborate to mediate centrosome cohesion. Since CDK5RAP2 depletion in human cells does not seem to affect AKAP450 localisation in interphase, and *vice versa* (Figure 4.1.2A and 4.1.4C), there may be another explanation for the apparent cooperation of CDK5RAP2 and AKAP450 in centrosome cohesion. If CDK5RAP2 and AKAP450 are mutually required to form a cohesive structure, the depletion of either protein alone would preclude the formation of such a structure. Alternatively, CDK5RAP2 and AKAP450 may also co-regulate centrosome cohesion by their effects on centrosomal-microtubule interactions (Jean et al., 1999; Meraldi and Nigg, 2001). AKAP450, like CDK5RAP2, can bind to microtubules (Kim et al., 2007) and has been proposed to regulate centrosome-mediated microtubule nucleation, since microtubule regrowth after nocodazole washout was slower in interphase cells depleted of AKAP450 (Larocca et al., 2006).

4.3.3 CDK5RAP2 is not required for the efficient localisation of γ -tubulin to mitotic centrosomes

My data reveal that CDK5RAP2 is not required for the localisation of γ -tubulin to the centrosome in mitosis. I saw an apparent reduction in γ -tubulin levels in the centrosome after siRNA depletion of CDK5RAP2, but this was not confirmed in the CDK5RAP2-depleted clonal cell lines: CDK5RAP2 hp1d and hp12d (Figure 4.2.1A, B). A lack of requirement for CDK5RAP2 in the recruitment of γ -tubulin to the centrosome is consistent with work from two other labs (Tim Megraw, Florida State University, USA and Andreas Merdes, Institut de Sciences et Technologies du Médicament de Toulouse, France, personal communications). However, it is inconsistent with work published by two other groups (Fong et al., 2008; Haren et al., 2009b). Both groups used siRNA depletion of CDK5RAP2 in HeLa cells and then

immunostained cells for γ -tubulin. Both saw a reduction in γ -tubulin at mitotic centrosomes after CDK5RAP2 depletion. Moreover, Fong *et al.* were able to detect an interaction between CDK5RAP2 and γ -tubulin and localise this interaction to the CNN1 domain of CDK5RAP2. This is similar to what has been shown for Cnn in *Drosophila* and mod20p in yeast (Samejima *et al.*, 2005; Terada *et al.*, 2003). I was unable to detect an interaction between endogenous CDK5RAP2 and γ -tubulin under numerous conditions (Figure 4.2.1C).

The difference between my results and those of Fong and Haren and their colleagues, is difficult to explain. However, in neither publication (Fong *et al.*, 2008; Haren *et al.*, 2009b) did the authors perform rescue experiments to prove beyond doubt that reduction in γ -tubulin was specifically due to the lack of CDK5RAP2 and not an off-target effect of the siRNA. Furthermore, the evidence for the reduction in γ -tubulin in mitotic centrosomes depleted of CDK5RAP2 in Fong *et al.* is weak. The authors show a plot of CDK5RAP2 centrosomal levels versus γ -tubulin centrosomal levels (Figure 5C in (Fong *et al.*, 2008)). The correlation between the two is low and three data points at one extreme of the graph are misleading. In the absence of a correlation coefficient or statistical analysis of their data it is difficult to draw a firm conclusion about the effects of CDK5RAP2 depletion on γ -tubulin centrosomal levels. Alternatively, the discrepancy between my data and that of Fong and Haren could be due to the incomplete depletion of CDK5RAP2 in my cells. However, if the data of Fong *et al.* are correct, I would expect to observe a reduction in γ -tubulin levels as soon as CDK5RAP2 levels start to decrease.

The observed interaction between γ -tubulin and CDK5RAP2 (Fong *et al.*, 2008) appears convincing. The reason why I was unable to observe such an interaction under the same immunoprecipitation conditions could be due to using different antibodies. For the immunoprecipitation shown in Figure 4.2.1C, I used the commercially available CDK5RAP2 A550 antibody. A550 antibody binds to CDK5RAP2 outside of the proposed γ -tubulin binding domain and therefore would not be expected to affect the interaction with γ -tubulin. Fong *et al.* used their own antibody. I requested and tested the Fong antibody and found that it recognised multiple bands of differing MWs on a Western blot and, under the same conditions outlined in (Fong *et al.*, 2008), I was unable to specifically immunoprecipitate CDK5RAP2 from HeLa cell extracts. Fong *et al.* used the same γ -tubulin antibody as

I did but I still failed to see the interaction by immunoprecipitation with this antibody (Figure 4.2.1C). Therefore, the reason for the observed difference in binding is not known.

4.3.4 Myomegalin and AKAP450

In contrast to CDK5RAP2, depletion of Myomegalin leads to an increase in AKAP450 levels in the mitotic centrosome (Figure 4.1.6). This is a very interesting result as it suggests that CDK5RAP2 and Myomegalin have opposite effects on AKAP450 localisation. Perhaps (in cells where Myomegalin is expressed in the centrosome) CDK5RAP2 and Myomegalin act together to regulate the amount of AKAP450 in the centrosome. The effects of having excess AKAP450 in the centrosome are unknown (published studies only overexpress part of this very large protein) and so why Myomegalin would be required to limit the amount of AKAP450 there is uncertain.

Chapter 5

CDK5RAP2 is required for centrosome attachment to spindle poles

All of my studies so far have used siRNA or shRNA to deplete CDK5RAP2 in human cells to investigate the function of this protein. This has proved useful since it has enabled me to uncover functions for CDK5RAP2 in centrosome cohesion and in the recruitment of AKAP450 to the mitotic centrosome. However, I did not see a mitotic defect in any of the CDK5RAP2-depleted cell lines. This was surprising considering the severe mitotic defects seen after mutation of Cnn in *Drosophila* embryos (Lucas and Raff, 2007; Megraw et al., 1999; Zhang and Megraw, 2007). While it is possible that Myomegalin is masking a mitotic function for CDK5RAP2, this seems unlikely, particularly in HeLa cells where Myomegalin is apparently not present in the centrosome (Chapter 3). I reasoned that the lack of mitotic phenotype could be due to the incomplete depletion of CDK5RAP2 by siRNA/shRNA, since I was never able to deplete CDK5RAP2 completely from the centrosome. Therefore, I decided to use another approach to study CDK5RAP2 function.

In this chapter, I used reverse genetics in the chicken B-cell line, DT40, to disrupt the evolutionarily conserved CNN1 and CNN2 domains of CDK5RAP2. DT40 cells exhibit a high ratio of homologous versus non-homologous targeting events, thus making them an ideal system to carry out precise genetic knockouts (Buerstedde and Takeda, 1991).

Using DT40 cells, I demonstrate that both the CNN1 and CNN2 domains of CDK5RAP2 are essential to maintain a link between the centrosome and the mitotic spindle poles. Furthermore, I find that the CNN1 domain is critical for the centrosomal recruitment of the PCM component, AKAP450 and the spindle pole protein and dynactin subunit, p150^{glued}. I propose that CDK5RAP2 maintains a link between centrosomes and spindle poles by providing docking sites for dynactin in the centrosome. DT40 cells lacking the CNN1 domain of CDK5RAP2 also exhibit premature centrosome splitting, similar to what was seen in CDK5RAP2 siRNA/shRNA. This provides further evidence for the requirement of the N-terminus of CDK5RAP2 to maintain centrosome cohesion.

(The majority of the work in this chapter has been published in (Barr et al., 2010) (see appendix).

5.1 Creation and characterisation of *cdk5rap2*-disrupted DT40 cell lines

5.1.1 *cdk5rap2* conservation between human and chicken

To investigate CDK5RAP2 in a clean genetic background, I wanted to assay CDK5RAP2 function using targeted gene disruption in the chicken B-cell line, DT40. Although targeted gene disruption is possible in mammalian cells (Shirasawa et al., 1993), DT40 cells represent a more convenient system to deliver gene-targeted mutations. DT40 cells can exhibit a targeting efficiency of up to 1:2 homologous versus non-homologous targeting events, which is orders of magnitude higher than that seen in mammalian cells (Buerstedde and Takeda, 1991; Winding and Berchtold, 2001).

DT40 cells are derived from an avian leukemia virus-transformed lymphoma in chicken. They exhibit a stable karyotype, with 11 autosomal macrochromosomes, 67 microchromosomes and the ZW sex chromosomes. They are near diploid, with the exception of chromosome 2, which is trisomic. The chicken genome is approximately one third smaller than that of mammalian genomes and, as such, introns are much smaller. This represents a further advantage over mammalian systems when disrupting genes by gene targeting. DT40 cells also have a fast propagation time – the length of the cell cycle being approximately 8-10 hours (Winding and Berchtold, 2001). Furthermore, the sequence of the chicken genome is publicly available, making the design of gene-targeting constructs straightforward (www.ensembl.org).

To see if chicken cells would be a useful system to study CDK5RAP2 function, I checked the conservation of chicken CDK5RAP2 to see if it had the conserved CNN1 and CNN2 domains. *Cdk5rap2* is a large 44-exon gene in chicken that spans 89 kb (Ensembl – www.ensembl.org). To ensure that the *Cdk5rap2* gene shown in Ensembl is annotated correctly, I searched chicken EST databases (BBSRC ChickEST database – www.chick.manchester.ac.uk). I found that the extreme C-terminus of *Gallus gallus* (Gg) *cdk5rap2* appeared to be annotated incorrectly. Ensembl indicates that the final exon of the gene is exon 44. However, I could find no EST for this exon and, moreover, this exon lacks a stop codon. Taking the intron between exon 43 and 44 revealed that there is an EST in this region. In addition, the protein product of this region is exactly conserved between chicken and another bird – the zebrafinch. To confirm which exons are expressed

(and, therefore, to check that *CDK5RAP2* is expressed at all in DT40), I extracted RNA from wild-type DT40 cells and generated cDNA. Using PCR, I checked which exons were present in the cDNA (Figure 5.1.1A). Sequencing of the PCR products showed the correct exon structure of the Gg *Cdk5rap2* gene to be the lower structure on the right of Figure 5.1.1A, that is that the Ensembl annotation is incorrect. PCR amplification of CDK5RAP2 cDNA in this way also confirmed that CDK5RAP2 is expressed in DT40 cells.

Taking the corrected Gg *Cdk5rap2* gene into consideration, chicken and human CDK5RAP2 proteins share significant sequence homology (41% overall identity) and the CNN1 and CNN2 domains are highly conserved in chicken (Figure 5.1.1B, C). This indicates that DT40 is a good model system for the analysis of vertebrate CDK5RAP2.

I also checked to see if the second CNN-domain containing protein, Myomegalin, was expressed in DT40. Using DT40 cDNA, I was able to confirm that Myomegalin is expressed in DT40 (Figure 5.1.1D). According to the annotation in Ensembl, the Gg *Myomegalin* gene lacks the CNN1 domain but has the CNN2 domain. Using BLAST searches of chicken EST databases, I also failed to find a CNN1 domain in Myomegalin.

Therefore, while DT40 expresses both CDK5RAP2 and Myomegalin, it appears that Myomegalin in DT40 may lack the CNN1 domain.

5.1.2 Gene-disruption of *cdk5rap2* in DT40 cells

As mentioned, the *cdk5rap2* locus spans 89 kb in the chicken genome. Theoretically, it is possible to delete a whole gene but recombination events become less efficient when the size of the targeted region exceeds 5 kb (Chapter 1 in (Buerstedde and Takeda, 2006) and KJ Patel, MRC-LMB, UK, personal communication). Therefore, I decided to target the evolutionarily conserved CNN1 and CNN2 domains of CDK5RAP2. I hypothesised that the function of CDK5RAP2 could require these conserved domains and in *Drosophila* embryos, the CNN1 domain is required for the majority of the functions of Cnn in the centrosome (Zhang and Megraw, 2007).

I designed gene-targeting constructs to disrupt the CNN1 and CNN2 domains in DT40 cells. The gene-targeting strategies that I used are shown in Figure 5.1.2A and are based on the procedures outlined in (Barr et al., 2009). Gene disruption is mediated by replacement of the part of the gene of interest with antibiotic resistance cassettes, under the control of the chicken β -actin promoter. Furthermore, the resistance cassette is flanked

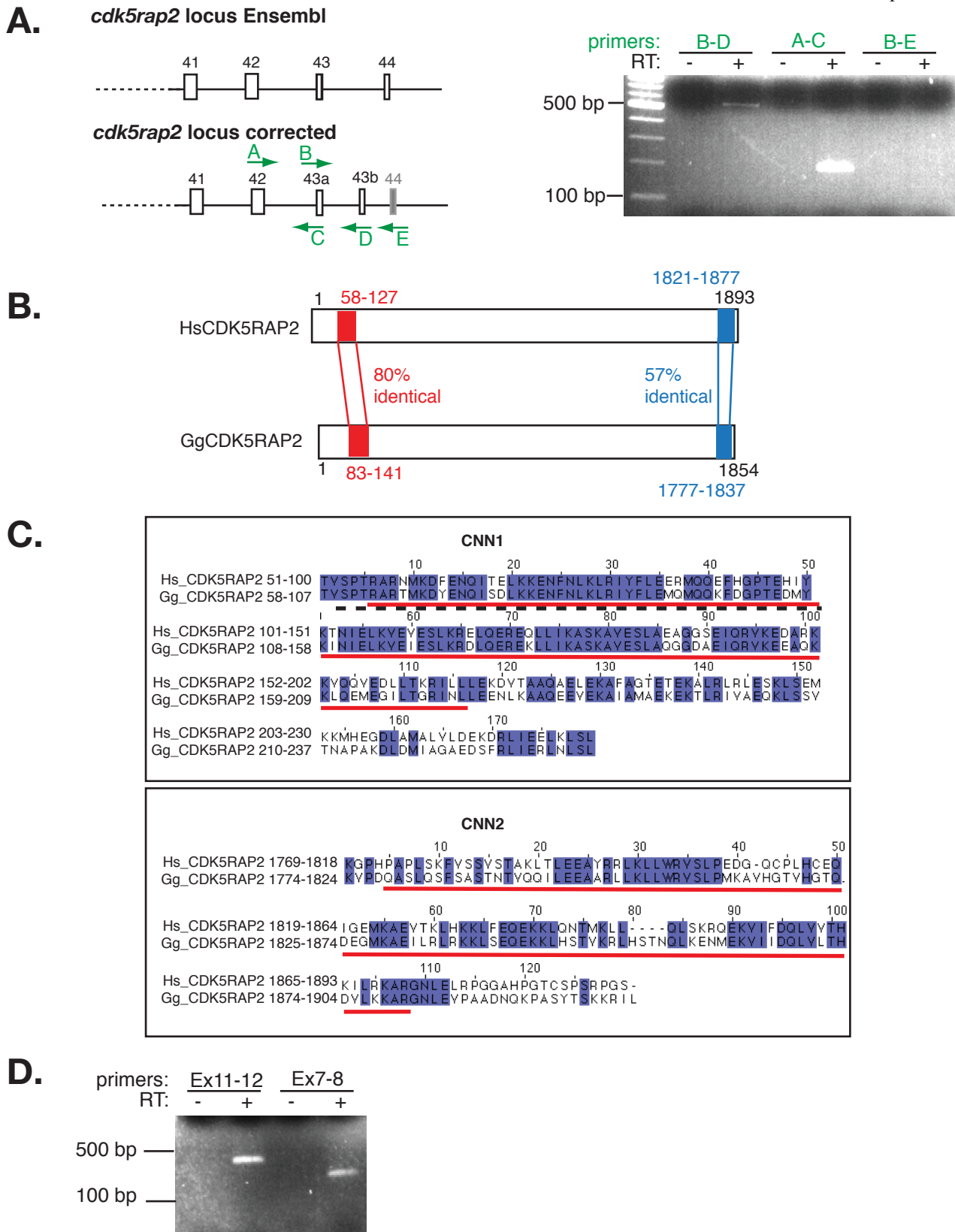


Figure 5.1.1. CDK5RAP2 conservation between human and chicken **A.** Schematics and EtBr-stained 2% agarose gel shows that the C-terminus of CDK5RAP2 is misannotated in Ensembl. **B.** Domain organisation in human and chicken CDK5RAP2 proteins. CNN1 motif is in red and CNN2 motif is in blue. **C.** Alignment of the conserved CNN1 and CNN2 domains in Hs and Gg CDK5RAP2. Red line marks amino acids removed by the knockout strategies in *cnn1*^{-/-} and *cnn2*^{-/-} cells (Figure 5.1.2A). Dotted line marks the γ -TuRC binding site (Fong *et al.*, 2008). The numbering of amino acids and sequence here refers to the product of a virtual cDNA assembled from similarity searches and RT PCRs (see A). **D.** EtBr-stained 2% agarose gel shows that Myomegalin is expressed in DT40 cells. ‘RT’ refers to presence or absence of reverse transcriptase in cDNA RT reaction. ‘Ex’ refers to exon pairs tested in PCR.

by loxP sites. LoxP sites allow cre recombinase-mediated recombination and recycling of the resistance cassettes, such that more genes can be targeted in the same cell line. The loxP sites have been designed in such a way that once recombined, the loxP site created is no longer recognised by cre recombinase and thus cannot be re-targeted by cre (Arakawa et al., 2001). This makes the recombined locus genetically stable. In designing the targeting constructs, I aimed to make the targeted regions as close in size as possible to the size of the antibiotic resistance cassettes used to disrupt the gene in order to maximise gene targeting efficiency.

Both alleles of the *Cdk5rap2* gene were disrupted by sequential gene targeting events. Targeted integration of the constructs into the *Cdk5rap2* genomic locus was confirmed by PCR on genomic DNA (Figure 5.1.2B and Table 2.4 in Materials and Methods for primer sequences). In confirming gene targeting by PCR, one primer must anneal within the resistance cassette and the second primer must be located outside of the gene targeting construct (see primer positions on Figure 5.1.2A). This is essential to confirm that the targeting construct is integrated in the correct genomic locus and is not randomly inserted into the genome.

In the case of CNN1 disruption, the gene-targeting efficiency for disruption of the first allele (*cnn1^{+/-}*) was 1 in 20. However, for homozygous gene disruption (*cnn1^{-/-}*), the gene-targeting efficiency was only 1 in 140. I obtained only two CNN1 homozygous-targeted clones. The first clone was in DT40 cells (*cnn1^{-/-}*; Figure 5.1.2A, B). The second clone was in a DT40 cell line that stably carries a tamoxifen-inducible cre recombinase (*cre-cnn1^{-/-}*; Figure 5.1.2A, B; (Arakawa et al., 2001)). However, *cre*-DT40 cells have been reported to have centrosome abnormalities ((Bree et al., 2007) and C. Morrison, NUI Galway, Ireland, personal communication) and therefore I carried out the majority of my analyses on the *cnn1^{-/-}* DT40 cell line. Where *cre-cnn1^{-/-}* DT40 cells were used is clearly indicated.

Gene targeting of the CNN2 domain of *Cdk5rap2* proved to be more straightforward than for CNN1. The gene-targeting efficiency for the homozygous disruption was 1 in 21 and thus I obtained multiple homozygous-targeted clones (*cnn2^{-/-}*; Figure 5.1.2A, B). Moreover, I transiently introduced cre recombinase into the *cnn1^{-/-}* clone to remove the antibiotic resistance cassettes and derive the *cnn1^{lox}* cell line (Figure 5.1.2C). I then used this to create a double *cnn1^{lox}cnn2^{-/-}* knockout cell line (Figure 5.1.2A).

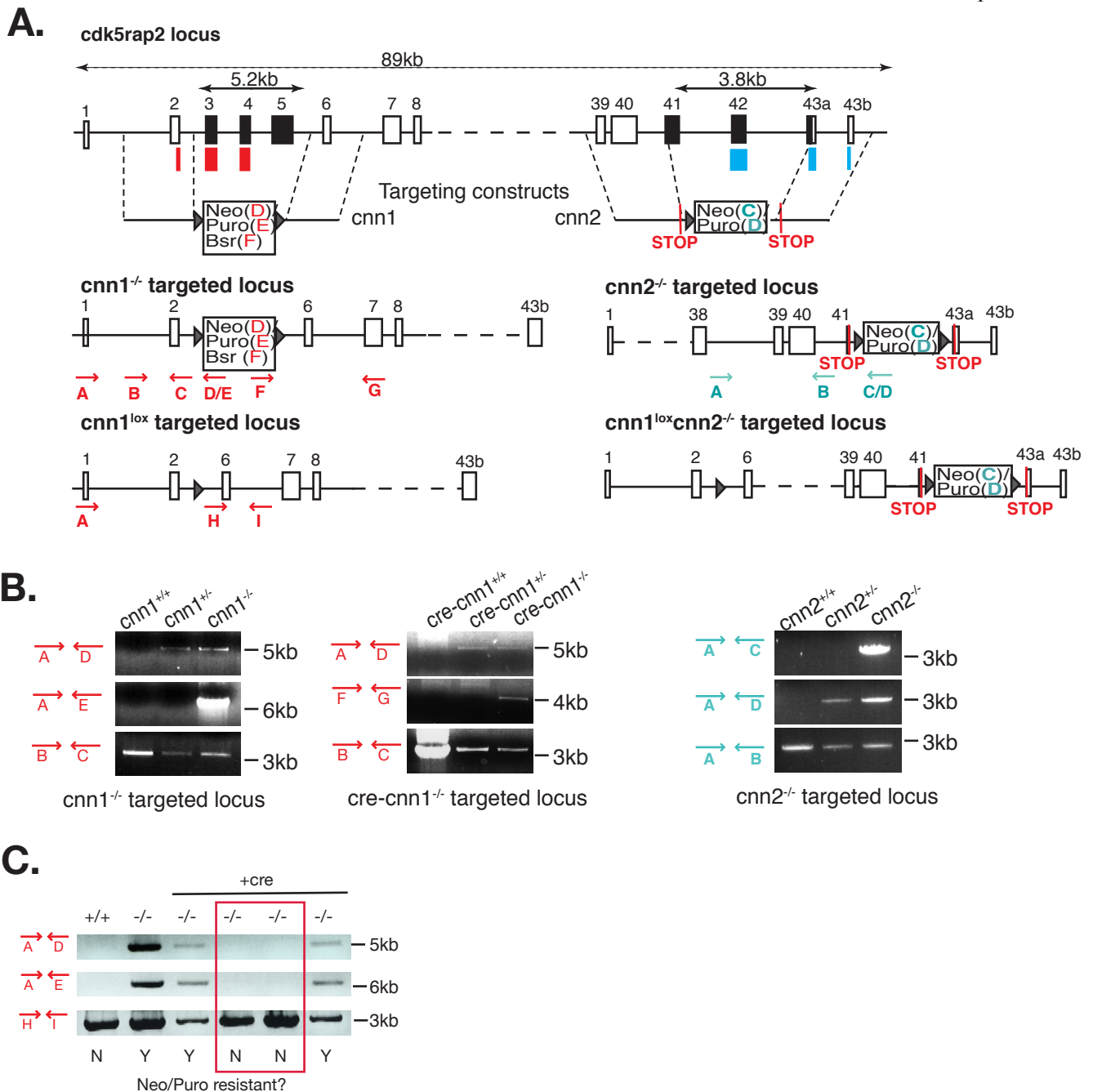


Figure 5.1.2 Gene-targeting strategy to disrupt the CNN1 and CNN2 domains of CDK5RAP2 in DT40. A. Schematic representation of the gene-targeting strategy in the *cdk5rap2* locus. The CNN1 domain maps to exons 2-4 of *cdk5rap2* (red bars). Exons 3-5 (black) were replaced by antibiotic resistance cassettes. Antibiotic resistance cassettes flanked by loxP sites (black triangles), were removed by cre recombinase ($cnn1^{lox}$). The CNN2 domain maps to exons 42-43b of *cdk5rap2* (blue bars). Exons 41-43a (black) were replaced by antibiotic resistance cassettes flanked by in-frame STOP codons. The same targeting constructs were introduced into $cnn1^{lox}$ cells to create the $cnn1^{lox};cnn2^{-/-}$ cells. **B.** EtBr stained 1% agarose gels confirming gene targeting events from A by PCR using genomic DNA extracted from wt and targeted cell lines. Primer positions are shown in A. **C.** EtBr stained 1% agarose gel showing cre-mediated recombination between loxP sites and removal of the antibiotic resistance cassettes. Surviving clones were assayed for antibiotic resistance (resistant (yes=Y), not resistant (no=N)) and for the presence of antibiotic resistance cassettes by PCR using genomic DNA. Primer pairs correspond to those shown in A. Examples of $cnn1^{lox}$ cells are in red box.

5.1.3 Characterisation of CNN1- and CNN2-disrupted DT40 cells

In wild-type DT40 cells, the SK56 CDK5RAP2 antibody recognised a protein of approximately 200 kDa on Western blots (Figure 5.1.3A). Immunostaining showed that CDK5RAP2 was centrosomal throughout the cell cycle in wild-type cells. In interphase cells I could detect a diffuse staining in the proximity of the centrosome, reminiscent of the Golgi apparatus staining observed in human cells (Figure 5.1.3B).

In *cnn1*^{-/-} and *cnn1*^{lox} cells, no CDK5RAP2 protein was detectable by Western blot or by immunostaining (Figure 5.1.3A, B). In *cnn2*^{-/-} cells, a truncated protein product (Δ CNN2) was detectable by Western blot that was absent from interphase centrosomes (Figure 5.1.3A, B). Centrosomal Δ CNN2 signal was, however, detectable in mitotic centrosomes, although at much lower levels than wild-type CDK5RAP2 (16 \pm 9% of wild-type levels; fluorescence intensity was measured in 18 centrosomes; see Section 2.5.2, Materials and Methods; Figure 5.1.3A, B; Table 5.1 below).

The targeted region in *cnn1*^{-/-} and *cnn1*^{lox} cells overlaps with the recognition site of the SK56 antibody, therefore this antibody could fail to detect a truncated protein lacking the CNN1 domain. To see if this was the case, I decided to tag the endogenous *Cdk5rap2* locus at the 3' end. To do this I used a protein G-TEV-Streptavidin-encoding tag (GS-TAP; (Burckstummer et al., 2006)). This tag contains a protein G moiety and a streptavidin binding moiety separated by a TEV protease cleavage site. Principally, GS-TAP was designed as a Tandem Affinity Purification (TAP) tag, but, due to the protein G moiety, it is also useful as an immunolocalisation tag since protein G can be detected by anti-protein G antibodies.

I designed and made targeting constructs and introduced the GS-TAP tag in-frame into a single allele of the *Cdk5rap2* gene in both *cnn1*^{lox} (tag-*cnn1*^{lox}) and wild-type (tag-wt) cells (Figure 5.1.3C). Targeted insertion of the GS-TAP tag into the *cdk5rap2* allele was checked by PCR on genomic DNA (Figure 5.1.3D). Western-blots of tag-wt and tag-*cnn1*^{lox} cell extracts revealed a prominent band of 210 kDa in tag-wt cells and the presence of a protein product (tag- Δ CNN1) in tag-*cnn1*^{lox} cells (Figure 5.1.3E). In immunostaining, anti-protein G stained both interphase and mitotic centrosomes in tag-wt cells. In the tag-*cnn1*^{lox} cell line tag- Δ CNN1 protein was only present in mitotic centrosomes (Figure 5.1.3F) corresponding to about 35 \pm 19% of tag-wt levels (fluorescence intensity was measured in 42 centrosomes; Table 5.1, below).

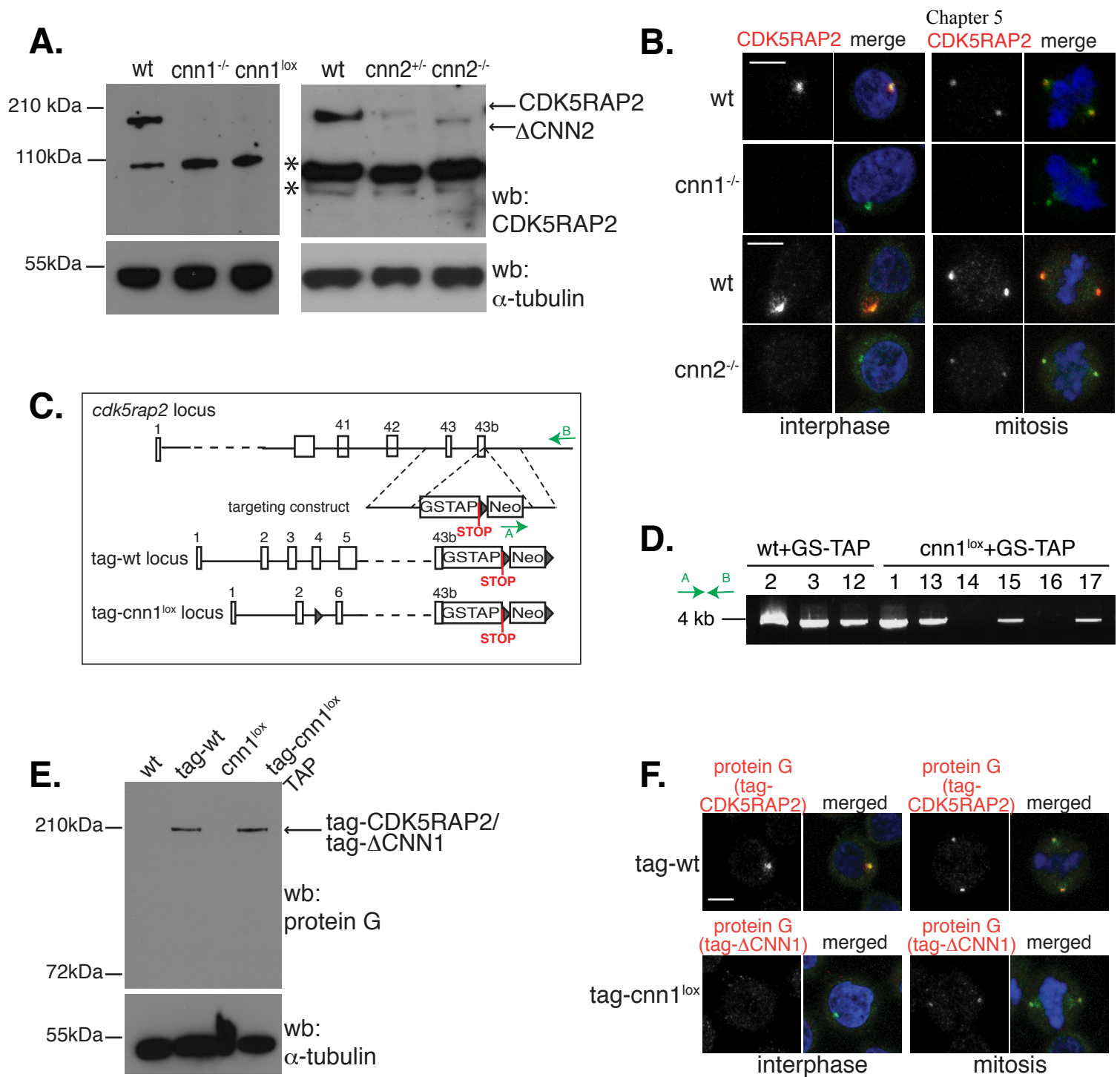


Figure 5.1.3 Characterisation of *cdk5rap2* in CNN1- and CNN2-disrupted DT40 cells **A.** Western blots of wt and gene-disrupted cells. α -tubulin serves as the loading control. Bands marked by asterisks are non-specific since *in situ* C-terminal tagging of CDK5RAP2 does not give rise to bands of these sizes (see below in E). **B.** Subcellular localisation of CDK5RAP2 in wild-type, *cnn1*^{-/-} and *cnn2*^{-/-} DT40 cells. DNA is blue, CDK5RAP2 is red and γ -tubulin is green in merged images. **C.** GS-TAP tagging of CDK5RAP2. Diagram shows targeting construct and knock-in strategy. GS-TAP was inserted in-frame into the wt or *cnn1*^{lox} allele of *cdk5rap2* just before the STOP codon. **D.** EtBr stained 1% agarose gel showing targeted integration of GS-TAP tag into wt-*cdk5rap2* allele (left hand side) or *cnn1*^{lox}-*cdk5rap2* allele (right hand side). *cnn1*^{lox} clones 14 and 16 do not have targeted integration of the construct. Green arrows refer to primers marked on schematic in C. **E.** Western blot of DT40 whole cell extracts. tag-wt and tag-*cnn1*^{lox} cells contain a protein G-encoding tag in one *cdk5rap2* allele. α -tubulin serves as the loading control. **F.** Subcellular localisation of tag-wt and tag-*cnn1*^{lox} in DT40 cells. DNA is blue, protein G is red and γ -tubulin is green in merged images. Scale bars are 5 μ m.

Since a protein product is made in the *cnn1*^{lox} cell line, I wondered if the *cdk5rap2* mRNA had undergone alternative splicing to generate a protein product lacking the CNN1 domain, or if translation had reinitiated downstream of the gene disruption. Therefore, I extracted RNA from wild-type, *cnn1*^{-/-} and *cnn1*^{lox} DT40 cells and generated cDNA. PCR of exons 1-6 of *cdk5rap2* cDNA (primers listed in Table 2.4, Materials and Methods) revealed that in both *cnn1*^{-/-} and *cnn1*^{lox} cells, *cdk5rap2* mRNA is alternatively spliced, such that exon 2 is spliced to exon 6. This product was not present in wild-type cells. Splicing of exon 2 to exon 6 generates an in-frame fusion (amino acids 62 to 177 on Figure 5.1.1C) and hence a CDK5RAP2 protein product lacking the majority of the CNN1 domain.

In summary, both *cnn1*^{lox} and *cnn2*^{-/-} cells express protein products (Table 5.1) and therefore represent powerful tools to study the respective roles of the CNN1 and CNN2 domains of CDK5RAP2. Moreover, the generation of cell lines carrying the GS-TAP tag in the endogenous *Cdk5rap2* and *cnn1*^{lox} *Cdk5rap2* loci, provide a powerful tool for identifying novel interacting partners of the wild-type and mutant CDK5RAP2 proteins by tandem affinity purification.

Table 5.1 Summary of *cdk5rap2* alleles generated in DT40

Cell lines	Protein product	Western blot	Subcellular localisation	Subcellular localisation
		Protein detectable	Interphase centrosome	Mitotic centrosome
wild-type	CDK5RAP2	✓	✓	✓
tag-wt	tag-CDK5RAP2	✓	✓	✓
<i>cnn1</i> ^{-/-}	ΔCNN1	?	?	?
tag- <i>cnn1</i> ^{lox}	tag-ΔCNN1	✓	X	✓ (35%)
<i>cnn2</i> ^{-/-}	ΔCNN2	✓	X	✓ (16%)
<i>cnn1</i> ^{lox} <i>cnn2</i> ^{-/-}	ΔCNN1ΔCNN2	?	?	?

Key to table: ✓ = yes, X = no, ? = unknown. Numbers in brackets refer to fluorescence intensity of CDK5RAP2 immunostaining at the centrosome measured relative to wild-type.

5.2 CDK5RAP2 connects centrosomes to mitotic spindle poles

5.2.1 Centrosomes detach from spindle poles in *cnn1*^{-/-} and *cnn2*^{-/-}

DT40 cells

I examined the morphology of the mitotic spindles in the DT40 mutant cell lines. In prophase, centrosome-associated microtubule asters appeared indistinguishable between wild-type and mutant cells (Figure 5.2.1A). However, in prometaphase, centrioles failed to colocalise with spindle poles in *cnn1*^{-/-} and *cnn2*^{-/-} cells (Figure 5.2.1B). This indicated that centrosomes were not tightly associated with spindle poles. Centrosomes that were separated from spindle poles were either fully detached from spindle poles (blue asterisk in Figure 5.2.1B) or only partially detached, where centrosomes still retained some association with their spindle pole of origin (yellow asterisks in Figure 5.2.1B). *cnn1*^{lox}, *cnn1*^{lox}*cnn2*^{-/-} and *cre-cnn1*^{-/-} cells displayed centrosome phenotypes identical to those seen in *cnn1*^{-/-} cells (Figure 5.2.1B, C). Importantly, partially or fully detached centrosomes were never observed in wild-type, heterozygous *cnn1*^{+/-}, *cre-cnn1*^{+/-} or *cnn2*^{+/-} DT40 cells. Centrosome detachment worsened during mitosis in mutant cells, such that by anaphase, almost half of *cnn1*^{-/-} spindles had lost both their centrosomes (Figure 5.2.1D). Detached centrosomes in anaphase and telophase raised the question of whether centrosomes could be unevenly segregated into daughter cells. I could not find individual *cnn1*^{-/-} cells that contained no centrosomes, but I noted a slight increase in both centrosome number (0.3±0.4% in wild-type and 2.7±0.8% in *cnn1*^{-/-} cells with greater than 2 centrosomes, based on γ -tubulin staining) and the frequency of multipolar spindles (4.6±3% in wild-type and 10±3% in *cnn1*^{-/-}). Cells with multiple centrosomes could arise from centrosome missegregation or failed mitosis and possible tetraploidisation. The percentage of cells with multiple centrosomes and spindle poles remained constant over several passages, suggesting that centrosome missegregation is a rare event or that such cells are eliminated from the population.

Truncated forms of CDK5RAP2, tag- Δ CNN1 and Δ CNN2, associated with detached centrosomes, but not with spindle poles (see example for tag- Δ CNN1 in Figure 5.1.3F and 5.2.1E). Levels of tag- Δ CNN1 at the centrosome did not correlate with centrosome

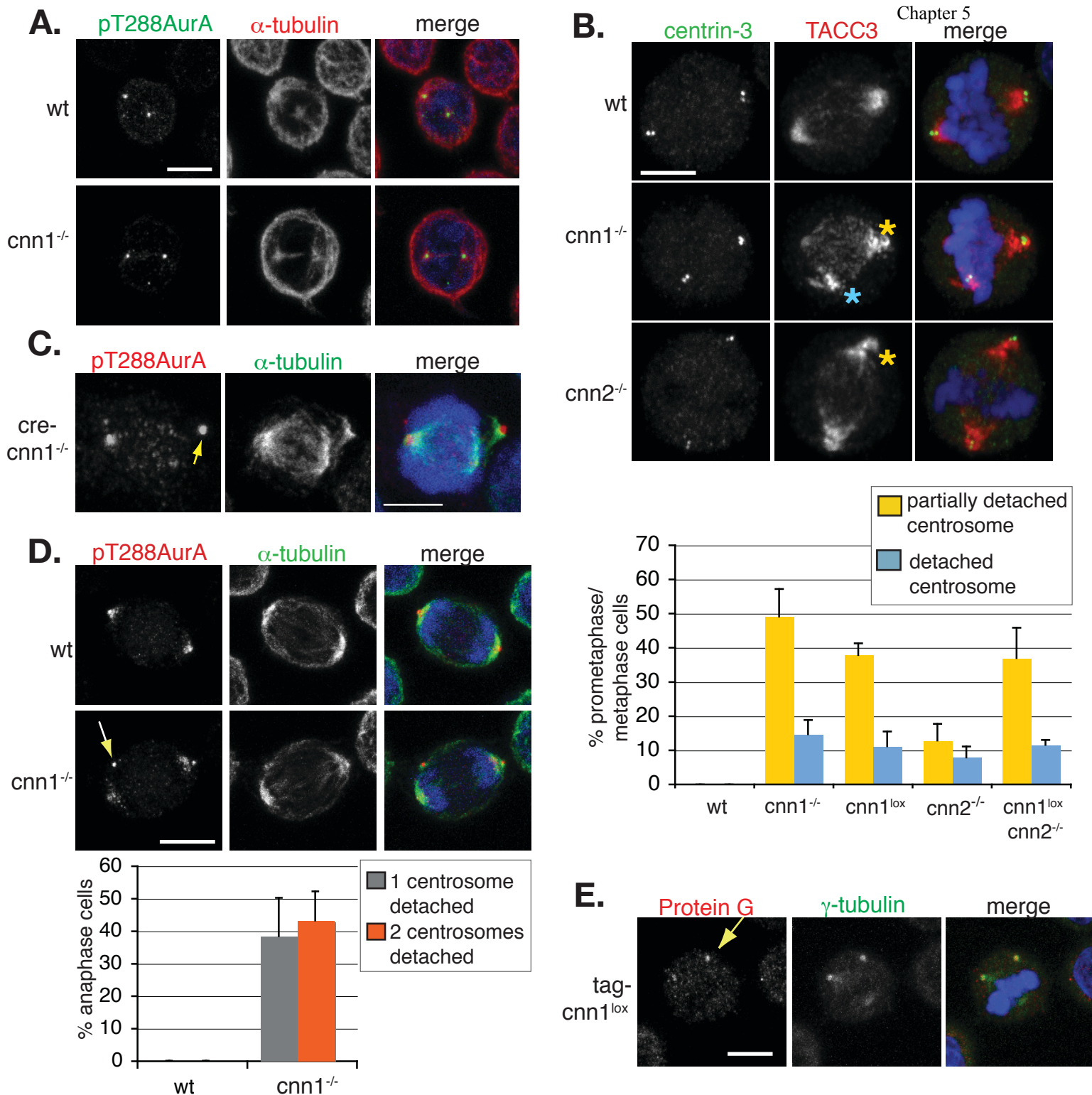


Figure 5.2.1 Centrosomes detach from spindle poles in *cnn1*^{-/-} and *cnn2*^{-/-} DT40 cells. **A.** Immunostaining of wt and *cnn1*^{-/-} cells. DNA is blue, pT288AurA is green and α -tubulin is red in merged images. **B.** In wt cells anti-centrin-3 antibody staining is confined to the tips of the two spindle pole regions marked by anti-TACC3 antibody (top panels). Partial detachment of centrosomes from spindle poles is marked with yellow asterisks and complete detachment with a blue asterisk in mutant cells. DNA is blue, TACC3 is red and centrin-3 is green in merged images. Graph shows quantification of the centrosome phenotypes seen in prometaphase/metaphase cells (n=4, 150 cells per experiment, error bars represent STD). **C.** Cre-*cnn1*^{-/-} cells display a mitotic phenotype similar to that seen in *cnn1*^{-/-} cells. Centrosomes are stained with anti-pT288AurA antibody. DNA is blue, pT288AurA is red and α -tubulin is green in merged image. **D.** In anaphase *cnn1*^{-/-} cells, pT288AurA staining frequently appears near the cortex away from the spindle poles (see arrow). DNA is blue, α -tubulin is green and pT288AurA is red in merged image. The graph shows quantification of centrosome phenotypes in anaphase cells (n=4, 150 cells per experiment, error bars represent STD). **E.** Centrosomal levels of Δ CNN1 protein do not correlate with centrosome detachment in tag-*cnn1*^{lox} cells. Arrow marks detached centrosome. DNA is blue, γ -tubulin is green and protein G is red in merged image. Scale bars are 5 μ m.

detachment arguing that the centrosome-detachment phenotype is not due to an overall decrease in CDK5RAP2 protein levels (Figure 5.2.1E).

The centrosome detachment phenotype was more severe in *cnn1*^{-/-} than in *cnn2*^{-/-} cells, therefore I focussed my detailed analysis on *cnn1*^{-/-} cells.

5.2.2 Expression of FLAG-FL CDK5RAP2 in *cnn1*^{lox} cells rescues centrosome detachment

I wanted to confirm that the mitotic defects I observed in Δ CNN1 cells were linked to the disruption of the *Cdk5rap2* gene. Therefore, first I transiently transfected *cnn1*^{-/-} cells with FLAG-tagged Full-Length human CDK5RAP2 cDNA (FLAG-FL; Figure 3.3.1A). In this experiment, partially and fully detached centrosomes were scored as one category. Transfected cells were identified by immunostaining with anti-FLAG antibody and looking for mitotic cells expressing FLAG. I observed 32 FLAG-FL transfected cells from three independent transfections and none of these had partially detached centrosomes, suggesting that FLAG-FL human CDK5RAP2 can rescue the centrosome detachment phenotype (Figure 5.2.2A). I also transiently transfected the FLAG-NT and FLAG-CT constructs (Figure 3.3.1A) into *cnn1*^{-/-} cells to see if constructs containing truncated CDK5RAP2 could rescue centrosome detachment. Both constructs can localise to centrosomes in mitosis (Figure 3.3.1) and therefore are present in the right cell cycle stage to rescue centrosome detachment. As Figure 5.2.2A shows, FLAG-NT could rescue the centrosome detachment phenotype (only 1 out of 23 cells had a partial or fully detached centrosome). FLAG-NT contains the CNN1 domain of CDK5RAP2 plus extra downstream sequence, but not the CNN2 domain. Therefore, rescue by FLAG-NT shows that restoration of the CNN1 domain can rescue centrosome detachment in *cnn1*^{-/-} cells. Consistent with this result, transfection of *cnn1*^{-/-} cells with FLAG-CT, which contains the CNN2 domain but lacks the CNN1 domain, failed to rescue centrosome detachment phenotypes (Figure 5.2.2A; 18 out of 29 cells still had a defect).

The transfection efficiency for transient transfection was very low. Therefore, to confirm the above results, I generated a stable cell line carrying FLAG-FL. I used the *cnn1*^{lox} cell line and introduced the FLAG-FL construct by electroporation, to promote random integration of the vector into the genome. I then selected single-cell clones with G418 antibiotic. Figure 5.2.2B suggests that FLAG-FL CDK5RAP2 expression in *cnn1*^{lox} cells is considerably higher than endogenous CDK5RAP2 expression in wild-type DT40 cells.

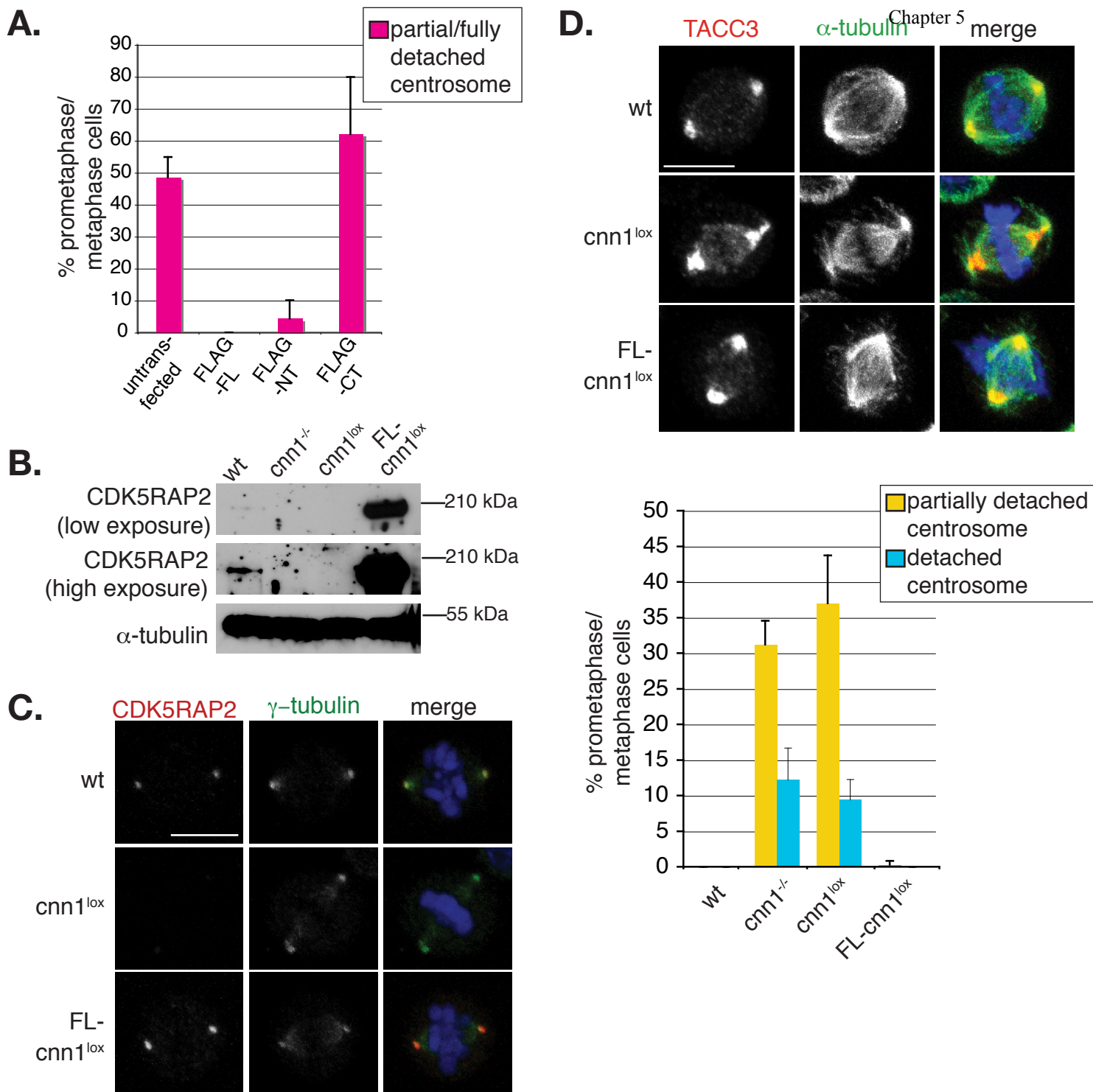


Figure 5.2.2 Expression of FLAG-FL CDK5RAP2 in *cnn1*^{-/-} cells rescues centrosome detachment.

A. Graph shows quantification of centrosome detachment phenotypes in *cnn1*^{-/-} cells 24 hr after transient transfection with FLAG-tagged human CDK5RAP2 constructs (Figure 3.1.3A). (n=3, 23-32 cells in total for each vector. Error bars represent STD). **B.** Western blot showing the levels of CDK5RAP2 protein in cytoplasmic extracts of wt, *cnn1*^{-/-}, *cnn1*^{lox} and FL-*cnn1*^{lox} cells. The FL-*cnn1*^{lox} line stably expresses FLAG-FL human CDK5RAP2. As FLAG-FL is expressed at considerably higher levels in FL-*cnn1*^{lox} cells than endogenous CDK5RAP2 in wt cells, different exposure times were used to visualise endogenous (high exposure) and exogenous (low exposure) proteins. α -tubulin serves as a loading control. **C.** FLAG-FL localises to the centrosomes in FL-*cnn1*^{lox} cells (bottom panels). DNA is blue, γ -tubulin is green and CDK5RAP2 is red in merged images. **D.** Complementing *cnn1*^{lox} cells with full-length human CDK5RAP2 rescues centrosome detachment. A representative image is shown for mitotic spindle morphology in each of wt, *cnn1*^{lox} and FL-*cnn1*^{lox} cells. DNA is blue, α -tubulin is green and TACC3 is red in merged images. Graph shows quantification of centrosome abnormalities in prometaphase/metaphase in mutant cell lines (n=3, 300 mitotic cells per experiment, error bars represent STD). FLAG-FL expression eliminates both partially detached and detached centrosome phenotypes seen in *cnn1*^{lox} cells. Scale bars are 5 μ m.

However, it is also worth noting that the SK56 CDK5RAP2 antibody was generated against a human CDK5RAP2 epitope and thus may have a higher affinity for the human CDK5RAP2 protein than the endogenous chicken protein. FLAG-FL human CDK5RAP2 localised to centrosomes in *cnn1*^{lox} cells, mimicking the localisation of endogenous chicken CDK5RAP2 (Figure 5.2.2C). Furthermore, complementation of *cnn1*^{lox} cells with FLAG-FL completely rescued the detached centrosome phenotype (Figure 5.2.2C,D). This confirms that the mitotic defects I have observed are due to disruption of the *Cdk5rap2* gene.

5.2.3 Centrosome detachment is a dynamic and reversible event

Since centrosomes were positioned normally in prophase, at the centre of microtubule asters in *cnn1*^{-/-} cells, I wanted to see at what point after NEBD centrosomes were detaching from mitotic spindles. In order to study the dynamics of centrosome detachment, I performed time-lapse imaging on *cnn1*^{-/-} cells transiently expressing GFP- α -tubulin (GFP-tubulin). I used two different time-intervals to image DT40 cells – filming at either 1-minute or 3-minute intervals. When imaged every minute, the GFP-signal started to bleach after about 100 minutes and cell survival decreased after 2 hours. When imaged every 3 minutes, the GFP signal remained prominent and cells showed little or no stress even when imaged for up to 3-4 hours. I noted that the average time from NEBD to anaphase onset is about 33 minutes in DT40 cells when the frames are acquired every minute compared to 23 minutes when acquired every 3 minutes (Figure 5.2.3A). Thus, cells seem to suffer some damage when imaged at higher temporal resolution, but this resolution is essential to follow spindle behaviour. Crucially, overall differences seen between wild-type and *cnn1*^{-/-} cells were consistent between the two imaging schedules. The following discussion of phenotypes is based on the 1-minute imaging schedule as this allowed a more detailed analysis of spindle assembly.

Following NEBD, *cnn1*^{-/-} cells were able to build a bipolar spindle with similar efficiency to wild-type. However, within a few minutes a small aster would detach from one or both spindle poles (Figure 5.2.3B, Movies 5.1-5.3 (see Supplementary CD)). Based on the striking similarities between spindle structures in live and fixed cells, I made the assumption that these small asters correspond to centrosomes. Bipolar spindle formation occurred simultaneously (within the same timepoint) in 3 out of 8 cells and preceded

A.

1 minute intervals	wt	cnn1 ^{-/-}		
	normal	normal	partial	detached
Total cell number	22	6	5	3
Cells that do not enter anaphase	0	0	2	3
Cells that fail cytokinesis	0	0	1	0
Average time period between NEBD and anaphase onset (minutes)	33.6	34.6	40	n/a

3 minute intervals	wt	cnn1 ^{-/-}		
	normal	normal	partial	detached
Total cell number	9	3	2	6
Cells that do not enter anaphase	0	0	0	1
Cells that fail cytokinesis	0	0	0	0
Average time period between NEBD and anaphase onset (minutes)	23.4	28.0	33.5	74.3

Figure 5.2.3 Centrosome detachment is a dynamic and reversible event A. Summary of time-lapse experiments. For *cnn1^{-/-}* cells I show the breakdown of mitotic timing and outcome according to centrosome phenotypes. The criteria for classification were the following: if at any point during imaging cells developed partially detached centrosomes they were included in ‘partial’, whereas cells with detached centrosomes or a combination of detached and partially detached centrosomes were scored in the ‘detached’ category. The three *cnn1^{-/-}* cells with detached centrosomes in the 1-minute interval filming schedule were followed for an average of 105 minutes after NEBD but they failed to initiate anaphase during filming.

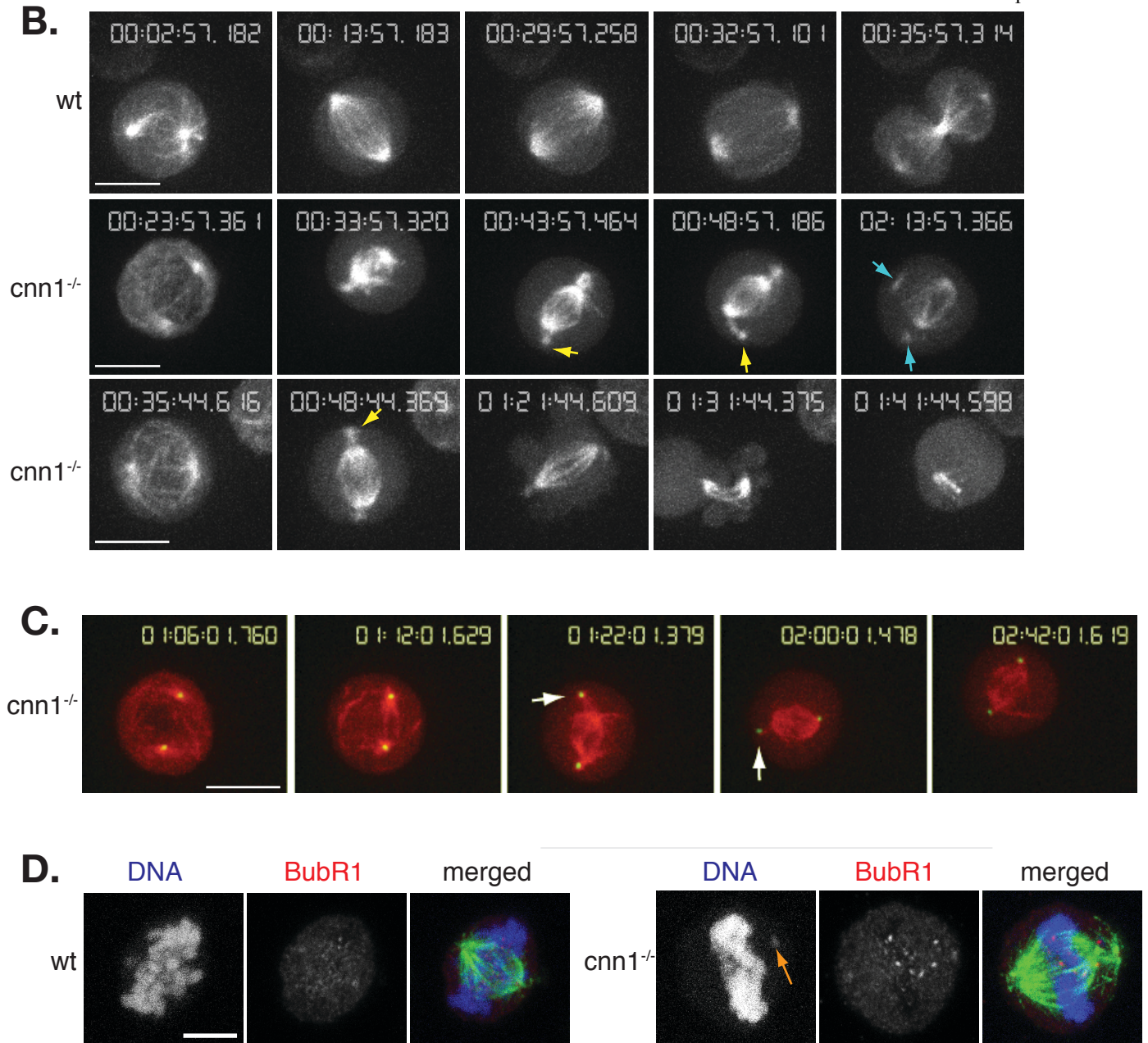


Figure 5.2.3 Centrosome detachment is a dynamic and reversible event (continued).

B. Still frames from time-lapse experiments following wt (see Movie 5.1) and *cnn1*^{-/-} cells (see Movies 5.2 and 5.3) through mitosis. Note that partially detached centrosomes (yellow arrows) appear soon after NEBD and precede the detached centrosome phenotype (blue arrows). The cell shown in the bottom panels initiates anaphase but fails to go through cytokinesis. **C.** *cnn1*^{-/-} cells (see Movie 5.4) were transiently transfected with mCherry-tubulin and GFP-PACT to image centrosomes and microtubules simultaneously. **D.** Immunofluorescence images of wt and *cnn1*^{-/-} cells. Orange arrow indicates unaligned chromosome close to a partially detached centrosome. DNA is blue, BubR1 is red and microtubules are green in merged images. Scale bars are 5 μ m.

centrosome detachment by 1-4 minutes in 4, and by 26 minutes in 1 cell. When fully detached from spindle poles, centrosomes moved rapidly around the cortex while still nucleating microtubules (middle panels in Figure 5.2.3B, Movie 5.2). Centrosomes were also observed to detach and re-attach to spindle poles, indicating that detachment is a dynamic and reversible event. *cnn1*^{-/-} cells with normal centrosome behaviour progressed through mitosis with similar timing to wild-type cells. However, *cnn1*^{-/-} cells with centrosome detachment phenotypes took longer to initiate anaphase (Figure 5.2.3A).

To visualise microtubules and centrosomes simultaneously, I co-transfected *cnn1*^{-/-} cells with mCherry- α -tubulin and a GFP fusion of PACT, the centrosomal targeting domain of AKAP450 (Gillingham and Munro, 2000). The GFP-PACT signal detached from the mitotic spindle poles as soon as a bipolar spindle became visible (Figure 5.2.3C; Movie 5.4 on Supplementary CD). This confirmed that the asters I saw detaching in GFP-tubulin only expressing cells were actually centrosomes. Thus it seems that centrosomes detach from spindle poles after NEBD, coincident with the time when microtubule attachment to kinetochores increases the tension at the spindle pole.

The delay in initiation of anaphase in *cnn1*^{-/-} cells with detached centrosome phenotypes could be due to the maintenance of the spindle assembly checkpoint (SAC). To determine whether abnormal centrosome attachment affects chromosome alignment, I scored mitotic cells with different centrosome phenotypes for the presence of the spindle assembly checkpoint component, BubR1 (Figure 5.2.3D) (Chan et al., 1999; Nishihashi et al., 2002; Taylor et al., 1998). My data revealed an inverse correlation between centrosome abnormalities and chromosome congression (percentage of BubR1-positive mitotic cells with normal, partially detached and fully detached centrosomes were 43%, 86% and 100%, respectively; 165 mitotic cells scored). Therefore, it seems that centrosome detachment can cause a delay in chromosome alignment and thus a delay in anaphase onset. The converse argument, that centrosome detachment is due to an extended mitotic arrest, is not true since centrosome detachment became apparent within 9 minutes after NEBD in 7 out of 8 cells and after 28 minutes in only 1 cell, when the metaphase to anaphase transition occurs after approximately 33 minutes on average in wild-type cells.

5.2.4 Dynamic microtubules are not required for centrosome detachment

CDK5RAP2 has been reported to regulate microtubule behaviour via its interaction with the microtubule plus end binding protein, Eb1 (Fong et al., 2008; Fong et al., 2009). Moreover, I have shown that CDK5RAP2 can bind to microtubule polymer in a microtubule spindown assay (Figure 3.3.4B). Therefore, I tested if abnormal microtubule dynamics contributed to centrosome detachment in *cnn1*^{-/-} cells. Microtubule dynamic instability was suppressed with a low dose of Taxol (Derry et al., 1998; Jordan et al., 1993). 2 hour treatment of *cnn1*^{-/-} cells with 5 nM Taxol interfered with chromosome congression to the metaphase plate without inducing microtubule bundling or multipolarity (Figure 5.2.4A). 5 nM Taxol increased the proportion of *cnn1*^{-/-} cells with fully detached centrosomes (Figure 5.2.4B). Thus, dynamic microtubules are not essential for centrosome detachment, but instead they may promote centrosome re-attachment to spindle poles.

5.2.5 Mitotic spindle pole organisation is intact in *cnn1*^{-/-} cells

Since the connection between centrosomes and spindle poles is lost in *cnn1*^{-/-} cells, I hypothesised that spindle pole organisation could be defective in these mutants. Centrosome detachment has been observed in cells where the function of the minus end directed motor protein, dynein, or its activator, dynactin, have been disrupted (Goshima and Vale, 2003; Maiato et al., 2004b; Merdes et al., 1996; Morales-Mulia and Scholey, 2005), or where the spindle pole matrix protein, NuMA has been depleted/mutated (Haren et al., 2009a; Silk et al., 2009). In all of these cases, bipolar spindles no longer focus at their minus ends and the centrosome detaches. Therefore, it was important to investigate if centrosomes were detaching in *cnn1*^{-/-} cells because of a lack of an organised spindle pole.

First I looked at the spindle microtubules at the poles. Spindle microtubules remain focussed in *cnn1*^{-/-} cells in spite of centrosome detachment (white arrow in Figure 5.2.5A). To see if spindle pole organisation is intact in *cnn1*^{-/-} cells, I examined the localisation of dynein/dynactin and NuMA. In both wild-type and *cnn1*^{-/-} cells the dynactin subunit p150^{glued} and NuMA localise in a crescent shape at the spindle poles (Figure 5.2.5B, C). A weak NuMA signal could also be detected in the detached centrosome, but I was unable to

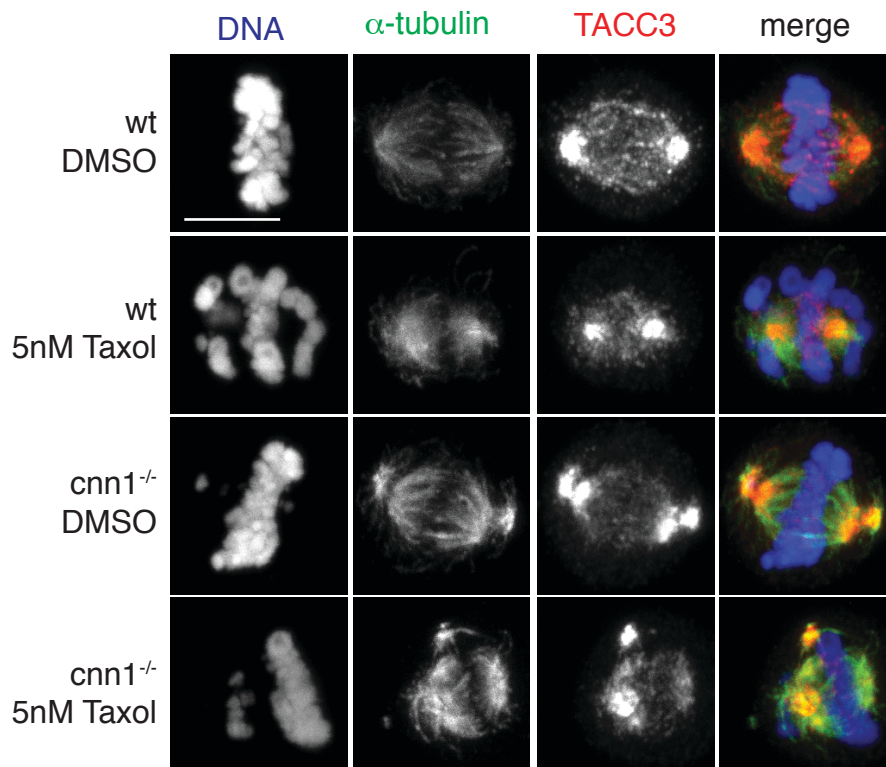
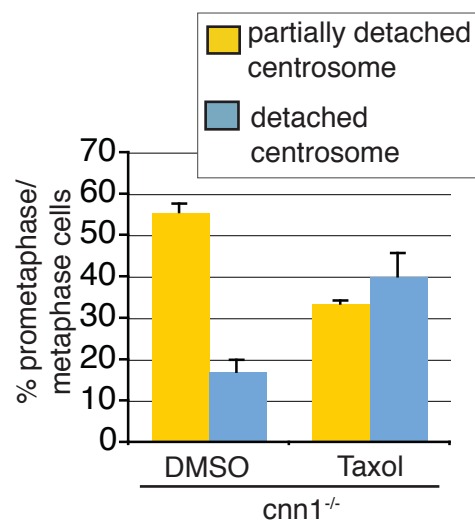
A.**B.**

Figure 5.2.4 Dynamic microtubules are not required for centrosome detachment.

A. Immunofluorescence images of DT40 cells treated with DMSO or a low dose (5 nM) of Taxol. DNA is blue, α -tubulin is green and TACC3 is red in merged image. **B.** Graph shows scoring of centrosome phenotypes (n=2; at least 150 cells were counted per experiment).

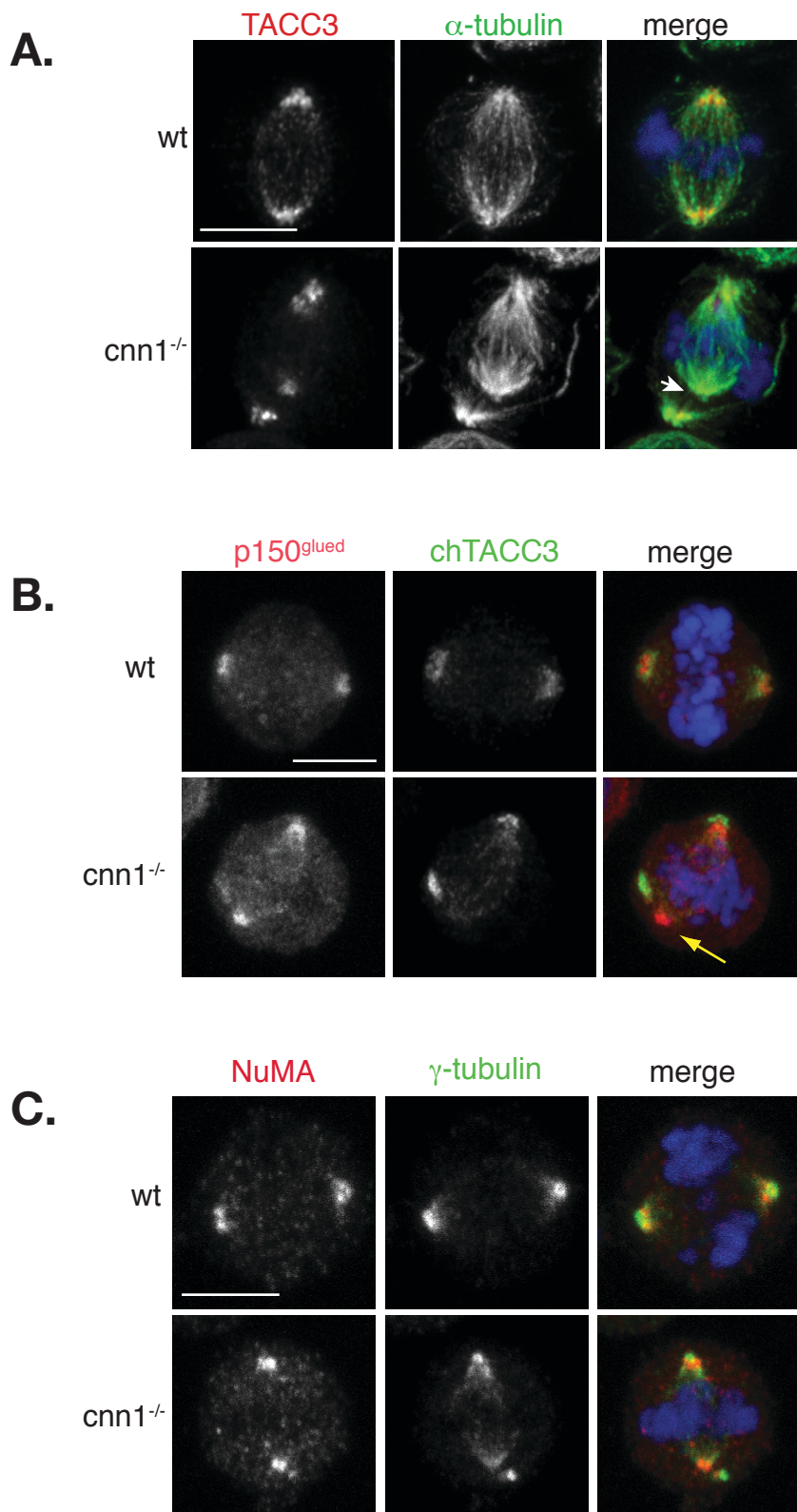


Figure 5.2.5 Mitotic spindle pole organisation is intact in *cnn1*^{-/-} cells. **A.** Immunofluorescence images of microtubules in wt and *cnn1*^{-/-} cells. Spindle poles remain focussed in *cnn1*^{-/-} cells even when centrosomes have detached (white arrow). DNA is blue, TACC3 is red and γ -tubulin is green in merged images. **B.** Subcellular localisation of the spindle pole organising protein, p150^{glued}, in wt and *cnn1*^{-/-} cells. Note that p150^{glued} localises to the spindle pole, even when centrosomes fully detach (yellow arrows). DNA is blue, p150^{glued} is red and TACC3 is green in merged images. **C.** Subcellular localisation of the spindle pole capping protein, NuMA, in wt and *cnn1*^{-/-} DT40 cells. DNA is blue, NuMA is red and γ -tubulin is green in merged images. Scale bars are 5 μ m.

visualise the centrosomal fraction of p150^{glued} in DT40 cells. Nonetheless, the CNN1 domain of CDK5RAP2 is dispensable for the spindle pole localisation and the microtubule-focussing activities of the NuMA/dynein/dynactin complex. Therefore, centrosome detachment is not due to impaired spindle pole focussing.

5.2.6 Centrosome structure is normal in *cnn1*^{-/-} cells

If the defect is not at the spindle pole in *cnn1*^{-/-} cells, then perhaps the centrosome structure is abnormal in these cells, thus leading to centrosome detachment. In order to do this I investigated centrosome structure by Transmission Electron Microscopy (TEM) on serially sectioned mitotic *cnn1*^{-/-} cells. Asynchronous DT40 cells were fixed in pre-warmed (37°C) glutaraldehyde (see Section 2.6 in Materials and Methods) to preserve microtubule structure. Fixed cells were embedded in an epon/epoxy resin before being serially-sectioned at 100 nm thickness. Mitotic cells could be identified in the microscope by the lack of nuclear envelope and the presence of condensed chromosomes. TEM revealed normal-looking, orthogonal centriole pairs in *cnn1*^{-/-} cells (Figure 5.2.6A, B). In addition, an electron-dense area was visible around the centrioles in both wild-type and *cnn1*^{-/-} centrioles, suggesting that PCM was recruited by *cnn1*^{-/-} centrioles (Figure 5.2.6B). Moreover, centriole length was normal in *cnn1*^{-/-} cells (data not shown).

I noticed that *cnn1*^{-/-} centrosomes appeared to associate with fewer microtubules. Microtubules are highlighted in red in Figure 5.2.6A for easier visualisation. All 7 wild-type centrosomes sectioned contained several microtubules. In contrast, of 9 *cnn1*^{-/-} centrosomes examined, microtubules focussed away from the centrosome in 3 (see Figure 5.2.6A for an example) and another 3 contained only a few microtubules. While caution should be exercised when interpreting such data from serially sectioned cells (as much depends on the angle of sectioning through the spindle), this may indicate that these *cnn1*^{-/-} centrosomes examined by TEM are separated from the mitotic spindle pole.

One *cnn1*^{-/-} centrosome was located near the cortex and associated with microtubules that were running along the cortex (Figure 5.2.6C). This pattern looked strikingly similar to the detached centrosome phenotype seen by immunofluorescence.

5.2.7 Visualising AKAP450 in DT40 cells

From my work in human cells, I know that CDK5RAP2 and the centrosomal scaffolding protein, AKAP450, interact (Figure 4.1.1B, C, D). Moreover, a reduction of CDK5RAP2

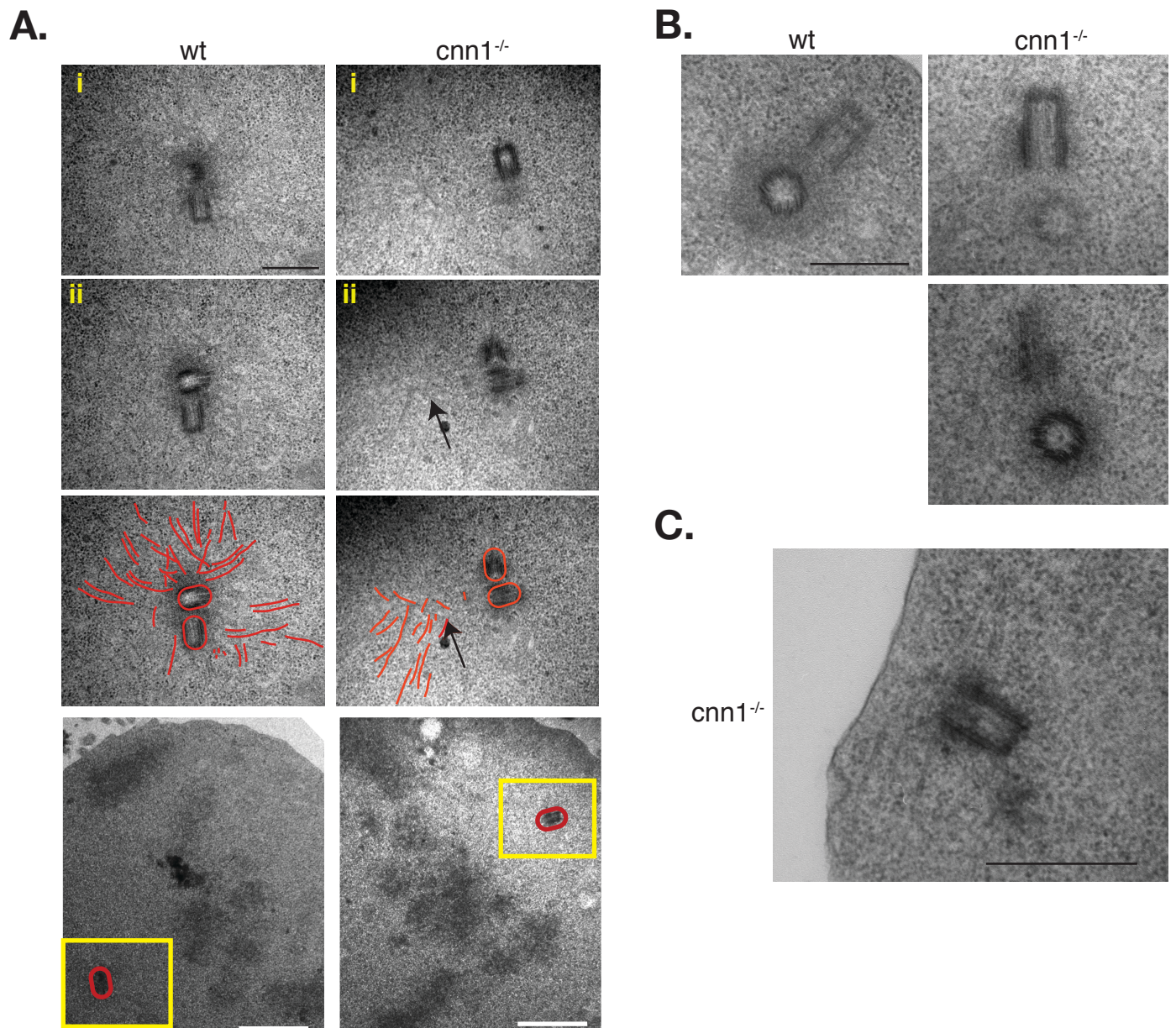


Figure 5.2.6 Centrosome structure is normal in $cnn1^{-/-}$ cells. **A.** TEM micrographs of serially sectioned prometaphase/metaphase cells. Two sections (i and ii) are shown for a single wt (left) and $cnn1^{-/-}$ cell (right). Third panels show replicates of sections 'ii' with microtubules highlighted in red to aid visualisation. While a large number of microtubules focus in the wt centrosome, microtubules seem to focus outside of the $cnn1^{-/-}$ centrosome. Arrows point to the area where a microtubule focus is visible in the $cnn1^{-/-}$ centrosome. Note that these are likely to be spindle microtubules as they occupy a position between the centrosomes and the chromosomes (chromosomes appear as electron-dense material in the whole-field view, bottom panels). **B.** Both wt and $cnn1^{-/-}$ centrioles are surrounded by an electron-dense matrix. **C.** This $cnn1^{-/-}$ centrosome is in close proximity to the cortex. Large bundles of cortical astral microtubules are visible around the centrosome. Black scale bars are 500 nm. White scale bars are 1 μ m.

protein in human cells leads to a decrease in the recruitment of AKAP450 to the mitotic centrosome (Figure 4.1.2A, B). Therefore I wanted to check the localisation of AKAP450 in *cnn1*^{-/-} cells. I tried multiple AKAP450 antibodies in DT40 cells in combination with a variety of fixation conditions, but unfortunately I could not detect the chicken protein with these antibodies despite extensive homology between chicken and human AKAP450 proteins (57% identical). Searching for AKAP450 ESTs in the BBSRC ChickEST database suggested that AKAP450 should be expressed in chicken. Therefore, I decided to use the GS-TAP tagging method to visualise endogenous AKAP450 in DT40 cells. I confirmed that the Ensembl annotation of Gg *Akap450* was correct by checking the predicted exons against the ChickEST database. In addition, the Ensembl-predicted C-terminus of AKAP450 is conserved in human and zebrafish and contains a stop codon. Therefore, I introduced a GS-TAP tag in-frame into the *Akap450* locus of wild-type, *cnn1*^{lox} and *cnn2*^{-/-} cells to generate tagAKAP-wt, tagAKAP-*cnn1*^{lox} and tagAKAP-*cnn2*^{-/-} cells, respectively (Figure 5.2.7A). Targeted insertions of the GS-TAP tag into the *Akap450* allele were confirmed by PCR on genomic DNA (Figure 5.2.7B). Note that the *Akap450* gene is present on chromosome two in the chicken genome, which is trisomic. Therefore, tagging one allele of AKAP450 in DT40 will label one third of the total protein.

Western blot analysis of AKAP450 GS-TAP targeted clones with anti-protein G antibody revealed a protein product (tag-AKAP450) of over 210 kDa in all three cell lines (Figure 5.2.7C). This is consistent with its predicted MW of 418 kDa. Anti-protein G antibody stained the centrosomes in tagAKAP-wt cells throughout the cell cycle (Figure 5.2.7D and 5.2.8A). Some signal was also visible in a broader area around the centrosome that likely corresponds to the Golgi (Figure 5.2.7D). A similar staining was visible in interphase tagAKAP-*cnn2*^{-/-} cells. However, in interphase tagAKAP-*cnn1*^{lox} cells, the same antibody gave a much weaker and highly variable staining (Figure 5.2.7D).

In summary, I have successfully created cell lines to analyse AKAP450 localisation in wild-type, *cnn1*^{lox} and *cnn2*^{-/-} cells. Moreover, localisation of AKAP450 to interphase centrosomes in *cnn1*^{lox} DT40 cells is perturbed.

In addition to allowing immunolocalisation of endogenous AKAP450 protein, GS-TAP tagging of AKAP450 could also help in the identification of novel interacting partners of AKAP450 by tandem affinity purification techniques.

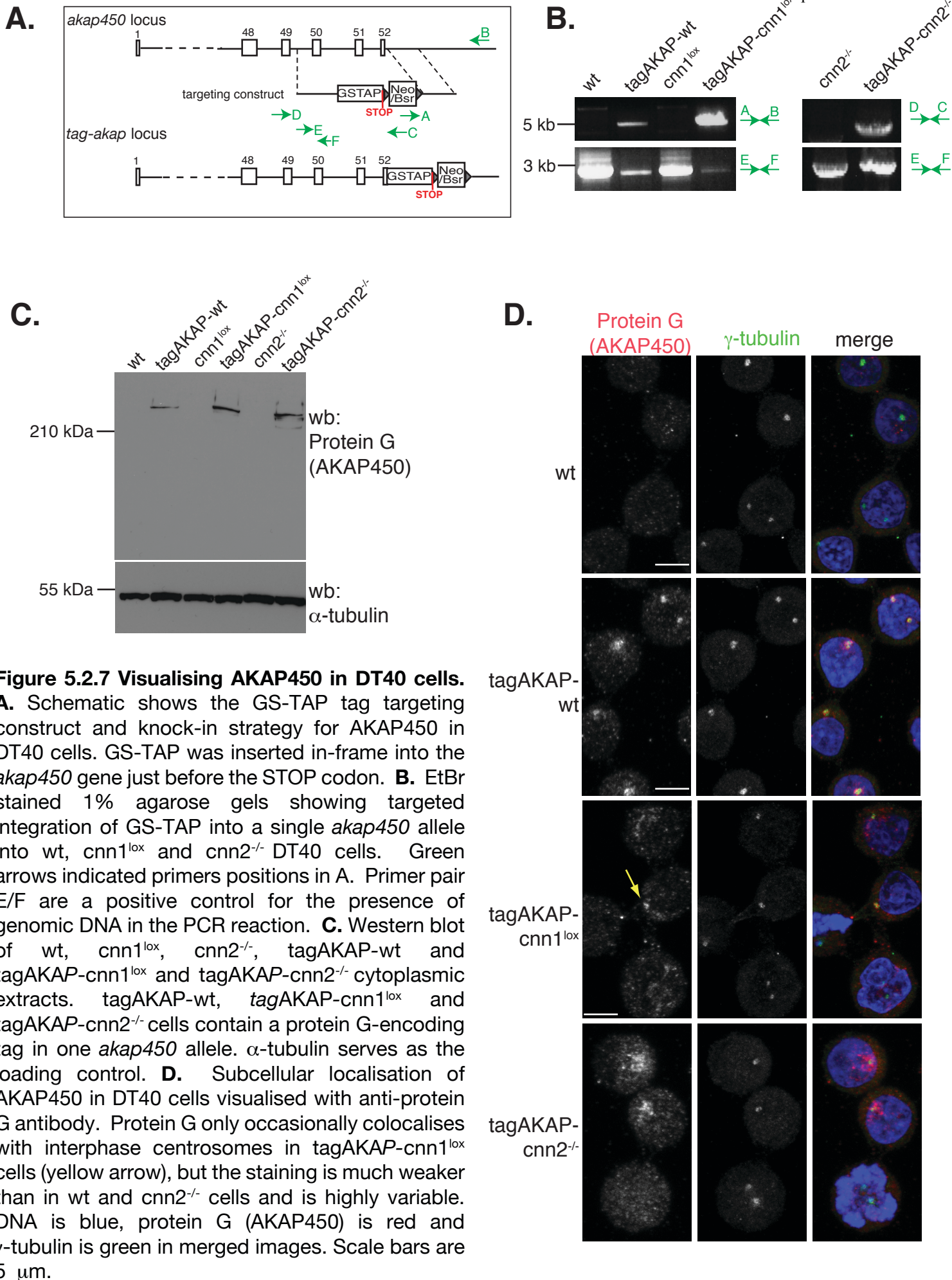


Figure 5.2.7 Visualising AKAP450 in DT40 cells.

A. Schematic shows the GS-TAP tag targeting construct and knock-in strategy for AKAP450 in DT40 cells. GS-TAP was inserted in-frame into the *akap450* gene just before the STOP codon. **B.** EtBr stained 1% agarose gels showing targeted integration of GS-TAP into a single *akap450* allele into wt, *cnn1^{lox}* and *cnn2^{-/-}* DT40 cells. Green arrows indicated primers positions in A. Primer pair E/F are a positive control for the presence of genomic DNA in the PCR reaction. **C.** Western blot of wt, *cnn1^{lox}*, *cnn2^{-/-}*, *tagAKAP-wt* and *tagAKAP-cnn1^{lox}* and *tagAKAP-cnn2^{-/-}* cytoplasmic extracts. *tagAKAP-wt*, *tagAKAP-cnn1^{lox}* and *tagAKAP-cnn2^{-/-}* cells contain a protein G-encoding tag in one *akap450* allele. α -tubulin serves as the loading control. **D.** Subcellular localisation of AKAP450 in DT40 cells visualised with anti-protein G antibody. Protein G only occasionally colocalises with interphase centrosomes in *tagAKAP-cnn1^{lox}* cells (yellow arrow), but the staining is much weaker than in wt and *cnn2^{-/-}* cells and is highly variable. DNA is blue, protein G (AKAP450) is red and γ -tubulin is green in merged images. Scale bars are 5 μ m.

5.2.8 CDK5RAP2 is critical for the centrosomal localisation of AKAP450

Importantly, while anti-protein G antibody stained the centrosomes in tagAKAP-wt mitotic cells, it failed to stain centrosomes in mitotic tagAKAP-cnn1^{lox} cells and tagAKAP-cnn2^{-/-} cells (Figure 5.2.8A). This is consistent with what I observed after depletion of CDK5RAP2 by siRNA in human cells. To confirm that AKAP450 was not localised to centrosomes in cnn1^{lox} and cnn2^{-/-} cells, I purified centrosomes from nocodazole-arrested DT40 cells (79.5% of wild-type and 80% of cnn1^{-/-} cells were in G2/M by flow cytometry – see plots in Figure 5.2.8B). PCM components could be affected by CNN1 deficiency (for example γ -tubulin), therefore I used the centrin-1 signal in fractions 3 and 4 for normalisation (Figure 5.2.8B). I found that the levels of AKAP450 were substantially reduced in purified CNN1-deficient centrosomes compared to wild-type centrosomes.

5.2.9 CDK5RAP2 is critical for the centrosomal localisation of p150^{glued}/dynactin

AKAP450 has been shown to interact with the p150^{glued} subunit of dynactin (Kim et al., 2007). Therefore, I wondered if the reduction in AKAP450 affected the amount of p150^{glued} present in purified mitotic CNN1-deficient centrosomes. I found that p150^{glued} was not detectable in purified CNN1-deficient centrosomes (Figure 5.2.8B). This suggested that the loss of p150^{glued} from centrosomes could be due to the reduction in AKAP450. However, it had not been shown if the interaction between AKAP450 and p150^{glued} was maintained in mitosis. Therefore, I immunoprecipitated p150^{glued} from nocodazole-arrested DT40 cell extracts. Immunoprecipitation of p150^{glued} coprecipitated AKAP450, indicating that the interaction is maintained in mitosis (Figure 5.2.9). CDK5RAP2 did not coprecipitate with p150^{glued} (Figure 5.2.9). These results raise the possibility that there are two subcomplexes in the PCM – one containing CDK5RAP2 and AKAP450 and the other containing AKAP450 and p150^{glued}.

When fused to GFP, the centrosomal targeting domain of AKAP450, PACT, is enriched in the centrosome of cnn1^{-/-} cells (Figure 5.2.3C). Thus, CDK5RAP2 is unlikely to anchor AKAP450 via the PACT domain.

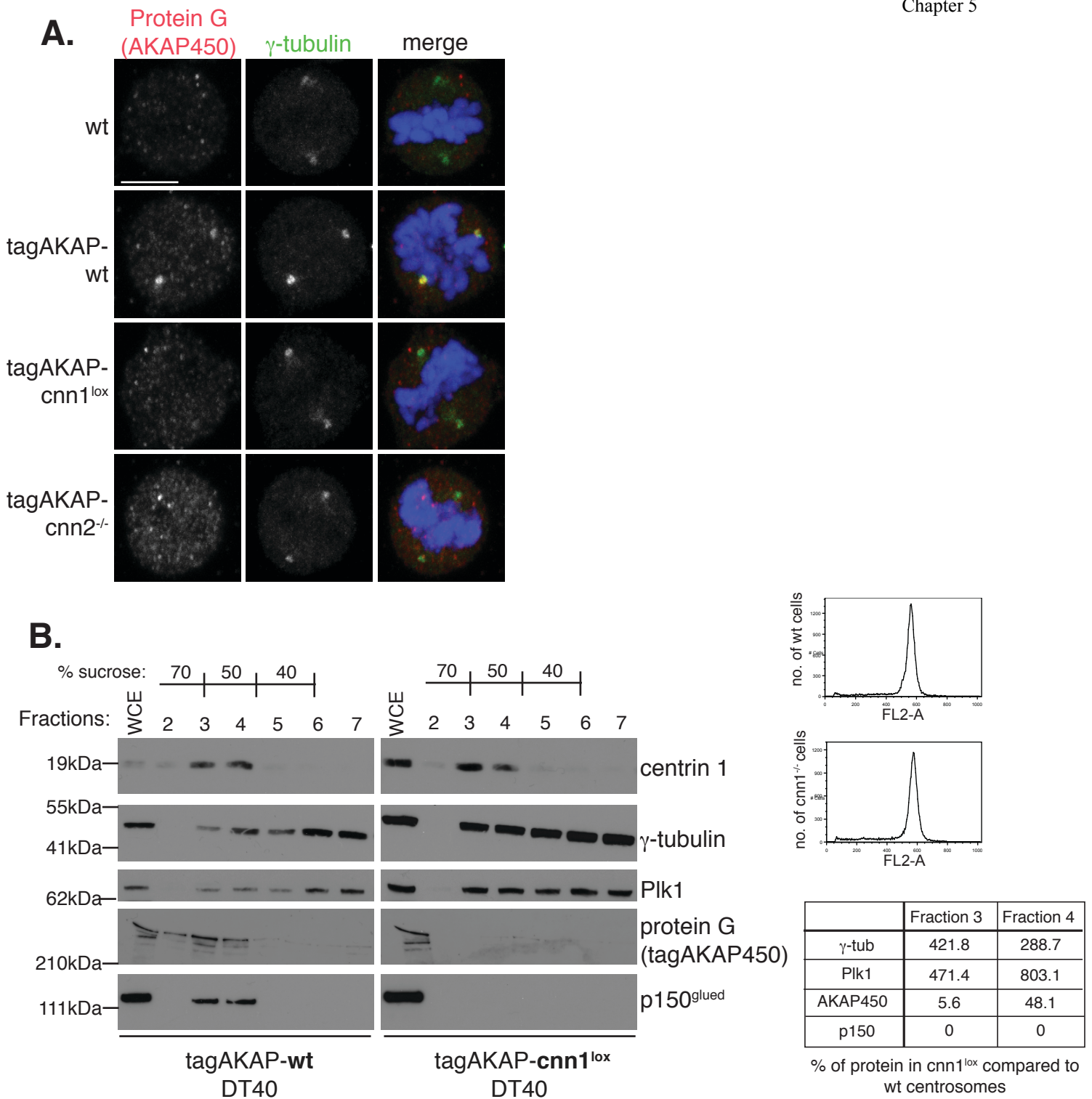


Figure 5.2.8 CDK5RAP2 is critical for the centrosomal localisation of AKAP450. **A.** Subcellular localisation of tagAKAP-wt, tagAKAP-cnn1^{lox} and tagAKAP-cnn2^{-/-} in mitotic DT40 cells. DNA is blue, protein G (AKAP450) is red and γ -tubulin is green in merged images. Scale bar is 5 μ m. **B.** Western blot showing protein fractions of centrosomes purified from nocodazole-arrested tagAKAP-wt (left) or tagAKAP-cnn1^{lox} (right) cells immunoblotted with antibodies against centrin-1 and various PCM components. Signal intensities in fractions 3 and 4 were normalised against the centrin signal in the same fraction. Table shows the percentage of each PCM component in tagAKAP-cnn1^{lox} centrosomal fractions compared to tagAKAP-wt fractions. Input represents 0.15% of Whole Cell Extract (WCE); 50% of final centrosome pellet was loaded in each fraction. Flow cytometry plots show efficiency of 12 hr nocodazole arrest.

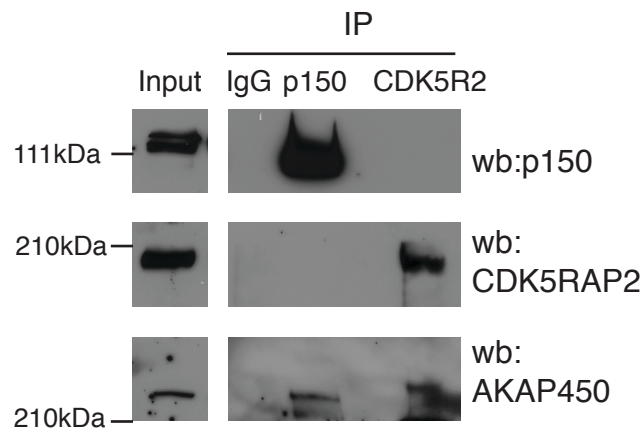


Figure 5.2.9 AKAP450 interacts with p150^{glued}/dynactin in mitosis. AKAP450 co-immunoprecipitates with p150^{glued} and CDK5RAP2 (CDK5R2) from nocodazole-arrested mitotic extracts of HeLa cells. A rabbit IgG mix was used as negative control. Input lane shows cytoplasmic extract prior to immunoprecipitation.

5.2.10 *cnn1*^{-/-} centrosomes contain reduced levels of γ -tubulin but are not deficient in microtubule nucleation

AKAP450 and CDK5RAP2 have been implicated in anchoring γ -tubulin complexes within the centrosome (Fong et al., 2008; Takahashi et al., 2002). Moreover, it has been reported that in human cells depleted of CDK5RAP2 by siRNA or shRNA, γ -tubulin is decreased in the mitotic centrosomes ((Fong et al., 2008; Haren et al., 2009b); Figure 4.2.1A, B). Fong *et al.* have mapped a γ -TuRC binding site in CDK5RAP2 to the CNN1 domain (Figure 5.1.1C). Therefore, I predicted that γ -tubulin recruitment would be perturbed in *cnn1*^{-/-} centrosomes. I could not detect any abnormalities in γ -tubulin localisation in interphase *cnn1*^{-/-} cells (Figures 5.1.3B, 5.2.7C and 5.3.1A). In G2 and mitosis, the mean fluorescent signal of γ -tubulin was similar between wild-type and mutant centrosomes (left graph in Figure 5.2.10A). However, the total volume of centrosomal γ -tubulin staining was slightly reduced in *cnn1*^{-/-} centrosomes (right graph in Figure 5.2.10A). This indicates that the CNN1 domain of CDK5RAP2 is required for the efficient concentration of γ -tubulin in the PCM.

γ -tubulin is a key factor in centrosomal microtubule nucleation (reviewed in (Raynaud-Messina and Merdes, 2007)). In addition, CDK5RAP2 has also been implicated in microtubule nucleation, at least in interphase cells (Fong et al., 2008). One way in which centrosome detachment might occur is if centrosomes were unable to nucleate sufficient microtubules, there would be fewer centrosomal microtubules to cross-link with the spindle microtubules. Therefore, I evaluated the microtubule nucleation ability of *cnn1*^{-/-} centrosomes in mitosis. Using centrin-3 to locate centrosomes and PHH3 staining to identify mitotic cells, I found that microtubule recovery from nocodazole-induced depolymerisation was indistinguishable between mitotic wild-type and *cnn1*^{-/-} centrosomes (Figure 5.2.10B). This indicates that *cnn1*^{-/-} centrosomes are not defective in microtubule nucleation. Furthermore, γ -tubulin was highly enriched in CNN1-deficient centrosomes purified from a mitotically-enriched cell population (Figure 5.2.8B). Perturbations in centrosomal γ -tubulin levels are therefore unlikely to explain the centrosome detachment phenotype.

If the microtubule-nucleation capacity is unperturbed in *cnn1*^{-/-} centrosomes, then perhaps centrosome detachment is due to a defect in microtubule anchoring. One could imagine that if the centrosome could not anchor the minus ends of spindle microtubules effectively then this could be one way that centrosomes detach. Therefore, I assayed the localisation

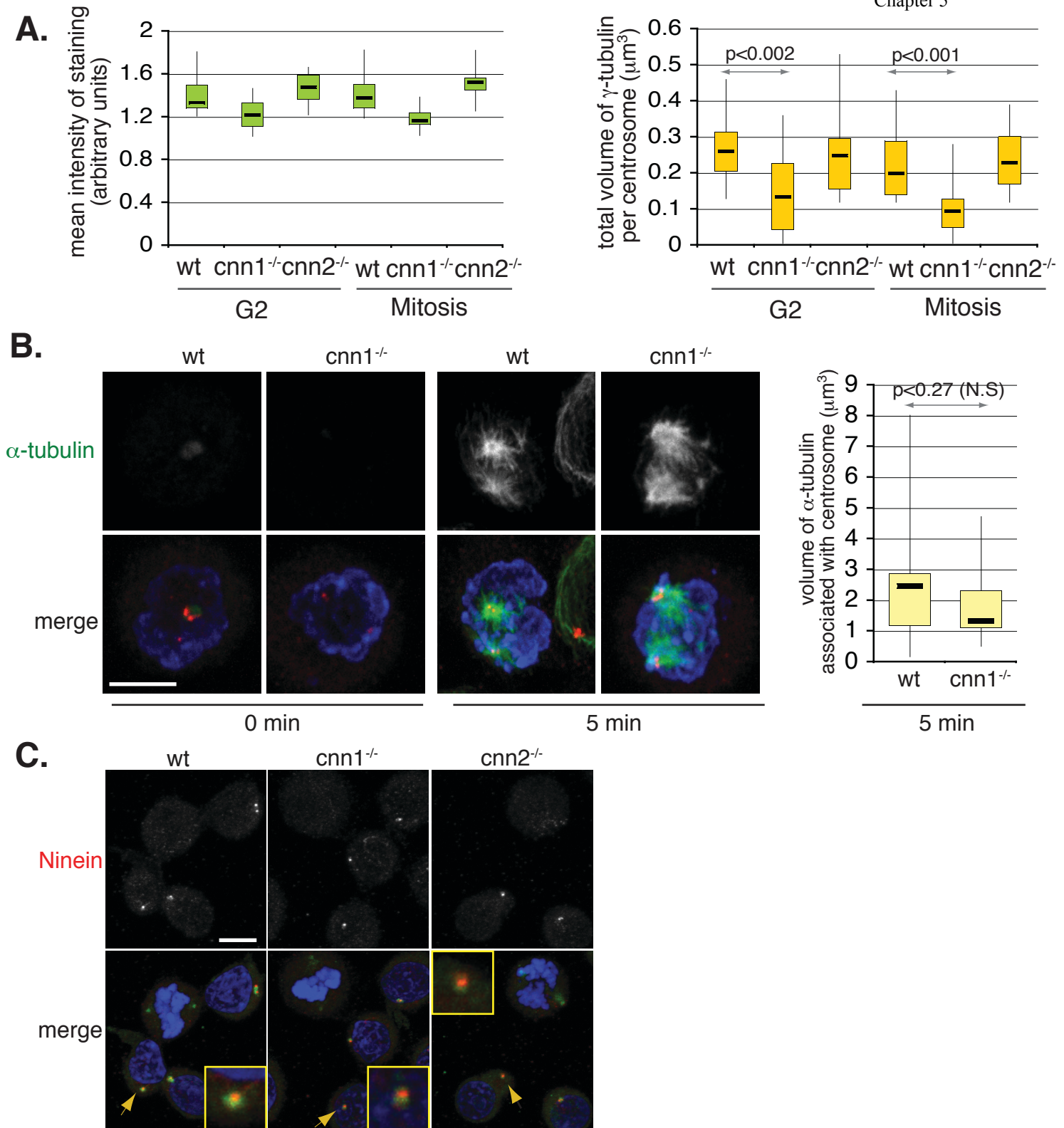


Figure 5.2.10 $cnn1^{-/-}$ centrosomes contain reduced levels of γ -tubulin but are not deficient in microtubule nucleation. **A.** Box plots show the distribution of the mean fluorescent intensity (left) or the total volume (right) of centrosomal γ -tubulin staining in G2 and mitotic cells. G2 cells were defined as cells that contain TACC3-positive centrosomes. 40 centrosomes were scored per cell line. **B.** $cnn1^{-/-}$ centrosomes regrow microtubules with similar efficiency to wt centrosomes after depolymerisation with 2 $\mu\text{g}/\text{ml}$ nocodazole treatment. Representative images are shown of cells at 0 and 5 minutes following nocodazole washout. Anti-PHH3 antibody was used to identify mitotic cells. PHH3 is blue, centrin-3 is red and α -tubulin is green in merged images. Box plots show distribution of total volume of α -tubulin staining associated with each centrosome in mitotic cells. 20 centrosomes were scored. **C.** Subcellular localisation of ninein in wt and $cnn1^{-/-}$ DT40 cells. As expected, ninein is present only in interphase centrosomes (Chen *et al.*, 2003). DNA is blue, ninein is red and γ -tubulin is green in merged images. Insets correspond to higher magnifications of centrosomes marked by arrowheads. Scale bars are 5 μm . p-values were calculated by two-tailed unpaired student's t-test.

of ninein, a centrosomal protein required for microtubule anchoring and nucleation during interphase (Delgehyr et al., 2005). There is controversy in the literature as to whether ninein localises to mitotic centrosomes or not (Bouckson-Castaing et al., 1996; Chen et al., 2003). Immunostaining of DT40 cells with ninein antibody showed that in DT40, ninein is not at the centrosome in mitosis (Figure 5.2.10C). However, in interphase I found that ninein was unperturbed in *cnn1*^{-/-} centrosomes (Figure 5.2.10C).

5.2.11 The CNN1 domain of CDK5RAP2 is dispensable for centrosome maturation

In *Drosophila* somatic cells, Cnn and Polo are essential for centrosome maturation and the two proteins are co-dependent for their centrosomal localisation (Dobbelaere et al., 2008). The orthologue of Polo in vertebrates is Polo-like kinase 1 (Plk1) and this is also required for centrosome maturation (Lane and Nigg, 1996). Plk1 has been implicated in the recruitment of CDK5RAP2 to centrosomes in human cells (Haren et al., 2009b). However, whether CDK5RAP2 can affect Plk1 localisation is not known.

To see if the disruption of the CNN1 domain of CDK5RAP2 affected Plk1 localisation, I immunostained DT40 cells with an antibody against Plk1. This immunostaining failed to reveal a difference between wild-type and *cnn1*^{-/-} cells (Figure 5.2.11A). Moreover, Plk-1 was enriched in mitotic centrosomes purified from *cnn1*^{-/-} cells (Figure 5.2.8B). Aurora A is another centrosomal protein kinase that is implicated in centrosome maturation and separation (reviewed in (Barr and Gergely, 2007), see appendix). Aurora A kinase autophosphorylates its T288 residue and this phosphorylation event is required for maximal activity of Aurora A (Barr and Gergely, 2007). I found that an antibody recognising phosphoT288 Aurora A colocalised with *cnn1*^{-/-} centrosomes (Figure 5.2.1D) and that the levels appeared similar between wild-type and *cnn1*^{-/-} cells. These results indicate that the role of the CNN1 domain in centrosome-to-spindle pole attachment is independent of centrosome maturation.

In *Drosophila* embryos, the CNN1 domain of Cnn is required for the recruitment of D-TACC and its binding partner, Msps (Mini-spindles) to the centrosome in mitosis (Zhang and Megraw, 2007). I found that TACC3 staining often appeared disorganised between partially detached centrosomes and spindle poles (Figure 5.2.1B). TACC proteins concentrate at spindle regions rich in microtubule minus ends (Barros et al., 2005; Cullen

and Ohkura, 2001; Gergely et al., 2000a). Also, since microtubule release from centrosomes increases in mitosis (Belmont et al., 1990), this pattern of TACC3 staining in *cnn1*^{-/-} cells is likely to reflect the presence of microtubule minus ends between the centrosome and the spindle pole, rather than a failure to recruit TACC3 to the centrosome. The TACC3-binding partner and Msp1 homologue, ch-Tog, is also recruited normally to *cnn1*^{-/-} centrosomes (Figure 5.2.11B). Therefore, in contrast to *Drosophila*, the CNN1 domain is dispensable for the centrosomal targeting of TACC3 and ch-Tog in vertebrates.

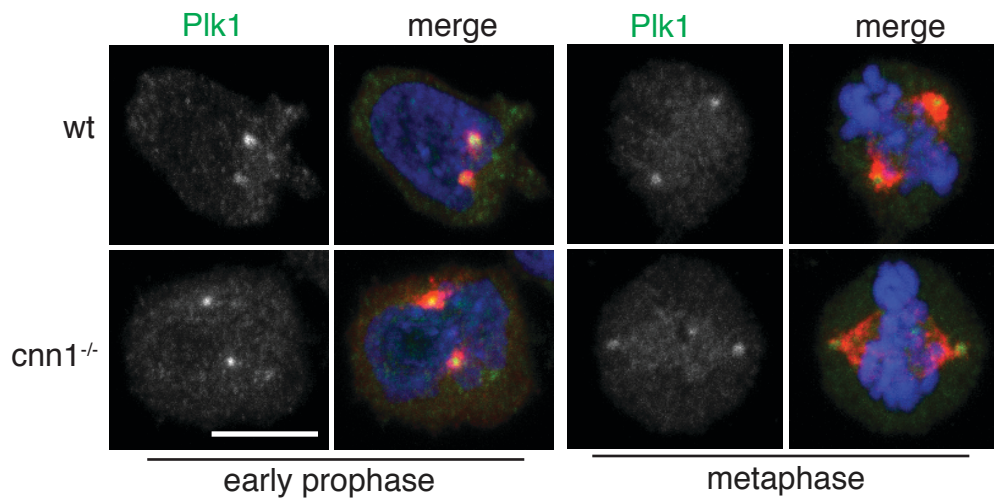
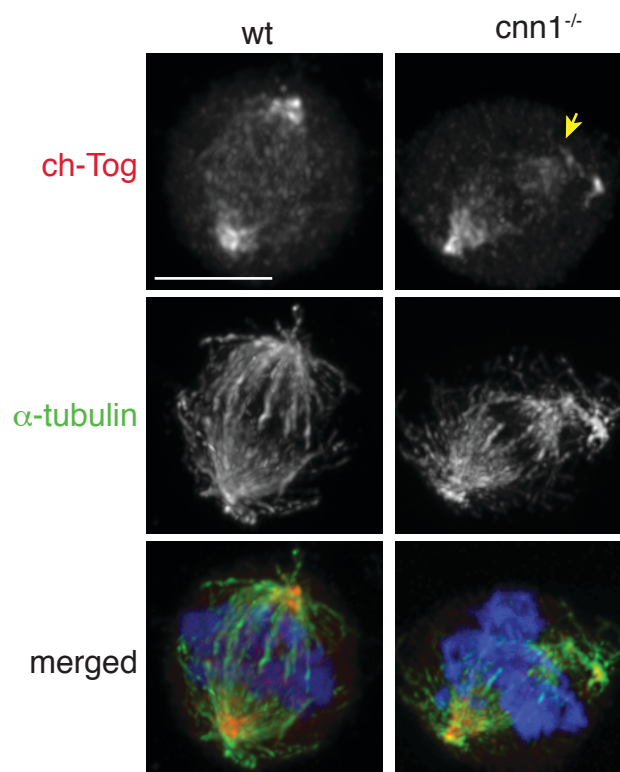
A.**B.**

Figure 5.2.11 The CNN1 domain of CDK5RAP2 is dispensable for centrosome maturation.

A. Subcellular localisation of Plk1 in prophase and prometaphase/metaphase *wt* and *cnn1^{-/-}* cells. DNA is blue, Plk1 is green and TACC3 is red in merged images. **B.** Subcellular localisation of ch-Tog. Ch-TOG accumulates at the spindle poles and on spindle microtubules in *wt* cells. In the *cnn1^{-/-}* cell shown, ch-Tog localises asymmetrically to the two halves of the spindle. Ch-Tog fails to accumulate on the spindle pole (yellow arrow) with a detached centrosome. DNA is blue, ch-Tog is red and α -tubulin is green in merged image. Scale bars are 5 μ m.

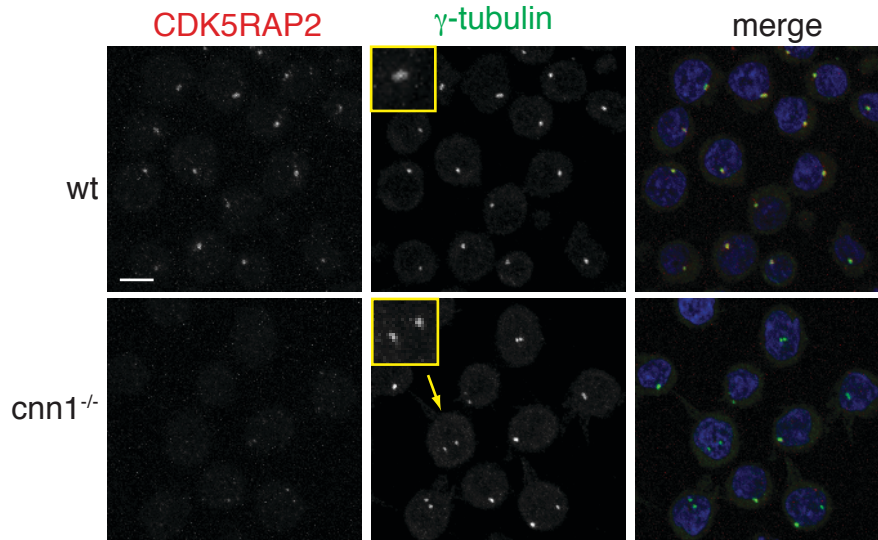
5.3 The CNN1, but not the CNN2, domain in CDK5RAP2 is required for centrosome cohesion

5.3.1 *cnn1*^{-/-}, but not *cnn2*^{-/-}, DT40 cells have defects in centrosome cohesion

CDK5RAP2 has been implicated in maintaining centrosome cohesion in human cells ((Graser et al., 2007a); Figure 3.2.2). Therefore I analysed centrosome splitting in wild-type, *cnn1*^{-/-} and *cnn2*^{-/-} DT40 cells. Using γ -tubulin as a marker, I found that split centrosomes were more frequent in *cnn1*^{-/-} than in wild-type or *cnn2*^{-/-} cells (Figure 5.3.1A, B). This could be due to either a delay in G2 or loss of cohesion between disengaged centrioles. Therefore, I co-stained cells with anti- γ -tubulin and anti-TACC3 antibodies. Like its human counterpart, the chicken TACC3 antibody associates with G2 centrosomes (Figure 5.2.11A)(Gergely et al., 2003; Gergely et al., 2000a). I found no evidence for a G2 delay in *cnn1*^{-/-} cells, but when scoring TACC3-negative cells (i.e. cells in G1 or S), I observed an increase in split centrosomes (Figure 5.3.1B). Therefore, this phenotype is similar to what I see in human cells depleted of CDK5RAP2 by siRNA or shRNA. The extent of centrosome splitting was less prominent in DT40 than in HeLa cells, representing a 2.5-fold instead of a 3.5-fold increase over background, but the small cytoplasmic volume of DT40 cells may limit the distances split centrosomes can travel.

I found that depletion of AKAP450 in human cells by siRNA also caused an increase in centrosome splitting (Figure 4.1.5). Interestingly, centrosome splitting in *cnn1*^{-/-} cells correlates with a perturbation in AKAP450 to centrosomes in interphase (Figure 5.2.7D). This provides further evidence that CDK5RAP2 and AKAP450 may be involved in the same pathway of mediating centrosome cohesion.

A.



B.

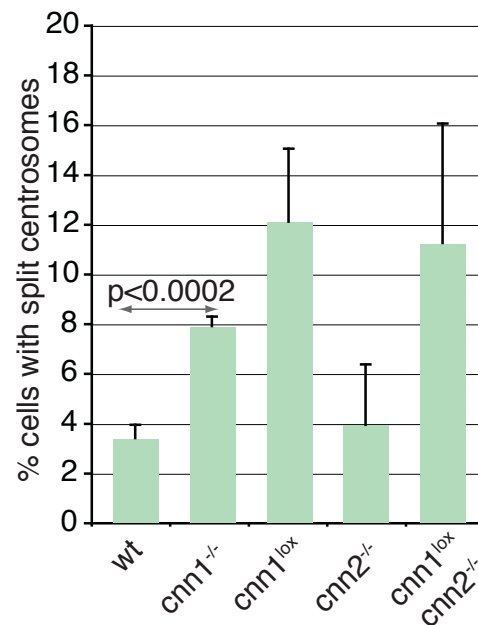


Figure 5.3.1 *cnn1*^{-/-}, but not *cnn2*^{-/-}, DT40 cells have defects in centrosome cohesion. **A.** Immunofluorescence images of wt and *cnn1*^{-/-} DT40 cells showing an increased frequency of centrosome splitting in *cnn1*^{-/-} cells. Insets represent close-ups of normal (wt) and split (*cnn1*^{-/-}) centrosomes. DNA is blue, CDK5RAP2 is red and γ -tubulin is green in merged images. Scale bar is 5 μ m. **B.** Graph shows quantification of centrosome splitting in wt and mutant cells (n=4, 150 cells per experiment, error bars represent STD). p-values were calculated by two-tailed unpaired Student's t-test.

5.4 Discussion

5.4.1 CDK5RAP2 is a critical regulator of centrosome to spindle pole attachment

My results suggest that CDK5RAP2 enables the centrosome to remain connected to spindle poles in the presence of microtubule-based forces such as the tension generated by kinetochore capture and bi-orientation of the mitotic spindle. I have shown that centrosome detachment in *cnn1*^{-/-} cells is not due to a reduction in nucleation capacity of the centrosome, mislocalisation of spindle pole focussing activities, abnormal microtubule dynamics or a defect in centrosome maturation. However, I believe that centrosomes detach due to the failure in AKAP450 recruitment to the centrosome in mitosis.

Loss of AKAP450 from mitotic centrosomes correlates with centrosome detachment defects in *cnn1*^{lox} and *cnn2*^{-/-} cells (Figure 5.2.8A). Since AKAP450 interacts with the dynactin subunit, p150^{glued}, ((Kim et al., 2007) and Figure 5.2.9), dynactin is required for the centrosomal accumulation of dynein (Quintyne and Schroer, 2002) and the NuMA/dynein/dynactin protein complex is required for centrosome to spindle pole attachment (Goshima and Vale, 2003; Haren et al., 2009a; Maiato et al., 2004b; Merdes et al., 1996; Morales-Mulia and Scholey, 2005; Silk et al., 2009), AKAP450 could connect centrosomes with spindle poles by acting as a PCM-resident receptor for spindle pole associated dynactin molecules. The absence of p150^{glued} from *cnn1*^{lox} centrosomes clearly favours this possibility (Figure 5.2.8B). Similar to their role on the Golgi (Kim et al., 2007; Rivero et al., 2009), the dynactin/AKAP450 complex could also contribute to microtubule anchoring in the mitotic PCM. While both the CNN1 and CNN2 domains are required for the mitotic recruitment of AKAP450, the weaker centrosome detachment phenotype of *cnn2*^{-/-} cells indicates that an intact CNN1 domain can partially aid centrosome attachment even when AKAP450 is absent. Intriguingly, the depletion of the centrosomal protein *cep72* has been shown to delocalise centrosomal AKAP450 during mitosis, leading to centrosome detachment from spindle poles (Oshimori et al., 2009).

Cells with detached centrosomes take longer to initiate anaphase (Figure 5.2.3). In fact, all three cells with detached centrosomes that were followed by time-lapse imaging failed to complete mitosis. While it is possible that some defects in these cells were exacerbated by laser damage induced by the extended period of time in mitosis, detached centrosomes do appear to lead to a delay in entering anaphase. Fixed cell analysis of BubR1

immunostaining showed a positive correlation between the severity of the centrosome detachment phenotype and BubR1 reactivity at kinetochores. In part, this may be due to chromosomes becoming associated with centrosomal microtubule asters that are not associated with the mitotic spindle (orange arrow, Figure 5.2.3D). However, the majority of chromosomes still align on the metaphase plate. Therefore it seems that once centrosomes do detach, they no longer play a role in spindle assembly. The reason for the delay in anaphase initiation could be that when centrosomes detach there may be fewer spindle microtubules and thus a reduced number of stable kinetochore-microtubule attachments, as has been shown for centrosome detachment after centrobilin depletion in human cells (Jeffery et al., 2010).

Disruption of the CNN1 and CNN2 domains in CDK5RAP2 in DT40 has many of the same phenotypes as conditional deletion of exon 22 of *Numa* in mouse (Silk et al., 2009). Live imaging of Δ exon22 mouse embryonic fibroblasts revealed that after NEBD, cells initially form a focussed bipolar spindle. However, after bipolar spindle formation, centrosomes detached from the spindle pole and spindle poles subsequently become unfocussed. This indicates that NuMA is required for centrosome to spindle pole attachment. The major difference between my data and the NuMA data is that in *cnn1*^{-/-} and *cnn2*^{-/-} DT40 cells, spindle poles remain focussed, whereas after gene-disruption of NuMA, they do not. This difference is because in *cnn1*^{-/-} DT40 cells, NuMA still localises to the spindle pole and therefore still coalesces the minus ends of microtubules into a focussed pole. Therefore, while gene disruption of NuMA and CDK5RAP2 appear to lead to similar phenotypes, their roles in centrosome to spindle pole attachment may be different.

Although spindles can form by centrosome-independent pathways, when centrosomes are present they act as the dominant sites in spindle assembly (Heald et al., 1997). What my data suggest is that, while centrosomes may be dominant in the initial stages of building a bipolar spindle, they are no longer dominant once a bipolar spindle is formed.

5.4.2 The CNN1, but not the CNN2, domain is required for centrosome cohesion

From my work in HeLa cells and from work published by others (Graser et al., 2007a), CDK5RAP2 was already known to play a role in mediating centrosome cohesion. However, by using targeted gene disruption in DT40, I now know that loss of centrosome

cohesion is specific to the disruption of the CNN1 domain, since *cnn2*^{-/-} cells behaved the same as wild-type (Figure 5.3.1).

My results reveal an inverse correlation between interphase centrosomal levels of AKAP450 and centrosome cohesion in *cnn1*^{lox} and *cnn2*^{-/-} cells (Figures 5.2.7D and 5.3.1B). Again, this supports the data I obtained about the interplay between CDK5RAP2 and AKAP450 in centrosome cohesion in human cells (Figure 4.1.5). However, in human cells I saw no effect on the interphase localisation of AKAP450 when CDK5RAP2 was depleted. The DT40 data show that CDK5RAP2 does regulate AKAP450 localisation in interphase and that this requires the CNN1 domain of CDK5RAP2. The reason I was unable to see this in human cells is likely to be due to the incomplete depletion of CDK5RAP2.

How the truncated Δ CNN2 product maintains centrosome cohesion and recruits AKAP450 to interphase centrosomes is an interesting question, since the Δ CNN2 protein product seems to be absent from interphase centrosomes (Figure 5.1.3B). Thus, these functions may require only small amounts (i.e. below the detection level) of Δ CNN2. Alternatively, it may be during mitosis when the CNN1 domain of CDK5RAP2 establishes centrosome cohesion and primes the centrosome for subsequent AKAP450 recruitment. The linker proteins are either absent (*cep68* and *rootletin*) or largely reduced (*c-Nap1*) in mitosis, anaphase and telophase (Bahe et al., 2005; Fry et al., 1998a; Graser et al., 2007a). Thus, the inter-centriolar linker is not present at the right time to maintain centrosome cohesion after centriole disengagement. CDK5RAP2 may be required to maintain centrosome cohesion immediately after centriole disengagement. This would ensure the centrioles remain paired and maintain cohesion during the subsequent interphase and extensive microtubule reorganisation after mitosis. Both Δ CNN1 and Δ CNN2 proteins are present in mitotic centrosomes. My data suggests that while the Δ CNN2 protein product is sufficient to maintain cohesion after centriole disengagement, the Δ CNN1 product is not. Δ CNN2 may establish centrosome cohesion at the end of mitosis and thus recruit AKAP450 to the centrosome, which is maintained there even after Δ CNN2 is lost from the centrosome in interphase. In the case of Δ CNN1 CDK5RAP2 DT40 cells, centrosome cohesion cannot be established and AKAP450 is not recruited.

5.4.3 GS-TAP tagging as a way to identify interacting partners of CDK5RAP2 and AKAP450

In this chapter, I have used the GS-TAP tagging approach as a label to visualise the localisation of endogenous CDK5RAP2 and AKAP450 in DT40. However, the GS-TAP tag was originally designed as a protein purification tag (Burckstummer et al., 2006). Therefore, I can now use these cell lines to tag the remaining allele of CDK5RAP2 and the remaining two alleles of AKAP450. These cell lines can then be used for purification of the TAP-tagged proteins to identify potential novel interacting partners. The GS-TAP purification has advantages over other immunoprecipitation methods for identifying interacting proteins as it relies on tandem purification (Burckstummer et al., 2006) and thus should reduce the number of non-specific binding partners.

DT40 cells are particularly useful for biochemical approaches, such as protein complex identification. Not only is it straightforward to tag the endogenous protein (and thus eliminate any false positive interactions generated by the overexpression of large, coiled-coil containing centrosomal proteins), but DT40 cells also grow quickly (doubling time of 8-10 hours), and, because they are a suspension cell line, they are easy to grow in large volumes. Also, since the chicken genome is publicly available, novel proteins can be identified easily. What would be a particularly powerful experiment to conduct would be to use SILAC (stable isotope labelling with amino acids in cell culture) techniques as a quantitative method to analyse the differential binding partners of the wt-tap and *cnn1*^{lox}-tap tagged CDK5RAP2 cell lines. This would be an excellent way to identify if there are other molecular players, apart from AKAP450, that are involved in centrosome to spindle pole attachment, or in centrosome cohesion.

Chapter 6

CDK5RAP2 is required for an efficient DNA damage response

The centrosome is known to play a role in the DNA damage response, in particular in maintaining an efficient G2 checkpoint (see Section 1.3.5). The DNA damage response has also been implicated in microcephaly, since the microcephaly protein – microcephalin, is required for efficient arrest after DNA damage and is involved in DNA repair (see Section 1.4.2.2). Therefore, I wanted to investigate if CDK5RAP2 also had a function in the DNA damage response.

In this chapter, using the CDK5RAP2 *cnn1*^{-/-} and *cnn2*^{-/-} DT40 cells described in Chapter 5, I have uncovered a role for CDK5RAP2 in maintaining an efficient G2 arrest after DNA damage. The CNN1 domain is essential for this function while the CNN2 domain is dispensable.

6.1 The CNN1 domain is required for an efficient G2 arrest after DNA damage

6.1.1 The CNN1 domain is essential for normal proliferation and clonogenic potential

I noticed while trying to obtain a homozygous $cnn1^{-/-}$ cell line that the gene-targeting efficiency was lower than expected (1 in 140). I reasoned that the low gene-targeting efficiency might be due to the homozygous disruption of the CNN1 domain affecting the growth of DT40 cells. Therefore I tested the capacity of individual cells to give rise to clones (i.e. clonogenic potential) by seeding single cells into 96-well plates and recording the percentage of cells that produced visible clones after 7 or 10 days (Figure 6.1.1). $cnn1^{-/-}$, $cre-cnn1^{-/-}$, $cnn1^{lox}$ and $cnn1^{lox}cnn2^{-/-}$ cell lines displayed reduced clonogenic potential. In contrast, wild-type, cre -wild-type and $cnn2^{-/-}$ cells had similar clonogenic potential. Moreover, the colonies that did form in $cnn1^{-/-}$, $cnn1^{lox}$, $cnn1^{lox}cnn2^{-/-}$ and $cre-cnn1^{-/-}$ cell lines were much smaller than those in wild-type and $cnn2^{-/-}$ cells. Reduction in clone formation reflected a genuine growth defect and was not due to impairment in cell-to-cell attachment, since I did not detect floating cells in the wells.

To try and determine why cells lacking the CNN1 domain of CDK5RAP2 had reduced clonogenic potential, I used time-lapse DIC (differential interference contrast) microscopy to film DT40 cells (see Movies 6.1-6.3 on Supplementary CD). Over a 26 hour period, I observed fewer cell divisions in $cnn1^{-/-}$ cells (42% of wild-type and 17% of $cnn1^{-/-}$ cells divided twice in 26 hours (92 wild-type and 77 $cnn1^{-/-}$ cells observed)). In addition, $cnn1^{-/-}$ cells were more prone to cell death: within 26 hours 11% of $cnn1^{-/-}$ cells died compared to only 1% in wild-type cells (9 out of 77 $cnn1^{-/-}$ cells and 1 out of 92 wild-type cells). Due to the centrosome detachment phenotype observed in $cnn1^{-/-}$ cells I wondered if the reduction in clonogenic potential was due to mitotic death. However, I only observed mitotic death in 2 out of 9 $cnn1^{-/-}$ cells. The majority of $cnn1^{-/-}$ cells died in interphase (7 out of 9 cells). This indicated that an increased rate of spontaneous cell death is likely to account for the lower proliferation potential.

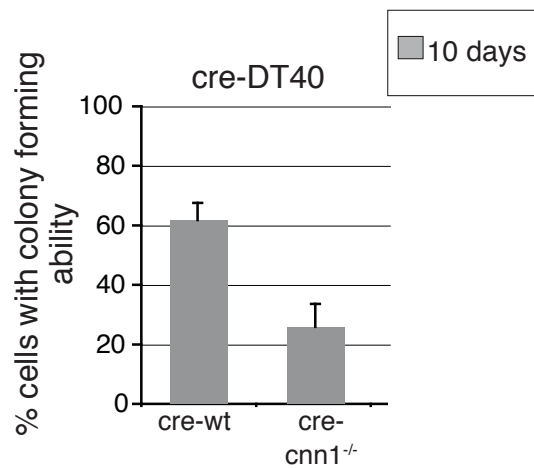
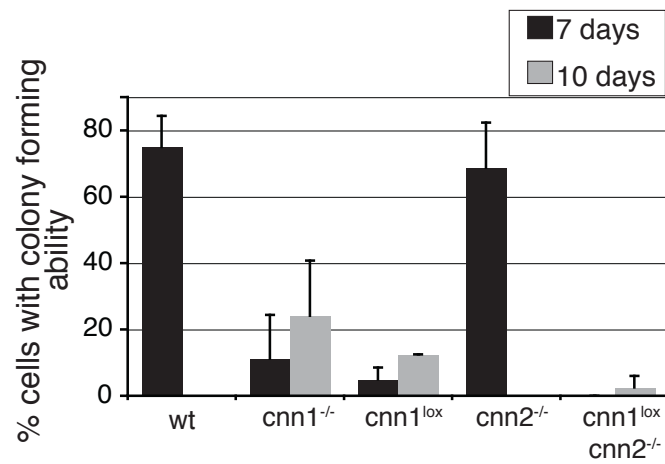


Figure 6.1.1 The CNN1 domain is essential for normal clonogenic potential. Graph shows percentage of cells that form a colony 7 or 10 days after plating. n=4, 40 cells per experiment. Error bars represent STD.

6.1.2 The CNN1 domain is required for effective DNA damage-induced G2 arrest

Both *cnn1*^{-/-} and *cnn2*^{-/-} cells display abnormal centrosome to spindle pole attachments but only *cnn1*^{-/-} cells are growth-impaired. Thus, the mitotic phenotype cannot be the sole reason for this impairment. Growth impairment is correlated with the defect in centrosome cohesion - that is it is present in *cnn1*^{-/-}, *cnn1*^{lox} and *cnn1*^{lox}*cnn2*^{-/-} and not in wild-type and *cnn2*^{-/-} cells. However, I did not observe a growth defect in CDK5RAP2-depleted HeLa cells with impaired centrosome cohesion. Also, it is difficult to imagine how a loss of centrosome cohesion could cause proliferation defects. Therefore, I favour the following explanation.

A decrease in proliferation rate in DT40 cells has been observed after gene-disruption of cell cycle checkpoint genes such as *chk1* (Zachos et al., 2003) and ATM (Takao et al., 1999). Moreover, Chk1 has been shown to accumulate at centrosomes and regulate mitotic entry, both in unperturbed cell cycles and after DNA damage (Kramer et al., 2004; Liu et al., 2000; Tibelius et al., 2009; Zachos et al., 2003) and see Section 1.3.5). One centrosomal protein mutated in microcephaly, microcephalin, is known to play a role in the DNA damage response (see Section 1.4.2.2). For these reasons, I wondered if CDK5RAP2 played a role in the centrosomal response to DNA damage.

To address this question, I irradiated asynchronous DT40 cells using a ¹³⁷Caesium gamma-irradiator. Ionising Radiation (IR) induces double-strand break formation in DNA and leads to the activation of ATM and ATR kinases. The irradiation dose of 20 Gy causes extensive DNA damage in DT40 cells, but, since these cells are deficient for p53, they cycle through S phase and accumulate in G2 phase in a Chk1 kinase-dependent manner (Takao et al., 1999; Zachos et al., 2003). Following irradiation, cells were incubated in nocodazole for 10 hours to trap cells that entered mitosis after DNA damage. Therefore, the mitotic index of these cells is in inverse relation with their ability to arrest in G2. Consistent with a tight cell cycle arrest, mitotic indices of wild-type and *cnn2*^{-/-} cells did not increase following irradiation (Figure 6.1.2A). In contrast, an increase in the mitotic index was detected in *cnn1*^{-/-} and *cnn1*^{lox}*cnn2*^{-/-} cells, indicative of an impaired G2 checkpoint (Figure 6.1.2A). These data imply that the CNN1 domain of CDK5RAP2 is required for a robust G2 arrest after IR.

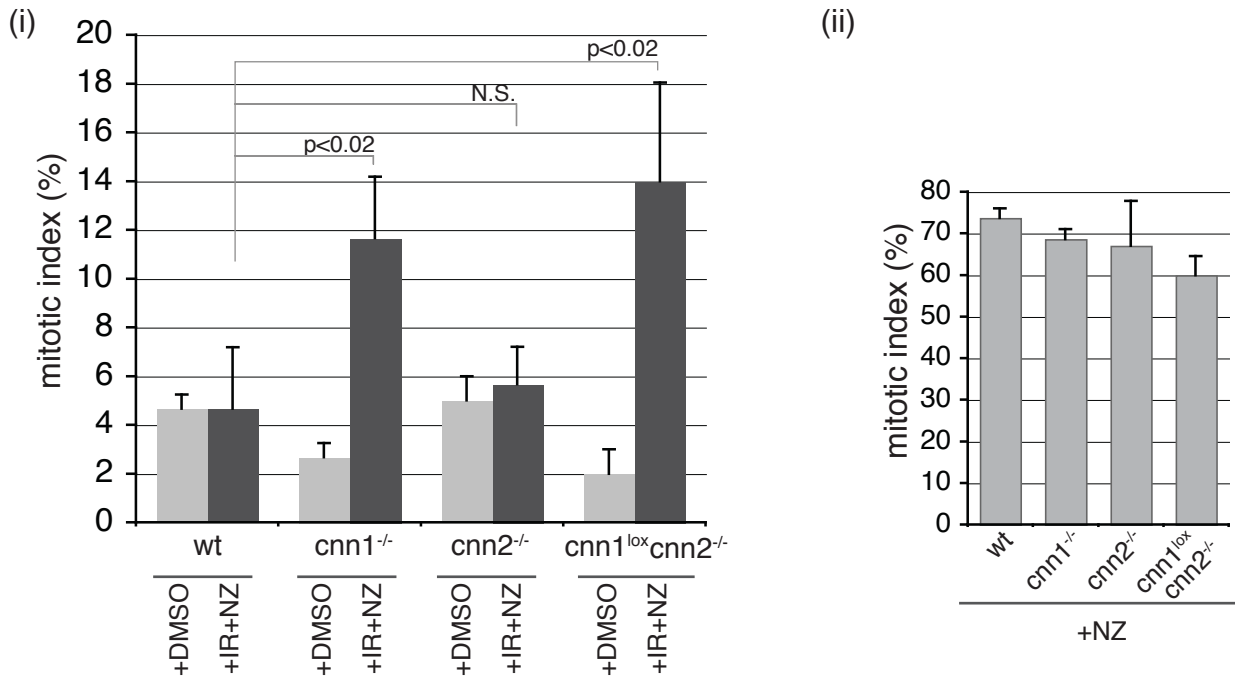
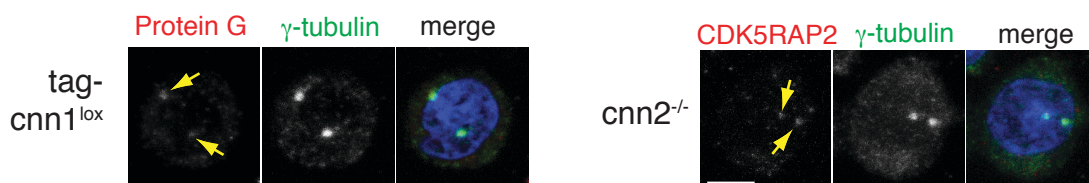
A.**B.**

Figure 6.1.2 The CNN1 domain is required for effective DNA damage-induced G2 arrest. **A.** Graph showing results of irradiation experiment. Mitotic index was determined for wt and gene-disrupted DT40 cells that were incubated in DMSO for 10 hours (+DMSO) or first irradiated with 20 Gy and then incubated in nocodazole for 10 hours (+IR +NZ; graph i) or incubated in nocodazole for 10 hours without irradiation (+NZ; graph ii). $n=3$, minimum of 3000 cells was scored per condition per experiment for each genotype. p -values were calculated by two-tailed unpaired Student's t -test.

B. Immunofluorescence images of $cnn1^{lox}$ and $cnn2^{-/-}$ DT40 cells. Yellow arrows indicate tag- Δ CNN1 and Δ CNN2 protein at the centrosomes. DNA is blue, proteinG/CDK5RAP2 is red and γ -tubulin is green in merged images. Scale bars are 5 μ m.

One reason for an impaired G2 arrest in *cnn1*^{-/-} and not *cnn2*^{-/-} cells could be that Δ CNN2 is present at centrosomes during G2 while tag- Δ CNN1 is not. In Chapter 5, I showed that neither tag- Δ CNN1 nor Δ CNN2 protein products localised to centrosomes in interphase (Figure 5.1.3B). However, I did not closely analyse G2 cells. Therefore, I re-examined the localisation of tag- Δ CNN1 and Δ CNN2 during G2. I found that both protein products were present on separated centrosomes prior to NEBD (Figure 6.1.2B). This suggested that both Δ CNN1 and Δ CNN2 proteins are present in the centrosome at the right cell cycle stage to mediate arrest in G2, yet only cells lacking the CNN1 domain have a defect in arresting after IR. Therefore, CDK5RAP2, and in particular the CNN1 domain, is required for efficient G2 arrest after DNA damage.

The mitotic index of both *cnn1*^{-/-} and *cnn1*^{lox}*cnn2*^{-/-} DMSO treated cells is lower than in the wild-type and *cnn2*^{-/-} cell lines. This may be due to the fact that in *cnn1*^{-/-} cells there is a higher rate of cell death in interphase (9% in *cnn1*^{-/-} vs 1% in wild-type cells; see Section 6.1.1). Since the analysis software may include a small proportion of these dead cells in the total cell count (and these would not score positive for PHH3), the proportion of PHH3 positive cells in the population could in fact be greater than my analysis suggests. This could also mean that the defect in G2 arrest observed after IR in these cells may actually be a slight underestimate.

6.1.3 The CNN1 domain is required for the centrosomal accumulation of Chk1

As mentioned before, centrosomal accumulation of Chk1 kinase prevents premature mitotic entry not only in the presence of DNA damage but also during unperturbed cell cycles (Kramer et al., 2004; Tibelius et al., 2009). In addition, in B-cells derived from microcephaly patients carrying mutations in the *microcephalin* gene, Chk1 is reduced in the centrosome (Tibelius et al., 2009). Therefore, I asked if levels of centrosomal Chk1 were affected in *cnn1*^{-/-} DT40 cells.

First, I tried to analyse Chk1 centrosomal levels by immunostaining. As expected, I did not observe Chk1 in mitotic centrosomes (Kramer et al., 2004). In interphase DT40 cells, I found that anti-Chk1 antibody gave a very weak and variable staining which I was unable to use for quantification. Therefore, I decided to analyse Chk1 centrosomal levels biochemically. I found that centrosomes purified from *cnn1*^{-/-} cells contained less Chk1

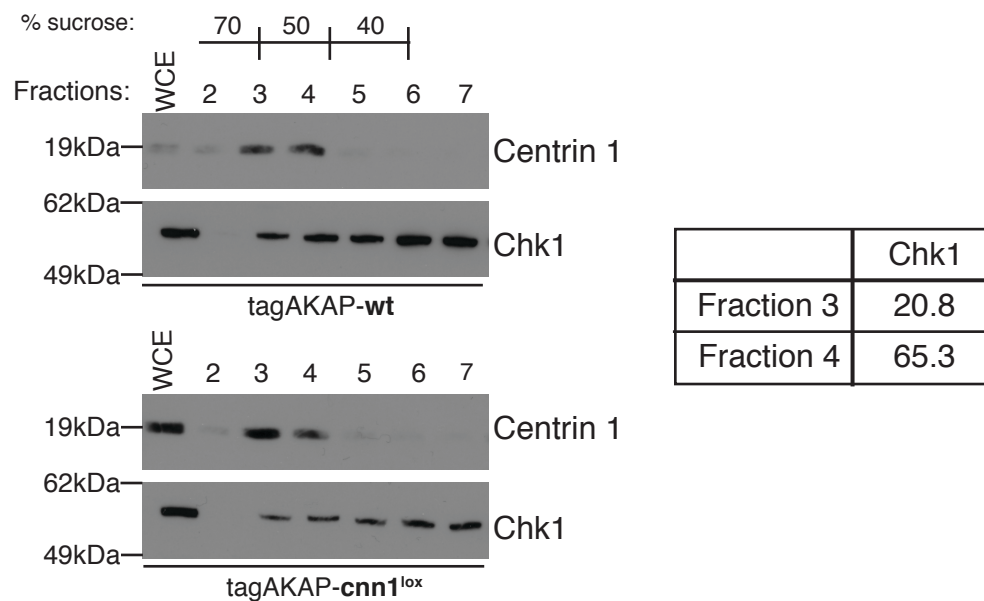


Figure 6.1.3 The CNN1 domain is required for the centrosomal accumulation of Chk1. Western blot showing that levels of Chk1 protein are reduced in CNN1-deficient centrosomes. Protein fractions containing centrosomes purified from tagAKAP-wt or tagAKAP-cnn1^{lox} cells (same purification as in Figure 5.2.8B) were immunoblotted with antibodies against centrin-1 and Chk1. Signal intensities of Chk1 in fractions 3 and 4 were normalised against the centrin signal in the same fraction. Table on right shows the percentage of Chk1 in tagAKAP-cnn1^{lox} compared to tagAKAP-wt centrosomal fractions.

than those purified from wild-type cells (Figure 6.1.3). These centrosomes were isolated from a nocodazole-arrested population (same experiment as in Figure 5.2.8B) in which 79.5% of wild-type and 80% of *cnn1*^{-/-} cells were in G2/M based on flow cytometry. Thus, at least 20% of purified centrosomes originate from cells in G1 or S phase. Since I cannot detect Chk1 in mitotic centrosomes, it is likely that the signal in purified centrosomes in Figure 6.1.3 is mostly contributed by interphase centrosomes.

In summary, the CNN1 domain of CDK5RAP2 is required for the efficient localisation of Chk1 to the centrosome.

6.1.4 The CNN1 domain is involved in centrosome amplification in response to aphidicolin but not to hydroxyurea

In response to IR and the subsequent G2 arrest, DT40 cells amplify their centrosomes ((Dodson et al., 2004) and see Section 1.3.5). DT40 cells also amplify their centrosomes after a prolonged (>12 hour) incubation with DNA replication fork-stalling agents such as aphidicolin or hydroxyurea (HU) (Dodson et al., 2004). Aphidicolin inhibits DNA polymerase α and thus inhibits DNA synthesis (Huberman, 1981). HU, on the otherhand, is an inhibitor of ribonucleotide reductase, an enzyme required to generate the precursors to dNTPs (Elford, 1968). Therefore, HU inhibits DNA replication fork progression by starving them of dNTPs. During shorter periods of incubation with aphidicolin or HU, DT40 cells arrest in S phase but prolonged incubation with these agents causes slippage out of the S phase arrest in DT40. Therefore, centrosome amplification during long incubation times in aphidicolin and HU may be occurring in G2 (Dodson et al., 2004). Importantly, centrosome amplification after either IR or DNA replication fork-stalling agents both require intact ATM/ATR kinase activities (Bourke et al., 2007; Dodson et al., 2004). With these data in mind I wondered if CDK5RAP2 played a role in the centrosomal response to DNA replication fork-stalling agents.

To analyse this, I treated DT40 cells for 16 hours with aphidicolin. I then fixed cells and analysed centrosome number by γ -tubulin staining. I found that 74% of wild-type DT40 cells contained two or more centrosomes but this was only 44% in *cnn1*^{-/-} cells (Figure 6.1.4A). It is important to state here that after a 16 hour aphidicolin treatment, I noted that a population of cells in both wild-type and *cnn1*^{-/-} DT40 stained positively for TACC3 and Plk1, markers of centrosomes in G2, consistent with previous findings (Dodson et al., 2004). Regardless of the cell cycle stage that amplification was occurring in, centrosome

amplification was mediated by ATM/ATR in both wild-type and *cnn1*^{-/-} cells, since co-treating cells with aphidicolin and caffeine, an inhibitor of ATM and ATR kinase activities, abolished centrosome amplification. These data imply that the CNN1 domain of CDK5RAP2 is not essential for centrosome amplification in response to aphidicolin-mediated cell cycle arrest but in the absence of the CNN1 domain, centrosome amplification is retarded.

Chk1 is required for centrosome amplification after IR-induced DNA damage, since *Chk1*^{-/-} DT40 cells do not amplify their centrosomes after IR treatment (Bourke et al., 2007). Moreover, centrosome amplification after DNA damage has been suggested to involve the centrosomal accumulation of Chk1 (Loffler et al., 2007). Therefore, the reduction in centrosomal Chk1 in *cnn1*^{-/-} cells may be the reason for the reduction in centrosome amplification after aphidicolin treatment. However, a recent paper has found that Chk1 is not required for centrosome amplification in response to a different DNA replication fork-stalling agent – HU (Bourke et al., 2010). Therefore, I was curious to see if *cnn1*^{-/-} cells amplified their centrosomes in response to HU treatment. Treatment of DT40 cells with HU leads to lower levels of centrosome amplification than treatment with aphidicolin. Because of this, to analyse centrosome amplification after HU treatment, I treated cells for 24 hours with HU, as in (Bourke et al., 2010). I found that after HU treatment, *cnn1*^{-/-} cells amplified their centrosomes equally well as wild-type cells (Figure 6.1.B). Thus, reduced centrosomal Chk1 in *cnn1*^{-/-} cells did not affect centrosome amplification in HU, in agreement with (Bourke et al., 2010).

Bourke and colleagues suggested that different centrosome amplification mechanisms must exist in response to IR (Chk1-dependent) and HU (Chk1-independent) (Bourke et al., 2010). My data suggest that different amplification mechanisms might exist even between the different DNA-replication fork stalling agents HU and aphidicolin. This might also explain the differences observed in the kinetics of centrosome amplification after either treatment (Figure 6.1.4).

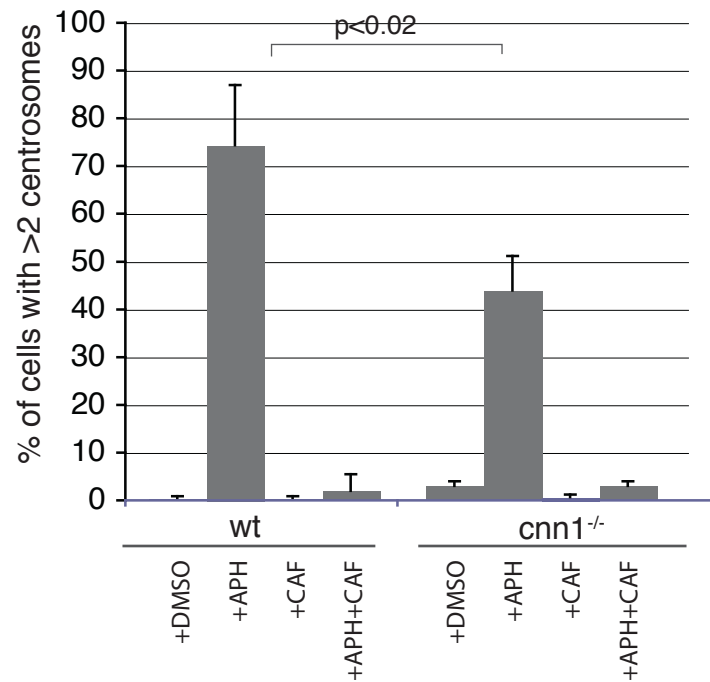
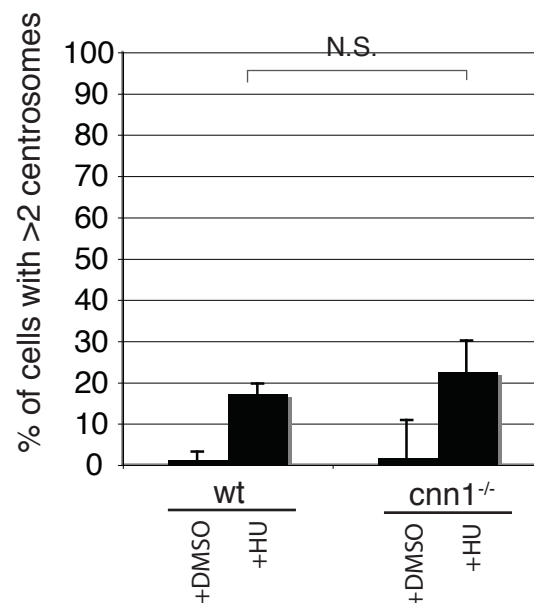
A.**B.**

Figure 6.1.4 The CNN1 domain is involved in centrosome amplification in response to aphidicolin but not to HU. **A.** Graph shows that 16 hr treatment with aphidicolin (+APH) induces centrosome overduplication in DT40 cells. Caffeine alone (+CAF) or with aphidicolin (+APH+CAF) does not cause centrosome overduplication. Centrosome number was determined using γ -tubulin staining. Note that *cnn1*^{-/-} cells contain slightly elevated centrosome numbers under all conditions (n= 3, at least 150 cells were scored per condition per experiment for each genotype). **B.** Graph shows that 24 hr treatment with hydroxyurea (+HU) induces centrosome amplification in DT40 cells. (n=4, at least 150 cells scored per condition, per experiment for each genotype). p values were calculated by two-tailed unpaired Student's t-test.

6.2 Discussion

6.2.1 The role of CDK5RAP2 in DNA-damage induced G2 arrest

In response to DNA damage or DNA replication fork-stalling agents, eukaryotic cells trigger checkpoint responses that facilitate DNA repair and delay cell cycle progression. The inefficient G2 arrest after irradiation observed in *cnn1*^{-/-} cells is similar to that reported in Chk1-deficient DT40 cells (Zachos et al., 2003). However, unlike Chk1-deficient cells, the majority of *cnn1*^{-/-} cells can still arrest in G2. This is not too surprising, since *cnn1*^{-/-} cells exhibit a reduction of approximately 55% instead of a complete loss of centrosomal Chk1 (Figure 6.1.3). Nonetheless, CDK5RAP2 plays a role in mediating the G2 checkpoint and its role in this process is likely to involve the recruitment and/or maintenance of Chk1 at the centrosome.

The requirement for CDK5RAP2 in the centrosomal recruitment of Chk1 is similar to the function described for a second microcephaly protein, microcephalin (Tibelius et al., 2009). Microcephalin has been found to mediate Chk1 localisation to the centrosome during unperturbed cell cycles (Tibelius et al., 2009). Therefore, perturbation of centrosomal Chk1 levels may represent a common mechanism in the cause of primary microcephaly (see Chapter 7: Discussion).

Intriguingly, the centrosomal protein, pericentrin, has also been shown to be required for the centrosomal recruitment of Chk1 (Tibelius et al., 2009). Mutations in pericentrin have been implicated in the microcephaly-related diseases, Majewski Osteoplasty Primordial Dwarfism type II (MOPD II) and Seckel syndrome (Griffith et al., 2008; Rauch et al., 2008). While these diseases are distinct from primary microcephaly, in that the overall growth of the affected individual is reduced, affected individuals do also present with microcephaly. CDK5RAP2 has been shown to be required for efficient pericentrin localisation to centrosomes in interphase (Graser et al., 2007a). Therefore, it is possible that CDK5RAP2 and pericentrin cooperate to recruit and/or maintain Chk1 in the centrosome. Since AKAP450 shares a high degree of homology with pericentrin, via their conserved C-terminal PACT domain, it may also be involved in this process.

6.2.2 The function of the CNN1 domain in centrosome amplification

In addition to its role in mediating G2 arrest after IR-induced DNA damage, CDK5RAP2 is also required for a maximal centrosome amplification response during prolonged treatment with the DNA replication fork-stalling agent, aphidicolin (Figure 6.1.4A). Chk1 has been shown to be required for centrosome amplification after IR (Bourke et al., 2007). Moreover, Loffler and colleagues showed that Chk1 accumulates at centrosomes after treatment with the DNA replication-fork stalling agent, HU, and that the forced centrosomal localisation of Chk1 can drive centrosome amplification (Loffler et al., 2007). For these reasons, I concluded that the reduction in centrosome amplification in *cnn1*^{-/-} cells, compared to wild-type, was likely to be due to the reduction in centrosomal Chk1 in *cnn1*^{-/-} cells (Figure 6.1.3; (Barr et al., 2010)).

However, a recent paper has questioned the requirement for Chk1 in centrosome-mediated amplification after treatment with the DNA replication fork-stalling agent, HU (Bourke et al., 2010). Chk1-disrupted DT40 cells arrested for 24 hours in HU were still able to amplify their centrosomes. Therefore, I treated wild-type and *cnn1*^{-/-} cells with HU and found that there was no difference in centrosome amplification between the two cell lines (Figure 6.1.4B). Thus, the reduction in centrosomal Chk1 in *cnn1*^{-/-} cells does not affect centrosome amplification after HU treatment. This is consistent with the results reported in (Bourke et al., 2010). These data raise the intriguing possibility that centrosome amplification in response to different DNA replication fork stalling agents is mediated by different mechanisms. A difference between the two mechanisms is further supported by the differences in the absolute number of wild-type DT40 cells that have amplified centrosomes after 16 hours in aphidicolin (74%) and 24 hours in HU (18%). Teasing apart the mechanisms underlying these observed differences in centrosome amplification pathways will be an important future area of research, especially since many human tumours contain cells with amplified centrosomes (reviewed in (Zyss and Gergely, 2009)).

6.2.3 The respective contributions of the CNN1 and CNN2 domains to CDK5RAP2 function

Table 6.1 summarises the different functions of the CNN1 and CNN2 domains of CDK5RAP2 in DT40 cells. In this respect, DT40 cells have proven to be extremely useful in delineating the respective contributions of these evolutionarily conserved domains to CDK5RAP2 function in vertebrate cells. I have found that the CNN1

domain is required for every function of CDK5RAP2 described so far. This is similar to what has been reported in *Drosophila* - that the majority of Cnn's functions are attributable to the CNN1 domain (Zhang and Megraw, 2007). This is perhaps not too surprising since this domain is also conserved in the single cell eukaryote - fission yeast. In vertebrate cells, the CNN1 domain of CDK5RAP2 is required for the localisation of AKAP450 to the centrosomes in mitosis and, as a consequence, for the attachment of centrosomes to spindle poles. The CNN1 domain is also required for centrosome cohesion, again a function that is likely to be due to its role in efficiently recruiting AKAP450 to the interphase centrosome. Finally, the CNN1 domain is required for the growth of DT40 and this may be due to its function in the DNA damage response and maintaining a robust G2 arrest. In contrast, I have found that the CNN2 domain only plays a role in the localisation of AKAP450 to mitotic centrosomes and, therefore, is required for centrosome to spindle pole attachment. It will be interesting to see if there are any functions of CDK5RAP2 that uniquely require the CNN2 domain.

Table 6.1 Functions of the CNN1 and CNN2 domains of CDK5RAP2 in DT40

Domain	CNN1	CNN2
Mitotic AKAP450 localisation	✓	✓
Centrosome-spindle pole attachment	✓	✓
Centrosome cohesion	✓	X
Interphase AKAP450 localisation	(✓)	X
Proliferation	✓	X
DNA damage induced G2 arrest	✓	X

Key to table: ✓ = required, (✓) = partially required, X = not required.

Overexpression studies of domains of CDK5RAP2 in human cells did give some clues as to the functions of the respective domains of CDK5RAP2. For example, overexpression of FLAG-CT in HeLa cells revealed that, although the C-terminus of CDK5RAP2 can localise to centrosomes in interphase, this localisation alone is not sufficient to maintain centrosome cohesion. This indicated that the N-terminus of CDK5RAP2 was important in mediating centrosome cohesion. This finding was then

further supported by gene-targeting of the CNN1 domain in DT40. However, the clonal nature of DT40 cell lines gives a clean genetic background when examining phenotypes without the concern of differential expression levels of overexpressed protein from cell to cell or the possible influence of epitope tags on protein function.

Chapter 7: Discussion

7.1 CDK5RAP2 is required for centrosome to spindle pole attachment

7.1.1 Attachment of centrosomes to spindle poles

During mitosis, the bipolar spindle is assembled by both centrosomal and non-centrosomal pathways (see Sections 1.3.3.5 and 1.3.4 and reviewed in (O'Connell and Khodjakov, 2007)). Non-centrosomally nucleated microtubules require an additional focussing step to generate the spindle structure. Microtubules are focussed at their minus ends by the activities of the microtubule motor protein, dynein and its activator dynactin. NuMA is transported to the spindle pole by dynein/dynactin, where it crosslinks focussed microtubules at their minus ends to form the spindle pole structure. Centrosome-nucleated microtubules are released from the centrosome in mitosis more readily than in interphase (Belmont et al., 1990). These microtubules may also be anchored in the spindle pole. However, since both the centrosome and the spindle pole contain a high density of microtubule minus ends, the relationship between them is not fully understood. In addition to its spindle pole focussing role, dynactin can also anchor microtubules in the centrosome and thus may provide a link between the centrosome and the spindle pole.

Disruption of the CNN1 and CNN2 domains of CDK5RAP2 in DT40 cells has revealed a new player in the attachment of centrosome to spindle poles. Disrupting either the CNN1 or CNN2 domain caused a dramatic detachment of centrosomes from spindle poles. Centrosome detachment occurs either concomitant with, or shortly after, bipolar spindle formation. Therefore, as microtubules capture kinetochores, increased force generated by spindle microtubules pulls the spindle pole away from the centrosome and the centrosome detaches. Cells with partially or fully detached centrosomes take longer to initiate anaphase and this is due to a delay in aligning chromosomes on the metaphase plate.

7.1.2 CDK5RAP2 maintains centrosome to spindle pole attachment via AKAP450 and dynactin

I have found that CDK5RAP2 interacts with the PCM scaffolding protein, AKAP450. Moreover, CDK5RAP2 is essential for the recruitment of AKAP450 to the centrosome in mitosis. Both the CNN1 and CNN2 domains of CDK5RAP2 are implicated in AKAP450 recruitment. Furthermore, AKAP450 interacts with the p150^{glued} subunit of dynactin (Kim et al., 2007), an interaction that I found to be maintained in mitosis. The CNN1 domain of CDK5RAP2 is required for the centrosomal accumulation of p150^{glued}, yet I could not detect an interaction between these two proteins. Therefore, I suggest a mechanism whereby CDK5RAP2 binds to and recruits AKAP450 to the mitotic centrosome. Once in the centrosome, AKAP450 binds to p150^{glued} and provides anchorage sites for the spindle poles in the centrosomes (Figure 7.1). I have found no evidence that CDK5RAP2, AKAP450 and p150^{glued} exist in the same molecular complex. Therefore, once CDK5RAP2 has recruited AKAP450 to the centrosome it may release it into the PCM where it can then provide its anchorage role (Figure 7.1).

In further support of this model is the fact that AKAP450 has already been implicated in centrosome attachment to spindle poles (Oshimori et al., 2009). siRNA-mediated depletion of the centrosomal protein, cep72, from HeLa cells caused a reduction in AKAP450 in the centrosome. Furthermore, cep72-depleted cells had defects in attachment between centrosomes and spindle poles in mitosis. The centrosome detachment defect was relatively mild in cep72-depleted HeLa cells, as compared to CNN1 and CNN2 deficient DT40 cells. However, these data still suggest a role for AKAP450 in centrosome to spindle pole attachment. Interestingly, Oshimori and colleagues attribute centrosome detachment to a reduction in the nucleation of microtubules from the centrosome in mitosis. I did not see any reduction in the microtubule nucleation capacity of centrosomes in cnn1^{-/-} cells and therefore my data suggest that this is not the primary mechanism of centrosome detachment in CNN1 disrupted cells.

AKAP450 is generally recognised as one of the scaffolding proteins in the centrosome, providing an anchor onto which other proteins can dock. Evidence for a scaffolding function comes from the observation that AKAP450 is required to anchor signalling enzymes at the centrosome – such as PKN, PKA and protein phosphatases

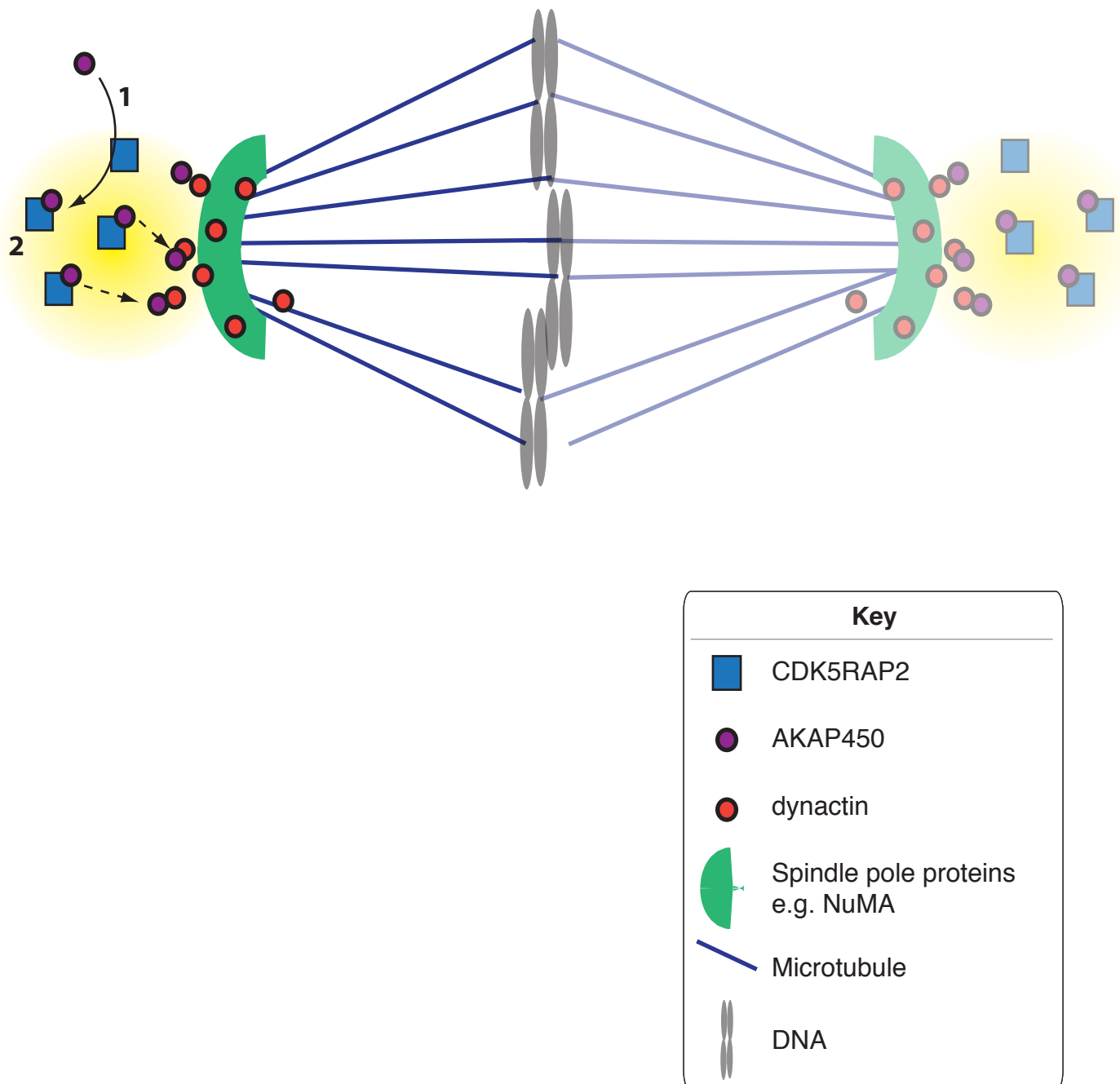


Figure 7.1 A model for how CDK5RAP2 mediates centrosome to spindle pole attachment via AKAP450 and dynactin. CDK5RAP2 recruits AKAP450 to the mitotic centrosome (1). It may also be required to maintain AKAP450 in the PCM (2). However, more likely is that CDK5RAP2 releases AKAP450 into the PCM (dashed arrows), where it can interact with the p150^{glued} subunit of dynactin. AKAP450 may provide docking sites for p150^{glued} in the PCM. In this way, spindle poles are linked to centrosomes by p150^{glued} binding to AKAP450 and bridging the centrosome and spindle pole.

1 and 2A (Takahashi et al., 1999). Moreover, FRAP studies in *Drosophila* embryos indicated a stable fraction of the PACT domain of AKAP450 associated with the centrosome (Martinez-Campos et al., 2004). However, apart from a mild reduction in γ -tubulin in the PCM, the overall PCM structure remained intact in *cnn1*^{-/-} DT40 cells. This brings into question the function of AKAP450 as a scaffolding protein. What is more likely is that AKAP450 is required for the anchorage of a subset of proteins in the PCM – for example p150^{glued} and the signalling enzymes mentioned above, but not for the overall integrity of the PCM. Therefore, AKAP450 may not be part of the ‘centromatrix’ discussed in Section 1.3.1.

To definitively prove that centrosome detachment is due to the lack of AKAP450 in the centrosome in CNN1 and CNN2 disrupted cells, it will be necessary to knockout the *akap450* gene in DT40. The difficulty with this is that *akap450* locus is very large in chicken – 74.9 kb - and thus it would be difficult to remove the whole gene. The Gg *akap450* gene is also present on chromosome 2, which is trisomic in chicken and therefore three independent gene targeting events would be required to disrupt *akap450*. Moreover, I still do not know which domains of AKAP450 might be important in centrosome to spindle pole anchoring and additional studies will be required to decide which domains to disrupt by gene targeting.

7.1.3 The relative contributions of the CNN1 and CNN2 domains in centrosome to spindle pole attachment

Although the centrosome detachment phenotype was obvious in both *cnn1*^{-/-} and *cnn2*^{-/-} DT40 cells, the extent of centrosome detachment was more severe in *cnn1*^{-/-} cells. I found that both the CNN1 and CNN2 domains of CDK5RAP2 were required to recruit AKAP450 to the centrosome in mitosis. Therefore, the CNN1 domain must also have an independent function in centrosome attachment to spindle poles outside of its role in AKAP450 recruitment. Since I have never detected CDK5RAP2 at the spindle pole, it is unlikely that CDK5RAP2 acts as a bridge itself between the centrosome and spindle pole. Therefore, the additional role of the CNN1 domain in centrosome to spindle pole attachment may involve other molecular players. One way to identify these would be to use the wt-TAP and *cnn1*^{lox}-TAP *cdk5rap2* DT40 cell lines to purify wild-type and Δ CNN1 CDK5RAP2 and look for differential interacting proteins by mass spectrometry.

In human cells, I found that the C-terminus of CDK5RAP2 is required for AKAP450 interaction, a region that includes the CNN2 domain. Therefore, one would predict that Δ CNN1 could still recruit AKAP450 to the centrosome. However, even when present at the centrosome in mitosis, Δ CNN1 CDK5RAP2 cannot recruit AKAP450. The data from human cells also suggests that in *cnn2*^{-/-} cells, CDK5RAP2 would not be able to interact with AKAP450 and recruit it to the centrosome. While this appears to be the case in mitosis, it is not consistent with the observation that in *cnn2*^{-/-} cells AKAP450 can localise to the centrosome in interphase, even when Δ CNN2 protein is apparently not there. These data suggest that perhaps neither Δ CNN1 nor Δ CNN2 can bind to AKAP450, maybe due to the low abundance of disrupted CDK5RAP2 protein or perturbations in the protein structure after the disruption of either CNN domain. This would explain why neither Δ CNN1 nor Δ CNN2 protein can recruit AKAP450 to the centrosome in mitosis. However, AKAP450 interphase recruitment in *cnn2*^{-/-} cells appears to be more complicated. Since the CNN1 domain is required for centrosome cohesion, if this cohesion is established at the end of mitosis during centriole disengagement then AKAP450 would be recruited to a cohesive structure (see Section 5.4.2 in Chapter 5). However, in *cnn1*^{-/-} cells, cohesion would not be established and therefore AKAP450 would not be recruited. GS-TAP tag–AKAP450 pull downs and identification of bound proteins by mass spectrometry would confirm if AKAP450 can bind to CDK5RAP2 protein lacking the CNN1 and/or CNN2 domains.

7.1.4 The interplay between CDK5RAP2 and dynein in the mitotic centrosome

At around the same time that we published a paper detailing the requirement for CDK5RAP2 in centrosome attachment to spindle poles (Barr et al., 2010), another paper was published that demonstrated a similar role for CDK5RAP2 in human cells (Lee and Rhee, 2010). The authors describe a detachment of centrosomes from spindle poles after depletion of CDK5RAP2 from HeLa cells by siRNA. Consistent with my data, Lee *et al.* also observed a reduction in dynein and AKAP450 in CDK5RAP2-depleted centrosomes. The centrosome detachment phenotype observed in HeLa cells is subtle and not as severe as the phenotype I observed in DT40 cells. This may be due to residual CDK5RAP2 protein after RNAi-knockdown in human cells.

Based on their data, Lee and colleagues propose a model whereby CDK5RAP2 leads to a reduction in dynein, and therefore a reduction in dynein-mediated transport to the centrosome. They do not demonstrate a molecular interaction between CDK5RAP2 and AKAP450, or indeed with dynein/dynactin. From these data, they deduce that AKAP450 is reduced in the centrosome due to a failure to recruit AKAP450 by a dynein-dependent mechanism. However, AKAP450 localisation to the centrosome has been shown to be microtubule independent (Kim et al., 2007). Microtubule-independent recruitment of AKAP450 to centrosomes is also consistent with my centrosome purification data. In the centrosome purification procedure, microtubules are depolymerised with nocodazole before cell lysis. Therefore, since AKAP450 still localises to wild-type DT40 centrosomes in the absence of microtubules, it must be recruited by a microtubule (and therefore dynein) independent mechanism. Furthermore, if CDK5RAP2 were required for dynein mediated transport then one would predict abnormal (i.e. unfocussed) spindle poles. However, after disruption of the CNN1 and CNN2 domains of CDK5RAP2 in DT40 (which both exhibit the centrosome detachment phenotype), spindle poles focus normally and accumulate NuMA. Therefore, my data suggest that the reduction in AKAP450 in mitotic centrosomes is due to a direct failure of CDK5RAP2 to recruit it to the PCM.

7.2 CDK5RAP2 and AKAP450 may mediate centrosome cohesion by regulating microtubule interactions with the centrosome

I have shown that CDK5RAP2 and AKAP450 are required to maintain centrosome cohesion in interphase. Specifically, the CNN1 domain of CDK5RAP2 is required to maintain cohesion whereas the CNN2 domain is dispensable for this process. CDK5RAP2 and AKAP450 are likely to cooperate in maintaining centrosome cohesion since siRNA-mediated depletion of both did not lead to an additional increase over depletion of either alone. Pericentrin is also likely to be part of this same mechanism, since CDK5RAP2 and pericentrin are mutually required for each other's localisation to the centrosome in interphase (Graser et al., 2007a). CDK5RAP2/AKAP450/pericentrin-mediated centrosome cohesion appears to be distinct from the c-Nap1/rootletin/cep68-mediated cohesion (Chapter 3 and (Graser et al., 2007a)). Therefore, the question remains as to how CDK5RAP2, AKAP450 and pericentrin mediate centrosome cohesion.

I suggest that the role of CDK5RAP2 in mediating centrosome cohesion may be in regulating centrosomal-microtubule interactions. The reason for this is as follows. An intact microtubule cytoskeleton is required to maintain centrosome cohesion by balancing the relative activities of kinases and phosphatases in the PCM (Jean et al., 1999; Meraldi and Nigg, 2001). An intact microtubule network would ensure that centrosomal recruitment of such kinases and phosphatases is intact. I have found that depolymerisation of microtubules by nocodazole in CDK5RAP2-depleted cells did not lead to a further increase in centrosome splitting over CDK5RAP2-depletion or nocodazole treatment alone. This suggests that CDK5RAP2 mediates centrosome cohesion by regulating interactions with the microtubule network. While overexpressed CDK5RAP2 can localise to microtubules, I have found no evidence that endogenous CDK5RAP2 does. However, CDK5RAP2 does localise to the centrosome and can bind to Taxol-stabilised microtubules. Therefore, CDK5RAP2 is in a prime position to regulate centrosome-microtubule interactions. Fong *et al.* have mapped the microtubule-binding region of CDK5RAP2 to the CNN1 domain (Fong et al., 2008). In human cells, I found that the N-terminus of CDK5RAP2 is required to

maintain centrosome cohesion. Moreover, in DT40, I found that specifically it is the CNN1 domain that is essential for centrosome cohesion. These data suggest that the microtubule-binding function of CDK5RAP2 could be important in maintaining centrosome cohesion.

AKAP450 has also been implicated in regulating centrosome-microtubule interactions (Kim et al., 2007; Larocca et al., 2006). Not only is AKAP450 able to bind to microtubules but microtubule regrowth after nocodazole washout is significantly retarded in AKAP450-depleted cells. In addition, the AKAP450 binding partner, p150^{glued}, is required for microtubule anchoring in the centrosome in interphase (Quintyne et al., 1999). Furthermore, overexpression of a dominant negative form of p150^{glued} has been shown to lead to a loss of centrosome cohesion (Quintyne and Schroer, 2002). My data suggests that in mitosis, CDK5RAP2 recruits AKAP450 to the centrosome and that AKAP450 then provides docking sites for spindle poles by a molecular interaction between AKAP450 and p150^{glued}. In interphase, this trio of proteins may also employ a similar mechanism for mediating centrosome cohesion. CDK5RAP2 may mediate the assembly of AKAP450 into cohesive complexes at the end of mitosis. AKAP450 may then provide centrosomal docking sites for p150^{glued} in the centrosome. In turn, p150^{glued} may then anchor microtubules in the centrosome and thus maintain centrosomal-microtubule interactions. Clearly, parts of this model remain to be tested. For example, we do not know what happens to p150^{glued} centrosomal localisation in interphase in the absence of CDK5RAP2 and/or AKAP450. Significantly, Lee *et al.* performed their centrosome purifications from asynchronous control- and CDK5RAP2-depleted HeLa cells and saw a significant reduction in dynein in these preparations (Lee and Rhee, 2010). Since one would expect that the majority of these cells would be in interphase then these data might suggest that dynein/dynactin may be reduced in interphase centrosomes after depletion of CDK5RAP2.

7.3 CDK5RAP2 plays a role in the DNA damage response

The poor clonogenic potential of *cnn1*^{-/-} cells prompted me to investigate if this was due to an impaired DNA damage response (Zachos et al., 2003). I found that the CNN1 domain of CDK5RAP2 is required for an efficient arrest in G2 after DNA damage. This may be due to a reduced capacity of *cnn1*^{-/-} cells to recruit Chk1 to the centrosome. Centrosomal recruitment of Chk1 has been implicated in regulating entry into mitosis in both unperturbed cell cycles and after DNA damage (Tibelius et al., 2009; Zachos et al., 2003). Chk1 at the centrosome maintains Cdk1 in an inactive state and thus inhibits entry into mitosis (see Section 1.3.5). Although I observed a defect in G2 arrest after DNA damage, I did not observe *cnn1*^{-/-} cells entering mitosis prematurely, for example with unduplicated centrosomes. Therefore, although *cnn1*^{-/-} cells have reduced Chk1 at their centrosomes, it seems that in unperturbed cell cycles this is sufficient to regulate normal mitotic entry. The problem only arises when cells incur DNA damage and extra centrosomal Chk1 is required, as suggested in (Loffler et al., 2007).

How CDK5RAP2 recruits Chk1 to centrosomes is still not known. For example, CDK5RAP2 may interact with Chk1 and recruit it directly to the centrosome. Alternatively, since CDK5RAP2 has been shown to be required for the efficient localisation of pericentrin to centrosomes in interphase (Graser et al., 2007a) and pericentrin has been shown to interact with and recruit Chk1 to the centrosome (Tibelius et al., 2009) then CDK5RAP2 may mediate Chk1 recruitment through pericentrin. It also remains to be seen if CDK5RAP2 can interact with pericentrin.

Apart from playing an indirect role in efficiently arresting the cell cycle after DNA damage, the centrosome also appears to act as an effector of DNA damage by amplifying in number. The reason this appears to be an effector mechanism rather than an indirect consequence of DNA damage is that it has the advantage that if cells slip out of a G2 arrest and into mitosis with DNA damage, cells with amplified centrosomes will assemble multipolar spindles. While mechanisms do exist to cluster multiple centrosomes (Kwon et al., 2008) and therefore generate a bipolar spindle with multiple centrosomes at each pole, an increased incidence of mitotic catastrophe in cells with amplified centrosomes has been reported (Dodson et al., 2007).

Therefore, this may be an elegant safeguard mechanism implemented by cells to eliminate cells with DNA damage and impaired cell cycle arrest from the population.

7.4 Similarities and differences between CDK5RAP2 and its lower eukaryotic homologues

7.4.1 Centrosome maturation

Drosophila Cnn and fission yeast mod20p both have in common the ability to bind to and recruit γ -tubulin to MTOCs. These functions require the CNN1 domain in both of these proteins (Samejima et al., 2008; Terada et al., 2003; Zhang and Megraw, 2007). siRNA/shRNA depletion of CDK5RAP2 in human cells did not lead to a defect in γ -tubulin recruitment. Gene-targeting of the CNN1 domain in DT40 appeared to lead to a small reduction in the amount of γ -tubulin at the centrosomes when examined by immunostaining but biochemical purification of centrosomes did not reveal a reduction in γ -tubulin. Importantly, the microtubule nucleating capacity of mitotic centrosomes in *cnn1*^{-/-} cells was equivalent to that in wild-type cells, further suggesting that γ -tubulin levels are not functionally reduced.

Reduction of γ -tubulin in mitotic centrosomes after CDK5RAP2 depletion has since been reported by two other groups (Fong et al., 2008; Haren et al., 2009b). Fong *et al.* reported that the CNN1 domain of CDK5RAP2 is able to interact with γ -tubulin and other members of the γ -TuRC (Fong et al., 2008). However, I have been unable to confirm these data. Furthermore, disruption of the CNN1 domain in DT40 cells did not affect the localisation of γ -tubulin to mitotic centrosomes, nor the ability of centrosomes to nucleate microtubules. Therefore, my results argue against the fact that recruitment of γ -tubulin to the centrosome in mitosis is a major function of the CNN1 domain in CDK5RAP2.

A siRNA screen to identify regulators of centrosome maturation in *Drosophila* S2 cells identified Cnn as being required (Dobbelaere et al., 2008). The screen actually used Cnn staining as a marker for PCM recruitment therefore, it may not seem surprising that Cnn was identified as being required. However, the authors did confirm a requirement for Cnn by siRNA depletion of Cnn in S2 cells and immunostaining with γ -tubulin antibody. Cnn has also been implicated in the localisation of Aurora A to the centrosome in S2 cells and *vice versa* (Terada et al., 2003). Zhang and colleagues identified the CNN1 domain of Cnn as being essential for the mitotic recruitment of D-TACC, its binding partner Msps and γ -tubulin to centrosomes (Zhang and Megraw, 2007). However, I have found no evidence for a

role of the CNN1 domain of CDK5RAP2 in centrosome maturation. This difference might be due to the differences between *Drosophila* and mammalian PCM organisation. Before G2, *Drosophila* centrosomes are essentially naked centrioles that recruit almost all of their PCM during centrosome maturation (reviewed in (Rusan and Rogers, 2009)). However, centrosomes in mammalian cells have PCM associated with them throughout the cell cycle, although the size of the PCM considerably increases in G2. Therefore, if CDK5RAP2 only had a moderate effect on centrosome maturation, this would result in only a subtle change in the PCM in G2 and mitosis. Cnn is phosphorylated in a Polo kinase-dependent manner (Dobbelaere et al., 2008). I have shown that CDK5RAP2 is phosphorylated in mitosis, although which residues are phosphorylated and by which kinase(s) is still unknown. GS-TAP tagging of endogenous CDK5RAP2 in DT40 could be a useful tool to map the phosphorylation sites in endogenous CDK5RAP2 and investigate if the phosphorylation of such sites changes throughout the cell cycle.

7.4.2 PCM structure

In *Drosophila*, Cnn is required for maintaining centrosome structure by keeping the PCM associated with the centrioles (Lucas and Raff, 2007). On first examination of the PCM protein TACC3 in *cnn1*^{-/-} and *cnn2*^{-/-} mitotic DT40 cells, it appeared that the link between the centrioles and PCM may also have been disturbed after disruption of *cdk5rap2* in vertebrate cells. In *cnn1*^{-/-} cells with partially and fully detached centrosomes, TACC3 is spread between the centrosomes and mitotic spindle poles and appears punctate. However, all of the other PCM components tested did not localise in this manner and instead concentrated around the centrioles. Since TACC3 interacts with microtubules (Gergely et al., 2000a) the localisation of TACC3 in this region is likely to reflect the presence of microtubule minus ends and not a general disorganisation of the PCM. Therefore, while CDK5RAP2 is required to maintain spindle pole proteins in the PCM, it does not seem to be required for the overall maintenance of centrosome integrity in the same way as Cnn. While some PCM proteins are reduced in CDK5RAP2-depleted or *cnn1*^{-/-} centrosomes (AKAP450 and p150^{glued}), the overall PCM structure appears to remain intact. One difference between Cnn and CDK5RAP2 functions in centrosome integrity might be the systems used to study these proteins. Cnn centrosome function has mostly been characterised

in syncytial embryos using overexpressed proteins, whereas that of CDK5RAP2 was examined in a cellular context. In the wild-type *Drosophila* syncytial embryo, live imaging of overexpressed PCM proteins suggests that PCM components exhibit centrosome ‘flaring’. Centrosome ‘flaring’ is a term used to describe the movement of PCM components away from the centrioles. It is unclear if this process occurs normally in the embryo or if it is a consequence of protein overexpression and saturation of binding sites in the PCM. Nevertheless, in *cnn* mutant embryos, increased centriole movement in combination with centrosome flaring leads to dispersal of PCM from around the centrioles and thus revealed the lost connection between centrioles and the PCM in *cnn* mutant flies. In cells, the presence of a cellular boundary might restrict the amount of centriole movement and centrosome flaring that can occur (if flaring occurs at all in vertebrates) since centrosomes are more restricted in their movements.

7.4.3 Centrosome to spindle pole attachment

Lucas and Raff also studied the function of Cnn in neuroblast divisions in the fly brain (Lucas and Raff, 2007). In *cnn* mutant flies, centrosomes could be seen to detach from spindle poles and move throughout the cytoplasm, indicating that Cnn may have a similar function to CDK5RAP2 in centrosome to spindle pole attachment. However, they did not characterise the mechanics of centrosome detachment in this system. Therefore, whether D-Plp (*Drosophila* Pericentrin like protein; orthologue of AKAP450 in fly) or dynactin are implicated is unknown.

7.4.4 Centrosome cohesion

CDK5RAP2 is required to maintain proper centrosome cohesion (Graser et al., 2007a). In the rapid syncytial divisions in *Drosophila* embryos, there is no interphase period and therefore Cnn has not been demonstrated to have a role in centrosome cohesion. Furthermore, the requirement for Cnn in centrosome cohesion in other *Drosophila* cell types has not been investigated.

7.4.5 Functions of the CNN2 domain

The CNN2 domain of Cnn has been shown to interact with Centrocortin and is required for cleavage furrow assembly in *Drosophila* embryos undergoing

cellularisation (Kao and Megraw, 2009; Vaizel-Ohayon and Schejter, 1999). The precise mechanism for how these two proteins regulate cleavage furrow assembly is still not understood but in embryos with a mutated CNN2 domain, actin filaments are not assembled correctly at the cleavage furrows (Kao and Megraw, 2009). Fission yeast Mod20p does not have a conserved CNN2 domain (see Figure 1.7). In vertebrate cells, cytokinesis may involve similar mechanisms to those required for cellularisation in the *Drosophila* embryo, since both require cleavage furrow assembly. However, I did not detect a defect in cytokinesis in *cnn2*^{-/-} DT40 cells. Therefore the significance of this function of the CNN2 domain in Cnn with respect to vertebrate CDK5RAP2 function is uncertain.

7.4.6 Does CDK5RAP2 function redundantly with Myomegalin?

Can the differences between CDK5RAP2 and Cnn function (for example in centrosome maturation) be explained by redundancy with the second Cnn orthologue in humans – Myomegalin? I have demonstrated that Myomegalin is not required for centrosome cohesion but have not extensively characterised this protein. I found that Myomegalin centrosomal localisation is variable between cell lines, which may imply that it is not an important centrosomal protein in all tissues. It is also possible that the antibody I used to study Myomegalin localisation (which is raised against the N-terminus of the protein, including the CNN1 domain) did not recognise other isoforms of Myomegalin that may localise to the centrosome. However, even if such isoforms did exist, this would indicate that Myomegalin at the centrosome in these cells lacked the CNN1 domain. My analysis of *Myomegalin* cDNA from HeLa (where I found that Myomegalin did not localise to centrosomes) and U251MG (where Myomegalin did localise to centrosomes), failed to reveal a difference in the exons expressed in these two cell lines. Importantly, from my data, I am unable to exclude the possibility that the exons expressed are on different transcripts and thus unable to exclude the presence of different isoforms. A Northern blot analysis with a variety of different anti-*Myomegalin* probes would be required to analyse the *Myomegalin* isoforms expressed.

While *Myomegalin* is expressed in DT40 cells, it does not seem to contain a CNN1 domain. Therefore, the phenotypes observed in CDK5RAP2 *cnn1*^{-/-} DT40 cells could be due to the complete absence of a CNN1 domain in these cells. This may explain

why *cnn1*^{-/-} cells have a more severe centrosome detachment phenotype than *cnn2*^{-/-} cells, since the CNN2 domain of Myomegalin may be able to take over part of this function. It would be interesting to target the CNN2 domain of *Myomegalin* in DT40 to see if this is also involved in centrosome-to-spindle pole attachment and if it exacerbates the centrosome detachment phenotype in *cnn2*^{-/-} CDK5RAP2 DT40 cells.

7.5 Inconsistencies between results obtained from DT40 and HeLa cell lines

The DT40 cell line is an extremely powerful system for studying gene function (Winding and Berchtold, 2001). Many of the phenotypes I observed after gene disruption in DT40 cells were similar to those after siRNA/shRNA of CDK5RAP2 in HeLa cells. Loss of AKAP450 from the mitotic centrosome was observed in both CDK5RAP2-depleted HeLa cells and after disruption of the CNN1 and CNN2 domains of CDK5RAP2 in DT40 cells. Loss of centrosome cohesion was also apparent both after depletion of CDK5RAP2 in HeLa cells and by disruption of the CNN1 domain in DT40. However, other phenotypes were only observed after gene disruption of *Cdk5rap2* in DT40 cells. This section describes the inconsistencies between the results obtained from DT40 and HeLa cell lines and why they may arise.

7.5.1 Centrosome detachment

Centrosome detachment from spindle poles was only observed in DT40 cells after the disruption of either the CNN1 or CNN2 domain of CDK5RAP2. This is in spite of the fact that AKAP450 also appeared to be absent from mitotic centrosomes in siRNA- and shRNA-depleted HeLa cells. I believe that this difference is due to the incomplete depletion of CDK5RAP2 from human cells by siRNA/shRNA. Even in the most efficient depletions of CDK5RAP2, there was always a small amount of CDK5RAP2 protein that remained in the centrosome. This small amount of CDK5RAP2 could be sufficient in itself to maintain centrosome attachment to spindle poles (since the CNN1 domain of CDK5RAP2 does seem to play a role in centrosome to spindle pole attachment outside of its ability to recruit AKAP450 to centrosomes). Alternatively, the small amount of endogenous CDK5RAP2 protein remaining in HeLa cells after siRNA/shRNA may still recruit a fraction of AKAP450 (i.e. below the detection level) to the mitotic centrosome, which could mediate anchorage of spindle poles.

A second reason may be that the centrosome detachment phenotype in HeLa cells is very subtle. siRNA depletion of CDK5RAP2 in HeLa cells has been reported to lead to centrosome detachment (Lee and Rhee, 2010). In HeLa cells depleted of CDK5RAP2, the authors observe centrosomes that are slightly displaced to one side

of the PCM but still very close to the spindle pole. Lee *et al.* classify these phenotypes as detached centrosomes. This classification is different to mine, in that if I had observed this phenotype in DT40, I would not have classified the centrosomes as either partially or fully-detached, but as normal. Partially and fully detached centrosomes were very clear in *cnn1*^{-/-} and *cnn2*^{-/-} DT40 cells and the separation between the centrosome and spindle pole was greater, even in partially detached centrosomes, than in CDK5RAP2-depleted HeLa cells. Therefore, in this aspect, DT40 cells proved to be a better system for studying the function of CDK5RAP2 in mitosis. The differences in centrosome detachment observed between DT40 and HeLa could be due to the incomplete depletion of CDK5RAP2 by siRNA in HeLa cells. Alternatively, the difference may arise from the fact that DT40 is a suspension cell line, while HeLa cells are adherent. Although HeLa cells do round up as they enter mitosis, they maintain actin-based retraction fibres that are able to exert an effect on spindle orientation (Kwon *et al.*, 2008). Therefore, the limited ability of HeLa mitotic spindles to rotate and change their position relative to the substratum may limit the capacity of the centrosome to detach and move around the cortex, as is seen in DT40. An interesting experiment would be to deplete CDK5RAP2 protein by siRNA in HeLa S3 cells, which are a suspension cell line, to see if this exacerbated the centrosome detachment phenotype.

7.5.2 AKAP450 localisation in interphase

In HeLa cells depleted of CDK5RAP2, AKAP450 was still present in abundance at the centrosome and Golgi in interphase cells. In *cnn2*^{-/-} DT40 cells, AKAP450 localisation was also unaffected in interphase. However, in *cnn1*^{-/-} cells, AKAP450 localisation in interphase was perturbed. Levels of AKAP450 in *cnn1*^{-/-} interphase cells were much lower and in most cells, AKAP450 was not visible at all. Again, the difference is likely to be due to the incomplete depletion of CDK5RAP2, such that the remaining protein is sufficient to localise AKAP450 to the centrosome.

7.5.3 CDK5RAP2 in centrosome cohesion

A loss of centrosome cohesion was observed after siRNA/shRNA depletion of CDK5RAP2 and disruption of the CNN1 domain in DT40 cells. Both overexpression of FLAG-CT in human cells and gene-disruption of the CNN1 domain in DT40,

revealed a requirement for the N-terminus of CDK5RAP2 in maintaining centrosome cohesion. The extent of centrosome splitting between HeLa and DT40 was quite different – being 2.5-fold higher in HeLa cells than in DT40. The reason for this discrepancy is not known. However, it may be due to the smaller cytoplasmic volume of DT40 cells compared to HeLa. In support of this is that time-lapse imaging of HeLa cells expressing GFP-centrin1 revealed that split centrosomes are very dynamic, with individual centrioles probing the cell cytoplasm and frequently moving apart and back together. The smaller volume of cytoplasm in DT40 cells means that centrioles have less freedom to move and thus would come together more frequently, even by chance.

7.6 Linking the function of CDK5RAP2 to microcephaly

How do mutations in *cdk5rap2* lead to microcephaly? Two scenarios in which a defect in CDK5RAP2 function could lead to microcephaly are outlined below.

7.6.1 Defects in spindle alignment

In mouse brain, the orientation of the cytokinetic plane determines whether apical progenitors undergo proliferative or neurogenic cell divisions in the neuroepithelium (see Figure 1.6 and also reviewed in (Farkas and Huttner, 2008)). Orientation of the mitotic spindle is regulated by centrosomal-nucleated astral microtubules and their interaction with the cell cortex (Toyoshima and Nishida, 2007). To generate a large stem-cell pool, the cytokinetic plane of dividing neuroepithelial cells must precisely bisect the apical membrane, such that both daughter cells remain anchored. If the link between centrosome and spindle poles is perturbed (such as is the case in *cdk5rap2* gene-disrupted DT40 cells), cortical cues would not be transmitted to the mitotic spindle and spindles could become misaligned. More recently, asymmetric centrosome inheritance (i.e. old versus new centrosome) has been suggested to be decisive in cell fate determination in mouse brain (Wang et al., 2009). Perturbations in spindle orientation would also be predicted to randomise the inheritance of the old and new centrosomes by daughter cells, and thus may affect cell fate.

In support of this argument is that in mice where the microcephaly protein, ASPM, has been depleted in the brain, spindle orientation was affected – leading to a premature switch from proliferative to neurogenic cell divisions and depletion of the stem-cell pool (Fish et al., 2006). Furthermore, like the disruption of the CNN1 and CNN2 domains in CDK5RAP2, depletion of ASPM in mouse brain caused centrosomes to detach from spindles. Centrosome detachment from spindles has also been observed in zebrafish null for the microcephaly protein, SIL (Pfaff et al., 2007), and in *Drosophila* embryos mutant for microcephalin (Brunk et al., 2007). Therefore, centrosome detachment may be a common mechanism in causing primary microcephaly.

7.6.2 Defects in arrest after DNA damage

I found that the CNN1 domain is required for efficient arrest in G2 after DNA damage. DT40 cells do not have functional p53 and therefore I was unable to use this system to investigate if CDK5RAP2 had functions in DNA damage checkpoints in G1 or intra-S. Mutations in DNA damage signalling and repair pathways can cause microcephaly phenotypes, including mutations in ATR, NBS1 and BRCA2 (reviewed in (McKinnon, 2009)). Furthermore, the primary microcephaly protein, microcephalin, has been extensively implicated in the DNA damage response and DNA repair. DNA repair is particularly important during early neurogenesis to repair replication-induced DNA damage generated when cells are undergoing rounds of rapid proliferation. In proliferating cells, this is repaired predominantly by homologous recombination (HR). As mentioned above, I am unable to make any statements about CDK5RAP2 function in pre-G2 checkpoints and hence in p53-mediated apoptosis of damaged cells. However, mutations in *cdk5rap2* may allow cells with damaged DNA to slip through the G2 checkpoint into mitosis. Cells entering mitosis with damaged DNA have been shown to form multipolar spindles with split centrioles (Hut et al., 2003). One would predict that these cells would undergo mitotic death, leading to depletion of the neuroepithelial stem cell, or neurogenic progenitor, pool. I would expect a similar phenotype if CDK5RAP2 is also required for G1 and intra-S phase checkpoints as presumably cells with damage would also skip these checkpoints in the presence of mutated *cdk5rap2*.

Why do mutations in *cdk5rap2* perturb cell division specifically in the neuroepithelium when CDK5RAP2 is a ubiquitously expressed protein? In humans there may be a CNN1-independent pathway that connects spindle poles with centrosomes in all cell types apart from neuroepithelial cells. Alternatively, CDK5RAP2 may function redundantly with Myomegalin in centrosome attachment to spindle poles. The CNN1 domain is absent from at least two splicing variants of human *Myomegalin*. Thus, if these variants are expressed in the developing neuroepithelium (or if *Myomegalin* is not expressed at all), CDK5RAP2 may be the only CNN1-containing protein available in the neuroepithelial cells. It will be important in future studies to assess the relative expression of CDK5RAP2 and Myomegalin in the developing neuroepithelium, and to characterise the isoforms of

both CDK5RAP2 and Myomegalin that are expressed there. Another reason why mutations in *cdk5rap2* may specifically affect brain development involves the requirement for CDK5RAP2 in the DNA damage response. Mutations in DNA damage repair pathways appear to have a predominant effect on the brain and nervous system. Therefore, it might be that the brain is exquisitely sensitive to DNA damage during development.

One of the reported *cdk5rap2* microcephaly mutations lies in the CNN1 domain (S81X; (Bond et al., 2005)). The second is further downstream but before the CNN2 domain (E385fsX4). It is not yet known if these mutations are hypomorphic or null for CDK5RAP2 protein. If truncated protein products are made these may lack CNN1 or CNN2 domains due to either reinitiation after the S81X mutation (Δ CNN1), or, in the case of E385fsX4, truncation before the CNN2 domain (Δ CNN2). Recently, microcephaly patient-derived B-cell lines from patients with mutations in *cdk5rap2* have become available (Geoff Woods, personal communication) and thus some of these questions can start to be answered.

In this thesis, I have described novel functions for CDK5RAP2 in the vertebrate centrosome. Moreover, through the study of CDK5RAP2, I have also characterised new functions for a second centrosomal protein, AKAP450. In addition, the study of CDK5RAP2 in DT40 cells has revealed a new mechanism for centrosome to spindle pole attachment in vertebrate cells. Ultimately, the question as to which functions of CDK5RAP2 are specifically required during brain development will only be answered by creating transgenic mice that mimic the microcephaly mutations found in humans. Analysis of the proliferation of neuroepithelial cells carrying such mutations would then indicate which aspects of CDK5RAP2 (and indeed centrosome) function are important during neurogenesis.

Chapter 8: Bibliography

- Acquaviva, C., and J. Pines. 2006. The anaphase-promoting complex/cyclosome: APC/C. *J Cell Sci.* 119:2401-4.
- Albee, A.J., and C. Wiese. 2008. Xenopus TACC3/maskin is not required for microtubule stability but is required for anchoring microtubules at the centrosome. *Mol Biol Cell.* 19:3347-56.
- Alderton, G.K., L. Galbiati, E. Griffith, K.H. Surinya, H. Neitzel, A.P. Jackson, P.A. Jeggo, and M. O'Driscoll. 2006. Regulation of mitotic entry by microcephalin and its overlap with ATR signalling. *Nat Cell Biol.* 8:725-733.
- Aleem, E., H. Kiyokawa, and P. Kaldis. 2005. Cdc2-cyclin E complexes regulate the G1/S phase transition. *Nat Cell Biol.* 7:831-6.
- Amos, L.A., and J. Lowe. 1999. How Taxol stabilises microtubule structure. *Chem Biol.* 6:R65-9.
- Andersen, J.S., C.J. Wilkinson, T. Mayor, P. Mortensen, E.A. Nigg, and M. Mann. 2003. Proteomic characterization of the human centrosome by protein correlation profiling. *Nature.* 426:570-574.
- Arakawa, H., D. Lodygin, and J.M. Buerstedde. 2001. Mutant loxP vectors for selectable marker recycle and conditional knock-outs. *BMC Biotechnol.* 1:7.
- Archer, J., and F. Solomon. 1994. Deconstructing the microtubule-organizing center. *Cell.* 76:589-91.
- Aubin, J.E., M. Osborn, and K. Weber. 1980. Variations in the distribution and migration of centriole duplexes in mitotic PtK2 cells studied by immunofluorescence microscopy. *J Cell Sci.* 43:177-94.
- Bahe, S., Y.-D. Stierhof, C.J. Wilkinson, F. Leiss, and E.A. Nigg. 2005. Rootletin forms centriole-associated filaments and functions in centrosome cohesion. *J. Cell Biol.* 171:27-33.
- Bahmanyar, S., D.D. Kaplan, J.G. DeLuca, T.H. Giddings, Jr., E.T. O'Toole, M. Winey, E.D. Salmon, P.J. Casey, W.J. Nelson, and A.I.M. Barth. 2008. -Catenin is a Nek2 substrate involved in centrosome separation. *Genes Dev.* 22:91-105.
- Barr, A.R., and F. Gergely. 2007. Aurora-A: the maker and breaker of spindle poles. *J Cell Sci.* 120:2987-96.

- Barr, A.R., and F. Gergely. 2008. MCAK-independent functions of ch-Tog/XMAP215 in microtubule plus-end dynamics. *Mol Cell Biol.* 28:7199-211.
- Barr, A.R., J.V. Kilmartin, and F. Gergely. 2010. CDK5RAP2 functions in centrosome to spindle pole attachment and DNA damage response. *J Cell Biol.* 189:23-39.
- Barr, A.R., D. Zyss, and F. Gergely. 2009. Knock-in and knock-out: the use of reverse genetics in somatic cells to dissect mitotic pathways. *Methods Mol Biol.* 545:1-19.
- Barr, F.A., and J. Egerer. 2005. Golgi positioning: are we looking at the right MAP? *J Cell Biol.* 168:993-8.
- Barr, F.A., and U. Gruneberg. 2007. Cytokinesis: placing and making the final cut. *Cell.* 131:847-60.
- Barros, T.P., K. Kinoshita, A.A. Hyman, and J.W. Raff. 2005. Aurora A activates D-TACC-Msps complexes exclusively at centrosomes to stabilize centrosomal microtubules. *J Cell Biol.* 170:1039-46.
- Bartek, J., and J. Lukas. 2003. Chk1 and Chk2 kinases in checkpoint control and cancer. *Cancer Cell.* 3:421-9.
- Bascom, R.A., S. Srinivasan, and R.L. Nussbaum. 1999. Identification and characterization of golgin-84, a novel Golgi integral membrane protein with a cytoplasmic coiled-coil domain. *J Biol Chem.* 274:2953-62.
- Basto, R., J. Lau, T. Vinogradova, A. Gardiol, C.G. Woods, A. Khodjakov, and J.W. Raff. 2006. Flies without centrioles. *Cell.* 125:1375-86.
- Belmont, L.D., A.A. Hyman, K.E. Sawin, and T.J. Mitchison. 1990. Real-time visualization of cell cycle-dependent changes in microtubule dynamics in cytoplasmic extracts. *Cell.* 62:579-89.
- Bettencourt-Dias, M., A. Rodrigues-Martins, L. Carpenter, M. Riparbelli, L. Lehmann, M.K. Gatt, N. Carmo, F. Balloux, G. Callaini, and D.M. Glover. 2005. SAK/PLK4 is required for centriole duplication and flagella development. *Curr Biol.* 15:2199-207.
- Bischoff, J.R., L. Anderson, Y. Zhu, K. Mossie, L. Ng, B. Souza, B. Schryver, P. Flanagan, F. Clairvoyant, C. Ginther, C.S. Chan, M. Novotny, D.J. Slamon, and G.D. Plowman. 1998. A homologue of Drosophila aurora kinase is oncogenic and amplified in human colorectal cancers. *Embo J.* 17:3052-65.

- Blangy, A., H.A. Lane, P. d'Herin, M. Harper, M. Kress, and E.A. Nigg. 1995. Phosphorylation by p34cdc2 regulates spindle association of human Eg5, a kinesin-related motor essential for bipolar spindle formation in vivo. *Cell*. 83:1159-69.
- Blasina, A., E.S. Paegle, and C.H. McGowan. 1997. The role of inhibitory phosphorylation of CDC2 following DNA replication block and radiation-induced damage in human cells. *Mol Biol Cell*. 8:1013-23.
- Bobinnec, Y., A. Khodjakov, L.M. Mir, C.L. Rieder, B. Edde, and M. Bornens. 1998a. Centriole disassembly in vivo and its effect on centrosome structure and function in vertebrate cells. *J Cell Biol*. 143:1575-89.
- Bobinnec, Y., M. Moudjou, J.P. Fouquet, E. Desbruyeres, B. Edde, and M. Bornens. 1998b. Glutamylation of centriole and cytoplasmic tubulin in proliferating non-neuronal cells. *Cell Motil Cytoskeleton*. 39:223-32.
- Bonaccorsi, S., M.G. Giansanti, and M. Gatti. 2000. Spindle assembly in *Drosophila* neuroblasts and ganglion mother cells. *Nat Cell Biol*. 2:54-6.
- Bond, J., E. Roberts, G.H. Mochida, D.J. Hampshire, S. Scott, J.M. Askham, K. Springell, M. Mahadevan, Y.J. Crow, A.F. Markham, C.A. Walsh, and C.G. Woods. 2002. ASPM is a major determinant of cerebral cortical size. *Nat Genet*. 32:316-20.
- Bond, J., E. Roberts, K. Springell, S.B. Lizarraga, S. Scott, J. Higgins, D.J. Hampshire, E.E. Morrison, G.F. Leal, E.O. Silva, S.M. Costa, D. Baralle, M. Raponi, G. Karbani, Y. Rashid, H. Jafri, C. Bennett, P. Corry, C.A. Walsh, and C.G. Woods. 2005. A centrosomal mechanism involving CDK5RAP2 and CENPJ controls brain size. *Nat Genet*. 37:353-5.
- Bond, J., S. Scott, D.J. Hampshire, K. Springell, P. Corry, M.J. Abramowicz, G.H. Mochida, R.C. Hennekam, E.R. Maher, J.P. Fryns, A. Alswaid, H. Jafri, Y. Rashid, A. Mubaidin, C.A. Walsh, E. Roberts, and C.G. Woods. 2003. Protein-truncating mutations in ASPM cause variable reduction in brain size. *Am J Hum Genet*. 73:1170-7.
- Bornens, M. 2002. Centrosome composition and microtubule anchoring mechanisms. *Curr Opin Cell Biol*. 14:25-34.
- Bornens, M., and M. Moudjou. 1999. Studying the composition and function of centrosomes in vertebrates. *Methods Cell Biol*. 61:13-34.

- Bouckson-Castaing, V., M. Moudjou, D.J. Ferguson, S. Mucklow, Y. Belkaid, G. Milon, and P.R. Crocker. 1996. Molecular characterisation of ninein, a new coiled-coil protein of the centrosome. *J Cell Sci.* 109 (Pt 1):179-90.
- Bourke, E., J.A. Brown, S. Takeda, H. Hohegger, and C.G. Morrison. 2010. DNA damage induces Chk1-dependent threonine-160 phosphorylation and activation of Cdk2. *Oncogene.* 29:616-24.
- Bourke, E., H. Dodson, A. Merdes, L. Cuffe, G. Zachos, M. Walker, D. Gillespie, and C.G. Morrison. 2007. DNA damage induces Chk1-dependent centrosome amplification. *EMBO Rep.* 8:603-9.
- Bradford, M.M. 1976. A rapid and sensitive method for the quantitation of microgram quantities of protein utilizing the principle of protein-dye binding. *Anal Biochem.* 72:248-54.
- Bree, R.T., X.Y. Lai, L.E. Canavan, and N.F. Lowndes. 2007. Comparisons between DT40 wildtype and DT40-Cre1 cells as suitable model systems for studying the DNA damage response. *Cell Cycle.* 6:2310-3.
- Brouhard, G.J., J.H. Stear, T.L. Noetzel, J. Al-Bassam, K. Kinoshita, S.C. Harrison, J. Howard, and A.A. Hyman. 2008. XMAP215 is a processive microtubule polymerase. *Cell.* 132:79-88.
- Brunk, K., B. Vernay, E. Griffith, N.L. Reynolds, D. Strutt, P.W. Ingham, and A.P. Jackson. 2007. Microcephalin coordinates mitosis in the syncytial *Drosophila* embryo. *J Cell Sci.* 120:3578-88.
- Buerstedde, J., and S. Takeda. 2006. Reviews and protocols in DT40 research. Springer Verlag. XII, 477 p., ISBN: 978-1-4020-4895-1.
- Buerstedde, J.M., and S. Takeda. 1991. Increased ratio of targeted to random integration after transfection of chicken B cell lines. *Cell.* 67:179-88.
- Burckstummer, T., K.L. Bennett, A. Preradovic, G. Schutze, O. Hantschel, G. Superti-Furga, and A. Bauch. 2006. An efficient tandem affinity purification procedure for interaction proteomics in mammalian cells. *Nat Methods.* 3:1013-9.
- Calegari, F., W. Haubensak, C. Haffner, and W.B. Huttner. 2005. Selective Lengthening of the Cell Cycle in the Neurogenic Subpopulation of Neural Progenitor Cells during Mouse Brain Development. *J. Neurosci.* 25:6533-6538.

- Calegari, F., and W.B. Huttner. 2003. An inhibition of cyclin-dependent kinases that lengthens, but does not arrest, neuroepithelial cell cycle induces premature neurogenesis. *J Cell Sci.* 116:4947-4955.
- Carazo-Salas, R.E., G. Guarguaglini, O.J. Gruss, A. Segref, E. Karsenti, and I.W. Mattaj. 1999. Generation of GTP-bound Ran by RCC1 is required for chromatin-induced mitotic spindle formation. *Nature.* 400:178-81.
- Chabin-Brion, K., J. Marceiller, F. Perez, C. Settegrana, A. Drechou, G. Durand, and C. Pous. 2001. The Golgi complex is a microtubule-organizing organelle. *Mol Biol Cell.* 12:2047-60.
- Chae, T., Y.T. Kwon, R. Bronson, P. Dikkes, E. Li, and L.H. Tsai. 1997. Mice lacking p35, a neuronal specific activator of Cdk5, display cortical lamination defects, seizures, and adult lethality. *Neuron.* 18:29-42.
- Chan, G.K., S.A. Jablonski, V. Sudakin, J.C. Hittle, and T.J. Yen. 1999. Human BUBR1 is a mitotic checkpoint kinase that monitors CENP-E functions at kinetochores and binds the cyclosome/APC. *J Cell Biol.* 146:941-54.
- Charrasse, S., M. Schroeder, C. Gauthier-Rouviere, F. Ango, L. Cassimeris, D.L. Gard, and C. Larroque. 1998. The TOGp protein is a new human microtubule-associated protein homologous to the Xenopus XMAP215. *J Cell Sci.* 111 (Pt 10):1371-83.
- Chen, C.H., S.L. Howng, T.S. Cheng, M.H. Chou, C.Y. Huang, and Y.R. Hong. 2003. Molecular characterization of human ninein protein: two distinct subdomains required for centrosomal targeting and regulating signals in cell cycle. *Biochem Biophys Res Commun.* 308:975-83.
- Chen, Z., V.B. Indjeian, M. McManus, L. Wang, and B.D. Dynlacht. 2002. CP110, a cell cycle-dependent CDK substrate, regulates centrosome duplication in human cells. *Dev Cell.* 3:339-50.
- Cheng, J., N. Turkel, N. Hemati, M.T. Fuller, A.J. Hunt, and Y.M. Yamashita. 2008. Centrosome misorientation reduces stem cell division during ageing. *Nature.* 456:599-604.
- Ching, Y.P., Z. Qi, and J.H. Wang. 2000. Cloning of three novel neuronal Cdk5 activator binding proteins. *Gene.* 242:285-94.
- Clark, I.B., and D.I. Meyer. 1999. Overexpression of normal and mutant Arp1alpha (centractin) differentially affects microtubule organization during mitosis and interphase. *J Cell Sci.* 112 (Pt 20):3507-18.

- Conde, C., and A. Caceres. 2009. Microtubule assembly, organization and dynamics in axons and dendrites. *Nat Rev Neurosci.* 10:319-32.
- Cullen, C.F., and H. Ohkura. 2001. Msps protein is localized to acentrosomal poles to ensure bipolarity of *Drosophila* meiotic spindles. *Nat Cell Biol.* 3:637-42.
- de Saint Phalle, B., and W. Sullivan. 1998. Spindle assembly and mitosis without centrosomes in parthenogenetic *Sciara* embryos. *J Cell Biol.* 141:1383-91.
- Debec, A., C. Detraves, C. Montmory, G. Geraud, and M. Wright. 1995. Polar organization of gamma-tubulin in acentriolar mitotic spindles of *Drosophila melanogaster* cells. *J Cell Sci.* 108 (Pt 7):2645-53.
- Delattre, M., C. Canard, and P. Gonczy. 2006. Sequential protein recruitment in *C. elegans* centriole formation. *Curr Biol.* 16:1844-9.
- Delattre, M., S. Leidel, K. Wani, K. Baumer, J. Bamat, H. Schnabel, R. Feichtinger, R. Schnabel, and P. Gonczy. 2004. Centriolar SAS-5 is required for centrosome duplication in *C. elegans*. *Nat Cell Biol.* 6:656-64.
- Delgehyr, N., J. Sillibourne, and M. Bornens. 2005. Microtubule nucleation and anchoring at the centrosome are independent processes linked by ninein function. *J Cell Sci.* 118:1565-75.
- Derry, W.B., L. Wilson, and M.A. Jordan. 1998. Low potency of taxol at microtubule minus ends: implications for its antimitotic and therapeutic mechanism. *Cancer Res.* 58:1177-84.
- Dicthenberg, J.B., W. Zimmerman, C.A. Sparks, A. Young, C. Vidair, Y. Zheng, W. Carrington, F.S. Fay, and S.J. Doxsey. 1998. Pericentrin and gamma-tubulin form a protein complex and are organized into a novel lattice at the centrosome. *J Cell Biol.* 141:163-74.
- do Carmo Avides, M., and D.M. Glover. 1999. Abnormal spindle protein, Asp, and the integrity of mitotic centrosomal microtubule organizing centers. *Science.* 283:1733-5.
- do Carmo Avides, M., A. Tavares, and D.M. Glover. 2001. Polo kinase and Asp are needed to promote the mitotic organizing activity of centrosomes. *Nat Cell Biol.* 3:421-4.
- Dobbelaere, J., Josu, Filipe, S. Suijkerbuijk, B. Baum, N. Tapon, and J. Raff. 2008. A Genome-Wide RNAi Screen to Dissect Centriole Duplication and Centrosome Maturation in *Drosophila*. *PLoS Biology.* 6:e224.

- Dodson, H., E. Bourke, L.J. Jeffers, P. Vagnarelli, E. Sonoda, S. Takeda, W.C. Earnshaw, A. Merdes, and C. Morrison. 2004. Centrosome amplification induced by DNA damage occurs during a prolonged G2 phase and involves ATM. *Embo J.* 23:3864-73.
- Dodson, H., S.P. Wheatley, and C.G. Morrison. 2007. Involvement of centrosome amplification in radiation-induced mitotic catastrophe. *Cell Cycle.* 6:364-70.
- Donaldson, M.M., A.A. Tavares, H. Ohkura, P. Deak, and D.M. Glover. 2001. Metaphase arrest with centromere separation in polo mutants of *Drosophila*. *J Cell Biol.* 153:663-76.
- Doxsey, S.J., P. Stein, L. Evans, P.D. Calarco, and M. Kirschner. 1994. Pericentrin, a highly conserved centrosome protein involved in microtubule organization. *Cell.* 76:639-50.
- Duensing, A., Y. Liu, M. Tseng, M. Malumbres, M. Barbacid, and S. Duensing. 2006. Cyclin-dependent kinase 2 is dispensable for normal centrosome duplication but required for oncogene-induced centrosome overduplication. *Oncogene.* 25:2943-9.
- Dutertre, S., M. Cazales, M. Quaranta, C. Froment, V. Trabut, C. Dozier, G. Mirey, J.P. Bouche, N. Theis-Febvre, E. Schmitt, B. Monsarrat, C. Prigent, and B. Ducommun. 2004. Phosphorylation of CDC25B by Aurora-A at the centrosome contributes to the G2-M transition. *J Cell Sci.* 117:2523-31.
- Elford, H.L. 1968. Effect of hydroxyurea on ribonucleotide reductase. *Biochem Biophys Res Commun.* 33:129-35.
- Endow, S.A., and D.J. Komma. 1997. Spindle dynamics during meiosis in *Drosophila* oocytes. *J Cell Biol.* 137:1321-36.
- Evans, T., E.T. Rosenthal, J. Youngblom, D. Distel, and T. Hunt. 1983. Cyclin: a protein specified by maternal mRNA in sea urchin eggs that is destroyed at each cleavage division. *Cell.* 33:389-96.
- Farkas, L.M., and W.B. Huttner. 2008. The cell biology of neural stem and progenitor cells and its significance for their proliferation versus differentiation during mammalian brain development. *Curr Opin Cell Biol.* 20:707-15.
- Faul, C., A. Dhume, A.D. Schechter, and P. Mundel. 2007. Protein Kinase A, Ca²⁺/Calmodulin-Dependent Kinase II, and Calcineurin Regulate the Intracellular Trafficking of Myopodin between the Z-Disc and the Nucleus of Cardiac Myocytes. *Mol. Cell. Biol.* 27:8215-8227.

- Fish, J.L., Y. Kosodo, W. Enard, S. Paabo, and W.B. Huttner. 2006. Aspm specifically maintains symmetric proliferative divisions of neuroepithelial cells. *Proc Natl Acad Sci U S A*. 103:10438-43.
- Fong, K.-W., Y.-K. Choi, J.B. Rattner, and R.Z. Qi. 2008. CDK5RAP2 Is a Pericentriolar Protein That Functions in Centrosomal Attachment of the γ -Tubulin Ring Complex. *Mol. Biol. Cell*. 19:115-125.
- Fong, K.W., S.Y. Hau, Y.S. Kho, Y. Jia, L. He, and R.Z. Qi. 2009. Interaction of CDK5RAP2 with EB1 to track growing microtubule tips and to regulate microtubule dynamics. *Mol Biol Cell*. 20:3660-70.
- Fry, A.M., T. Mayor, P. Meraldi, Y.-D. Stierhof, K. Tanaka, and E.A. Nigg. 1998a. C-Nap1, a Novel Centrosomal Coiled-Coil Protein and Candidate Substrate of the Cell Cycle-regulated Protein Kinase Nek2. *J. Cell Biol.* 141:1563-1574.
- Fry, A.M., P. Meraldi, and E.A. Nigg. 1998b. A centrosomal function for the human Nek2 protein kinase, a member of the NIMA family of cell cycle regulators. *Embo J*. 17:470-81.
- Fry, A.M., S.J. Schultz, J. Bartek, and E.A. Nigg. 1995. Substrate specificity and cell cycle regulation of the Nek2 protein kinase, a potential human homolog of the mitotic regulator NIMA of *Aspergillus nidulans*. *J Biol Chem*. 270:12899-905.
- Gaglio, T., M.A. Dionne, and D.A. Compton. 1997. Mitotic spindle poles are organized by structural and motor proteins in addition to centrosomes. *J Cell Biol*. 138:1055-66.
- Galjart, N. 2005. CLIPs and CLASPs and cellular dynamics. *Nat Rev Mol Cell Biol*. 6:487-98.
- Gard, D.L., and M.W. Kirschner. 1987. A microtubule-associated protein from *Xenopus* eggs that specifically promotes assembly at the plus-end. *J Cell Biol*. 105:2203-15.
- Gavet, O., and J. Pines. 2010a. Activation of cyclin B1-Cdk1 synchronizes events in the nucleus and the cytoplasm at mitosis. *J Cell Biol*. 189:247-59.
- Gavet, O., and J. Pines. 2010b. Progressive activation of CyclinB1-Cdk1 coordinates entry to mitosis. *Dev Cell*. 18:533-43.
- Gergely, F., V.M. Draviam, and J.W. Raff. 2003. The ch-TOG/XMAP215 protein is essential for spindle pole organization in human somatic cells. *Genes Dev*. 17:336-41.

- Gergely, F., C. Karlsson, I. Still, J. Cowell, J. Kilmartin, and J.W. Raff. 2000a. The TACC domain identifies a family of centrosomal proteins that can interact with microtubules. *Proc Natl Acad Sci U S A*. 97:14352-7.
- Gergely, F., D. Kidd, K. Jeffers, J.G. Wakefield, and J.W. Raff. 2000b. D-TACC: a novel centrosomal protein required for normal spindle function in the early *Drosophila* embryo. *Embo J*. 19:241-52.
- Giet, R., D. McLean, S. Descamps, M.J. Lee, J.W. Raff, C. Prigent, and D.M. Glover. 2002. *Drosophila* Aurora A kinase is required to localize D-TACC to centrosomes and to regulate astral microtubules. *J Cell Biol*. 156:437-51.
- Gillingham, A.K., and S. Munro. 2000. The PACT domain, a conserved centrosomal targeting motif in the coiled-coil proteins AKAP450 and pericentrin. *EMBO Rep*. 1:524-9.
- Glotzer, M., A.W. Murray, and M.W. Kirschner. 1991. Cyclin is degraded by the ubiquitin pathway. *Nature*. 349:132-8.
- Goshima, G., M. Mayer, N. Zhang, N. Stuurman, and R.D. Vale. 2008. Augmin: a protein complex required for centrosome-independent microtubule generation within the spindle. *J Cell Biol*. 181:421-9.
- Goshima, G., and R.D. Vale. 2003. The roles of microtubule-based motor proteins in mitosis: comprehensive RNAi analysis in the *Drosophila* S2 cell line. *J Cell Biol*. 162:1003-16.
- Goshima, G., R. Wollman, S.S. Goodwin, N. Zhang, J.M. Scholey, R.D. Vale, and N. Stuurman. 2007. Genes required for mitotic spindle assembly in *Drosophila* S2 cells. *Science*. 316:417-21.
- Gould, R.R., and G.G. Borisy. 1977. The pericentriolar material in Chinese hamster ovary cells nucleates microtubule formation. *J Cell Biol*. 73:601-15.
- Graser, S., Y.-D. Stierhof, and E.A. Nigg. 2007a. Cep68 and Cep215 (Cdk5rap2) are required for centrosome cohesion. *J Cell Sci*. 120:4321-4331.
- Graser, S., Y.D. Stierhof, S.B. Lavoie, O.S. Gassner, S. Lamla, M. Le Clech, and E.A. Nigg. 2007b. Cep164, a novel centriole appendage protein required for primary cilium formation. *J Cell Biol*. 179:321-30.
- Griffith, E., S. Walker, C.A. Martin, P. Vagnarelli, T. Stiff, B. Vernay, N. Al Sanna, A. Sagar, B. Hamel, W.C. Earnshaw, P.A. Jeggo, A.P. Jackson, and M. O'Driscoll. 2008. Mutations in pericentrin cause Seckel syndrome with defective ATR-dependent DNA damage signaling. *Nat Genet*. 40:232-6.

- Gruss, O.J., R.E. Carazo-Salas, C.A. Schatz, G. Guarguaglini, J. Kast, M. Wilm, N. Le Bot, I. Vernos, E. Karsenti, and I.W. Mattaj. 2001. Ran induces spindle assembly by reversing the inhibitory effect of importin alpha on TPX2 activity. *Cell*. 104:83-93.
- Hadjihannas, M.V., M. Bruckner, and J. Behrens. 2010. Conductin/axin2 and Wnt signalling regulates centrosome cohesion. *EMBO Rep*. 11:317-24.
- Haren, L., N. Gnadt, M. Wright, and A. Merdes. 2009a. NuMA is required for proper spindle assembly and chromosome alignment in prometaphase. *BMC Res Notes*. 2:64.
- Haren, L., and A. Merdes. 2002. Direct binding of NuMA to tubulin is mediated by a novel sequence motif in the tail domain that bundles and stabilizes microtubules. *J Cell Sci*. 115:1815-24.
- Haren, L., T. Stearns, and J. Luders. 2009b. Plk1-Dependent Recruitment of gamma-Tubulin Complexes to Mitotic Centrosomes Involves Multiple PCM Components. *PLoS ONE*. 4:e5976.
- Hauf, S., I.C. Waizenegger, and J.M. Peters. 2001. Cohesin cleavage by separase required for anaphase and cytokinesis in human cells. *Science*. 293:1320-3.
- Hayden, J.H., S.S. Bowser, and C.L. Rieder. 1990. Kinetochores capture astral microtubules during chromosome attachment to the mitotic spindle: direct visualization in live newt lung cells. *J Cell Biol*. 111:1039-45.
- Heald, R., R. Tournebize, T. Blank, R. Sandaltzopoulos, P. Becker, A. Hyman, and E. Karsenti. 1996. Self-organization of microtubules into bipolar spindles around artificial chromosomes in *Xenopus* egg extracts. *Nature*. 382:420-5.
- Heald, R., R. Tournebize, A. Habermann, E. Karsenti, and A. Hyman. 1997. Spindle assembly in *Xenopus* egg extracts: respective roles of centrosomes and microtubule self-organization. *J Cell Biol*. 138:615-28.
- Helps, N.R., X. Luo, H.M. Barker, and P.T. Cohen. 2000. NIMA-related kinase 2 (Nek2), a cell-cycle-regulated protein kinase localized to centrosomes, is complexed to protein phosphatase 1. *Biochem J*. 349:509-18.
- Hertig, A.T., and E.C. Adams. 1967. Studies on the human oocyte and its follicle. I. Ultrastructural and histochemical observations on the primordial follicle stage. *J Cell Biol*. 34:647-75.

- Hinchcliffe, E.H., F.J. Miller, M. Cham, A. Khodjakov, and G. Sluder. 2001. Requirement of a Centrosomal Activity for Cell Cycle Progression Through G1 into S Phase. *Science*. 291:1547-1550.
- Hirokawa, N., Y. Noda, and Y. Okada. 1998. Kinesin and dynein superfamily proteins in organelle transport and cell division. *Curr Opin Cell Biol*. 10:60-73.
- Hochegger, H., D. Dejsuphong, E. Sonoda, A. Saberi, E. Rajendra, J. Kirk, T. Hunt, and S. Takeda. 2007. An essential role for Cdk1 in S phase control is revealed via chemical genetics in vertebrate cells. *J Cell Biol*. 178:257-68.
- Hornig, N.C., P.P. Knowles, N.Q. McDonald, and F. Uhlmann. 2002. The dual mechanism of separase regulation by securin. *Curr Biol*. 12:973-82.
- Horvath, S., B. Zhang, M. Carlson, K.V. Lu, S. Zhu, R.M. Felciano, M.F. Lurance, W. Zhao, S. Qi, Z. Chen, Y. Lee, A.C. Scheck, L.M. Liao, H. Wu, D.H. Geschwind, P.G. Febbo, H.I. Kornblum, T.F. Cloughesy, S.F. Nelson, and P.S. Mischel. 2006. Analysis of oncogenic signaling networks in glioblastoma identifies ASPM as a molecular target. *Proc Natl Acad Sci U S A*. 103:17402-7.
- Howard, J., and A.A. Hyman. 2007. Microtubule polymerases and depolymerases. *Curr Opin Cell Biol*. 19:31-5.
- Howard, J., and A.A. Hyman. 2009. Growth, fluctuation and switching at microtubule plus ends. *Nat Rev Mol Cell Biol*. 10:569-74.
- Hsu, W.B., L.Y. Hung, C.J. Tang, C.L. Su, Y. Chang, and T.K. Tang. 2008. Functional characterization of the microtubule-binding and -destabilizing domains of CPAP and d-SAS-4. *Exp Cell Res*. 314:2591-602.
- Huang, J., and J.W. Raff. 1999. The disappearance of cyclin B at the end of mitosis is regulated spatially in *Drosophila* cells. *Embo J*. 18:2184-95.
- Huberman, J.A. 1981. New views of the biochemistry of eucaryotic DNA replication revealed by aphidicolin, an unusual inhibitor of DNA polymerase alpha. *Cell*. 23:647-8.
- Hudson, D.F., K.M. Marshall, and W.C. Earnshaw. 2009. Condensin: Architect of mitotic chromosomes. *Chromosome Res*. 17:131-44.
- Hung, L.Y., H.L. Chen, C.W. Chang, B.R. Li, and T.K. Tang. 2004. Identification of a novel microtubule-destabilizing motif in CPAP that binds to tubulin heterodimers and inhibits microtubule assembly. *Mol Biol Cell*. 15:2697-706.

- Hut, H.M., W. Lemstra, E.H. Blaauw, G.W. Van Cappellen, H.H. Kampinga, and O.C. Sibon. 2003. Centrosomes split in the presence of impaired DNA integrity during mitosis. *Mol Biol Cell*. 14:1993-2004.
- Ishikawa, H., A. Kubo, and S. Tsukita. 2005. Odf2-deficient mother centrioles lack distal/subdistal appendages and the ability to generate primary cilia. *Nat Cell Biol*. 7:517-24.
- Izraeli, S., L.A. Lowe, V.L. Bertness, D.J. Good, D.W. Dorward, I.R. Kirsch, and M.R. Kuehn. 1999. The SIL gene is required for mouse embryonic axial development and left-right specification. *Nature*. 399:691-4.
- Jackman, M., C. Lindon, E.A. Nigg, and J. Pines. 2003. Active cyclin B1-Cdk1 first appears on centrosomes in prophase. *Nat Cell Biol*. 5:143-8.
- Jackson, A.P., H. Eastwood, S.M. Bell, J. Adu, C. Toomes, I.M. Carr, E. Roberts, D.J. Hampshire, Y.J. Crow, A.J. Mighell, G. Karbani, H. Jafri, Y. Rashid, R.F. Mueller, A.F. Markham, and C.G. Woods. 2002. Identification of microcephalin, a protein implicated in determining the size of the human brain. *Am J Hum Genet*. 71:136-42.
- Jean, C., Y. Tollon, B. Raynaud-Messina, and M. Wright. 1999. The mammalian interphase centrosome: two independent units maintained together by the dynamics of the microtubule cytoskeleton. *Eur J Cell Biol*. 78:549-60.
- Jeffers, L.J., B.J. Coull, S.J. Stack, and C.G. Morrison. 2008. Distinct BRCT domains in Meph1/Brit1 mediate ionizing radiation-induced focus formation and centrosomal localization. *Oncogene*. 27:139-44.
- Jeffery, J.M., A.J. Urquhart, V.N. Subramaniam, R.G. Parton, and K.K. Khanna. 2010. Centrobin regulates the assembly of functional mitotic spindles. *Oncogene*.
- Jin, P., Y. Gu, and D.O. Morgan. 1996. Role of inhibitory CDC2 phosphorylation in radiation-induced G2 arrest in human cells. *J Cell Biol*. 134:963-70.
- Jordan, M.A., R.J. Toso, D. Thrower, and L. Wilson. 1993. Mechanism of mitotic block and inhibition of cell proliferation by taxol at low concentrations. *Proc Natl Acad Sci U S A*. 90:9552-6.
- Joshi, H.C., M.J. Palacios, L. McNamara, and D.W. Cleveland. 1992. Gamma-tubulin is a centrosomal protein required for cell cycle-dependent microtubule nucleation. *Nature*. 356:80-3.

- Jurczyk, A., A. Gromley, S. Redick, J.S. Agustin, G. Witman, G.J. Pazour, D.J.M. Peters, and S. Doxsey. 2004. Pericentrin forms a complex with intraflagellar transport proteins and polycystin-2 and is required for primary cilia assembly. *J. Cell Biol.* 166:637-643.
- Kalab, P., R.T. Pu, and M. Dasso. 1999. The ran GTPase regulates mitotic spindle assembly. *Curr Biol.* 9:481-4.
- Kao, L.R., and T.L. Megraw. 2009. Centrocortin cooperates with centrosomin to organize Drosophila embryonic cleavage furrows. *Curr Biol.* 19:937-42.
- Kapitein, L.C., E.J. Peterman, B.H. Kwok, J.H. Kim, T.M. Kapoor, and C.F. Schmidt. 2005. The bipolar mitotic kinesin Eg5 moves on both microtubules that it crosslinks. *Nature.* 435:114-8.
- Kardon, J.R., and R.D. Vale. 2009. Regulators of the cytoplasmic dynein motor. *Nat Rev Mol Cell Biol.* 10:854-65.
- Kasbek, C., C.H. Yang, A.M. Yusof, H.M. Chapman, M. Winey, and H.A. Fisk. 2007. Preventing the degradation of mps1 at centrosomes is sufficient to cause centrosome reduplication in human cells. *Mol Biol Cell.* 18:4457-69.
- Keryer, G., B. Di Fiore, C. Celati, K.F. Lehtreck, M. Mogensen, A. Delouvee, P. Lavia, M. Bornens, and A.M. Tassin. 2003. Part of Ran is associated with AKAP450 at the centrosome: involvement in microtubule-organizing activity. *Mol Biol Cell.* 14:4260-71.
- Khodjakov, A., R.W. Cole, B.R. Oakley, and C.L. Rieder. 2000. Centrosome-independent mitotic spindle formation in vertebrates. *Curr Biol.* 10:59-67.
- Khodjakov, A., and C.L. Rieder. 1999. The sudden recruitment of gamma-tubulin to the centrosome at the onset of mitosis and its dynamic exchange throughout the cell cycle, do not require microtubules. *J Cell Biol.* 146:585-96.
- Khodjakov, A., and C.L. Rieder. 2001. Centrosomes Enhance the Fidelity of Cytokinesis in Vertebrates and Are Required for Cell Cycle Progression. *J. Cell Biol.* 153:237-242.
- Kim, H.S., M. Takahashi, K. Matsuo, and Y. Ono. 2007. Recruitment of CG-NAP to the Golgi apparatus through interaction with dynein-dynactin complex. *Genes Cells.* 12:421-34.
- Kinoshita, K., T.L. Noetzel, L. Pelletier, K. Mechtler, D.N. Drechsel, A. Schwager, M. Lee, J.W. Raff, and A.A. Hyman. 2005. Aurora A phosphorylation of

- TACC3/maskin is required for centrosome-dependent microtubule assembly in mitosis. *J Cell Biol.* 170:1047-55.
- Kirkham, M., T. Müller-Reichert, K. Oegema, S. Grill, and A.A. Hyman. 2003. SAS-4 Is a *C. elegans* Centriolar Protein that Controls Centrosome Size. *Cell.* 112:575-587.
- Kirschner, M., and T. Mitchison. 1986. Beyond self-assembly: from microtubules to morphogenesis. *Cell.* 45:329-42.
- Klausner, R.D., J.G. Donaldson, and J. Lippincott-Schwartz. 1992. Brefeldin A: insights into the control of membrane traffic and organelle structure. *J Cell Biol.* 116:1071-80.
- Kleylein-Sohn, J., J. Westendorf, M. Le Clech, R. Habedanck, Y.D. Stierhof, and E.A. Nigg. 2007. Plk4-induced centriole biogenesis in human cells. *Dev Cell.* 13:190-202.
- Kochanski, R.S., and G.G. Borisy. 1990. Mode of centriole duplication and distribution. *J Cell Biol.* 110:1599-605.
- Koffa, M.D., C.M. Casanova, R. Santarella, T. Kocher, M. Wilm, and I.W. Mattaj. 2006. HURP is part of a Ran-dependent complex involved in spindle formation. *Curr Biol.* 16:743-54.
- Kohlmaier, G., J. Loncarek, X. Meng, B.F. McEwen, M.M. Mogensen, A. Spektor, B.D. Dynlacht, A. Khodjakov, and P. Gonczy. 2009. Overly long centrioles and defective cell division upon excess of the SAS-4-related protein CPAP. *Curr Biol.* 19:1012-8.
- Komarova, Y.A., I.A. Vorobjev, and G.G. Borisy. 2002. Life cycle of MTs: persistent growth in the cell interior, asymmetric transition frequencies and effects of the cell boundary. *J Cell Sci.* 115:3527-39.
- Kosodo, Y., K. Roper, W. Haubensak, A.M. Marzesco, D. Corbeil, and W.B. Huttner. 2004. Asymmetric distribution of the apical plasma membrane during neurogenic divisions of mammalian neuroepithelial cells. *Embo J.* 23:2314-24.
- Kouprina, N., A. Pavlicek, N.K. Collins, M. Nakano, V.N. Noskov, J. Ohzeki, G.H. Mochida, J.I. Risinger, P. Goldsmith, M. Gunsior, G. Solomon, W. Gersch, J.H. Kim, J.C. Barrett, C.A. Walsh, J. Jurka, H. Masumoto, and V. Larionov. 2005. The microcephaly ASPM gene is expressed in proliferating tissues and encodes for a mitotic spindle protein. *Hum Mol Genet.* 14:2155-65.

- Kozminski, K.G., K.A. Johnson, P. Forscher, and J.L. Rosenbaum. 1993. A motility in the eukaryotic flagellum unrelated to flagellar beating. *Proc Natl Acad Sci U S A.* 90:5519-23.
- Kramer, A., N. Mailand, C. Lukas, R.G. Syljuasen, C.J. Wilkinson, E.A. Nigg, J. Bartek, and J. Lukas. 2004. Centrosome-associated Chk1 prevents premature activation of cyclin-B-Cdk1 kinase. *Nat Cell Biol.* 6:884-891.
- Kumar, A., S.C. Girimaji, M.R. Duvvari, and S.H. Blanton. 2009. Mutations in STIL, encoding a pericentriolar and centrosomal protein, cause primary microcephaly. *Am J Hum Genet.* 84:286-90.
- Kuriyama, R., and G.G. Borisy. 1981. Microtubule-nucleating activity of centrosomes in Chinese hamster ovary cells is independent of the centriole cycle but coupled to the mitotic cycle. *J Cell Biol.* 91:822-6.
- Kwon, M., S.A. Godinho, N.S. Chandhok, N.J. Ganem, A. Azioune, M. They, and D. Pellman. 2008. Mechanisms to suppress multipolar divisions in cancer cells with extra centrosomes. *Genes Dev.* 22:2189-203.
- Lacey, K.R., P.K. Jackson, and T. Stearns. 1999. Cyclin-dependent kinase control of centrosome duplication. *Proc Natl Acad Sci U S A.* 96:2817-22.
- Lane, H.A., and E.A. Nigg. 1996. Antibody microinjection reveals an essential role for human polo-like kinase 1 (Plk1) in the functional maturation of mitotic centrosomes. *J Cell Biol.* 135:1701-13.
- Larocca, M.C., M. Jin, and J.R. Goldenring. 2006. AKAP350 modulates microtubule dynamics. *Eur J Cell Biol.* 85:611-9.
- Larocca, M.C., R.A. Shanks, L. Tian, D.L. Nelson, D.M. Stewart, and J.R. Goldenring. 2004. AKAP350 interaction with cdc42 interacting protein 4 at the Golgi apparatus. *Mol Biol Cell.* 15:2771-81.
- Lawo, S., M. Bashkurov, M. Mullin, M.G. Ferreria, R. Kittler, B. Habermann, A. Tagliaferro, I. Poser, J.R.A. Hutchins, B. Hegemann, D. Pinchev, F. Buchholz, J.-M. Peters, A.A. Hyman, A.-C. Gingras, and L. Pelletier. 2009. HAUS, the 8-Subunit Human Augmin Complex, Regulates Centrosome and Spindle Integrity. *Current Biology.* 19:816-826.
- Lee, M.J., F. Gergely, K. Jeffers, S.Y. Peak-Chew, and J.W. Raff. 2001. Msp/XMAP215 interacts with the centrosomal protein D-TACC to regulate microtubule behaviour. *Nat Cell Biol.* 3:643-9.

- Lee, S., and K. Rhee. 2010. CEP215 is involved in the dynein-dependent accumulation of pericentriolar matrix proteins for spindle pole formation. *Cell Cycle*. 9.
- Leidel, S., and P. Gonczy. 2003. SAS-4 is essential for centrosome duplication in *C. elegans* and is recruited to daughter centrioles once per cell cycle. *Dev Cell*. 4:431-9.
- LeRoy, P.J., J.J. Hunter, K.M. Hoar, K.E. Burke, V. Shinde, J. Ruan, D. Bowman, K. Galvin, and J.A. Ecsedy. 2007. Localization of human TACC3 to mitotic spindles is mediated by phosphorylation on Ser558 by Aurora A: a novel pharmacodynamic method for measuring Aurora A activity. *Cancer Res*. 67:5362-70.
- Lew, J., Q.Q. Huang, Z. Qi, R.J. Winkfein, R. Aebersold, T. Hunt, and J.H. Wang. 1994. A brain-specific activator of cyclin-dependent kinase 5. *Nature*. 371:423-6.
- Lew, J., R. Winkfein, H. Paudel, and J. Wang. 1992. Brain proline-directed protein kinase is a neurofilament kinase which displays high sequence homology to p34cdc2. *J. Biol. Chem*. 267:25922-25926.
- Liang, Y., H. Gao, S.Y. Lin, G. Peng, X. Huang, P. Zhang, J.A. Goss, F.C. Brunnicardi, A.S. Multani, S. Chang, and K. Li. 2010. BRIT1/MCPH1 is essential for mitotic and meiotic recombination DNA repair and maintaining genomic stability in mice. *PLoS Genet*. 6:e1000826.
- Lin, S.Y., R. Rai, K. Li, Z.X. Xu, and S.J. Elledge. 2005. BRIT1/MCPH1 is a DNA damage responsive protein that regulates the Brca1-Chk1 pathway, implicating checkpoint dysfunction in microcephaly. *Proc Natl Acad Sci U S A*. 102:15105-9.
- Littlepage, L.E., H. Wu, T. Andresson, J.K. Deanehan, L.T. Amundadottir, and J.V. Ruderman. 2002. Identification of phosphorylated residues that affect the activity of the mitotic kinase Aurora-A. *Proc Natl Acad Sci U S A*. 99:15440-5.
- Liu, Q., S. Guntuku, X.S. Cui, S. Matsuoka, D. Cortez, K. Tamai, G. Luo, S. Carattini-Rivera, F. DeMayo, A. Bradley, L.A. Donehower, and S.J. Elledge. 2000. Chk1 is an essential kinase that is regulated by Atr and required for the G(2)/M DNA damage checkpoint. *Genes Dev*. 14:1448-59.

- Loffler, H., T. Bochtler, B. Fritz, B. Tews, A.D. Ho, J. Lukas, J. Bartek, and A. Kramer. 2007. DNA damage-induced accumulation of centrosomal Chk1 contributes to its checkpoint function. *Cell Cycle*. 6:2541-8.
- Loffler, H., J. Lukas, J. Bartek, and A. Kramer. 2006. Structure meets function--Centrosomes, genome maintenance and the DNA damage response. *Experimental Cell Research*. 312:2633-2640.
- Logarinho, E., and C.E. Sunkel. 1998. The Drosophila POLO kinase localises to multiple compartments of the mitotic apparatus and is required for the phosphorylation of MPM2 reactive epitopes. *J Cell Sci*. 111 (Pt 19):2897-909.
- Lucas, E.P., and J.W. Raff. 2007. Maintaining the proper connection between the centrioles and the pericentriolar matrix requires Drosophila Centrosomin. *J Cell Biol*. 178:725-732.
- Luders, J., and T. Stearns. 2007. Microtubule-organizing centres: a re-evaluation. *Nat Rev Mol Cell Biol*. 8:161-167.
- Lupas, A., M. Van Dyke, and J. Stock. 1991. Predicting coiled coils from protein sequences. *Science*. 252:1162-1164.
- Maiato, H., J. DeLuca, E.D. Salmon, and W.C. Earnshaw. 2004a. The dynamic kinetochore-microtubule interface. *J Cell Sci*. 117:5461-77.
- Maiato, H., C.L. Rieder, and A. Khodjakov. 2004b. Kinetochore-driven formation of kinetochore fibers contributes to spindle assembly during animal mitosis. *J Cell Biol*. 167:831-40.
- Malmanche, N., A. Maia, and C.E. Sunkel. 2006. The spindle assembly checkpoint: preventing chromosome mis-segregation during mitosis and meiosis. *FEBS Lett*. 580:2888-95.
- Maney, T., M. Wagenbach, and L. Wordeman. 2001. Molecular dissection of the microtubule depolymerizing activity of mitotic centromere-associated kinesin. *J Biol Chem*. 276:34753-8.
- Maresca, T.J., and E.D. Salmon. Welcome to a new kind of tension: translating kinetochore mechanics into a wait-anaphase signal. *J Cell Sci*. 123:825-35.
- Maresca, T.J., and E.D. Salmon. 2009. Intrakinetochore stretch is associated with changes in kinetochore phosphorylation and spindle assembly checkpoint activity. *J Cell Biol*. 184:373-81.

- Margolis, R.L., and L. Wilson. 1978. Opposite end assembly and disassembly of microtubules at steady state in vitro. *Cell*. 13:1-8.
- Marshall, W.F. 2007. What is the function of centrioles? *J Cell Biochem*. 100:916-22.
- Martinez-Campos, M., R. Basto, J. Baker, M. Kernan, and J.W. Raff. 2004. The *Drosophila* pericentrin-like protein is essential for cilia/flagella function, but appears to be dispensable for mitosis. *J Cell Biol*. 165:673-83.
- Mastronarde, D.N., K.L. McDonald, R. Ding, and J.R. McIntosh. 1993. Interpolar spindle microtubules in PTK cells. *J Cell Biol*. 123:1475-89.
- Mayor, T., Y.D. Stierhof, K. Tanaka, A.M. Fry, and E.A. Nigg. 2000. The centrosomal protein C-Nap1 is required for cell cycle-regulated centrosome cohesion. *J Cell Biol*. 151:837-46.
- McKinnon, P.J. 2009. DNA repair deficiency and neurological disease. *Nat Rev Neurosci*. 10:100-12.
- McNally, F.J., and S. Thomas. 1998. Katanin is responsible for the M-phase microtubule-severing activity in *Xenopus* eggs. *Mol Biol Cell*. 9:1847-61.
- Megraw, T.L., L.-R. Kao, and T.C. Kaufman. 2001. Zygotic development without functional mitotic centrosomes. *Current Biology*. 11:116-120.
- Megraw, T.L., K. Li, L.R. Kao, and T.C. Kaufman. 1999. The centrosomin protein is required for centrosome assembly and function during cleavage in *Drosophila*. *Development*. 126:2829-2839.
- Meraldi, P., J. Lukas, A.M. Fry, J. Bartek, and E.A. Nigg. 1999. Centrosome duplication in mammalian somatic cells requires E2F and Cdk2-cyclin A. *Nat Cell Biol*. 1:88-93.
- Meraldi, P., and E.A. Nigg. 2001. Centrosome cohesion is regulated by a balance of kinase and phosphatase activities. *J Cell Sci*. 114:3749-57.
- Merdes, A., K. Ramyar, J.D. Vechio, and D.W. Cleveland. 1996. A Complex of NuMA and Cytoplasmic Dynein Is Essential for Mitotic Spindle Assembly. *Cell*. 87:447-458.
- Mikhailov, A., R.W. Cole, and C.L. Rieder. 2002. DNA damage during mitosis in human cells delays the metaphase/anaphase transition via the spindle-assembly checkpoint. *Curr Biol*. 12:1797-806.
- Mitchison, T., L. Evans, E. Schulze, and M. Kirschner. 1986. Sites of microtubule assembly and disassembly in the mitotic spindle. *Cell*. 45:515-27.

- Mitchison, T., and M. Kirschner. 1984a. Dynamic instability of microtubule growth. *Nature*. 312:237-42.
- Mitchison, T., and M. Kirschner. 1984b. Microtubule assembly nucleated by isolated centrosomes. *Nature*. 312:232-7.
- Mitchison, T.J. 1989. Polewards microtubule flux in the mitotic spindle: evidence from photoactivation of fluorescence. *J Cell Biol*. 109:637-52.
- Mitra, J., and G.H. Enders. 2004. Cyclin A/Cdk2 complexes regulate activation of Cdk1 and Cdc25 phosphatases in human cells. *Oncogene*. 23:3361-7.
- Mogensen, M.M., A. Malik, M. Piel, V. Bouckson-Castaing, and M. Bornens. 2000. Microtubule minus-end anchorage at centrosomal and non-centrosomal sites: the role of ninein. *J Cell Sci*. 113 (Pt 17):3013-23.
- Morales-Mulia, S., and J.M. Scholey. 2005. Spindle pole organization in *Drosophila* S2 cells by dynein, abnormal spindle protein (Asp), and KLP10A. *Mol Biol Cell*. 16:3176-86.
- Morris, V.B., J. Brammall, J. Noble, and R. Reddel. 2000. p53 localizes to the centrosomes and spindles of mitotic cells in the embryonic chick epiblast, human cell lines, and a human primary culture: An immunofluorescence study. *Exp Cell Res*. 256:122-30.
- Murphy, D.B., K.A. Johnson, and G.G. Borisy. 1977. Role of tubulin-associated proteins in microtubule nucleation and elongation. *J Mol Biol*. 117:33-52.
- Nachury, M.V., T.J. Maresca, W.C. Salmon, C.M. Waterman-Storer, R. Heald, and K. Weis. 2001. Importin beta is a mitotic target of the small GTPase Ran in spindle assembly. *Cell*. 104:95-106.
- Nakajima, H., F. Toyoshima-Morimoto, E. Taniguchi, and E. Nishida. 2003. Identification of a consensus motif for Plk (Polo-like kinase) phosphorylation reveals Myt1 as a Plk1 substrate. *J Biol Chem*. 278:25277-80.
- Nakamura, M., X.Z. Zhou, and K.P. Lu. 2001. Critical role for the EB1 and APC interaction in the regulation of microtubule polymerization. *Curr Biol*. 11:1062-7.
- Nasmyth, K. 2002. Segregating sister genomes: the molecular biology of chromosome separation. *Science*. 297:559-65.
- Nezi, L., and A. Musacchio. 2009. Sister chromatid tension and the spindle assembly checkpoint. *Curr Opin Cell Biol*. 21:785-95.

- Nigg, E.A., and J.W. Raff. 2009. Centrioles, centrosomes, and cilia in health and disease. *Cell*. 139:663-78.
- Nikolic, M., H. Dudek, Y.T. Kwon, Y.F. Ramos, and L.H. Tsai. 1996. The cdk5/p35 kinase is essential for neurite outgrowth during neuronal differentiation. *Genes Dev*. 10:816-25.
- Nishihashi, A., T. Haraguchi, Y. Hiraoka, T. Ikemura, V. Regnier, H. Dodson, W.C. Earnshaw, and T. Fukagawa. 2002. CENP-I is essential for centromere function in vertebrate cells. *Dev Cell*. 2:463-76.
- Nogales, E., S.G. Wolf, I.A. Khan, R.F. Luduena, and K.H. Downing. 1995. Structure of tubulin at 6.5 Å and location of the taxol-binding site. *Nature*. 375:424-7.
- Nousiainen, M., H.H.W. Sillje, G. Sauer, E.A. Nigg, and R. Korner. 2006. Phosphoproteome analysis of the human mitotic spindle. *PNAS*. 103:5391-5396.
- O'Brien, L.L., A.J. Albee, L. Liu, W. Tao, P. Dobrzyn, S.B. Lizarraga, and C. Wiese. 2005. The *Xenopus* TACC homologue, maskin, functions in mitotic spindle assembly. *Mol Biol Cell*. 16:2836-47.
- O'Connell, C.B., and A.L. Khodjakov. 2007. Cooperative mechanisms of mitotic spindle formation. *J Cell Sci*. 120:1717-22.
- O'Connell, C.B., J. Loncarek, P. Kalab, and A. Khodjakov. 2009. Relative contributions of chromatin and kinetochores to mitotic spindle assembly. *J Cell Biol*. 187:43-51.
- O'Connell, K.F., C. Caron, K.R. Kopish, D.D. Hurd, K.J. Kempfues, Y. Li, and J.G. White. 2001. The *C. elegans* zyg-1 gene encodes a regulator of centrosome duplication with distinct maternal and paternal roles in the embryo. *Cell*. 105:547-58.
- Oakley, C.E., and B.R. Oakley. 1989. Identification of gamma-tubulin, a new member of the tubulin superfamily encoded by mipA gene of *Aspergillus nidulans*. *Nature*. 338:662-4.
- Ohi, R., and K.L. Gould. 1999. Regulating the onset of mitosis. *Curr Opin Cell Biol*. 11:267-73.
- Ohshima, T., J.M. Ward, C.G. Huh, G. Longenecker, Veeranna, H.C. Pant, R.O. Brady, L.J. Martin, and A.B. Kulkarni. 1996. Targeted disruption of the cyclin-dependent kinase 5 gene results in abnormal corticogenesis, neuronal pathology and perinatal death. *Proc Natl Acad Sci U S A*. 93:11173-8.

- Okuda, M., H.F. Horn, P. Tarapore, Y. Tokuyama, A.G. Smulian, P.K. Chan, E.S. Knudsen, I.A. Hofmann, J.D. Snyder, K.E. Bove, and K. Fukasawa. 2000. Nucleophosmin/B23 is a target of CDK2/cyclin E in centrosome duplication. *Cell*. 103:127-40.
- Oshimori, N., X. Li, M. Ohsugi, and T. Yamamoto. 2009. Cep72 regulates the localization of key centrosomal proteins and proper bipolar spindle formation. *Embo J*. 28:2066-76.
- Paintrand, M., M. Moudjou, H. Delacroix, and M. Bornens. 1992. Centrosome organization and centriole architecture: their sensitivity to divalent cations. *J Struct Biol*. 108:107-28.
- Paramasivam, M., Y.J. Chang, and J.J. Loturco. 2007. ASPM and Citron Kinase Co-Localize to the Midbody Ring During Cytokinesis. *Cell Cycle*. 6.
- Paudel, H.K., J. Lew, Z. Ali, and J.H. Wang. 1993. Brain proline-directed protein kinase phosphorylates tau on sites that are abnormally phosphorylated in tau associated with Alzheimer's paired helical filaments. *J Biol Chem*. 268:23512-8.
- Peel, N., N.R. Stevens, R. Basto, and J.W. Raff. 2007. Overexpressing centriole-replication proteins in vivo induces centriole overduplication and de novo formation. *Curr Biol*. 17:834-43.
- Pelletier, L., E. O'Toole, A. Schwager, A.A. Hyman, and T. Muller-Reichert. 2006. Centriole assembly in *Caenorhabditis elegans*. *Nature*. 444:619-23.
- Peng, G., E.K. Yim, H. Dai, A.P. Jackson, I. Burgt, M.R. Pan, R. Hu, K. Li, and S.Y. Lin. 2009. BRIT1/MCPH1 links chromatin remodelling to DNA damage response. *Nat Cell Biol*. 11:865-72.
- Peset, I., J. Seiler, T. Sardon, L.A. Bejarano, S. Rybina, and I. Vernos. 2005. Function and regulation of Maskin, a TACC family protein, in microtubule growth during mitosis. *J Cell Biol*. 170:1057-66.
- Petretti, C., M. Savoian, E. Montembault, D.M. Glover, C. Prigent, and R. Giet. 2006. The PITSLRE/CDK11p58 protein kinase promotes centrosome maturation and bipolar spindle formation. *EMBO Rep*. 7:418-24.
- Pfaff, K.L., C.T. Straub, K. Chiang, D.M. Bear, Y. Zhou, and L.I. Zon. 2007. The zebra fish *cassiopeia* mutant reveals that SIL is required for mitotic spindle organization. *Mol Cell Biol*. 27:5887-97.

- Piehl, M., U.S. Tulu, P. Wadsworth, and L. Cassimeris. 2004. Centrosome maturation: measurement of microtubule nucleation throughout the cell cycle by using GFP-tagged EB1. *Proc Natl Acad Sci U S A*. 101:1584-8.
- Piel, M., P. Meyer, A. Khodjakov, C.L. Rieder, and M. Bornens. 2000a. The respective contributions of the mother and daughter centrioles to centrosome activity and behavior in vertebrate cells. *J Cell Biol*. 149:317-30.
- Piel, M., J. Nordberg, U. Euteneuer, and M. Bornens. 2001. Centrosome-dependent exit of cytokinesis in animal cells. *Science*. 291:1550-3.
- Pines, J., and T. Hunter. 1991. Human cyclins A and B1 are differentially located in the cell and undergo cell cycle-dependent nuclear transport. *J Cell Biol*. 115:1-17.
- Prosser, S.L., K.R. Straatman, and A.M. Fry. 2009. Molecular dissection of the centrosome overduplication pathway in S-phase-arrested cells. *Mol Cell Biol*. 29:1760-73.
- Puntoni, F., and E. Villa-Moruzzi. 1997. Protein phosphatase-1 alpha, gamma 1, and delta: changes in phosphorylation and activity in mitotic HeLa cells and in cells released from the mitotic block. *Arch Biochem Biophys*. 340:177-84.
- Quintyne, N.J., S.R. Gill, D.M. Eckley, C.L. Crego, D.A. Compton, and T.A. Schroer. 1999. Dynactin is required for microtubule anchoring at centrosomes. *J Cell Biol*. 147:321-34.
- Quintyne, N.J., and T.A. Schroer. 2002. Distinct cell cycle-dependent roles for dynactin and dynein at centrosomes. *J Cell Biol*. 159:245-54.
- Rai, R., H. Dai, A.S. Multani, K. Li, K. Chin, J. Gray, J.P. Lahad, J. Liang, G.B. Mills, F. Meric-Bernstam, and S.Y. Lin. 2006. BRIT1 regulates early DNA damage response, chromosomal integrity, and cancer. *Cancer Cell*. 10:145-57.
- Rainey, M.D., E.J. Black, G. Zachos, and D.A. Gillespie. 2008. Chk2 is required for optimal mitotic delay in response to irradiation-induced DNA damage incurred in G2 phase. *Oncogene*. 27:896-906.
- Rattner, J.B., and M.W. Berns. 1976. Centriole behavior in early mitosis of rat kangaroo cells (PTK2). *Chromosoma*. 54:387-95.
- Rauch, A., C.T. Thiel, D. Schindler, U. Wick, Y.J. Crow, A.B. Ekici, A.J. van Essen, T.O. Goecke, L. Al-Gazali, K.H. Chrzanowska, C. Zweier, H.G. Brunner, K. Becker, C.J. Curry, B. Dallapiccola, K. Devriendt, A. Dorfler, E. Kinning, A. Megarbane, P. Meinecke, R.K. Semple, S. Spranger, A. Toutain, R.C.

- Trembath, E. Voss, L. Wilson, R. Hennekam, F. de Zegher, H.-G. Dorr, and A. Reis. 2008. Mutations in the Pericentrin (PCNT) Gene Cause Primordial Dwarfism. *Science*:1151174.
- Raynaud-Messina, B., and A. Merdes. 2007. Gamma-tubulin complexes and microtubule organization. *Curr Opin Cell Biol.* 19:24-30.
- Reynolds, E.S. 1963. The use of lead citrate at high pH as an electron-opaque stain in electron microscopy. *J Cell Biol.* 17:208-12.
- Rhind, N., and P. Russell. 2000. Chk1 and Cds1: linchpins of the DNA damage and replication checkpoint pathways. *J Cell Sci.* 113 (Pt 22):3889-96.
- Rickmyre, J.L., S. Dasgupta, D.L. Ooi, J. Keel, E. Lee, M.W. Kirschner, S. Waddell, and L.A. Lee. 2007. The Drosophila homolog of MCPH1, a human microcephaly gene, is required for genomic stability in the early embryo. *J Cell Sci.* 120:3565-77.
- Rieder, C.L., and S.P. Alexander. 1990. Kinetochores are transported poleward along a single astral microtubule during chromosome attachment to the spindle in newt lung cells. *J Cell Biol.* 110:81-95.
- Rieder, C.L., R.W. Cole, A. Khodjakov, and G. Sluder. 1995. The checkpoint delaying anaphase in response to chromosome monoorientation is mediated by an inhibitory signal produced by unattached kinetochores. *J Cell Biol.* 130:941-8.
- Rios, R.M., A. Sanchis, A.M. Tassin, C. Fedriani, and M. Bornens. 2004. GMAP-210 recruits gamma-tubulin complexes to cis-Golgi membranes and is required for Golgi ribbon formation. *Cell.* 118:323-35.
- Ripoll, P., S. Pimpinelli, M.M. Valdivia, and J. Avila. 1985. A cell division mutant of Drosophila with a functionally abnormal spindle. *Cell.* 41:907-12.
- Rivero, S., J. Cardenas, M. Bornens, and R.M. Rios. 2009. Microtubule nucleation at the cis-side of the Golgi apparatus requires AKAP450 and GM130. *Embo J.* 28:1016-28.
- Roberts, E., D.J. Hampshire, L. Pattison, K. Springell, H. Jafri, P. Corry, J. Mannon, Y. Rashid, Y. Crow, J. Bond, and C.G. Woods. 2002. Autosomal recessive primary microcephaly: an analysis of locus heterogeneity and phenotypic variation. *J Med Genet.* 39:718-21.
- Rogalski, A.A., and S.J. Singer. 1984. Associations of elements of the Golgi apparatus with microtubules. *J Cell Biol.* 99:1092-100.

- Rosenblatt, J., L.P. Cramer, B. Baum, and K.M. McGee. 2004. Myosin II-dependent cortical movement is required for centrosome separation and positioning during mitotic spindle assembly. *Cell*. 117:361-72.
- Rusan, N.M., and G.C. Rogers. 2009. Centrosome function: sometimes less is more. *Traffic*. 10:472-81.
- Saladino, C., E. Bourke, P.C. Conroy, and C.G. Morrison. 2009. Centriole separation in DNA damage-induced centrosome amplification. *Environ Mol Mutagen*. 50:725-32.
- Samejima, I., P.C. Lourenco, H.A. Snaith, and K.E. Sawin. 2005. Fission yeast mto2p regulates microtubule nucleation by the centrosomin-related protein mto1p. *Mol Biol Cell*. 16:3040-51.
- Samejima, I., V.J. Miller, L.M. Groocock, and K.E. Sawin. 2008. Two distinct regions of Mto1 are required for normal microtubule nucleation and efficient association with the gamma-tubulin complex in vivo. *J Cell Sci*. 121:3971-80.
- Sandoval, I.V., J.S. Bonifacino, R.D. Klausner, M. Henkart, and J. Wehland. 1984. Role of microtubules in the organization and localization of the Golgi apparatus. *J Cell Biol*. 99:113s-118s.
- Saredi, A., L. Howard, and D.A. Compton. 1996. NuMA assembles into an extensive filamentous structure when expressed in the cell cytoplasm. *J Cell Sci*. 109 (Pt 3):619-30.
- Satir, P., and S.T. Christensen. 2007. Overview of structure and function of mammalian cilia. *Annu Rev Physiol*. 69:377-400.
- Sato, N., K. Mizumoto, M. Nakamura, and M. Tanaka. 2000. Radiation-induced centrosome overduplication and multiple mitotic spindles in human tumor cells. *Exp Cell Res*. 255:321-6.
- Saunders, R.D., M.C. Avides, T. Howard, C. Gonzalez, and D.M. Glover. 1997. The *Drosophila* gene abnormal spindle encodes a novel microtubule-associated protein that associates with the polar regions of the mitotic spindle. *J Cell Biol*. 137:881-90.
- Sawin, K.E., P.C.C. Lourenco, and H.A. Snaith. 2004. Microtubule Nucleation at Non-Spindle Pole Body Microtubule-Organizing Centers Requires Fission Yeast Centrosomin-Related Protein mod20p. *Current Biology*. 14:763-775.

- Schmidt, T.I., J. Kleylein-Sohn, J. Westendorf, M. Le Clech, S.B. Lavoie, Y.D. Stierhof, and E.A. Nigg. 2009. Control of centriole length by CPAP and CP110. *Curr Biol.* 19:1005-11.
- Scholey, J.M. 2008. Intraflagellar transport motors in cilia: moving along the cell's antenna. *J Cell Biol.* 180:23-9.
- Serrano, M., A.W. Lin, M.E. McCurrach, D. Beach, and S.W. Lowe. 1997. Oncogenic ras Provokes Premature Cell Senescence Associated with Accumulation of p53 and p16INK4a. *Cell.* 88:593-602.
- Sherr, C.J. 1993. Mammalian G1 cyclins. *Cell.* 73:1059-65.
- Shiloh, Y. 2003. ATM and related protein kinases: safeguarding genome integrity. *Nat Rev Cancer.* 3:155-68.
- Shima, T., T. Kon, K. Imamula, R. Ohkura, and K. Sutoh. 2006. Two modes of microtubule sliding driven by cytoplasmic dynein. *Proc Natl Acad Sci U S A.* 103:17736-40.
- Shirasawa, S., M. Furuse, N. Yokoyama, and T. Sasazuki. 1993. Altered growth of human colon cancer cell lines disrupted at activated Ki-ras. *Science.* 260:85-8.
- Shorter, J., and G. Warren. 2002. Golgi architecture and inheritance. *Annu Rev Cell Dev Biol.* 18:379-420.
- Silk, A.D., A.J. Holland, and D.W. Cleveland. 2009. Requirements for NuMA in maintenance and establishment of mammalian spindle poles. *J Cell Biol.* 184:677-90.
- Smith, E., D. Dejsuphong, A. Balestrini, M. Hampel, C. Lenz, S. Takeda, A. Vindigni, and V. Costanzo. 2009. An ATM- and ATR-dependent checkpoint inactivates spindle assembly by targeting CEP63. *Nat Cell Biol.* advanced online publication.
- Stevens, N.R., J. Dobbelaere, K. Brunk, A. Franz, and J.W. Raff. 2010. Drosophila Ana2 is a conserved centriole duplication factor. *J Cell Biol.* 188:313-23.
- Stucki, M., and S.P. Jackson. 2006. gammaH2AX and MDC1: anchoring the DNA-damage-response machinery to broken chromosomes. *DNA Repair (Amst).* 5:534-43.
- Sullivan, W. 2009. Centrosomes: CNN's Broadcast Reaches the Cleavage Furrow. *Current Biology.* 19:R513-R515.

- Sun, D., C.L. Leung, and R.K. Liem. 1996. Phosphorylation of the high molecular weight neurofilament protein (NF-H) by Cdk5 and p35. *J Biol Chem.* 271:14245-51.
- Sunkel, C.E., and D.M. Glover. 1988. polo, a mitotic mutant of *Drosophila* displaying abnormal spindle poles. *J Cell Sci.* 89 (Pt 1):25-38.
- Szollosi, D., P. Calarco, and R.P. Donahue. 1972. Absence of centrioles in the first and second meiotic spindles of mouse oocytes. *J Cell Sci.* 11:521-41.
- Takada, S., A. Kelkar, and W.E. Theurkauf. 2003. *Drosophila* checkpoint kinase 2 couples centrosome function and spindle assembly to genomic integrity. *Cell.* 113:87-99.
- Takahashi, M., H. Shibata, M. Shimakawa, M. Miyamoto, H. Mukai, and Y. Ono. 1999. Characterization of a novel giant scaffolding protein, CG-NAP, that anchors multiple signaling enzymes to centrosome and the golgi apparatus. *J Biol Chem.* 274:17267-74.
- Takahashi, M., A. Yamagiwa, T. Nishimura, H. Mukai, and Y. Ono. 2002. Centrosomal proteins CG-NAP and kendrin provide microtubule nucleation sites by anchoring gamma-tubulin ring complex. *Mol Biol Cell.* 13:3235-45.
- Takahashi, T., R.S. Nowakowski, and V.S. Caviness, Jr. 1995. The cell cycle of the pseudostratified ventricular epithelium of the embryonic murine cerebral wall. *J. Neurosci.* 15:6046-6057.
- Takao, N., H. Kato, R. Mori, C. Morrison, E. Sonada, X. Sun, H. Shimizu, K. Yoshioka, S. Takeda, and K. Yamamoto. 1999. Disruption of ATM in p53-null cells causes multiple functional abnormalities in cellular response to ionizing radiation. *Oncogene.* 18:7002-9.
- Tang, C.J., R.H. Fu, K.S. Wu, W.B. Hsu, and T.K. Tang. 2009. CPAP is a cell-cycle regulated protein that controls centriole length. *Nat Cell Biol.* 11:825-31.
- Taylor, S.S., E. Ha, and F. McKeon. 1998. The human homologue of Bub3 is required for kinetochore localization of Bub1 and a Mad3/Bub1-related protein kinase. *J Cell Biol.* 142:1-11.
- Terada, Y., Y. Uetake, and R. Kuriyama. 2003. Interaction of Aurora-A and centrosomin at the microtubule-nucleating site in *Drosophila* and mammalian cells. *J. Cell Biol.* 162:757-764.

- Theurkauf, W.E., and R.S. Hawley. 1992. Meiotic spindle assembly in *Drosophila* females: behavior of nonexchange chromosomes and the effects of mutations in the nod kinesin-like protein. *J Cell Biol.* 116:1167-80.
- Thompson, H.M., H. Cao, J. Chen, U. Euteneuer, and M.A. McNiven. 2004. Dynamin 2 binds gamma-tubulin and participates in centrosome cohesion. *Nat Cell Biol.* 6:335-42.
- Tibelius, A., J. Marhold, H. Zentgraf, C.E. Heilig, H. Neitzel, B. Ducommun, A. Rauch, A.D. Ho, J. Bartek, and A. Kramer. 2009. Microcephalin and pericentrin regulate mitotic entry via centrosome-associated Chk1. *J Cell Biol.* 185:1149-57.
- Toyoshima, F., and E. Nishida. 2007. Spindle orientation in animal cell mitosis: roles of integrin in the control of spindle axis. *J Cell Physiol.* 213:407-11.
- Trimborn, M., S.M. Bell, C. Felix, Y. Rashid, H. Jafri, P.D. Griffiths, L.M. Neumann, A. Krebs, A. Reis, K. Sperling, H. Neitzel, and A.P. Jackson. 2004. Mutations in microcephalin cause aberrant regulation of chromosome condensation. *Am J Hum Genet.* 75:261-6.
- Trimborn, M., D. Schindler, H. Neitzel, and T. Hirano. 2006. Misregulated chromosome condensation in MCPH1 primary microcephaly is mediated by condensin II. *Cell Cycle.* 5:322-6.
- Tsai, L.H., I. Delalle, V.S. Caviness, Jr., T. Chae, and E. Harlow. 1994. p35 is a neural-specific regulatory subunit of cyclin-dependent kinase 5. *Nature.* 371:419-23.
- Tsou, M.-F.B., and T. Stearns. 2006a. Mechanism limiting centrosome duplication to once per cell cycle. *Nature.* 442:947-951.
- Tsou, M.F., and T. Stearns. 2006b. Controlling centrosome number: licenses and blocks. *Curr Opin Cell Biol.* 18:74-8.
- Tsou, M.F., W.J. Wang, K.A. George, K. Uryu, T. Stearns, and P.V. Jallepalli. 2009. Polo kinase and separase regulate the mitotic licensing of centriole duplication in human cells. *Dev Cell.* 17:344-54.
- Tsvetkov, L., X. Xu, J. Li, and D.F. Stern. 2003. Polo-like kinase 1 and Chk2 interact and co-localize to centrosomes and the midbody. *J Biol Chem.* 278:8468-75.
- Turner, N.C., C.J. Lord, E. Iorns, R. Brough, S. Swift, R. Elliott, S. Rayter, A.N. Tutt, and A. Ashworth. 2008. A synthetic lethal siRNA screen identifying genes mediating sensitivity to a PARP inhibitor. *Embo J.* 27:1368-77.

- Uchida, K.S., K. Takagaki, K. Kumada, Y. Hirayama, T. Noda, and T. Hirota. 2009. Kinetochore stretching inactivates the spindle assembly checkpoint. *J Cell Biol.* 184:383-90.
- Uehara, R., R.S. Nozawa, A. Tomioka, S. Petry, R.D. Vale, C. Obuse, and G. Goshima. 2009. The augmin complex plays a critical role in spindle microtubule generation for mitotic progression and cytokinesis in human cells. *Proc Natl Acad Sci U S A.* 106:6998-7003.
- Uetake, Y., J. Loncarek, J.J. Nordberg, C.N. English, S. La Terra, A. Khodjakov, and G. Sluder. 2007. Cell cycle progression and de novo centriole assembly after centrosomal removal in untransformed human cells. *J Cell Biol.* 176:173-82.
- Uhlmann, F., F. Lottspeich, and K. Nasmyth. 1999. Sister-chromatid separation at anaphase onset is promoted by cleavage of the cohesin subunit Scc1. *Nature.* 400:37-42.
- Uhlmann, F., and K. Nasmyth. 1998. Cohesion between sister chromatids must be established during DNA replication. *Curr Biol.* 8:1095-101.
- Vagnarelli, P., C. Morrison, H. Dodson, E. Sonoda, S. Takeda, and W.C. Earnshaw. 2004. Analysis of Scc1-deficient cells defines a key metaphase role of vertebrate cohesin in linking sister kinetochores. *EMBO Rep.* 5:167-71.
- Vaisberg, E.A., M.P. Koonce, and J.R. McIntosh. 1993. Cytoplasmic dynein plays a role in mammalian mitotic spindle formation. *J Cell Biol.* 123:849-58.
- Vaizel-Ohayon, D., and E.D. Schejter. 1999. Mutations in centrosomin reveal requirements for centrosomal function during early *Drosophila* embryogenesis. *Current Biology.* 9:889-898.
- van der Voet, M., C.W. Berends, A. Perreault, T. Nguyen-Ngoc, P. Gonczy, M. Vidal, M. Boxem, and S. van den Heuvel. 2009. NuMA-related LIN-5, ASPM-1, calmodulin and dynein promote meiotic spindle rotation independently of cortical LIN-5/GPR/Galpha. *Nat Cell Biol.* 11:269-77.
- Vandre, D.D., F.M. Davis, P.N. Rao, and G.G. Borisy. 1984. Phosphoproteins are components of mitotic microtubule organizing centers. *Proc Natl Acad Sci U S A.* 81:4439-43.
- Vasquez, R.J., B. Howell, A.M. Yvon, P. Wadsworth, and L. Cassimeris. 1997. Nanomolar concentrations of nocodazole alter microtubule dynamic instability in vivo and in vitro. *Mol Biol Cell.* 8:973-85.

- Verde, I., G. Pahlke, M. Salanova, G. Zhang, S. Wang, D. Coletti, J. Onuffer, S.L.C. Jin, and M. Conti. 2001. Myomegalin Is a Novel Protein of the Golgi/Centrosome That Interacts with a Cyclic Nucleotide Phosphodiesterase. *J. Biol. Chem.* 276:11189-11198.
- Vitre, B., F.M. Coquelle, C. Heichette, C. Garnier, D. Chretien, and I. Arnal. 2008. EB1 regulates microtubule dynamics and tubulin sheet closure in vitro. *Nat Cell Biol.* 10:415-21.
- Walter, A.O., W. Seghezzi, W. Korver, J. Sheung, and E. Lees. 2000. The mitotic serine/threonine kinase Aurora2/AIK is regulated by phosphorylation and degradation. *Oncogene.* 19:4906-16.
- Wang, X., Y.P. Ching, W.H. Lam, Z. Qi, M. Zhang, and J.H. Wang. 2000. Identification of a common protein association region in the neuronal Cdk5 activator. *J Biol Chem.* 275:31763-9.
- Wang, X., J.W. Tsai, J.H. Imai, W.N. Lian, R.B. Vallee, and S.H. Shi. 2009. Asymmetric centrosome inheritance maintains neural progenitors in the neocortex. *Nature.* 461:947-55.
- Waterman-Storer, C.M., S. Karki, and E.L. Holzbaur. 1995. The p150Glued component of the dynactin complex binds to both microtubules and the actin-related protein centractin (Arp-1). *Proc Natl Acad Sci U S A.* 92:1634-8.
- Waterman-Storer, C.M., and E.D. Salmon. 1997. Microtubule dynamics: Treadmilling comes around again. *Current Biology.* 7:R369-R372.
- Winding, P., and M.W. Berchtold. 2001. The chicken B cell line DT40: a novel tool for gene disruption experiments. *J Immunol Methods.* 249:1-16.
- Wong, C., and T. Stearns. 2003. Centrosome number is controlled by a centrosome-intrinsic block to reduplication. *Nat Cell Biol.* 5:539-44.
- Wood, J.L., K. Li, Y. Liang, and J. Chen. 2008. Microcephalin/MCPH1 associates with the condensin II complex to function in homologous recombination repair. *J. Biol. Chem.* 283:29586-92.
- Wood, J.L., N. Singh, G. Mer, and J. Chen. 2007. MCPH1 functions in an H2AX-dependent but MDC1-independent pathway in response to DNA damage. *J Biol Chem.* 282:35416-23.
- Wu, X., G. Mondal, X. Wang, J. Wu, L. Yang, V.S. Pankratz, M. Rowley, and F.J. Couch. 2009. Microcephalin regulates BRCA2 and Rad51-associated DNA double-strand break repair. *Cancer Res.* 69:5531-6.

- Xie, Z., L.Y. Moy, K. Sanada, Y. Zhou, J.J. Buchman, and L.-H. Tsai. 2007. Cep120 and TACCs Control Interkinetic Nuclear Migration and the Neural Progenitor Pool. *Neuron*. 56:79-93.
- Xu, X., J. Lee, and D.F. Stern. 2004. Microcephalin is a DNA damage response protein involved in regulation of CHK1 and BRCA1. *J Biol Chem*. 279:34091-4.
- Yamashita, Y.M., and M.T. Fuller. 2008. Asymmetric centrosome behavior and the mechanisms of stem cell division. *J. Cell Biol.*:180: 261-6.
- Yang, J., M. Adamian, and T. Li. 2006. Rootletin interacts with C-Nap1 and may function as a physical linker between the pair of centrioles/basal bodies in cells. *Mol Biol Cell*. 17:1033-40.
- Yang, S.Z., F.T. Lin, and W.C. Lin. 2008. MCPH1/BRIT1 cooperates with E2F1 in the activation of checkpoint, DNA repair and apoptosis. *EMBO Rep*. 9:907-15.
- Zachos, G., M.D. Rainey, and D.A. Gillespie. 2003. Chk1-deficient tumour cells are viable but exhibit multiple checkpoint and survival defects. *Embo J*. 22:713-23.
- Zhang, J., and T.L. Megraw. 2007. Proper Recruitment of γ -Tubulin and D-TACC/Msps to Embryonic Drosophila Centrosomes Requires Centrosomin Motif 1. *Mol. Biol. Cell*. 18:4037-4049.
- Zhao, L., C. Jin, Y. Chu, C. Varghese, S. Hua, F. Yan, Y. Miao, J. Liu, D. Mann, X. Ding, J. Zhang, Z. Wang, Z. Dou, and X. Yao. 2010. Dimerization of CPAP orchestrates centrosome cohesion plasticity. *J Biol Chem*. 285:2488-97.
- Zhao, Z.S., J.P. Lim, Y.W. Ng, L. Lim, and E. Manser. 2005. The GIT-associated kinase PAK targets to the centrosome and regulates Aurora-A. *Mol Cell*. 20:237-49.
- Zhong, X., L. Liu, A. Zhao, G.P. Pfeifer, and X. Xu. 2005. The abnormal spindle-like, microcephaly-associated (ASPM) gene encodes a centrosomal protein. *Cell Cycle*. 4:1227-9.
- Zhong, X., G.P. Pfeifer, and X. Xu. 2006. Microcephalin encodes a centrosomal protein. *Cell Cycle*. 5:457-8.
- Zyss, D., and F. Gergely. 2009. Centrosome function in cancer: guilty or innocent? *Trends Cell Biol*. 19:334-46.

Appendix

Appendix 1

Supplementary CD with figure legends for movies.

Appendix 2

Parts of this thesis have been published in the following article:

Barr, A.R., J.V. Kilmartin, and F. Gergely. 2010. CDK5RAP2 functions in centrosome to spindle pole attachment and DNA damage response. *J Cell Biol.* 189:23-39.

The following articles are also referenced in the text:

Barr, A.R., and F. Gergely. 2007. Aurora-A: the maker and breaker of spindle poles. *J Cell Sci.* 120:2987-96.

Barr, A.R., and F. Gergely. 2008. MCAK-independent functions of ch-Tog/XMAP215 in microtubule plus-end dynamics. *Mol Cell Biol.* 28:7199-211.

All of these articles have been printed and included in the appendix of this thesis.

Appendix 1: Figure legends for Supplementary movies (see Supplementary CD)

Supplementary movies for Figure 3.2.5

Movie 3.1 Control hp1-1 cell transfected with GFP-centrin1.

Movie 3.2 CDK5RAP2 hp1d cells transfected with GFP-centrin1.

Movie 3.3 Control hp1-1 cell transfected with GFP-centrin1. Note the presence of two pairs of centrioles at the start of the filming period.

Supplementary movies for Figure 5.2.3

Movie 5.1 Wild-type DT40 cell transfected with GFP-tubulin.

Movie 5.2 *cnn1*^{-/-} DT40 cell transfected with GFP-tubulin.

Movie 5.3 *cnn1*^{-/-} DT40 cell transfected with GFP-tubulin.

Movie 5.4 *cnn1*^{-/-} DT40 cell transfected with GFP-PACT, to visualise the centrosomes (green) and mCherry-tubulin to visualise the microtubule cytoskeleton (red).

Supplementary movies to accompany text in 6.1.1

(Z-stack images were taken every 15 minutes for at least 26 hours. See Materials and Methods for details).

Movie 6.1 Wild-type DT40 cell filmed by DIC microscopy.

Movie 6.2 *cnn1*^{-/-} DT40 cell filmed by DIC microscopy.

Movie 6.3 *cnn1*^{-/-} DT40 cell filmed by DIC microscopy